| AD NUMBER |
| --- |
| **ADB202472** |
| LIMITATION CHANGES |
| TO:<br>**Approved for public release; distribution is unlimited.** |
| FROM:<br>**DTIC users only.** |
| AUTHORITY |
| **ONR ltr dtd 13 May 1970** |

UNITED STATES NAVY
AND
UNITED STATES AIR FORCE

# PROJECT SQUID

## ANNUAL PROGRAM REPORT

1 January, 1950

POLYTECHNIC INSTITUTE OF BROOKLYN
CORNELL AERONAUTICAL LABORATORY
UNIVERSITY OF DELAWARE
JOHNS HOPKINS UNIVERSITY
NEW YORK UNIVERSITY
PRINCETON UNIVERSITY
PURDUE UNIVERSITY

ANNUAL PROGRAM REPORT

# PROJECT SQUID

*A COOPERATIVE PROGRAM*
*OF FUNDAMENTAL RESEARCH IN JET PROPULSION*
*FOR THE*
*OFFICE OF NAVAL RESEARCH, DEPARTMENT OF THE NAVY*
*AND THE*
*OFFICE OF AIR RESEARCH, DEPARTMENT OF THE AIR FORCE*

- - - - -

CONTRACTS AND NR NUMBERS

NYU - N6-ORI-11, Task Order 2, NR 220-040
PIB - N6-ORI-98, Task Order 2, NR 220-039
PRF - N6-ORI-104, Task Order 1, NR 220-042
CAL - N6-ORI-119, Task Order 1, NR 220-041
PRIN- N6-ORI-105, Task Order 3, NR 220-038
DEL - N8-ONR-74000 and 74001, NR 220-063
JHU - N6-ONR-243, Task Order 20, NR 220-088

1 January 1950

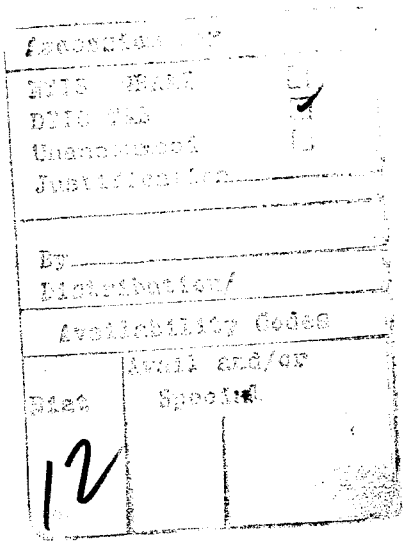

# TABLE OF CONTENTS

# I. JET PROPULSION ENGINES

## A. *EXPERIMENTAL INVESTIGATION OF THE EFFECT OF COMBUSTION CHAMBER PRESSURE UPON ROCKET MOTOR PERFORMANCE. (PRF-7R8)*

*Submitted by: C.M. Beighley, Purdue University*

The object of this problem is to obtain experimental data regarding the effect of combustion chamber pressure upon the performance of rocket motors employing white fuming nitric acid and AN-F-58 jet engine fuel for propellants. The theoretical work in connection with the above has been reported by C.H. Trent and M.J. Zucrow.[1]

A series of rocket motors is being designed with a constant $L^* = 60$ in. and an aspect ratio of 2 for operation at the following combustion chamber pressures: 500, 700, and 1000 psi. No investigation is contemplated, at this time, of the effect of $L^*$ on performance. The effect of mixture ratio (oxidizer/fuel) at each chamber pressure, however, is to be investigated. Figure 1 illustrates the internal configurations of the rocket motors to be used in the investigations.

The thrust cylinder, nozzle, and injector for each rocket motor is to be fabricated from Type 347 stainless steel. The combustion chambers and nozzles are to be water-cooled, with helical flow around the combustion chamber walls and approximately longitudinal flow over the nozzle walls. All injectors are of the 2 to 1 symmetrical impingement type (two acid streams impinging on 1 fuel stream) with four impingement points. If the cooling problem becomes too severe for water-cooling, Niafrax ceramic liners will be employed, or film cooling.

## B. *PRELIMINARY ANALYSIS OF HEAT TRANSFER IN HIGH PRESSURE ROCKET MOTOR. (PRF-7R2).*

*Submitted by: C.F. Warner and M.J. Zucrow, Purdue University*

Insofar as is possible, theoretical analysis is utilized in this problem to estimate the severity of the heat transfer problems in rocket motors operating at high combustion

[1] C.H. Trent and M.J. Zucrow, *The Calculated Performance of Hydrocarbon-White Fuming Nitric Acid Propellants at High Chamber Pressures,* Project Squid, Technical Memorandum No. Pur-6.

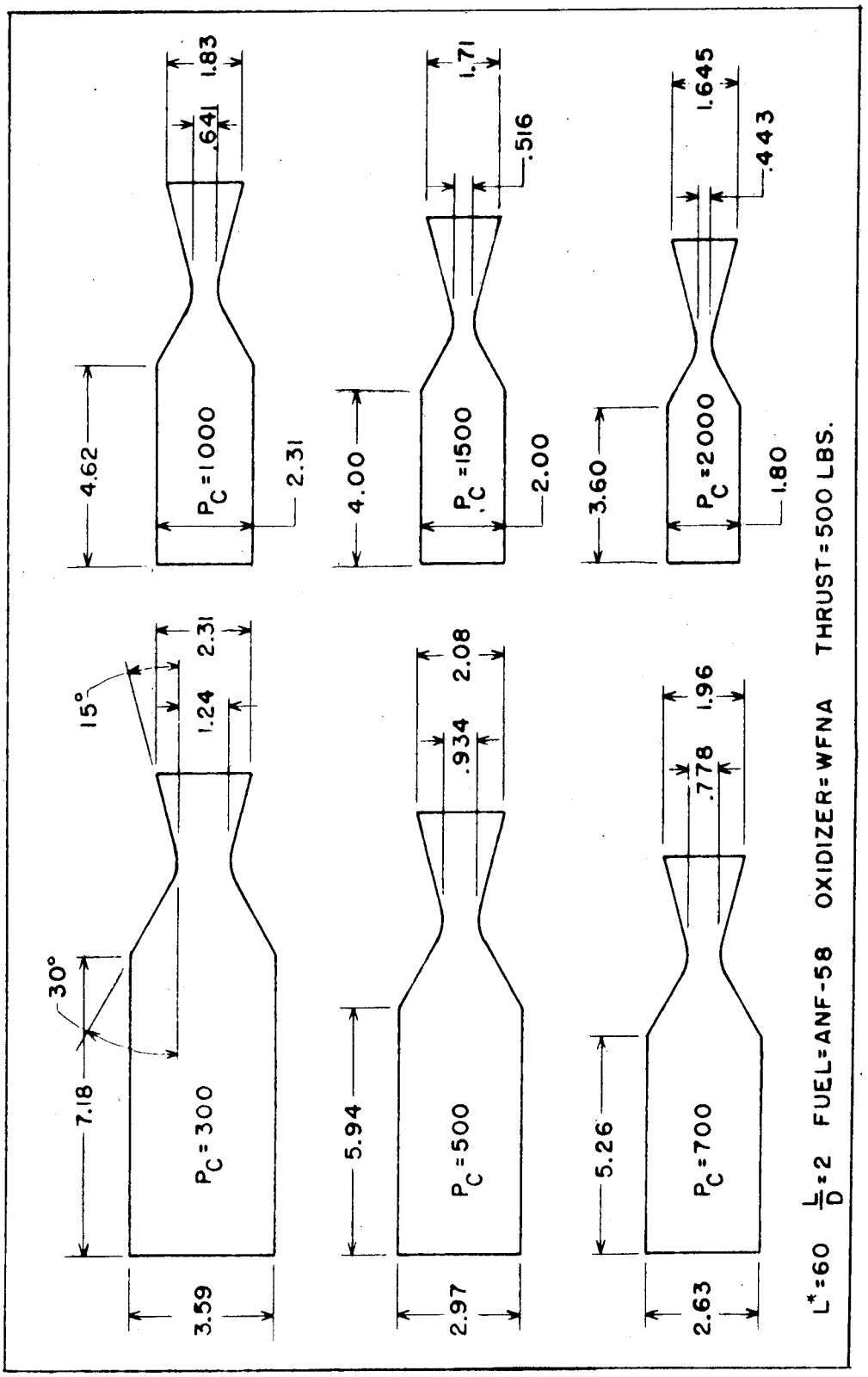


Fig. 1. Proposed rocket motors for the investigation of combustion chamber pressure upon motor performance.

chamber pressures with WFNA and AN-F-58 jet engine fuel as propellants. For comparison the heat transfer with the WFNA-Aniline propellant system was also investigated. A technical report on the above subject has been transmitted to Project Squid, Princeton, New Jersey.

In making the analysis it was assumed that the combustion gases and the flame temperatures were those presented by C.H. Trent and M.J. Zucrow.[2]

The rocket motors analyzed were assumed to have the following characteristics: constant thrust of 500 pounds; constant $L^* = 100$ inches; constant aspect ratio of 2, and variable chamber and throat dimensions. Figure 2 presents the principal results of the analysis.

The convective heat transfer rates were calculated by W.H. McAdams in equation 4c, of his book entitled, *Heat Transmission.*[3]

The radiation from the combustion gases was determined by means of the method of Hottel and Egbert.[4]

The main conclusions derived from the analysis are as follows:

The rate of heat transfer to the combustion chamber and nozzle increases practically linearly with the combustion chamber pressure; this effect of pressure has been substantiated experimentally at lower combustion chamber pressures.

The heat transfer rate in the nozzle throat becomes extremely large at high chamber pressures. If the predicted values are actually realized, it may not be possible to cool the throat section of the nozzle adequately with regenerative cooling alone.

The heat transfer rates in a rocket motor employing WFNA and octane as propellants are practically the same as for the WFNA and aniline propellants.

There is a lack of experimental data on the thermal conductivity properties and viscosities of gases and gas mixtures at high temperatures. Such data are needed for making reliable correlations of heat transfer test data.

---

[2]Trent and Zucrow, Tech. Memo. Pur-6.

[3]W.H. McAdams, *Heat Transmission,* McGraw-Hill Book Company, New York, p. 168.

[4]H.C. Hottel and R.B. Egbert, "Radiant Heat Transmission for Water Vapor," *Trans. Amer. Inst. of Chem. Engineers,* Vol. 38, 1942, p. 531.

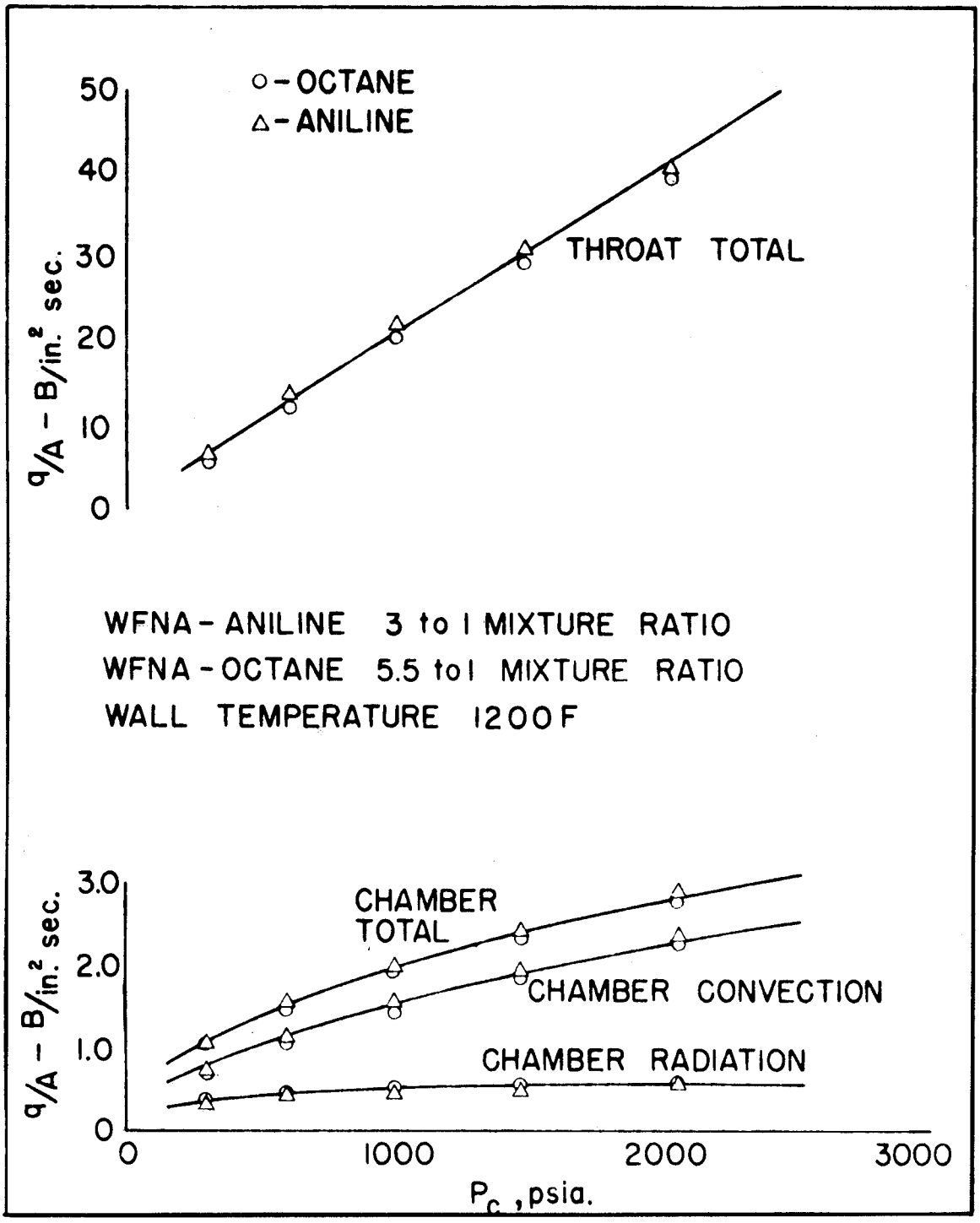


Fig. 2. Heat transfer rates as a function of chamber pressure for a 500 pound thrust motor.

## C. *EXPERIMENTAL INVESTIGATION OF THE EFFECT OF COMBUSTION CHAMBER PRESSURE UPON HEAT TRANSFER IN ROCKET MOTORS. (PRF-7R9).*

*Submitted by: C.F. Warner, Purdue University*

This problem seeks to provide the experimental data regarding the influence of combustion chamber pressure upon the heat transfer in rocket motors. The work is the experimental counterpart of the theoretical analysis described in Section B.

For the experiments a series of water-cooled 500-pound-thrust rocket motors are being designed for operation with combustion pressure ranges of 300, 500, 700, and 1000 psi.

The data obtained from testing at 1000 psi will govern the direction of future investigations. As far as possible, the same type of injector design is to be used with each rocket to reduce the effect of injector design upon the heat transfer data. The 300-psi rocket motor has been fabricated, and preliminary tests have been conducted with it.

All motors are equipped with separate cooling jackets for the thrust cylinder and the exhaust nozzle, thus permitting the independent determination of the overall heat transfer in the combustion chamber and nozzle sections. The bulk temperature of the coolant is to be measured at several locations in the cooling jacket. The same rocket motors discussed under Section A are to be used for this investigation. All of the experiments will be with WFNA and AN-F-58 jet engine fuel as propellants.

A water-cooled motor designed for 300 psi combustion chamber pressure is currently being tested to obtain the heat transfer data at 300 psi that are to serve as the basis of comparison with the heat transfer at higher pressures. To eliminate, as far as possible, the influence of injector design upon heat transfer, the aforementioned motor has been built with an $L^* = 100$ in. and the injector is of the 1 to 1 impingement type (1 fuel system and 1 oxidizer stream) with 6 impingement points. Too few data have been obtained to warrant reporting at this time.

## D. *STUDIES OF THE PRINCIPLES OF THE RAM ROCKET. (Pr-Ph.3).*

*Submitted by: J.V. Charyk, Princeton University*

From practical application considerations a ducted rocket or ram rocket appears to have certain inherent advantages over the ramjet or rocket motor alone. These advantages

can be summarized as follows:

Since the rocket jet has been shown to be able to induce an air flow amounting to 10 to 15 times its propellant weight flow, thrust augmentation in the static case of the order of at least 50 per cent should be able to be realized. This induction action by the rocket, however, falls off rather rapidly with forward velocity, and operation of the device then depends on ram pressure which increases with forward velocity.

The products of combustion of a rocket motor are exhausted at such a temperature that they contain large quantities of combustible products such as free hydrogen ($H_2$), carbon monoxide (CO), and smaller quantities of H, OH, etc. In the ram rocket engine, these products react with the oxygen in the secondary air so that the resultant percentage of the energy available in the rocket fuel that is converted into useful work is considerably higher than in the case of the rocket alone. When the rocket is used in connection with a ramjet, these products provide part of, or all of, the ramjet fuel by reacting with the air entering the ramjet.

In such a device the presence of the rocket motor eliminates the problem of ignition and also does away with the need for drag producing flame holders. Altitude limitations and ramjet combustion chamber velocity limitations are also largely eliminated. Since the rocket exhaust products are at a very high temperature and of very simple chemical composition, high combustion efficiencies should be obtained.

**Rocket Motor Development.** The original development of the small liquid propellant rocket is described in the annual progress report of January 1949. Since that time the rocket has been used in connection with a duct which makes it merely one component of the overall *ram rocket,* or ducted rocket, and consequently the performance criteria are no longer those of a rocket alone. The functions of the rocket in the ram rocket power plant are: to supply thrust which compares favorably to that of a rocket when used as the sole power source; to serve as a gaseous fuel injector to supply large quantities of CO, $H_2$, etc. to be burned in the downstream duct; and to act as the primary jet of an ejector which induces free air for thrust augmentation in the static case and at low flight velocities.

In order to satisfy these additional requirements, the choice of propellants for the ram rocket will not necessarily be the same as those for ordinary rocket applications. Furthermore, the mixture ratio used will not be the same as that for optimum performance of the rocket alone. Rather, a much richer fuel-oxidizer ratio is desirable. Three fuel combinations are tabulated in Table I in order to show the variation in their useful

Table I. Comparison of Three Rocket Fuels.

$P_c$ = 300 lb./in.$^2$ Abs.
$I_s$ = 225-230 sec.
All on rich range. All values in BTU/lb.

| | | 75% $C_2H_5OH$ 25% $H_2O$ | $C_2H_5OH$ | $C_8H_{18}$ |
|---|---|---|---|---|
| 1. | Specific Impulse $I_s$ sec. | 225 | 229 | 225 |
| 2. | Mixture Ratio O/F | 1.0 | 1.1 | 1.4 |
| 3.* | Low heating value BTU/lb. of fuel | 8950 | 11930 | 19250 |
| 4. | BTU/lb. of total propellant (at above mixture ratio) | 4475 | 5680 | 8030 |
| 5.** | Temperature at exhaust °F (frozen equilibrium) | 2200 | 2050 | 1580 |
| 6.** *** | Enthalpy of exhaust products $h_{ex}$ | 1350 | 1070 | 930 |
| 7.*** | Low heating values of CO, $H_2$, and H $h_c$ | 2035 | 3340 | 6105 |
| 8. | K.E. of exhaust gases $\frac{1}{J}\frac{1}{2}\frac{WV^2}{g}$ $h_{ke}$ | 1050 | 1090 | 1050 |
| 9. | 6+7+8=4 | 4435 | 5500 | 8085 |
| 10. | Ratio $\frac{h_{ex}+h_c}{h_{ke}}$ | 3.0 | 4.1 | 6.7 |

* *Marks Handbook*
** North American and Bell Aircraft Reports
*** Bureau of Standards Values (1947). Base = -460°F

exhaust products. Item 10 is a ratio of the available exhaust energy to the kinetic energy, which determines the thrust of the rocket alone. The figures in the table are for octane rather than for the diesel oil, which was used in some of the experimental work, since the latter figures were not readily available.

The purely physical requirement that the rocket motor be streamlined when used in connection with the duct, necessitated further changes in the rocket motor design. Figure 3 shows the latest motor mounted on the test stand, supported by an airfoil section strut

which contains the coolant, propellant, and pressure lines and ignition wire. A streamlined cowling (not shown) covers the entire motor. An assembly drawing of the unit is shown in Figure 4 and a break-down of the motor components in Figure 5. It will be noted that the original design features of having no welded parts, thereby allowing inspection and replacement of parts, has been maintained in this model.

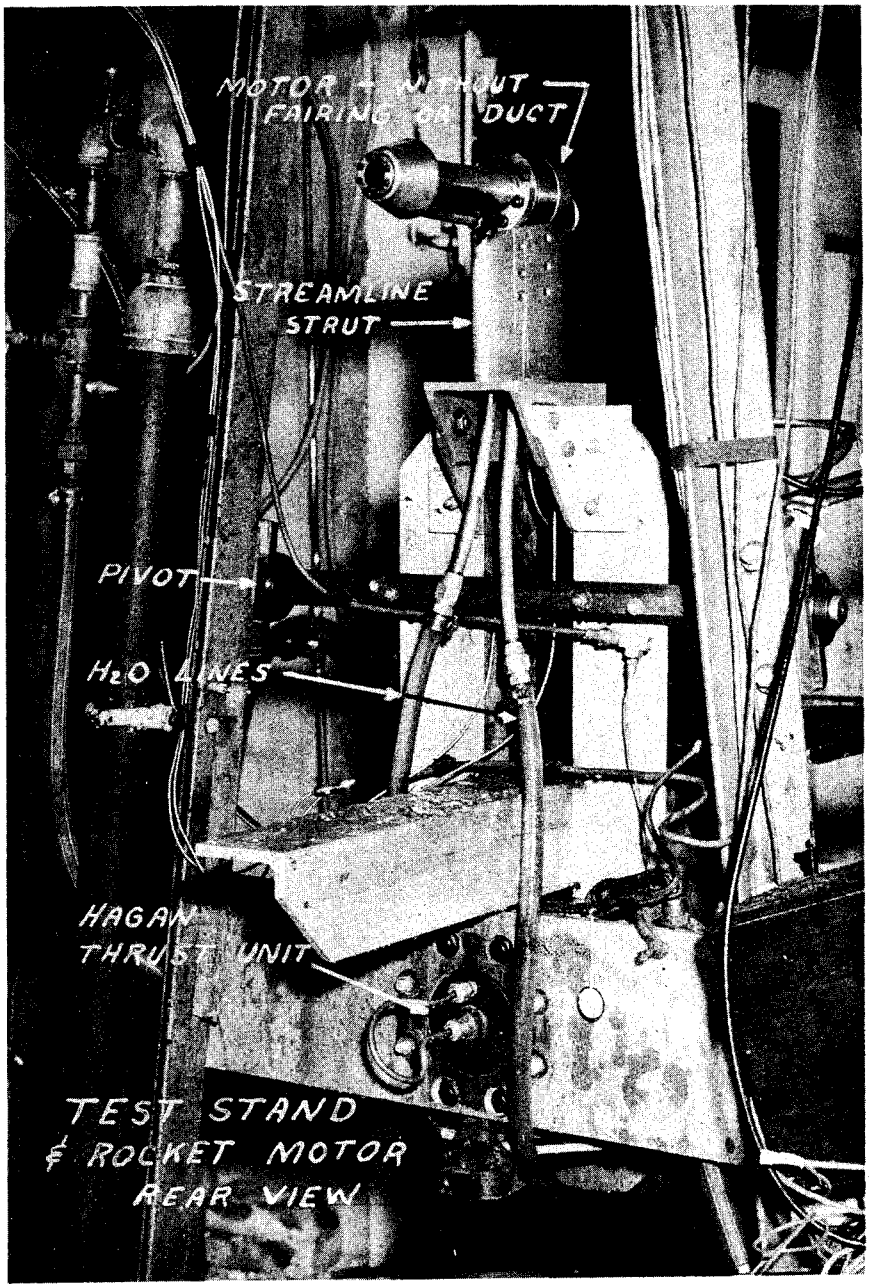


**Fig. 3.** Fifty-pound thrust rocket motor on stand.

After the installation of the downstream duct, it was no longer practicable to obtain ignition by means of a spark from a wire inserted into the throat of the motor. By slightly modifying the injector, a small model engine spark plug was incorporated in the design. This gave immediate ignition with either alcohol or diesel oil as a fuel. The life of these plugs is approximately five runs of three minutes duration. The position relation to the surface of the injector head, however, is rather critical. Satisfactory ignition occurs when the plug is recessed about $\frac{1}{10}$ inch into the head. If it is located further back, it is less effective, and if it is flush or protruding into the chamber, the electrodes tend to burn more rapidly.

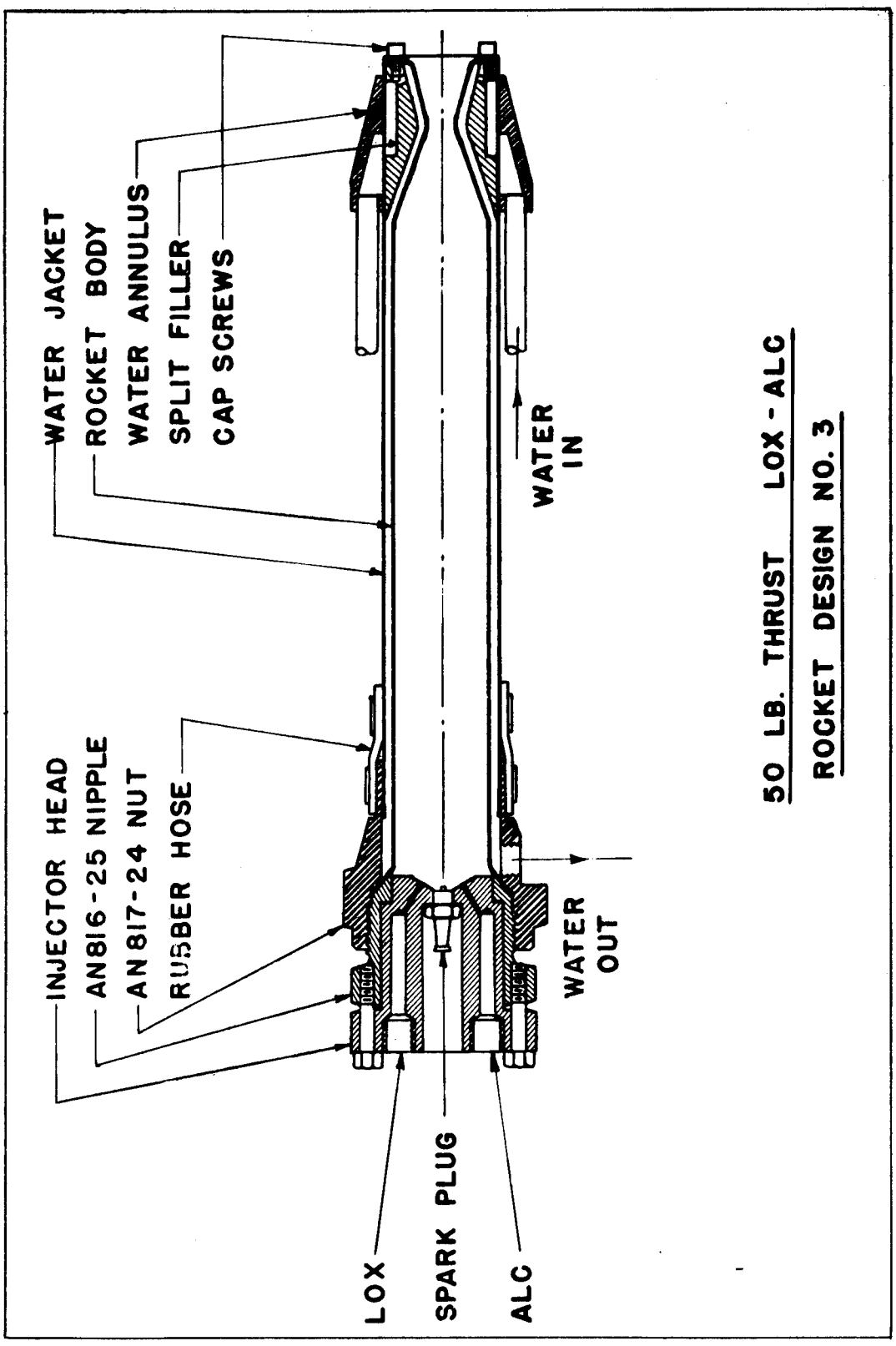
WATER JACKET
ROCKET BODY
WATER ANNULUS
SPLIT FILLER
CAP SCREWS
WATER IN
INJECTOR HEAD
AN816-25 NIPPLE
AN817-24 NUT
RUBBER HOSE
WATER OUT
LOX
SPARK PLUG
ALC
50 LB. THRUST LOX-ALC
ROCKET DESIGN NO. 3

Fig. 4.

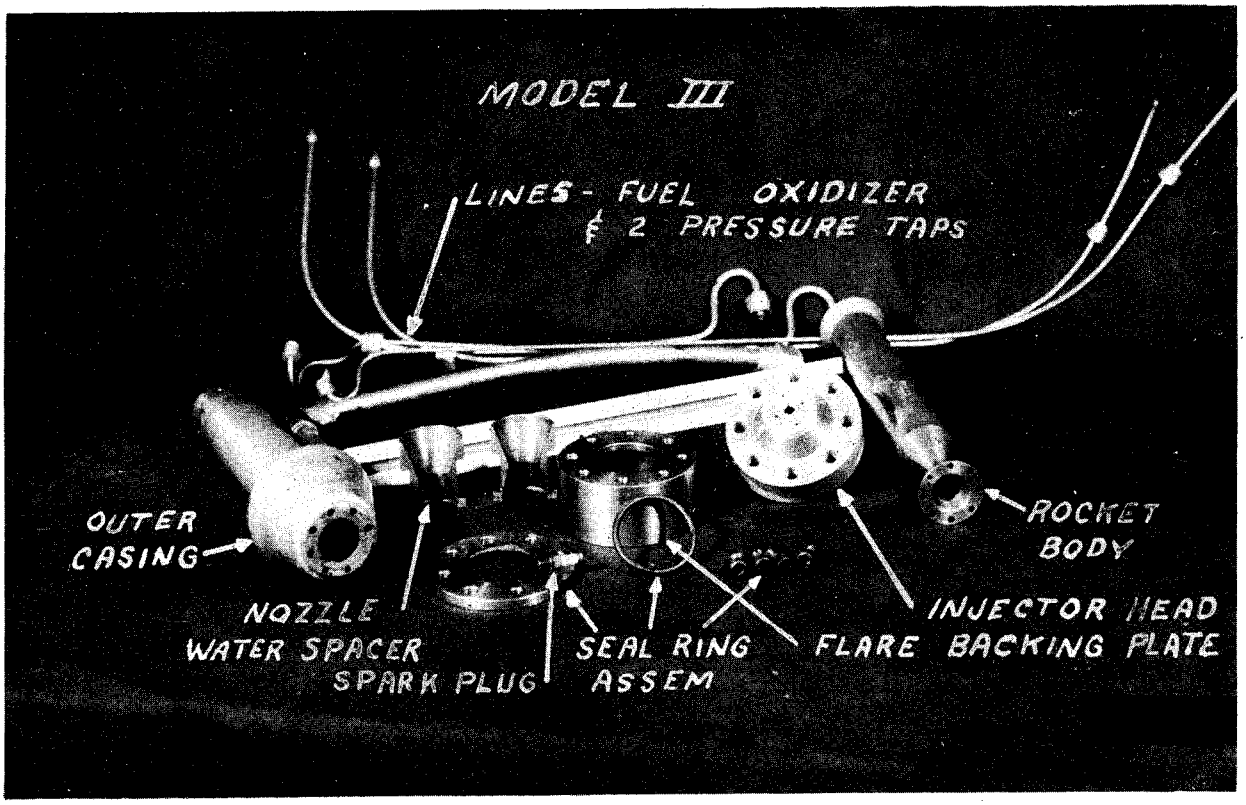


Fig. 5. Breakdown of rocket motor components.

The rocket performance appears to be satisfactory for the work in connection with ram rockets. Specific impulse as a function of mixture ratio is shown in Fig. 6 for two fuels as well as the theoretical values for frozen equilibrium. Figure 7 shows thrust variation with chamber pressure for a number of runs. The scatter is due to variation of mixture ratio of the motor and inaccuracy of instrumentation.

**Duct Development.** The previously described rocket motor is mounted on a thrust stand as shown in Figure 3. Ducts of various configurations, one of which is shown in Figure 8, are installed on a separate thrust stand which reads the net thrust (gross thrust minus internal drag). For the initial tests of the ram rocket at simulated forward velocities, it is planned to modify the existing air ejector facility to product a free jet, approximately 6 inches in diameter. Results of the air ejector studies indicate Mach numbers up to about 0.6 can be produced. A smaller rocket motor than that used in the static work would be necessary in such a test configuration.

A series of 30 static ram rocket runs have been made to date, using rockets of two different propellant combinations at different mixture ratios. Data taken in a typical ram

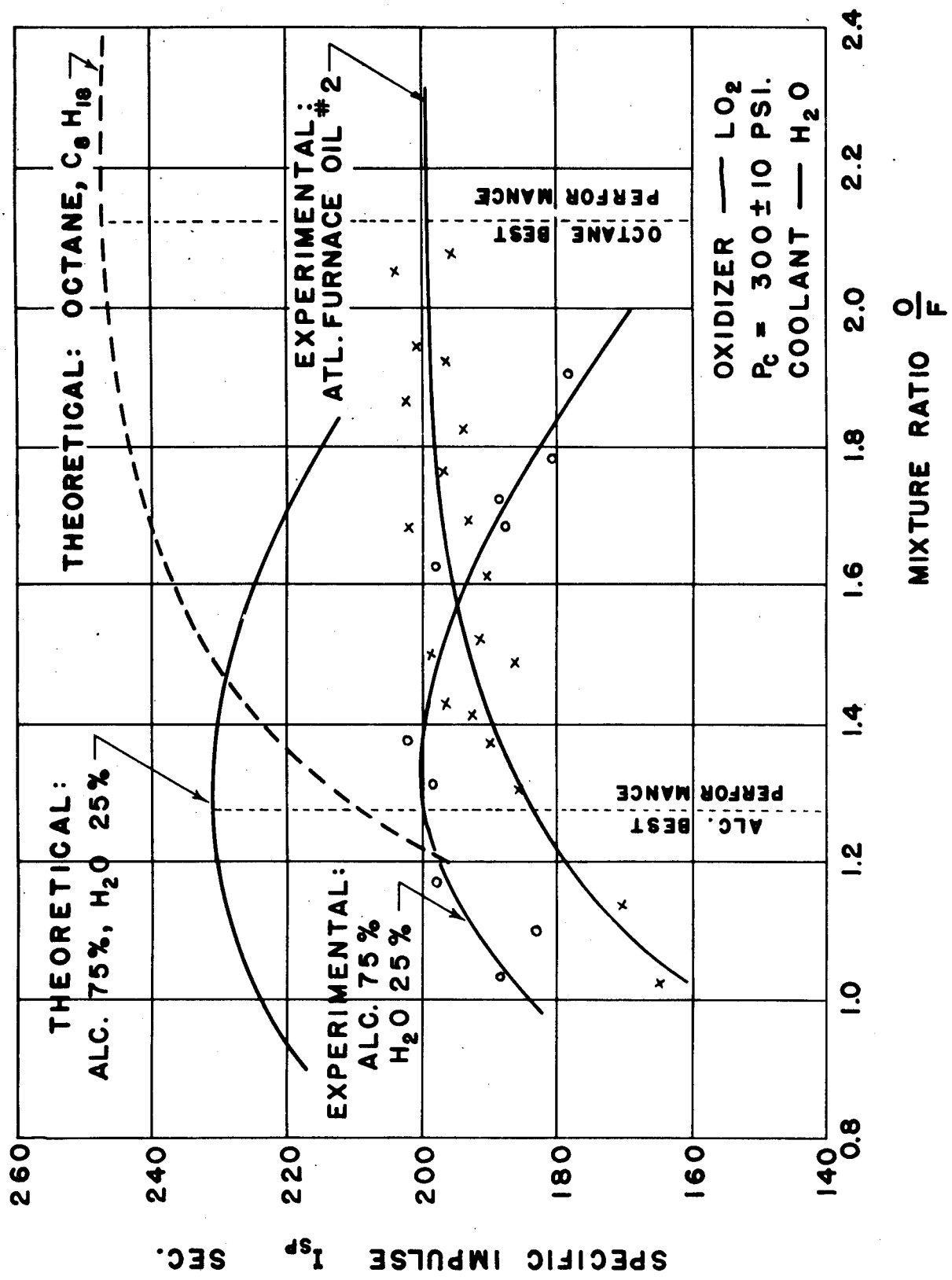
THEORETICAL: OCTANE, $C_8H_{18}$
EXPERIMENTAL: ATL. FURNACE OIL #2
OCTANE BEST PERFORMANCE
OXIDIZER — $LO_2$
$P_c$ = 300 ± 10 PSI.
COOLANT — $H_2O$
THEORETICAL: ALC. 75%, $H_2O$ 25%
EXPERIMENTAL: ALC. 75% $H_2O$ 25%
ALC. BEST PERFORMANCE
SPECIFIC IMPULSE $I_{sp}$ SEC.
MIXTURE RATIO $\frac{O}{F}$
260
240
220
200
180
160
140
0.8
1.0
1.2
1.4
1.6
1.8
2.0
2.2
2.4

Fig. 6

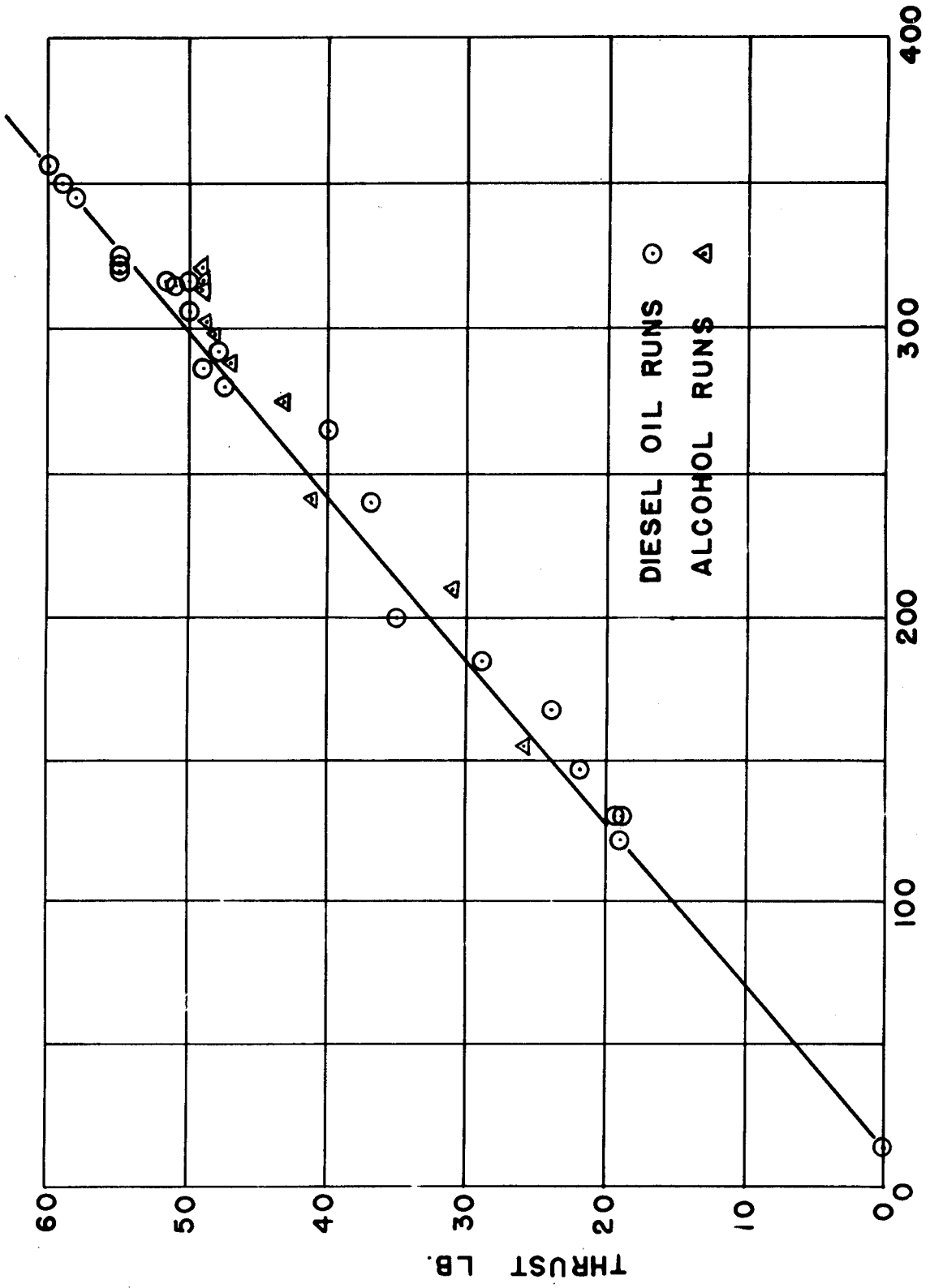
DIESEL OIL RUNS ⊙
ALCOHOL RUNS △
THRUST LB.
0
10
20
30
40
50
60
100
200
300
400
$P_c$ PSIA

Fig. 7.

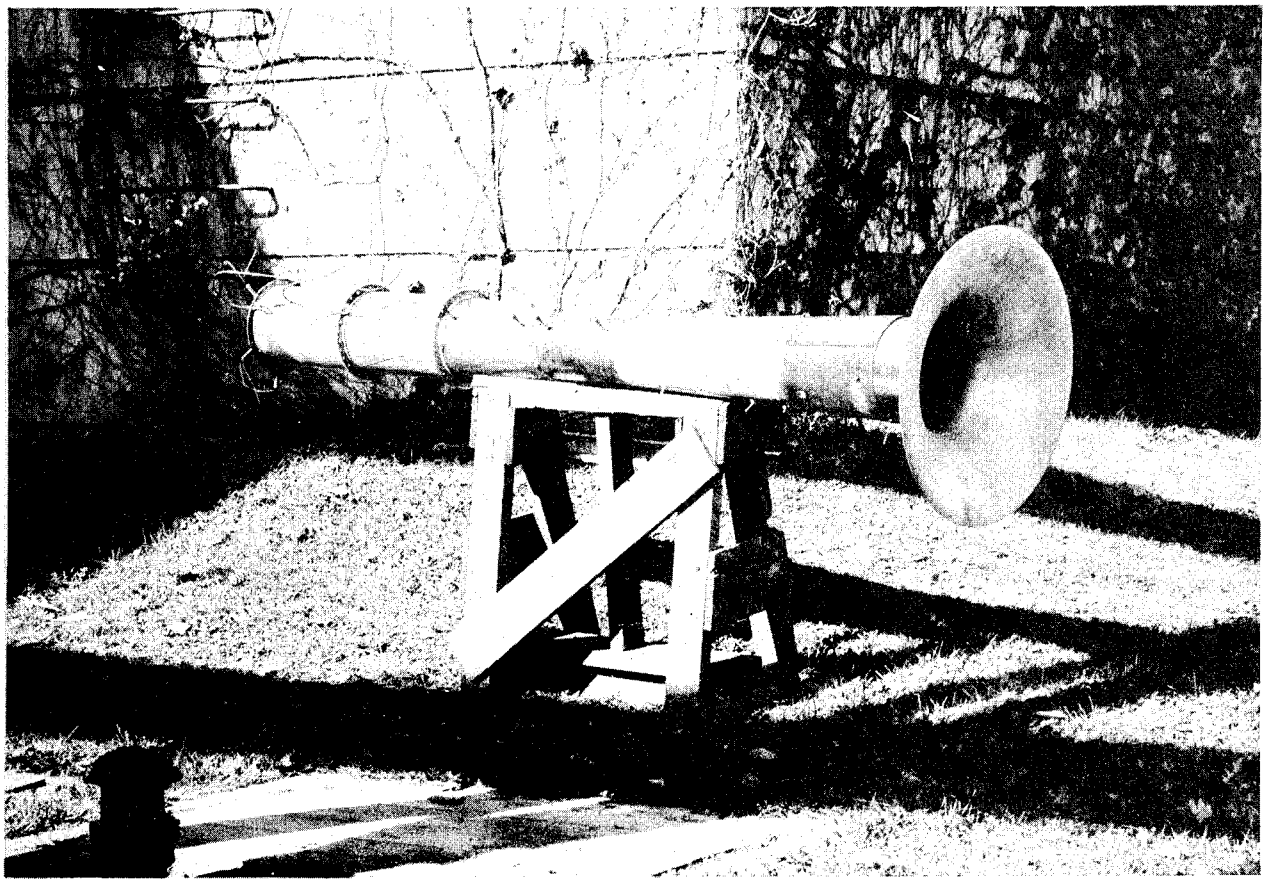

Fig. 8. Typical duct used in connection with fifty-pound rocket motor.

rocket run are as follows: thrust on rocket (Manometer and Recorder); chamber pressure (gauge and recorder); oxidizer flow to rocket; fuel flow to rocket; thrust on duct; air flow induced into duct; total head traverse at end of duct; thermocouple traverse at end of duct; static pressure distribution along duct (12 stations); and exhaust analysis at end of duct.

The first tests were made using a stainless steel duct six inches in diameter and nine feet long to determine whether the duct, thermocouples, and total head tubes would operate satisfactorily and to obtain rough estimates of the magnitude of the quantities to be measured. The next tests were conducted with the system modified by the addition of an inlet cone and an outlet diffuser similar to those used with good results in the cold jet case. (These gave 70 per cent augmentation in the cold case.) The purpose of these tests was to get a direct comparison with the cold jet results and to establish the validity of the simple constant area ejector theory modified by a heat addition parameter. As would be expected, the gross performance data as well as the static pressure distribution were markedly affected as a result of the large thermal and chemical energy made available by the rocket.

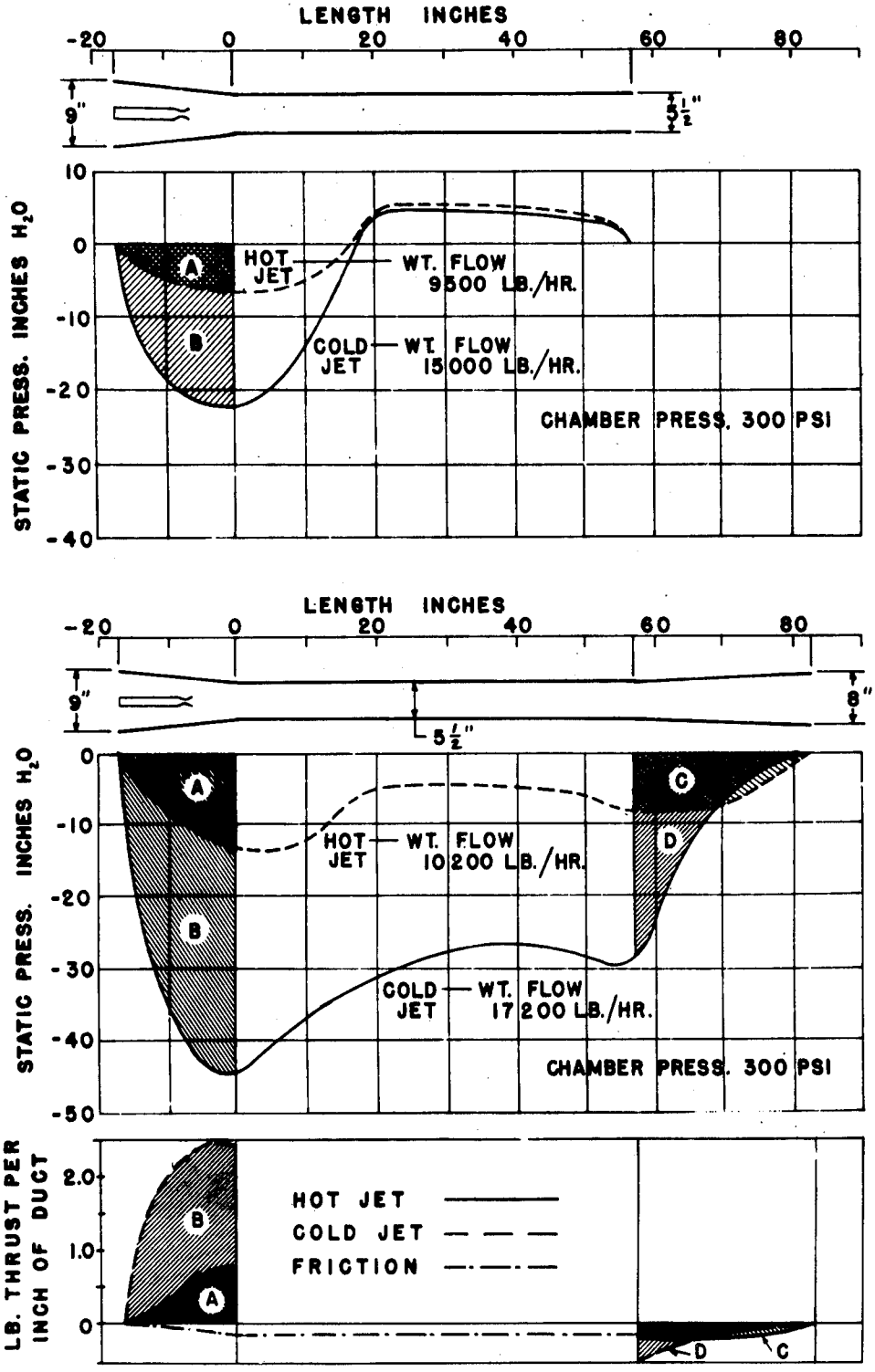


Fig. 9. Static pressure and thrust distribution: air ejector *vs* rocket ejector.

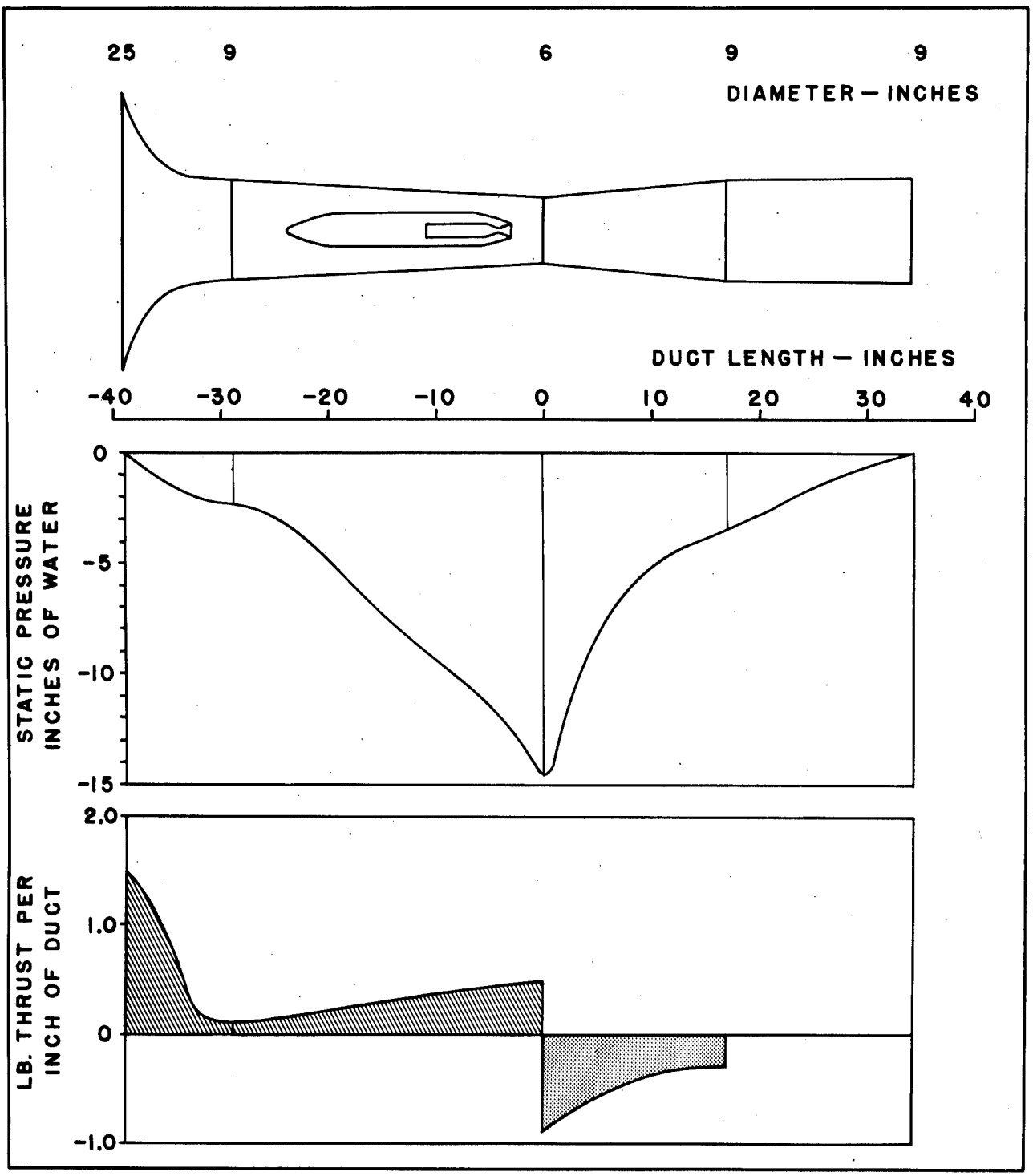
25
9
6
9
9
DIAMETER — INCHES
DUCT LENGTH — INCHES
-40
-30
-20
-10
0
10
20
30
40
STATIC PRESSURE
INCHES OF WATER
0
-5
-10
-15
LB. THRUST PER
INCH OF DUCT
2.0
1.0
0
-1.0

Fig. 10.

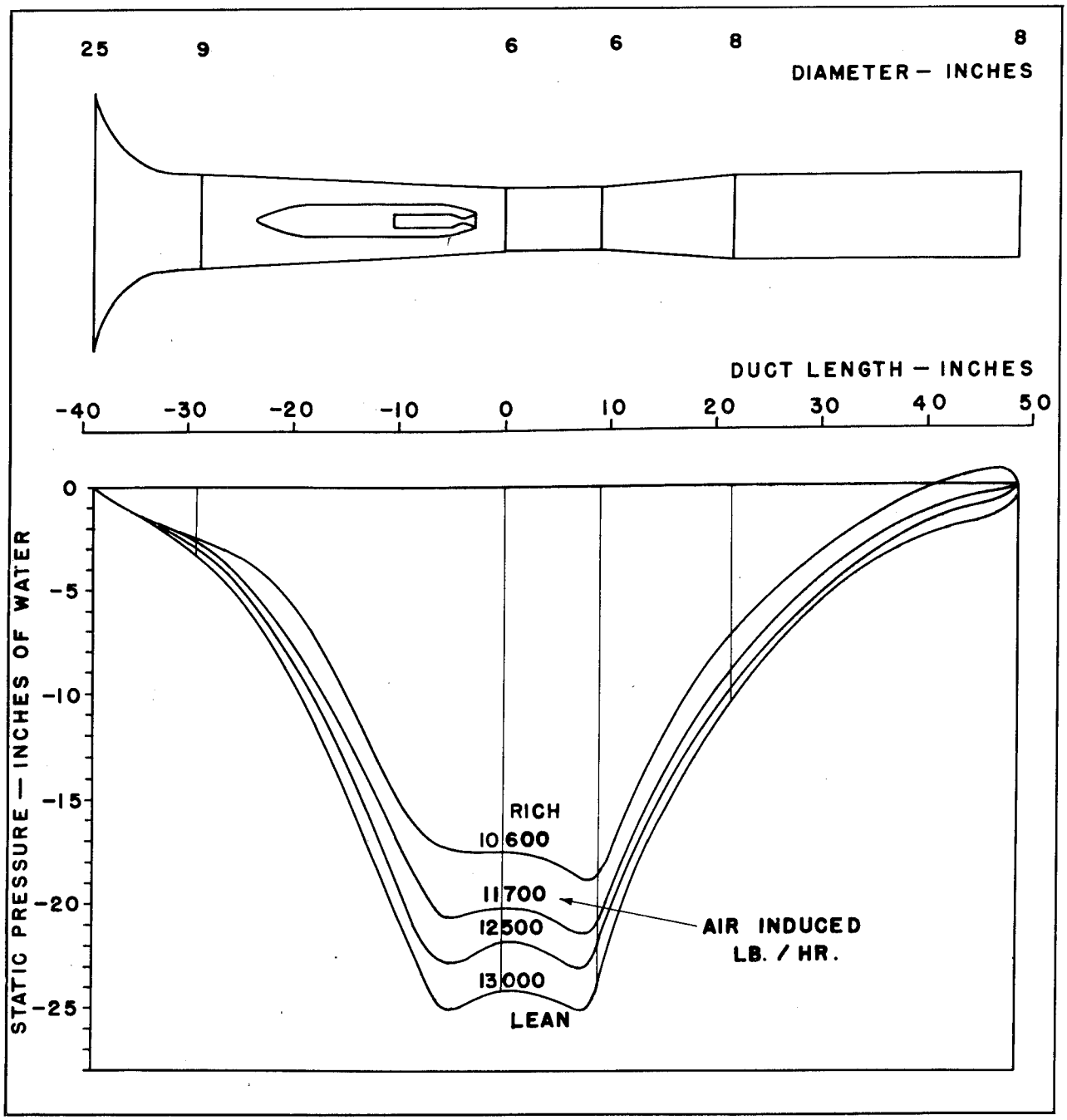
25
9
6
6
8
8
DIAMETER – INCHES
DUCT LENGTH – INCHES
-40
-30
-20
-10
0
10
20
30
40
50
0
-5
-10
-15
-20
-25
STATIC PRESSURE – INCHES OF WATER
RICH
10 600
11 700
12 500
13 000
LEAN
AIR INDUCED
LB. / HR.

Fig. 11.

To investigate the effects of the ratio of primary jet area to duct area in this case, a series of tests was made with a smaller rocket with resultant higher ratios of induced air to primary jet mass flow. Figure 9 shows a comparison of the hot and cold jet cases for similar ducts, both with and without exit diffusers. In both hot and cold cases, the net thrust is, of course, the integral of the pressure over the non-constant area sections minus the friction forces. As would be expected, the pressure distribution curves in Figure 9 indicate very little thrust augmentation in the case of a constant area mixing section with large heat addition. The mass of air induced decreases rapidly with heat addition in the constant area duct. The cold jet ejector tests exhibit thrust augmentations of the order of 40-70 per cent in the cases plotted (Area B - area D - friction).

Succeeding tests were made using a duct configuration with a diverging section downstream of the rocket as shown in Figure 10 with a resultant increase in the mass of air induced and in thrust augmentation. Tests were conducted over a range of rocket propellant mixture ratios with the results illustrated in Figures 10 and 11.

To study static performance of the ram rocket, further tests are contemplated with more rapidly diverging sections downstream of the rocket. It is intended to explore the effect of key variables such as the optimum configuration of the inlet cone and exit diffuser, duct length, rocket location, etc. The extent of the validity of the conventional one-dimensional treatments is also being investigated.

## *E. INVESTIGATION OF A VALVELESS INTERMITTENT RAMJET ENGINE. (Pr-Ph.4)*

*Submitted by: A. Kahane, Princeton University*

An experimental and theoretical program was initiated in March 1948, to determine the possibilities of an intermittent ramjet engine. Exploratory combustion experiments carried out in a 4-inch square tube in a 0.5 Mach number 4-inch diameter jet, indicated that a combustion pressure rise of one atmosphere was obtainable with gasoline-air mixtures. (See Project Squid, Annual Report, January 1949, for test setup details.) Theoretical calculations indicated that with a combustion pressure rise of this order of magnitude, the ideal specific impulse of the intermittent ram jet is superior to the steady ramjet, especially at flight Mach numbers less than 2.

The experimental objectives of the annual period reported herein have been to obtain smooth and repeatable intermittent combustion and to determine the optimum configuration and

thrust and fuel consumption characteristics of a subsonic engine. Theoretical studies of the gas dynamic cycle of a subsonic engine, of the gas dynamics of the combustion process, and of the spillage phenomena encountered at the inlet have been made. ( See Page 24 for theoretical analyses.)

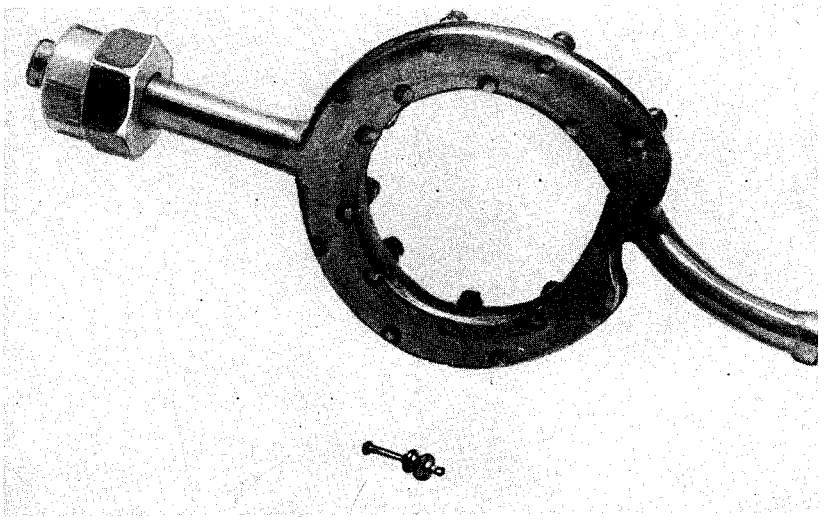

Fig. 12. Injection Nozzle 4. Individual valve with spring in in foreground.

**Nozzle Development.** In order to attain the objective of smooth and repeatable intermittent combustion, a satisfactory fuel injection nozzle had to be developed. Nozzle 3 (described in Project Squid Annual Report, January 1948) proved unsatisfactory because complete cutoff of the injection was not obtained due to the distance between the fuel flow valve and the nozzle orifices. Considerable dripping of the fuel occurred between injections. Nozzle 4 (see Figure 12) was then built in an attempt to eliminate this dripping. This nozzle utilized the same diesel type fuel flow valves (mounted on the wall of the tube) as nozzle 3, but each of the 16 orifices (8 connected to each side of the two-cylinder fuel pump) was fitted with an externally-seated spring-loaded fuel flow valve. Dripping was not eliminated, however, probably because oscillations took place between the main fuel flow valve and the orifice valves. In addition, severe difficulties were encountered with the fuel flow valves used with both nozzle 3 and nozzle 4. This valve would tend to score during operation, altering the injection pattern and duration, apparently since operating frequencies were much higher than encountered in ordinary diesel use. Nozzle 5 (see Figure 13) was designed and built by the Fiedler-Sellers Corporation. This nozzle has 16 individual spring-loaded valves, 8 connected to each side of the two-cylinder pump. These valves have been designed to eliminate the necessity of using an auxilliary fuel flow valve. The individual valve construction is schematically indicated in Figure 14. Both the conical end of the valve stem and the valve stem are lap fitted into the valve seat and body respectively, so that no leakage occurs when the valve is in the closed position. Opening of the valve occurs when fuel under high pressure enters the valve cylinder and exerts a pressure on the valve face. The valve is closed by the action of a cantilever leaf spring which rests on the rear of the valve stem. An insert is located

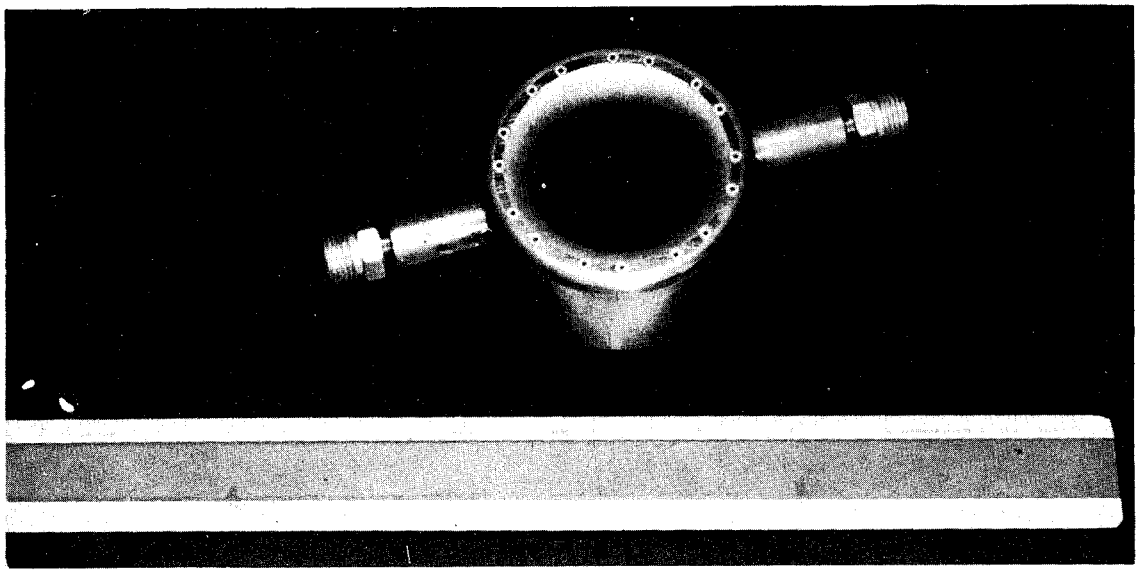

Fig. 13 (a). Injection side of nozzle 5.

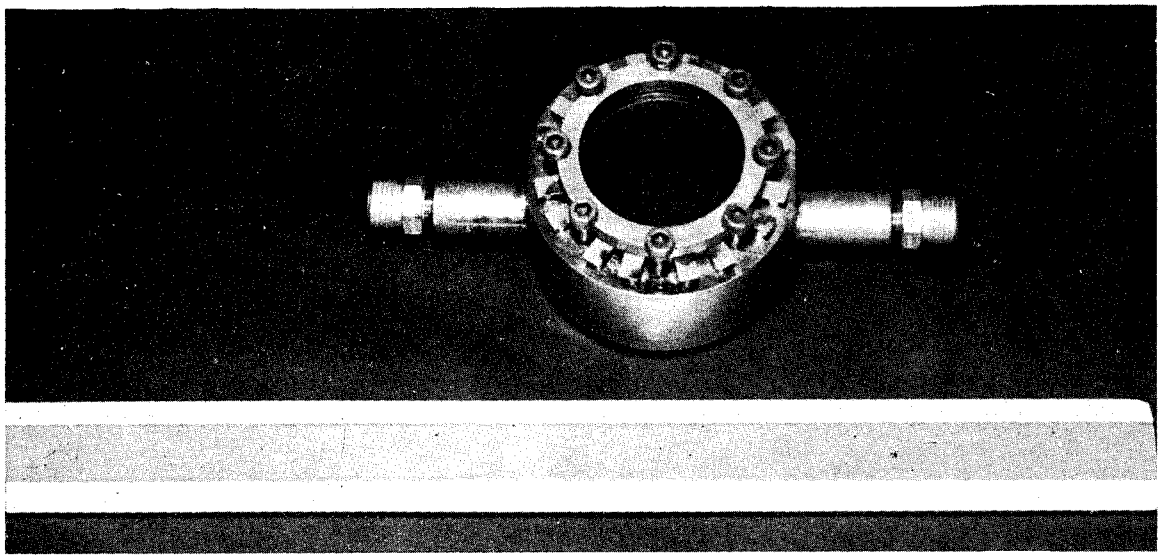

Fig. 13 (b). Spring side of nozzle 5.

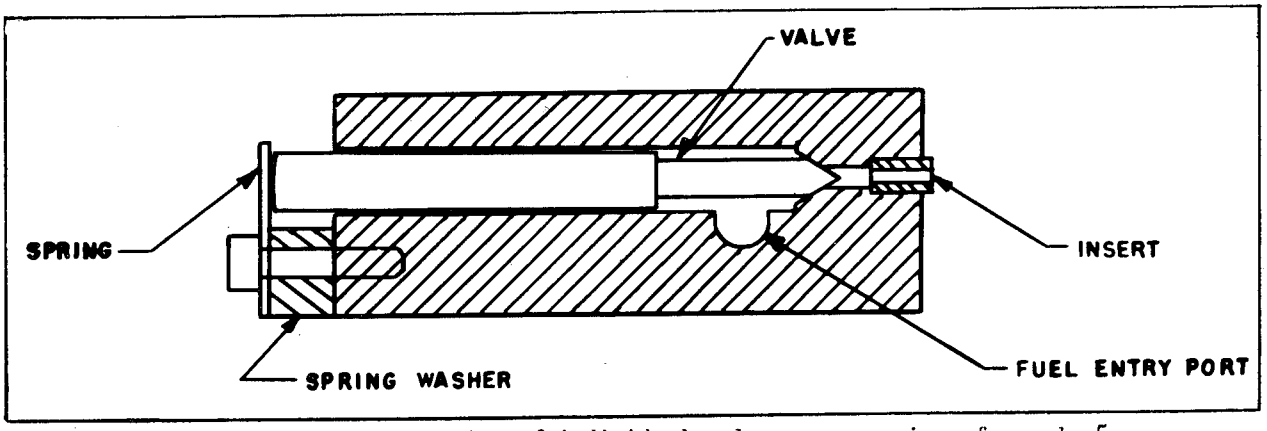


**Fig. 14.** Schematic drawing of individual valve construction of nozzle 5.

at the spray orifice. The inserts are removable, and variation of the orifice length-diameter ratio (the spray shape is dependent on this ratio) and spray direction can easily be accomplished. This valve is set for an injection pressure of 1800 psi. This can be varied, however, by changing the initial spring tension by altering the thickness of the spring washer. The injection duration of nozzle 5 is about 15 degrees of crank angle. Difficulties with spring breakage were encountered in initial tests of this nozzle. Re-design of the spring after some experimentation seems to have remedied this. Since the nozzle with redesigned spring was delivered only a month prior to this writing, no conclusive remarks as to its adequacy can be made. Its operation in preliminary tests, however, has been satisfactory.

**Combustion Pressure Rise.** Although repeatable measurements of peak pressure rise during intermittent combustion could not be made because of the defects of nozzles 3 and 4, some trends were observed. The most significant was the trend of variation of peak pressure rise with blower jet speed, which is shown in Figure 15. These tests indicated a marked increase of pressure rise with jet speed. The explanation for this relationship appears to be that higher flame velocities occur at higher jet speeds because of the greater turbulent fluctuation velocities existing. It is well known that the turbulent fluctuation velocities due to pipe flow and flow past a grid (in this case past the nozzle) vary directly with flow velocity. Experimental and theoretical studies of the influence of turbulence on flame velocity[5,6] indicate a direct variation of flame velocity with turbulence fluctuation velocity. The gas dynamic theory of the combustion process (See Project Squid, Annual Report, January 1949) shows, furthermore, that for a given fuel-air ratio, the pressure rise increases with

[5] G. Damkohler, *The Effect of Turbulence on the Flame Velocity in Gas Mixtures,* National Advisory Committee for Aeronautics T.M. No. 1112, April 1947.

[6] K.I. Shelkin, *On Combustion in a Turbulent Flow,* National Advisory Committee for Aeronautics T.M. 1110, February 1947.

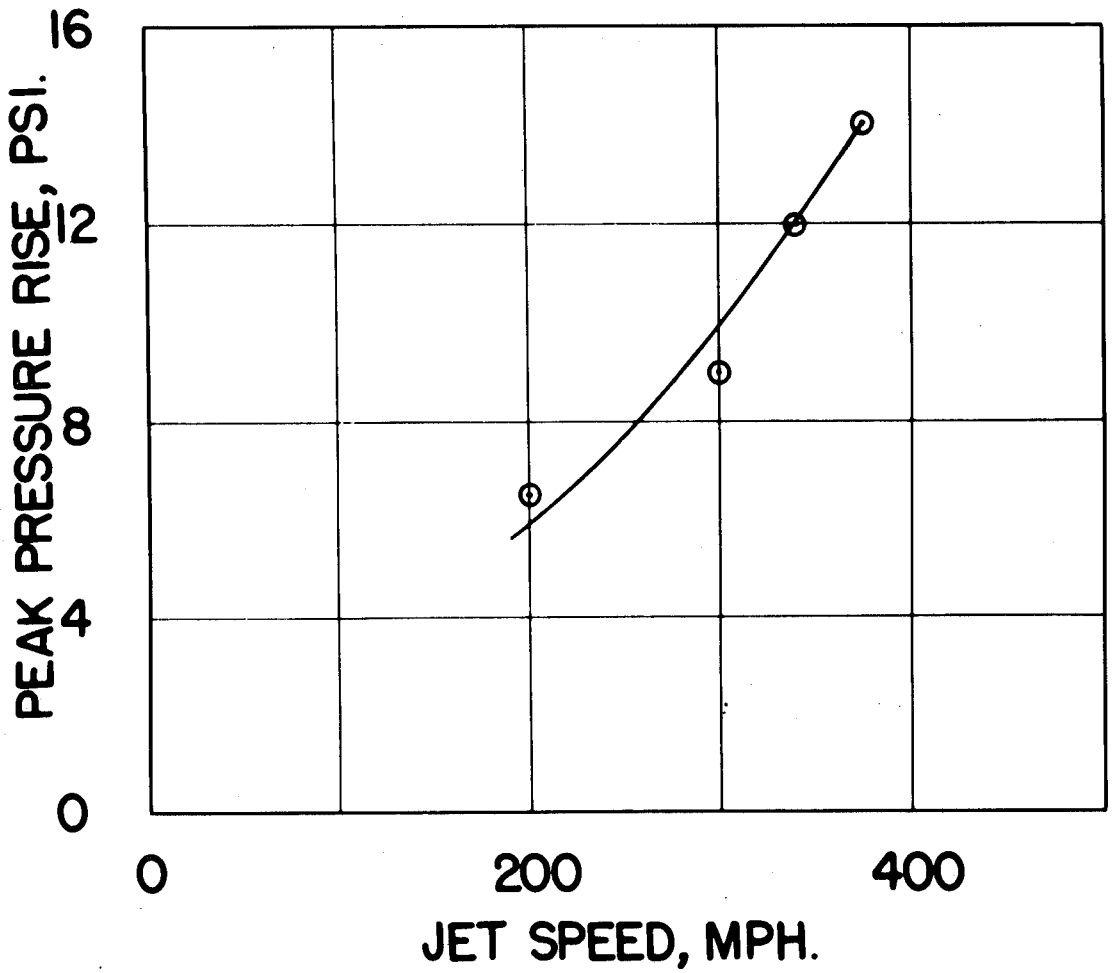


Fig. 15. Variation of peak pressure rise during intermittent combustion with blower jet speed, injection frequency 25 cycles per second.

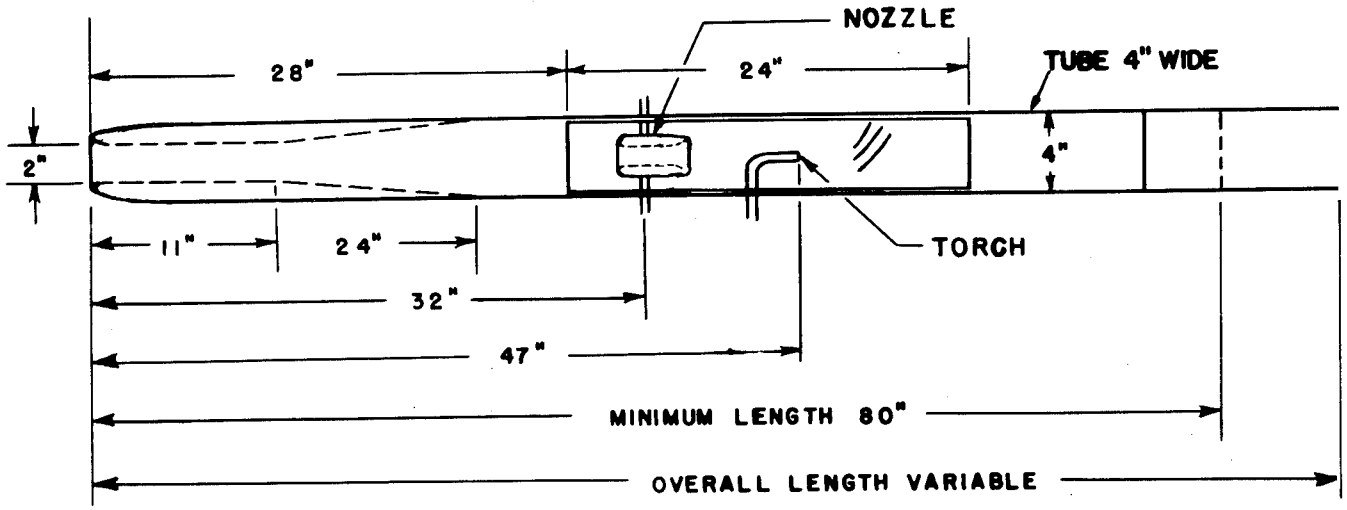


Fig. 16. Initial subsonic engine configuration tested. Overall length 140 inches.

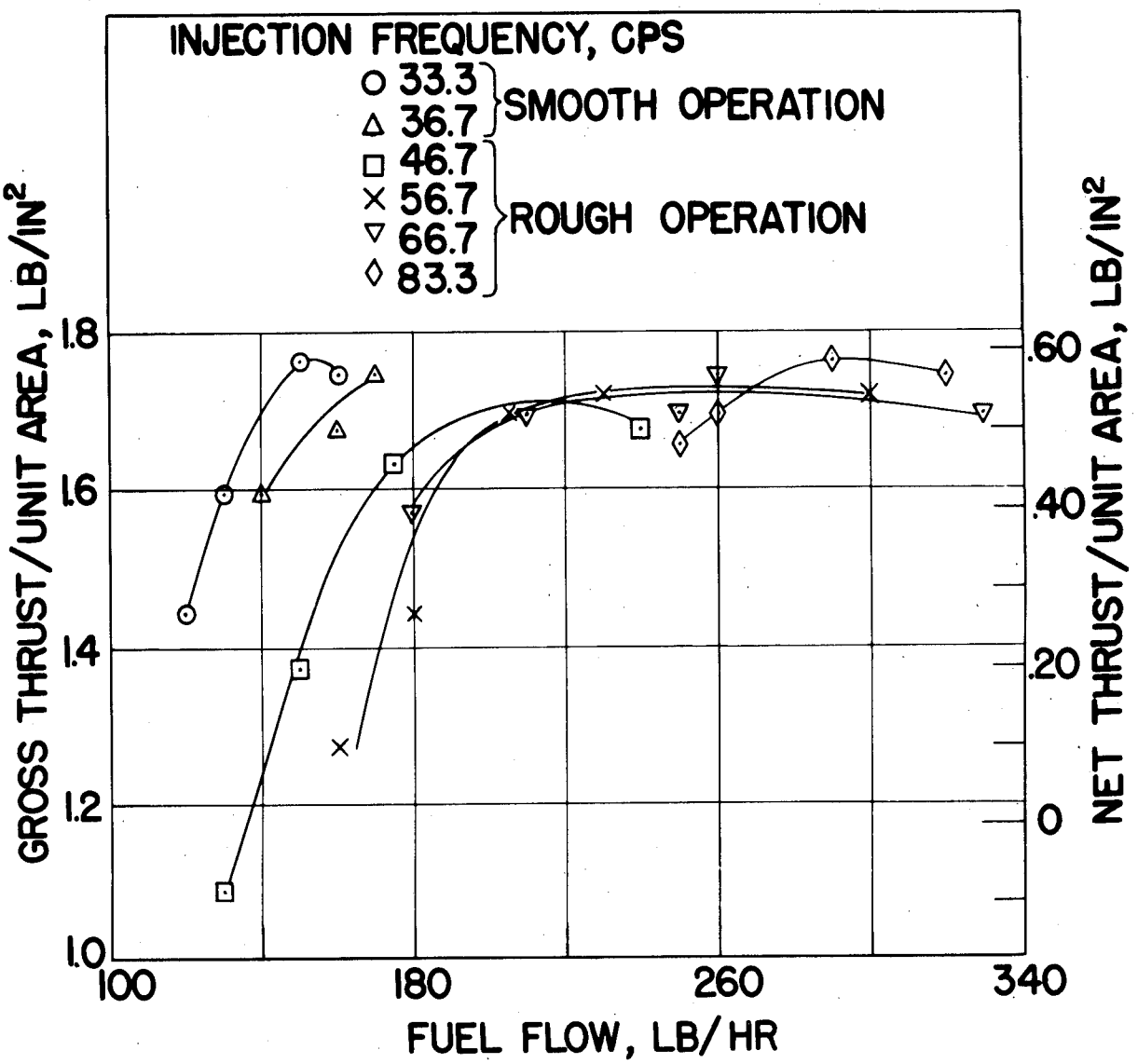


Fig. 17. Variation of gross and net thrust per unit combustion chamber area with fuel flow and injection frequency at 0.5 Mach number.

increasing flame velocity. Plans include construction of the simple hot wire anemometer, described by Kovasznay,[7] to be used for measurement of the turbulence intensity and scale in the combustion chamber. High speed motion picture studies of the flame motion are also contemplated.

[7] L.S.G. Kovasznay, *Simple Hot Wire Anemometer*, Aero.-J.H.U., C.M.-573, September 20, 1949.

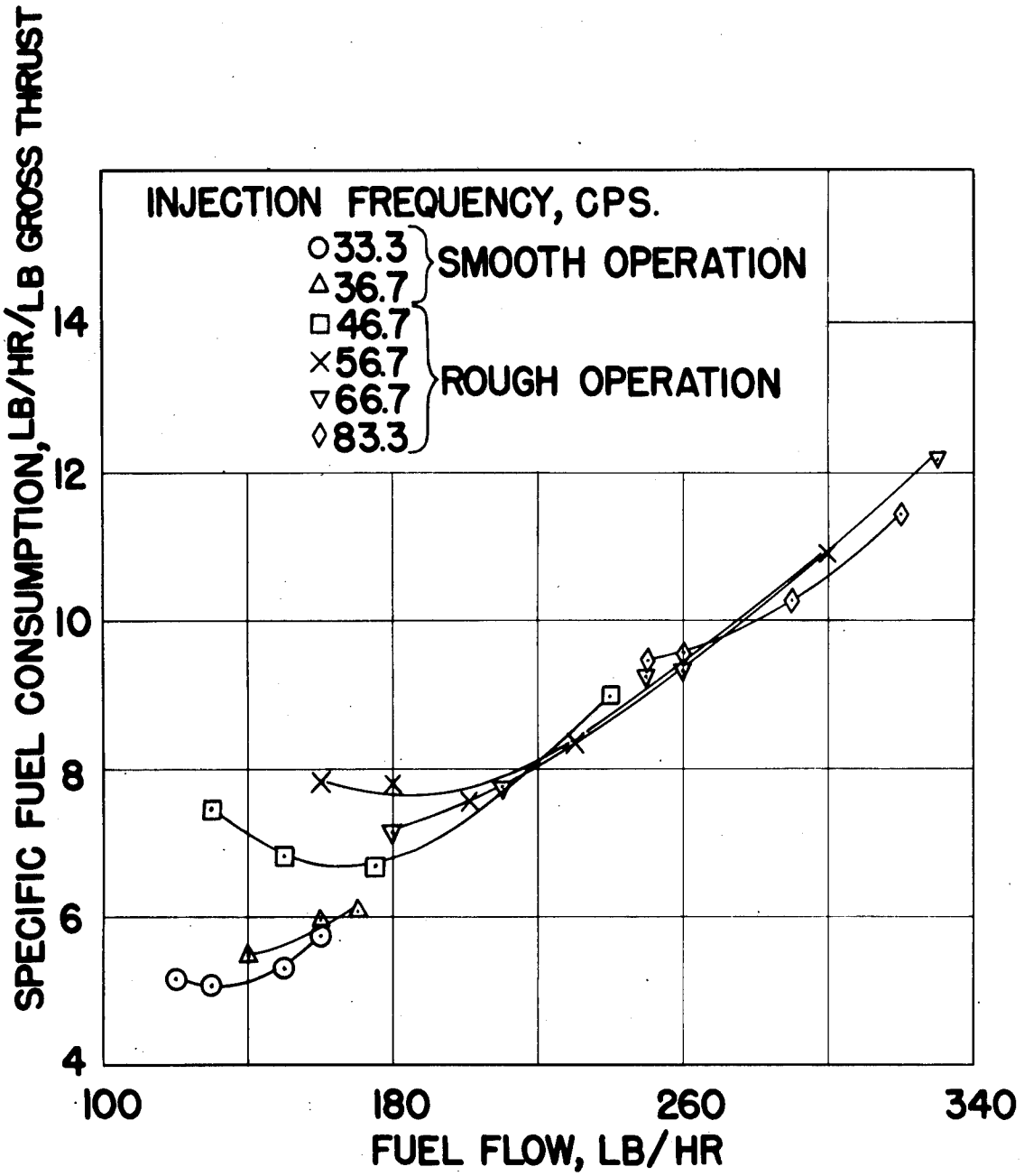


Fig. 18. Variation of specific fuel consumption with fuel flow and injection frequency at 0.5 Mach number.

Tests of a Preliminary Subsonic Engine Configuration. The obtaining of a pressure rise of one atmosphere during intermittent combustion in a flowing gas indicated that the intermittent ramjet engine was feasible from a combustion point of view. Efforts were then directed towards the determination of an optimum subsonic configuration (at least for 0.5 Mach

number due to limited air capacity) and the determination of the specific thrust and fuel consumption characteristics of this engine. These tests have been delayed because of the time-consuming nozzle development. A preliminary test, however, at 0.5 Mach number in the 4-inch diameter air jet with injection nozzle 5 (spray in upstream direction) is reported. The engine configuration tested is shown in Figure 16, page 21, The overall length was 140 inches. A subsonic diffuser is utilized, and the tail pipe was of constant area equal to combustion chamber area. Values of gross thrust and net thrust per unit combustion chamber area are plotted against fuel flow in Figure 17 for several values of injection frequency. Specific fuel consumption based on gross thrust is shown in Figure 18. (Net thrust is defined as thrust measured by balance. Gross thrust is net thrust plus cold drag.) Smooth operation was attained only at the two lowest injection frequencies of 33.3 and 36.7 cycles per second. The rough operation at the higher frequencies apparently resulted from the improper ratio of tail pipe length to overall engine length. This ratio would be expected to be most critical for high frequency operation. Figure 17 shows that peak thrust was about the same for all test injection frequencies. Minimum specific fuel consumption of 5.1 lb/hr/lb gross thrust, was obtained at the lowest frequency of 33.3 cps.

Plans include tests with various engine configurations (tail pipe lengths, inlet diffusers, tail pipe shape) with the objective of obtaining smooth operation at high injection frequencies and improved performance.

Ideal Specific Impulse. The ideal specific impulse (assuming no losses, constant ratio of specific heats $\gamma=1.4$, and neglecting dissociation) of the intermittent ramjet engine has been calculated using the *universal thrust equation* of Zwicky.[8] Since this equation has been derived for steady flow engines, its application to an unsteady engine cannot be considered absolutely correct. However, it is believed that the calculations afford some indication of the comparison of the impulse of the ideal intermittent and steady ramjets. The results which are shown in Figures 19a and 19b indicate larger ideal specific impulse for the intermittent ramjet engine, especially at Mach numbers less than 2. (The steady ramjet is represented by $P_{c/P_b} = 1$; the intermittent processes correspond to $P_{c/P_b} > 1$)

The minimum specific fuel consumption obtained in tests of the initial subsonic configuration of the intermittent ramjet was 5.1 lb/hr/lb. (See preceding section.) This corresponds to a value of specific impulse of 706 sec. Placing this value on Figure 19 indicates that

[8]F. Zwicky, *Morphology of Aerial Propulsion,* Helvetica Physica Acta, Volume XXI, 1948.

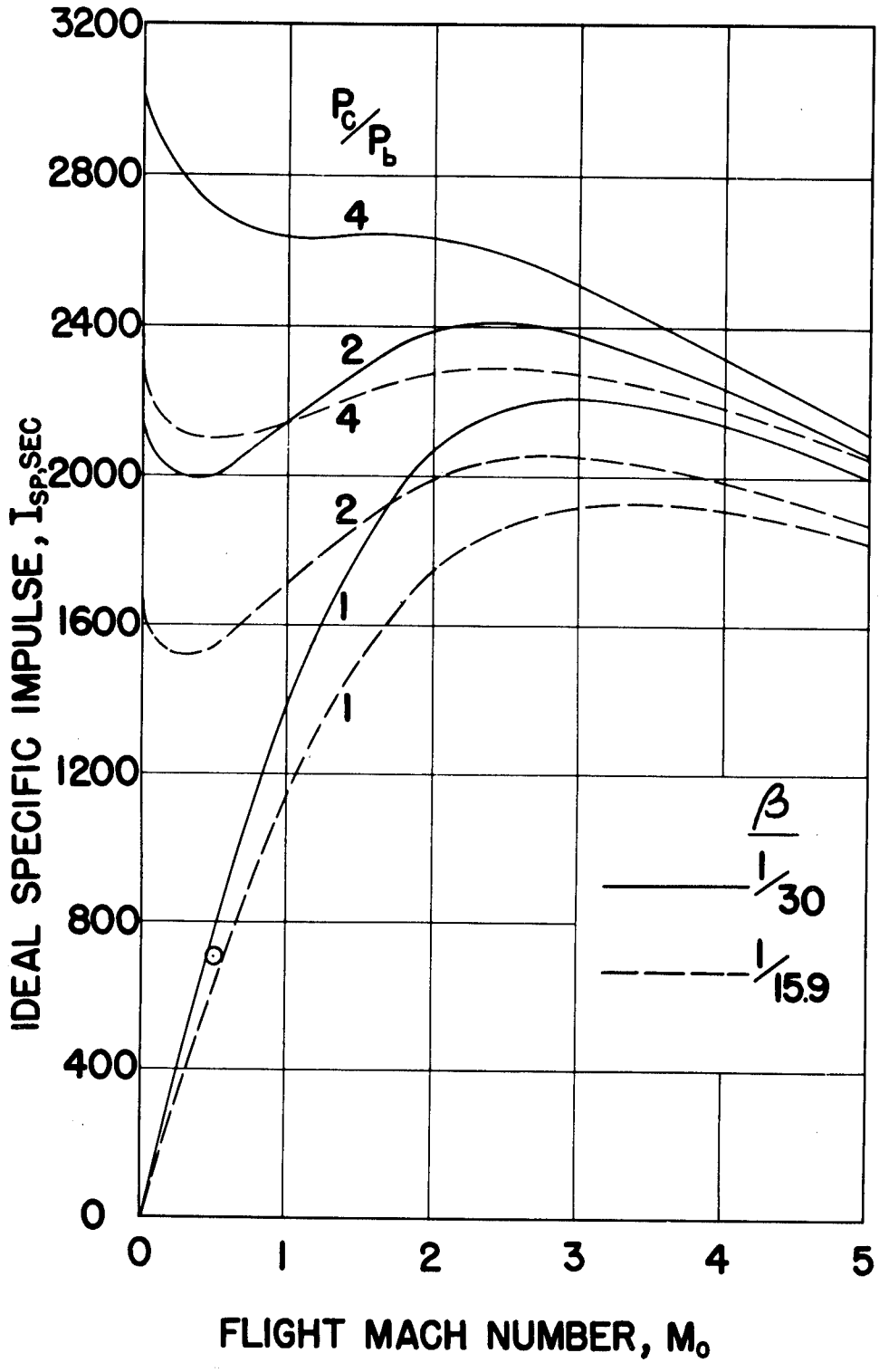


**Fig. 19a.** Variation of ideal specific impulse with flight Mach number at sea level. $P_c/P_b$, combustion pressure ratio; $\beta = \frac{W_f}{W_f + W_a}$, fuel parameter; $W_a$, weight flow of air; $W_f$, weight flow of fuel; $P_b$, pressure before combustion (ram pressure); $P_c$, pressure after combustion.

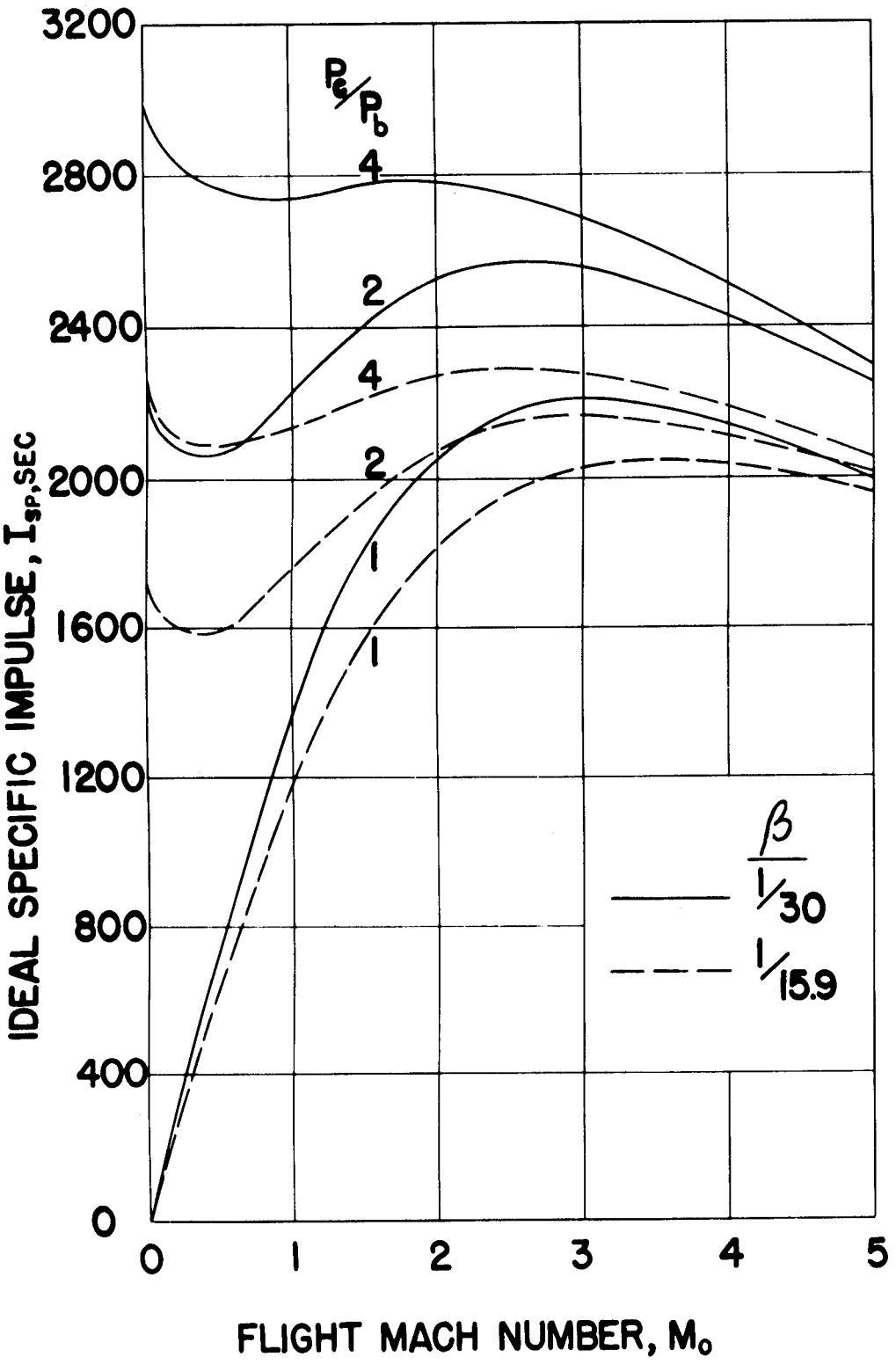


Fig. 19b. Variation of ideal specific impulse with flight Mach number at 40,000 ft. altitude. $P_{c/P_b}$, combustion pressure ratio; $\beta = \frac{W_f}{W_f + W_a}$, fuel parameter; $W_a$, weight flow of air; $W_f$, weight flow of fuel;

this experimental value corresponds closely to *ideal* steady ramjet specific impulse at M=0.5. This comparison may be regarded as experimental justification of the theoretical relative superiority of the intermittent process, despite the crudeness of this theoretical approach.

**Gas Dynamics of Combustion Process and Wave Processes in Engines.** The theory of the gas dynamics of the combustion process reported in the Project Squid, Annual Report, January 1949, was extended to include effects of variable specific heats and mol number. The general theory with applications to flame propagation in open and closed flame tubes as well as intermittent combustion in a flowing gas, will be issued shortly in report form.

A characteristic calculation of the wave processes in a subsonic engine with a diffuser inlet has been carried out for flight Mach number of 0.4. The inlet spillage phenomena has been examined (See Project Squid, Quarterly Report, July 1949.) and a formula derived for maximum pressure rise of the shock wave striking the inlet, for which no spillage results. The characteristic engine calculation and the spillage phenomena are discussed in detail in a report now being completed.

Plans include carrying out a characteristic calculation of a subsonic configuration at 0.8 flight Mach number and investigating methods of making more exact performance calculations.

## *F. INVESTIGATION OF VALVELESS PULSEJETS. (CAL-1R7).*

*Submitted by: J.V. Foa and G. Rudinger, Cornell Aeronautical Laboratory.*

The elimination of the valves of a pulsejet should lead to an engine of greatly improved reliability and increased useful life. Experiments with small scale models have been continued. These models consist of ducts similar to those of conventional pulsejets but their front ends are closed. In this manner, the pressure waves arriving at the front end just before combustion are not required to close any valve and therefore retain more of their strength upon reflection. The pulsations set up by the first explosion are found to be maintained under suitable conditions of (continuous) air and fuel injection.

The optimum shape of the duct is not necessarily the same as that for a conventional pulsejet and it was found during the experimental work that minor modifications could influence the performance considerably. Performance was also affected to a considerable extent by the type of fuel injection and the fuel used. It appeared that for any type of fuel injection system used, a different optimum shape of the duct would be required. Fuels used were

methane, propane and gasoline. The fuel was injected either directly into the combustion chamber at one or more points or premixed with the air supply. In all experiments, mean fuel flow was measured by a commercial rotameter and mean thrust was determined either on a small dynamometer thrust stand or by means of a thrust plate. From these measurements the specific impulse could also be determined. A report on a series of such measurements was issued.[9] These experiments have been continued. One of the latest models (Model 20) had a combustion chamber that was 3 inches in diameter and 6 inches long; the corresponding dimensions for the tailpipe were 2.5 inches and 16 in. - 20 in. (adjustable), respectively; these two parts were joined by a conical section of 3.5 inches length; the tailpipe exit was slightly flared. Fuel was injected separately from the air at three points of the combustion chamber. The thrust obtained with this model, corrected for the thrust produced by the air flow alone without combustion, was, under optimum conditions, about 11 pounds (1.5 pounds per square inch combustion chamber area) at a specific impulse of about 2500 seconds. The fuel used was propane.

A small series of experiments was also carried out with a model consisting of a straight telescopic tube of 3-inches diameter and having a slightly flared exit (Model 21). The air supply and fuel injection system were the same as for Model 20. At a total length of the tube of 27 inches the thrust produced was 13.2 pounds (about 1.9 pounds per square inch) but the specific impulse was only 1850 seconds.

It is planned to test valveless pulsejet models in a fast airstream to measure their performance with ram air under various flying conditions. In this connection, proper design of the inlet configuration will be of importance. Some thought was given to designs which would utilize the experimentally observed tendency of flows to follow a convex curvature of a wall on one side without any constraining wall on the other (Coanda effect). If such a scheme were successful, inflow into the combustion chamber of the pulsejet could take place through a practically open inlet tube while the reverse flow could be deflected by the Coanda effect and exhausted downstream.

A preliminary series of experiments on the Coanda effect was undertaken with a two-dimensional model. Some carbon dioxide was added to the air to visualize the flow. Figure 20 shows the strong deflection of the jet without any constraining wall. The experiments were

[9] J.G. Logan, Jr., *Valveless Pulsejet Investigations. Part I. Test of Small Scale Models,* Project Squid, Technical Memorandum CAL-27, May 1949.

carried out both with steady and with pulsating flow. The rotary interrupter valve is visible in the lower left corner of Figure 20. No difference was noted between the effect in steady and pulsating flow.

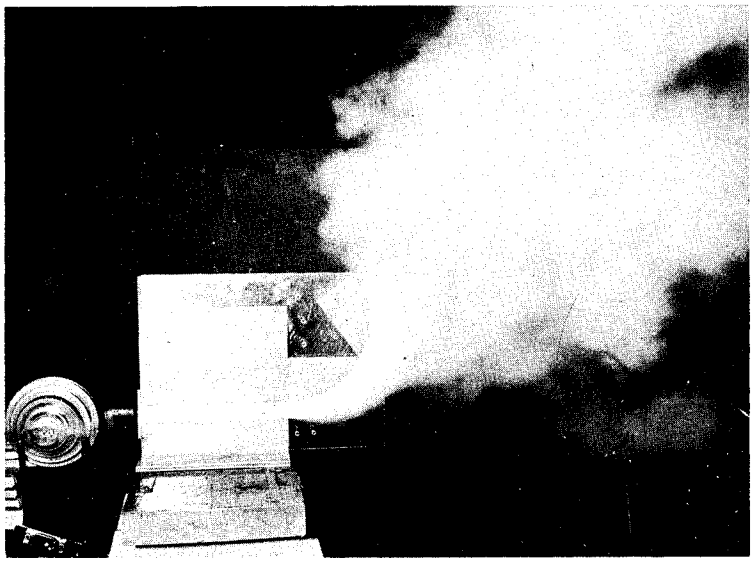

Fig. 20. Coanda effect in intermittent flow.

It appeared that the valveless pulsejet could be developed into a powerplant suitable for helicopters. Preliminary swirling arm tests were successfully carried out. In any helicopter application, it would be very important to build the propulsion unit as compactly as possible. Attempts will be made to obtain particularly short models with as little as possible increase of the maximum engine diameter by telescoping the combustion chamber and tail pipe. One model of this type, 3.5 inches diameter and 9 inches long, was built. This model resonated and produced some thrust; however, no actual measurements were taken. Further work along these lines is planned.

Both theoretical and experimental attempts were made to gain a better insight into the mechanism of valveless pulsejets. A two-dimensional model of a valveless pulsejet with Vicor glass side walls was built for observation by means of high speed motion pictures. At first, it appeared as if the rectangular cross section of this model had some effect on the combustion phenomena since it would not operate as smoothly as an ordinary cylindrical model. However, no difficulties were encountered with a similar model built entirely of steel. It was then suspected that the observed difficulties had been due to either leakage or lack of sufficient rigidity. Another more rigid model was therefore constructed. In preliminary tests, flash photographs and high speed motion pictures were taken and indicated satisfactory operation. It is planned to use this model to obtain simultaneous records of pressure variations and flow phenomena. So far, these experiments have been used mainly to determine the best locations for the fuel injector.

By means of the method of characteristics, it was possible to obtain agreement with the experimental results with regard to thrust, specific impulse and operating frequency on the

basis of reasonable assumptions concerning the initial conditions. Unfortunately, the same results could apparently be obtained by different sets of initial conditions. Therefore no definite conclusions regarding the mechanism of the engine could be drawn. Further work of this nature has been suspended until experimental or theoretical data will become available that would make this approach promising.

However, two interesting side results have been obtained during this investigation. It was noted that whenever an interface between hot and cold gases reached the open end of the tailpipe, very strong pressure waves could be produced in cases where the flow velocity was sufficiently high. If, for example, the cold gas leaves the tailpipe at a Mach number of 1.0, the pressure at the exit may be considerably higher than ambient. When the interface reaches the open end, the Mach number in the hot gas behind it drops to a value less than 1.0, an expansion wave can travel into the duct and the high pressure at the exit can no longer be maintained.

It was also found that when heat is being steadily released in a limited region of a duct, pressure oscillations may occur due to wave reflections at the interface between burning and non-burning gas. The frequency of these oscillations does not depend on the length of the duct but on that of the heating region and its location with respect to the closed end of the duct. These pressure oscillations are caused by the disturbances produced at the instant of ignition which are repeatedly reflected both at the closed end and at the interface between burning and non-burning gas. In the examples carried out, the rate of energy release was assumed to be constant and unaffected by pressure waves. In this case the oscillations rapidly died out. These oscillations may, however, be amplified by the effect of the pressure waves on the combustion process. This phenomenon may lead to some insight into the mechanism of *rough burning* in ramjets.

## G. *STUDY OF THE OPERATION OF SHROUDED PULSEJETS. (CAL-1R8).*

*Submitted by: J.V. Foa and G. Rudinger, Cornell Aeronautical Laboratory.*

An investigation has been started to study the operation of ducted pulsejets. The thrust developed by a conventional pulsejet decreases sharply at flight velocities of a few hundred miles per hour and at flight Mach numbers of about 0.6 its operation stops altogether. This failure to operate is due to the increasing difference between the ram pressure at the inlet and the static pressure at the tailpipe exit. To eliminate the detrimental effect of this pressure difference, the pulsejet is placed inside a surrounding duct which is designed to

keep the Mach number of the internal flow sufficiently low. Power plants of this type are known as ducted (or shrouded) pulsejets and may have better performance than either the pulsejet or the ramjet in some range of flight velocities. This is a problem of non-steady flow because of the intermittent combustion process in the pulsejet. However, since it does not seem possible at the present time to treat the periodic phenomena that occur in the duct with any accuracy at all, calculations have been based on *effective* mean flow parameters to reduce the treatment to one of steady flow. Such an analysis may lead to useful information on some of the effects of size and shape of the shroud but it cannot be expected to include the coupling effects that may occur between oscillations in the duct and in the pulsejet.

The first problem to be investigated was an evaluation of the range of flight Mach number in which the ducted pulsejet could be expected to give a better performance than either the conventional pulsejet or the ramjet. The analysis was, therefore, always carried out for the optimum configuration at any flight Mach number. A similar analysis was also carried out for the ramjet since a comparison of theoretical results based on the same assumptions should be more significant than a comparison of theoretical results for the ducted pulsejet with actual performance data for ramjets or theoretical results based on different assumptions.

In the configuration investigated, the pulsejet was submerged in a constant area duct connected to an inlet diffuser. This duct was of sufficient length to insure complete mixing of the pulsejet exhaust gases and the surrounding flow and the exit was formed by a nozzle designed for complete expansion. The thrust of the pulsejet alone was assumed to be proportional to the static pressure of the flow at the diffuser exit and was taken as 360 pounds per square foot at sea level pressure; the specific impulse of the pulsejet alone was assumed to be constant and equal to 1100 seconds, On the basis of the assumptions made, the optimum duct configuration, thrust and specific impulse could be calculated for any altitude and flight Mach number.

A report on this part of the investigation has been prepared.[10] The main results may be summarized as follows: At flight Mach numbers lower than about 0.25, the conventional pulsejet would be superior to the ducted pulsejet both with regard to specific thrust and specific impulse. At higher flight Mach numbers, the conventional pulsejet would still be capable of producing higher specific thrust perhaps up to flight Mach numbers of 0.5 while the ducted

[10] G. Rudinger, *An Evaluation of the Potential Merits of Ducted Pulse Jets,* Project Squid Technical Memorandum CAL-32, October 1949.

pulsejet would then have a considerably higher specific impulse. At Mach numbers greater than about 0.6, the comparison becomes meaningless since the conventional pulsejet would not operate in this speed range.

The comparison calculations for the ramjet were, at first, based on an air/fuel ratio of 25. In this case, the ramjet could produce the higher specific thrust for flight Mach numbers greater than 0.6. At M=1.5, the specific thrust of the ramjet was more than twice as high as that of the ducted pulsejet. However, the specific impulse of the ramjet was then only about 60 per cent of that of the ducted pulsejet. The two values became comparable only at flight Mach numbers above 2.0.

By increasing the air/fuel ratio of the ramjet a higher specific impulse could be obtained at the expense of some loss of thrust. If, in this manner, the specific thrust of the ramjet was made equal to that of the ducted pulsejet, the latter still had a higher specific impulse up to flight Mach numbers of about 1.5.

For a ducted pulsejet in which the ratio of maximum pulsejet area to maximum duct area was 0.4, typical performance data obtained were: a specific thrust of 250 pounds per square foot at an altitude of 10000 feet; and a specific impulse of 1860 seconds. A ramjet operating with an air/fuel ratio of 100 would give the same specific thrust but its specific impulse would only be 1180 seconds. It was concluded that the ducted pulsejet should be a valuable powerplant in the range of high subsonic or low supersonic flight velocities.

This work is being continued along two main lines of approach. One is the extension of the analysis outlined above to a study of off-design performance. This phase has only been started and no results are as yet available. It is planned later to carry on testing of actual models using either conventional or valveless pulsejets. The other line of approach is a more detailed study of the phenomena connected with the operation of ducted pulsejets. If one imagines that the instantaneous values of all state and flow parameters could be measured, their mean value would, in general, not form a set of flow conditions that could simultaneously be satisfied by a steady flow unless the amplitude of the oscillations were small. This is due to the complicated non-linear relations between the parameters. The assumption of an *equivalent steady flow* made above can, therefore, only be a rough approximation.

For the purpose of checking the accuracy of the steady flow assumption, a series of experiments has been started to study pressure disturbances in a ducted pulsejet. The pulsejet was simulated by a mechanically controlled intermittent air jet discharging into a constant

area duct. The injector nozzle was surrounded by streamlined bodies blocking various fractions of the duct. Instantaneous pressure recordings were obtained at various points along the duct and for various frequencies of the injected flow. The pressure records obtained showed a considerable amount of high frequency disturbances which have not yet been explained. It is suspected that they were caused by shock reflections across the duct. However, these records have already indicated that the disturbances that are propagated upstream may have a considerably reduced amplitude compared to those propagated downstream. Attempts will also be made to study the concepts of an equivalent steady flow theoretically by means of the method of characteristics or some other procedure.

The pressure waves and their reflections inside the duct produce a complicated flow pattern that must depend to a great extent on the geometry and particularly the longitudinal dimensions of the duct. No theoretical method appears to be available for such investigations and all the work will have to be done experimentally. The water analogy may be a useful tool for investigations of this nature.

The investigations of shock oscillations in a diffuser under the influence of pressure disturbances - as discussed under the problem of stability of shock waves in supersonic diffusers (Div. II, Sec. A)- will also be of importance in the study of ducted pulsejets for the supersonic range of flight Mach numbers.

Exploratory studies have been carried out along two lines; generalization of the theory of jet propulsion, and search for improved pulsejet configurations. The following is a brief outline of the work done to date.

An attempt has been made to evolve a theory whereby the performance of all air-breathing jet engines could be calculated through a common set of equations. The investigation has been carried out so far only for single-flow jet engines. The performance of this class of engines is expressed in terms of parameters that can be varied continuously over their respective ranges of practical significance. The results are presented in the form of a *performance spectrum* which extends from the ideal constant-volume pulsejet to the isothermal ramjet or turbojet. This continuous spectrum makes it possible: to obtain a direct comparison of the performance of existing jet power plants under any desired operating condition; to evaluate the present performance of existing power plants in relation to their respective theoretical optima; to determine which parameters are to be considered of importance in any attempt to improve the performance of existing types of jet engines; and to estimate the performance of nonexisting but conceivable new types of jet engines, and perhaps also to suggest new avenues

of propulsion development. A memorandum covering this phase of the investigation is now being prepared.

The information acquired in the study of shock motions has led to new ideas concerning the improvements of pulsejets. The basic principle is periodically to open and close the inlet and exit of a duct. The interruption of the exit flow produces a shock wave that is reflected forward and backward in the duct. Its strength is maintained by correctly timed intermittent combustion cycles. By conserving the wave energy of the shock, the combustion process takes place in precompressed gas thus resulting in a high thermal efficiency. A preliminary characteristics diagram indicated the essential feasibility of such engines. It is planned to investigate these ideas further.

## *H. THEORY OF PULSEJETS. (NYU-3R7)*

*Submitted by: G.E. Hudson, New York University*

An estimate has been made during the past year of the thrust exerted on pulsating jet devices operating statically, for which a periodic reversal of flow takes place at their exhaust ends. This estimate is based on an idealized model of the flow at and near the exhaust port where it is supposed that the fluid moves incompressibly. Furthermore, in this model the effect of loss of kinetic energy and momentum by actual transport of fluid from the exhaust port in the jet, a phenomenon which might be termed *jet detachment*, as well as any intake effects at the front end of the device, are neglected. Several cases which are approximately realizable in practice are discussed below.

The flow patterns in and out of the exhaust port during a cycle are similar (but opposed in direction) and are like those for incompressible potential flow in or out of a tube. In this case, if $Z$ is the amplitude of the motion of the fluid inside the tube near the exhaust port, $\omega$ is $2\pi$ times the frequency of the oscillation, $\rho$ is the density of the medium outside the tube, and $A$ is the cross-sectional area of the exhaust port, the thrust averaged over a cycle is $\bar{T} = \frac{1}{4} \rho A \omega^2 Z^2$. In this estimate, the effect of the pressure decrease at the edge of the exhaust port as the fluid flows around it is neglected.

The outflow and inflow patterns are dissimilar, the inflow may be likened to a potential flow into a tube, while on the outflow a jet is formed which is brought to rest just prior to the inflow. In this case the thrust is half of the value calculated in the preceding paragraph. This case is more likely to approximate actual pulsating flows, except when the edge

of the exhaust port is flared, inhibiting the jet formation, to which the case discussed above is more applicable.

In both these cases, the thrust is expressed in terms of parameters describing the motion of the fluid near the open end of the tailpipe. If the fluid in the tube is incompressible, as in a Bodine piston device operating under water, these formulas give estimates of the effect of outflow and inflow, neglecting the important phenomenon of jet detachment as mentioned above. However, if the fluid in the tube is compressible, the motion at the open end may be considered to be produced by a piston oscillating at the far end of the tube, with the compressible gas acting somewhat like a massive spring interposed between the piston and the open end. Hence, as the piston frequency nears the natural frequency of oscillation of the system, the amplitude of motion at the open end becomes very great, showing that the thrust should increase greatly near resonance due to the backflow effect. At the same time, of course, the effect of jet detachment would become very large, with a probably positive contribution to the thrust, but with the simultaneous effect of limiting the amplitude of the motion at the open end (by dissipation of the energy).

Further theoretical developments in this direction await the solution of various special theoretical problems as well as more experimental information concerning the effects of variation of certain parameters.

## *I. EXPERIMENTAL STUDY OF AN IDEALIZED PULSEJET. (NYU-6R1)*

*Submitted by: G.E. Hudson, New York University*

During the past year, a small pulsejet was developed that has transparent side walls and a constant cross-sectional area from the valve bank to the exhaust port. The preliminary investigation of the characteristics of such an engine was done by mounting the valve head of a Dynajet engine on a 2¼-inch diameter pipe. It was found that this combination ran best when the length of the pipe was 26 inches. The 2¼-inch pipe was then replaced by a square tube (2¼ in. $x$ 2¼ in. $x$ 36 in.) so that the later models could be constructed with transparent side walls without modification of the internal cross section. The static thrust of this particular model was found to be of the order of 2 pounds. To make the air flow through the valves substantially two-dimensional, which is desirable when observing flow with a Schlieren system, a new valve bank was then developed which had two horizontal slots as inlet passages. High speed photographs of the operation of an engine (2¼ in. $x$ 2¼ in. $x$ 37 in.) with such a two-dimensional valve bank and transparent side walls showed that the entering charge was

compressed and expanded many times before it was expelled at the tailpipe rather than just twice as in the Dynajet. This may have been due to the restricted movement of the valves which limited the amount of fresh mixture induced during each cycle, rather than to the uniform cross section of the engine. Since the engine was now running best at a length considerably longer than the Dynajet, a one-half scale model was built to make it possible to take Schlieren pictures of most of the engine at one time. The stepwise development described above now proved to be extremely helpful since previous experience aided greatly in the solution of the problems of the smaller engine 1¼ in. x 1¼ in. x 27½ in. which was found to be considerably more critical to changes in dimensions than the reduction in scale would indicate. High speed motion pictures will be taken of the operation of this engine as soon as time permits.

Two other brief investigations of allied problems were made during the past year as a result of ideas derived from the work on flame tubes, Div. IV, Sec. A, and the mathematical theory of pulse jets, Div. I, Sec.H.

The effect of inserting a grid (Div. IV, Sec. A) in a standard pulsejet engine was tested by equipping a glass-walled model of the Dynajet engine with a grid 2 inches downstream of the intake valves. A comparison of high speed Schlieren photographs of the flame and particle motions in this engine with those taken when the grid was not in place indicated that no marked change in flow pattern occurred. This might be attributed to the fact that a great deal of turbulent motion is already present.

As a result of the observation that most of the gases flowing back into the tailpipe of a pulsejet come in radially from the sides, a brief investigation has been made of the effect on static thrust of placing exhaust gas ducting behind a small pulsejet engine. Both the diameter of the duct and the axial distance between the end of the tailpipe and the beginning of the duct were varied. The results of these tests indicated that the static thrust of the combination may vary as much as 10 per cent within the range of lengths tested (6 in. to 52 in), even if the duct diameter and axial spacing are optimum. Maximum thrust was obtained when the pipe was the proper length to resonate at the fundamental frequency or at the first overtone of the engine noise. Though insignificant increases of the order of 2 per cent over the rated thrust of the pulsejet engine alone were obtained, it is felt that this method offers a suitable means of ducting the exhaust gases, provided a reasonable amount of air can be supplied at the junction between the engine and the duct. A technical memorandum on this subject is now being prepared.

# II. FLUID MECHANICS

## A. *PROPAGATION AND STABILITY OF SHOCK WAVES IN SUPERSONIC DIFFUSERS. (CAL-1R6).*

*Submitted by: J.V. Foa and G. Rudinger, Cornell Aeronautical Laboratory.*

If the back pressure in a supersonic diffuser is varied, the shock either moves to a new equilibrium position within the diffuser or it may be forced out of it depending on the magnitude of the pressure variation. If such variations, however, occur periodically at high frequency, the shock may oscillate entirely inside the diffuser even if the pressure reached values that are considerably higher than would be permissible in steady flow. In various practical applications (*e.g.*, supersonic ducted pulsejet, see below) it would be important to know for a given diffuser the relation between amplitude and frequency of pressure oscillations that would be permissible without forcing the shock ahead of the throat.

As a first step in approaching this problem, the complete interruption of flows for a short period has been studied. The shock produced by closing a gate decays as it is overtaken by the expansion wave resulting from the reopening of the gate. The approximate analytical method that was previously developed[1] could not be used to determine the state of the gas at the location of the interrupting gate. The method of characteristics had to be applied in order to acquire deeper insight into the behavior of the mass flow following the opening of the gate. If the original flow is supersonic, one would expect that this initial mass flow following the removal of the interrupting gate would be higher than the original value since the mean mass flow during the transient from the the initial interruption until reestablishment of the original flow must be equal to the original mass flow. Instead, the mass flow at the first instant after opening was noted to be lower than the mean and to reach a higher value only during the later part of the transient. A plot of the instantaneous mass flow versus time was given in a previous progress report.[2] A complete report on this work will be prepared.

An attempt was made to determine the shock motion in a diffuser by an analytical method. The method was based on the assumption that the static pressure distribution between the

[1]Project Squid, Annual Program Report, January 1949, Cornell Aeronautical Laboratory, p. 115.

[2]Project Squid, Quarterly Progress Report, July 1949, Cornell Aeronautical Laboratory, p. 42.

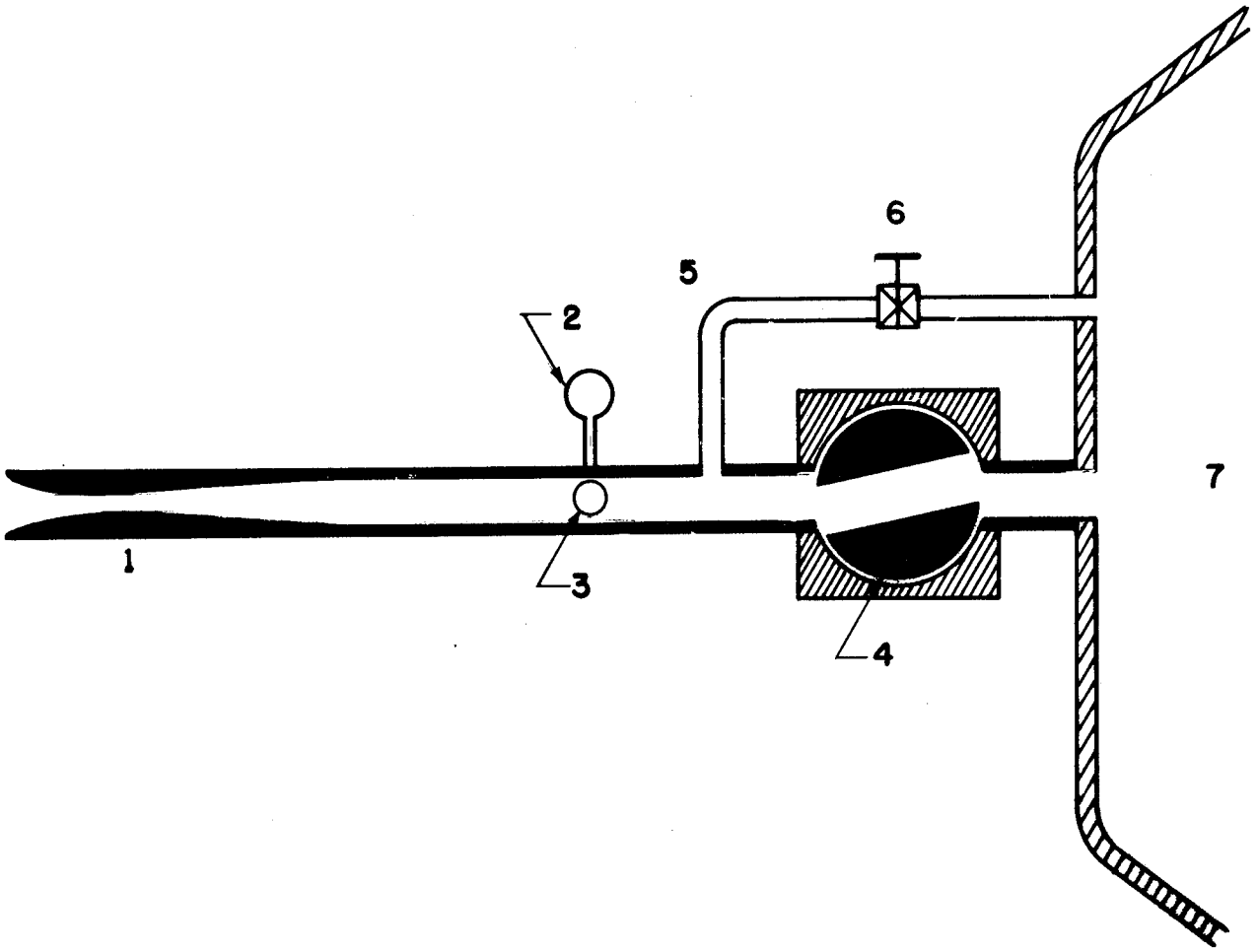


Fig. 1. Experimental setup for observation of oscillating shock waves.

1. Two-dimensional diffuser
2. Manometer (Mean pressure)
3. Pressure gauge (Instantaneous pressure).
4. Rotating valve (Driven by variable speed motor)
5. By-pass
6. Manually controlled valve.
7. Low pressure reservoir (altitude chamber)

moving shock and the end of the diffuser was the same as in steady isentropic flow with the same back pressure. In other words, the entropy gradient which existed downstream of the shock during its motion was assumed to be entirely due to a departure of the static temperature distribution from that corresponding to isentropic flow. Comparison of the results obtained in this way and by means of the method of characteristics indicated some discrepancies, the most serious of which was found to occur at the approach to the final steady state: the analytical method led to an asymptotic approach whereas the method of characteristics indicated a slight overshooting of the final shock position in the course of the transient.

It was then decided to build two-dimensional diffuser models and study shock motions experimentally. The experimental arrangement is shown schematically in Figure 1. A two-dimensional diffuser was connected through a rotating valve to the Cornell Aeronautical Laboratory altitude chamber which acted as a low pressure reservoir. Air was sucked in through the inlet and a shock occurred within the diffuser somewhere between the throat and the exit. The valve was driven by a variable speed motor and interrupted the flow periodically. The amplitude of the pressure oscillations produced in this manner could be varied by a manually adjusted by-pass to the valve.

As long as the shock oscillations took place entirely within the chanel, *i.e.*, as long as the flow was supersonic in some part of the channel, the flow interruptions at the valve could not be heard outside. Increasing the pressure amplitude by closing the by-pass would eventually push the shock out of the channel during part of the cycle. This transition was clearly audible and it was thus possible to correlate the frequency of the pressure pulses and their amplitude to keep the shock entirely within the channel for various mean exit pressures.

The instantaneous pressures in the channel near the rotating valve were recorded by means of a condenser-type pressure gauge[3] and the mean pressure was read on a manometer. Numerous static pressure measurements along the diffuser were also taken in steady flow to check the results against one-dimensional theory. Three diffusers were used in these experiments. Their lengths were about 12 inches, 21 inches and 36 inches, respectively. All had the same throat area of about 0.5 square inch and an exit area of about 1.0 square inch. A Schlieren system was used to visualize the shock pattern.

An attempt was made to observe the shock motion through a stroboscopic disc placed in the light path of the Schlieren system. However, the motion was not regular enough for satisfactory observation in this manner. Successful high speed Schlieren motion pictures were taken with speeds up to about 7000 frames per second using a Fastax camera with a special control unit (*Goose*). The instantaneous pressure at the diffuser exit was recorded simultaneously. The film showed the complete motion of the shock oscillating at about 100 cycles per second.

The tests yielded the unexpected result that the pressure pulses that were permissible without pushing the shock out of the throat could in some cases have lower frequency or higher amplitude in a short than in a long diffuser. This was believed to be due to boundary layer

[3]Project Squid, Annual Program Report, January 1948, New York University, p. 17.

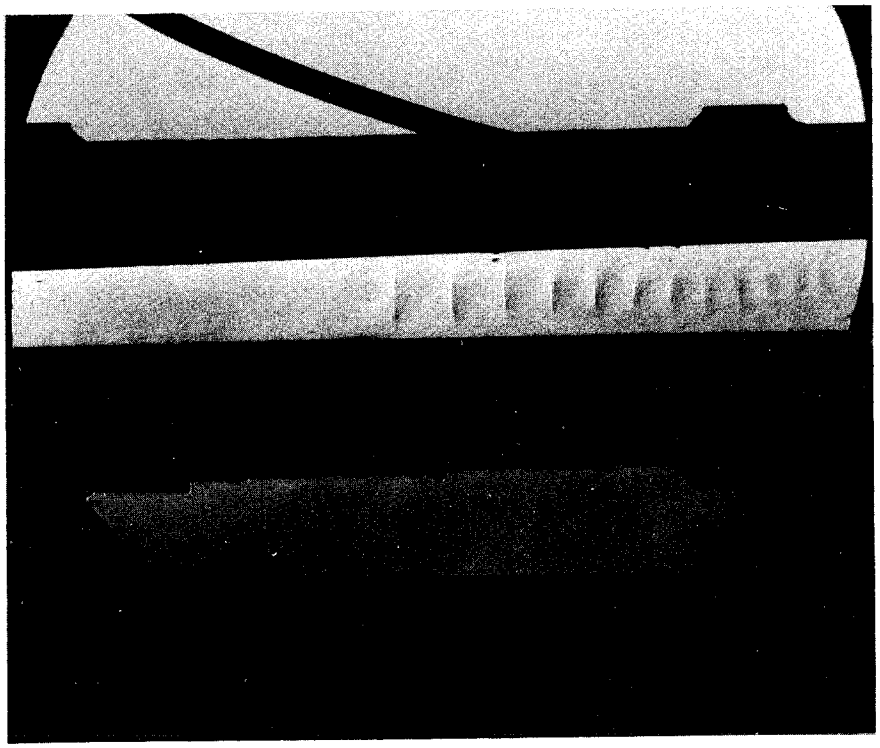

Fig. 2. Steady flow multiple shock pattern in small diffuser model (about 1.0 foot long)

effects which could be very important in models of such small size. Observation during steady flow did not reveal a single normal shock but a pattern of multiple shocks as in Figure 2 showing that the boundary layer occupied an appreciable portion of the cross section. The motion pictures showed that the shock pattern underwent considerable modifications during oscillations and was reduced to a single normal shock during part of the cycle. Figures 3a and 3b show two random flash exposures (4 microseconds) taken during shock oscillations in the shortest diffuser.

The result of all these experiments will be reported after all data have been evaluated. Work has been started on the design and construction of models for similar experiments on a larger scale so that boundary layer effects will not be of such major importance.

## *B. INVESTIGATION OF EJECTOR PERFORMANCE AND THE MIXING OF SUPERSONIC AND SUBSONIC FLUID STREAMS. (Pr-Phase 3)*

*Submitted by: J.V. Charyk, Princeton University.*

One of the key problems involved in the performance of propulsive devices of the ducted type is that of the mixing of the primary jet with the secondary air stream. The primary jet ordinarily will involve supersonic exhaust velocities, will be characterized by a high stagnation temperature and will have a density rather different from that of the incoming air. The theoretical study of such problems has been limited almost invariably to a one-dimensional treatment which simply equates the total original mass, momentum, and energy of the two

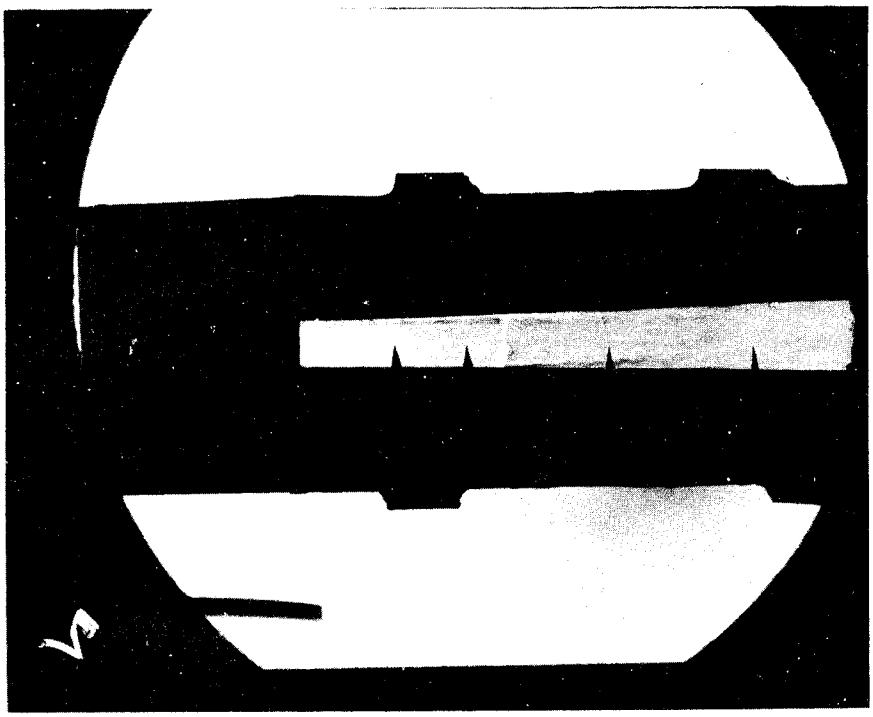

Fig. 3a.

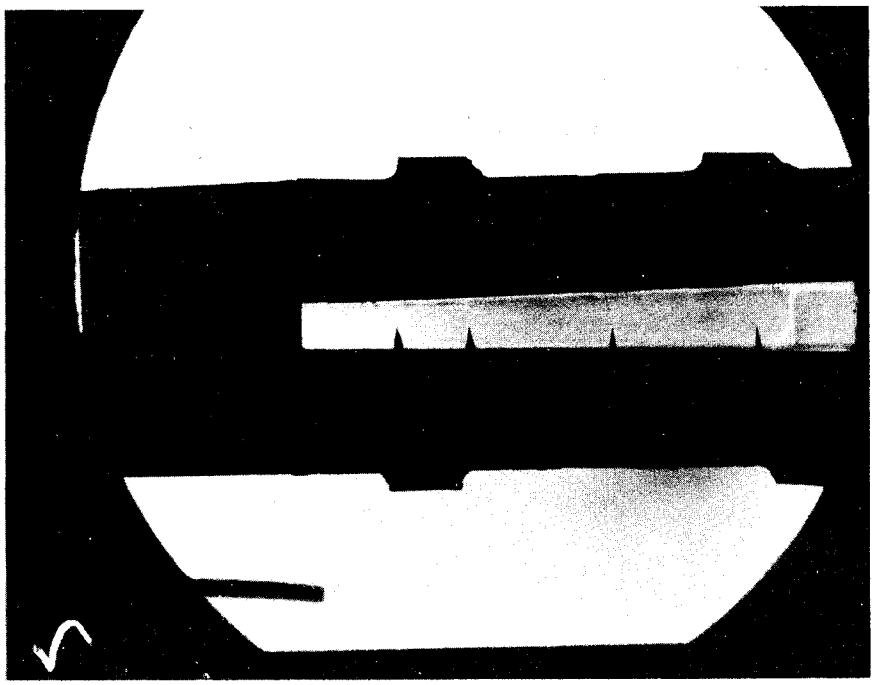

Fig. 3b.
Random flash exposures of oscillating shock patterns in small diffuser model (about 1.0 foot long)

streams to the same quantities after mixing is complete. Such a treatment can handle only the problems of constant area mixing and constant pressure mixing; it will, of course, give no insight into conditions at intermediate stations, and will give no indication of the duct length required for complete mixing. The latter factor is of primary importance from the standpoint of practical application of such devices. The experimental data available has been limited and on the whole has been confined to a rather narrow range of the significant parameters.

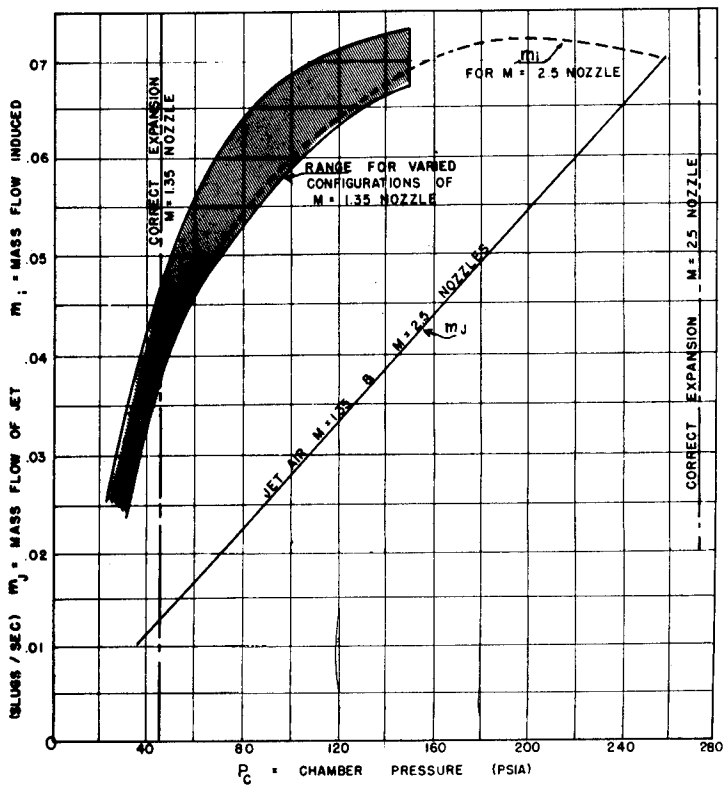


Fig. 4. Mass induction data for two-dimensional ejector.

One of the efforts of the experimental work has been to study this mixing problem over a wide variation in the key parameters, to explore the validity and limitations of the simplified theories, and to provide more specific information for use in making performance studies of ducted propulsive devices.

Initial ejector studies were made in a two-dimensional channel equipped with flexible walls so that the configuration could be readily varied and studies could easily be made of cases other than constant pressure and constant area mixing, the two amenable to theoretical calculation. These studies were confined to the case of the mixing of two air streams with approximately the same stagnation temperature. Two primary jet nozzles were employed in these studies, one designed for an exit Mach number of 1.35, and the other for a Mach number of 2.5. Ejector performance data consisting of the determination of the mass ratio of induced to primary air and kinetic energy of the induced air were obtained as a function of the stagnation pressure of the primary jet. Such studies were carried out over a very wide variation in the value of the area ratio of the primary stream to the secondary stream and in the duct configuration. The results of many of these tests are summarized in Figure 4.

Figure 5 illustrates the results of tests made, varying the ratio of the area of the throat to the area of the jet and carried out at the optimum stagnation pressure of 90 pounds per

square inch. The mass flow of the induced air and the kinetic energy of the induced air are plotted as a function of the area ratio. Range X in Figure 5 would normally define the operational limits for ejector performance. Whether maximum mass flow or maximum kinetic energy is desired will depend on the specific application in mind.

In addition, pressure and velocity surveys were made in certain special cases in order to gain insight into the mixing process. Temperature measurements were also made employing thermocouple techniques. The difficulties of obtaining proper thermocouple correction factors limited the accuracy of these measurements.

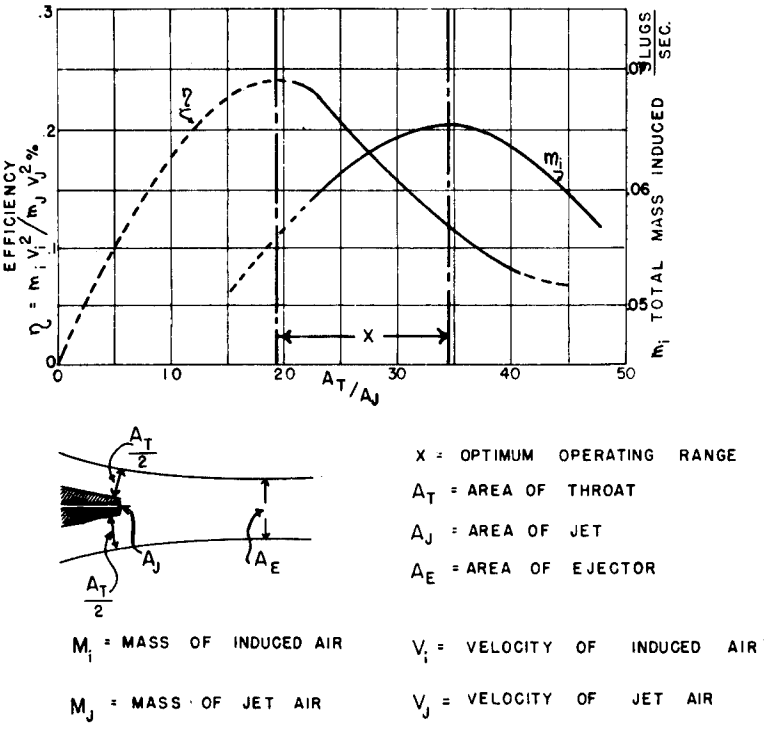


Fig. 5. Performance of two-dimensional ejector as function of secondary to primary area ratio.

The chief difficulty experienced with the two-dimensional channel was the dominant effect of side wall friction resulting from the narrow channel width. This exhibited itself, of course, not only in the channel surveys but in the performance data which gave ratios of induced mass to primary mass of the order of only 65 per cent to 75 per cent of the theoretical value, neglecting friction. Even greater deviation was experienced between the experimental and theoretical values of the Mach number of the induced air stream at the beginning of mixing. Part of this discrepancy, however, is due to the fact that the geometrical configuration of the apparatus was such as to exclude the attainment of strictly constant area mixing of two parallel streams. Rather, the experimental arrangement corresponded more closely to a constant pressure section followed by a constant area mixing section. Accordingly, a theoretical estimate of the magnitude of this correction was attempted. Briefly, a formulation of the problem for the system indicated in Figure 6 was made. The result can be expressed in terms of the same parameters as in the cases of constant area and constant pressure mixing plus the variables $\theta$ and $A_3/A_1$. This general formulation reduces neatly to the simpler cases of constant area and constant pressure mixing with the selection of the appropriate values for these new parameters. The effect of these calculations was to bring the theoretical and experimental mass ratios and the values of the inlet Mach number into much better agreement.

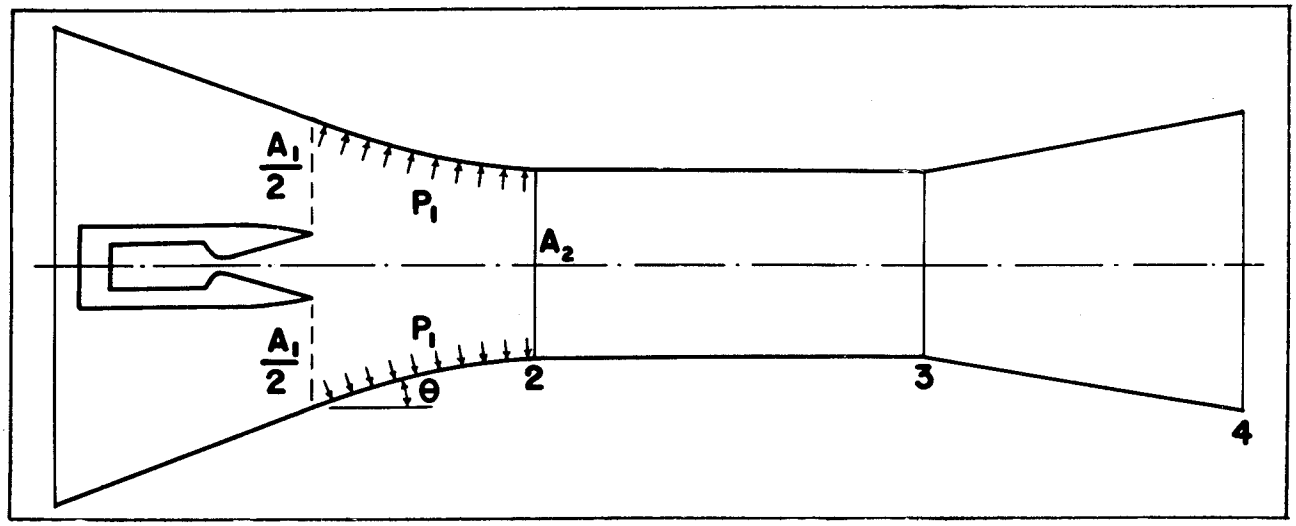


Fig. 6. Diagrammatic sketch of constant area ejector with constant pressure induction section.

Unfortunately, air supply limitations prevented the use of a more satisfactory channel width and it was felt that it would be wise to abandon temporarily the two-dimensional studies and to go instead to a simple axially symmetric arrangement as shown in Figure 7 in order to obtain additional ejector performance data.

This ejector consists of a standard rocket body adapted to the air supply system used in the previous test work. The supersonic jet is directed into a 5½ inch plexiglass duct that can be adjusted to any fixed length and can readily be fitted with appropriate inlet and exit sections. The duct is mounted so as to move freely along its center line and the net thrust can be measured by a platform scale through the linkage as shown in the figure. The present studies involving this apparatus have been confined to the case of constant area mixing and have been intended to yield experimental data for comparison with the simplified theory, to establish limitations of the theory and to yield data not obtainable by calculation, such as the mixing length required, the pressure distribution along the duct during mixing, and an estimate of the friction losses.

The studies have involved, in addition to the measurement of the static pressure distribution, the determination of the mass of air induced, the velocity profile of the stream at the end of the constant area section, the characteristics of the primary jet, and the thrust augmentation produced by the duct.

A study has been made of the effect of the following variables: length of constant area duct; inlet and exit section configurations; ratio of primary jet area to duct area; degree of

under- and over-expansion of primary jet; location of primary jet; and physical properties of primary fluid.

The stagnation pressure of the primary air has been treated as the independent variable and tests have been conducted up to pressures of the order of 350 pounds per square inch.

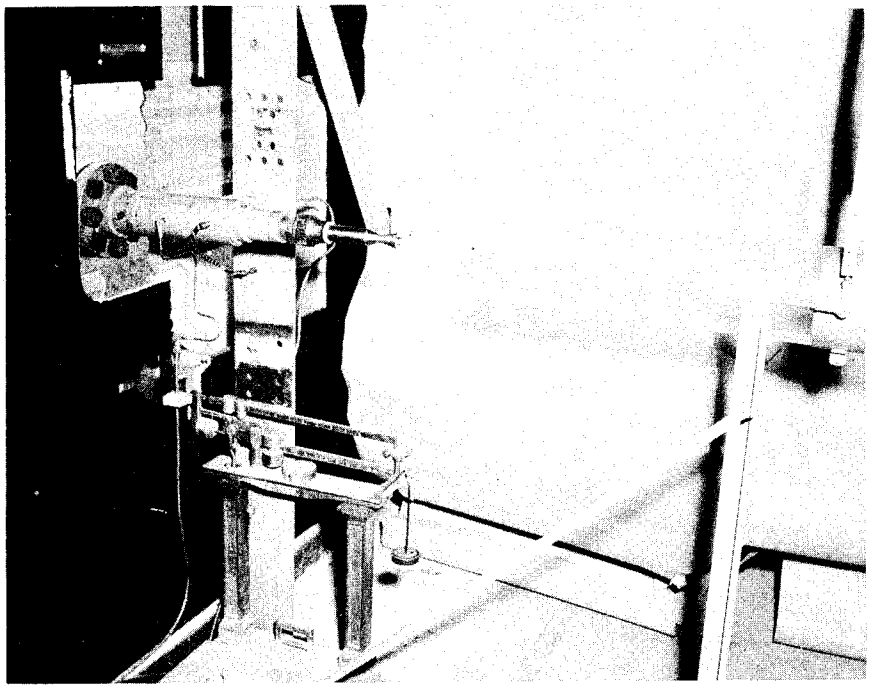

Fig. 7. Experimental test rig - axially symmetric ejector.

Figure 8 illustrates typical gross performance data for a particular configuration. Of particular value have been the static pressure distribution measurements. In addition to furnishing insight into ejector action, they have been of assistance in furnishing a means of specifying the required duct length for optimum performance as a function of the other basic parameters. Typical pressure distribution curves are illustrated in Figure 9.

An extensive series of tests has been made to study experimentally the effects of various inlet and exit section configurations. Figure 10 illustrates, for example, the effect on static pressure distribution resulting from the addition of the specific exit diffuser as indicated, and Figure 11 compares the gross performance.

To investigate the effects of under- and over-expansion of the primary jet, tests were conducted with nozzles of varying exit area, ranging from the case with no divergent section to cases of such large overexpansion that separation occurred over the entire range of stagnation pressures. Thrust data appears to be relatively insensitive to under- or over- expansion; the maximum variation noted was of the order of 10 per cent.

A series of tests has been conducted to investigate the effect of primary jet location on the mass of air induced and on the thrust augmentation. The results are summarized in Fig. 12 for a specific duct configuration.

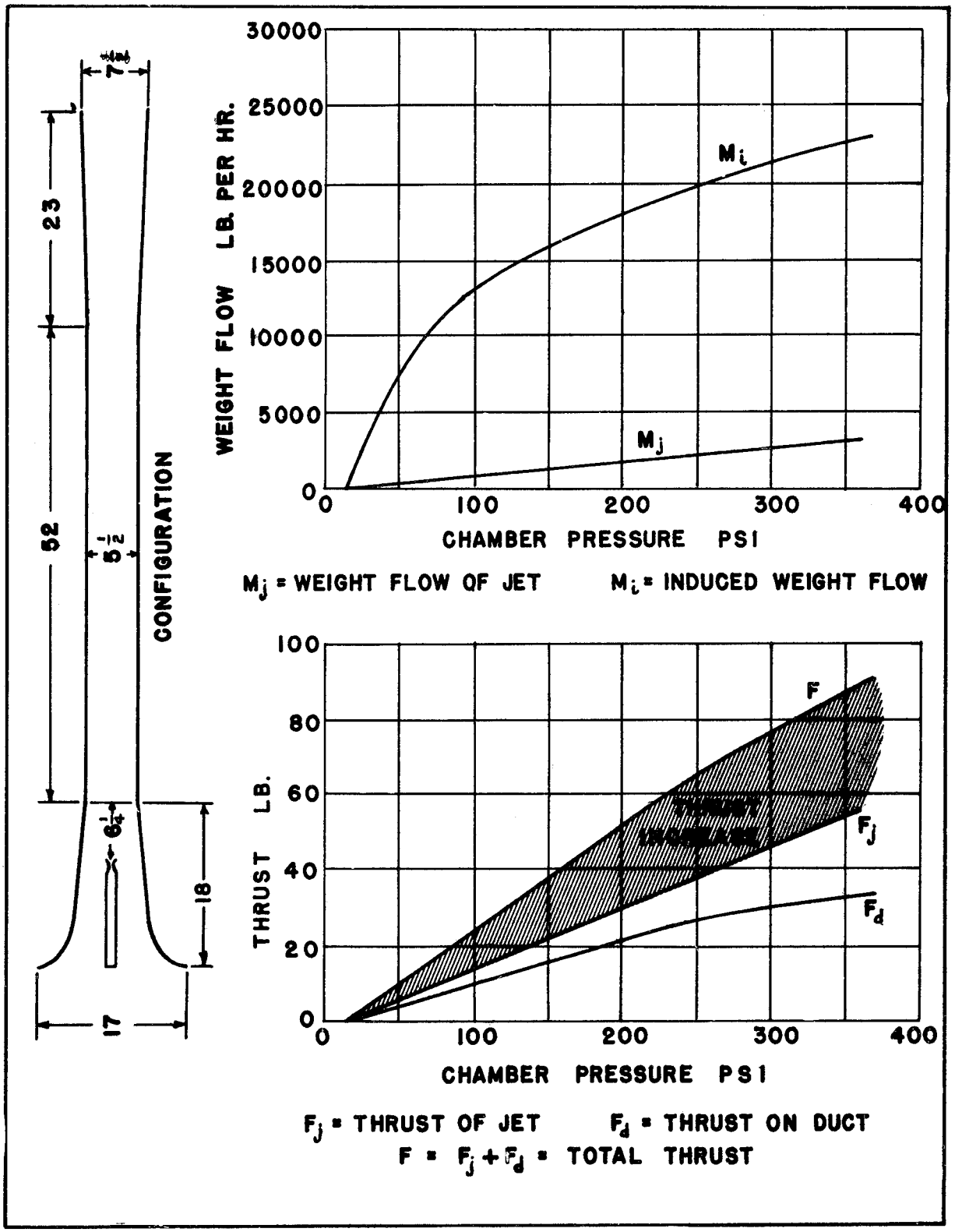


Fig. 8. Typical performance data axially symmetric ejector.

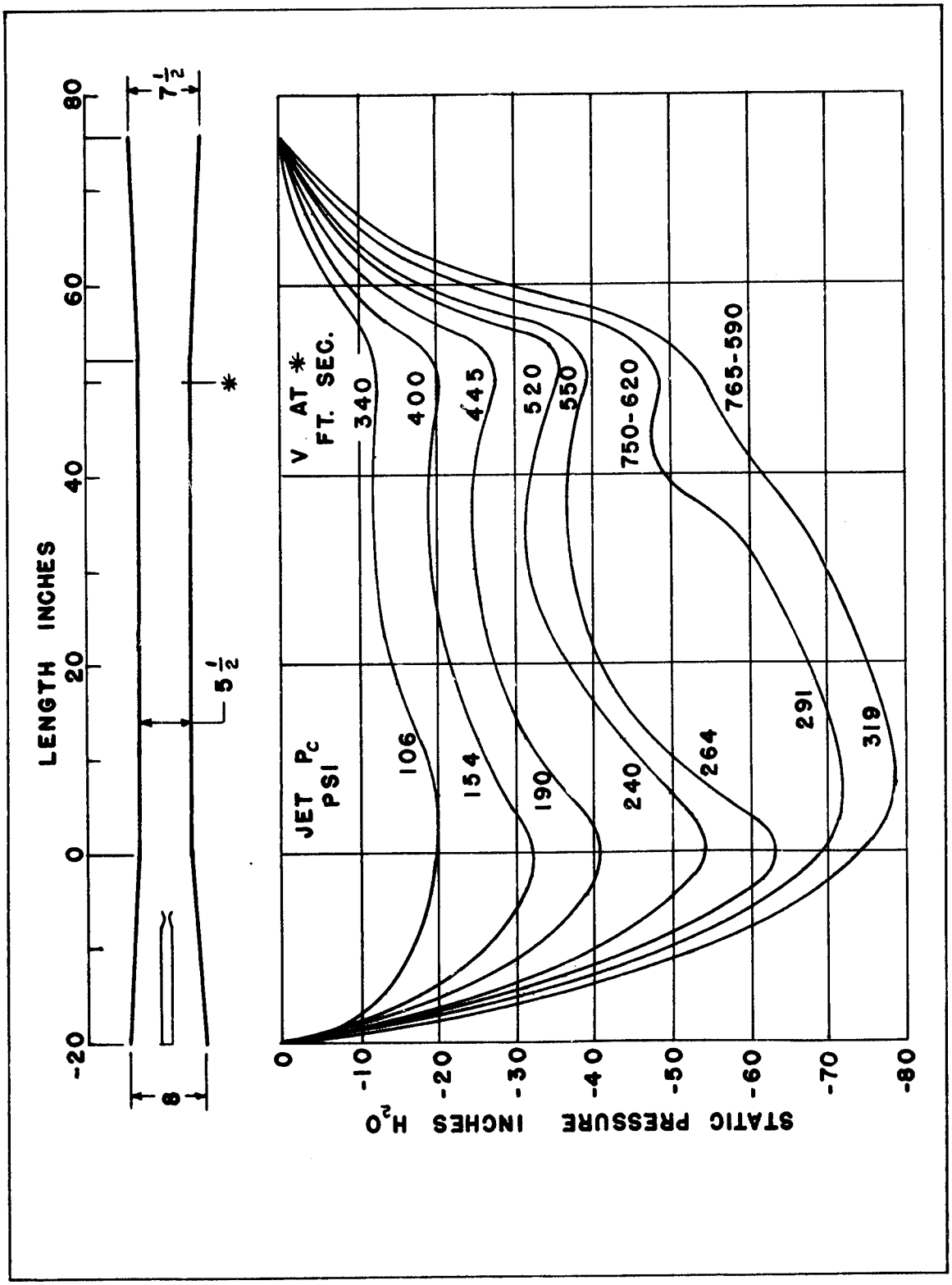


Fig. 9. Static pressure distribution axially symmetric ejector.

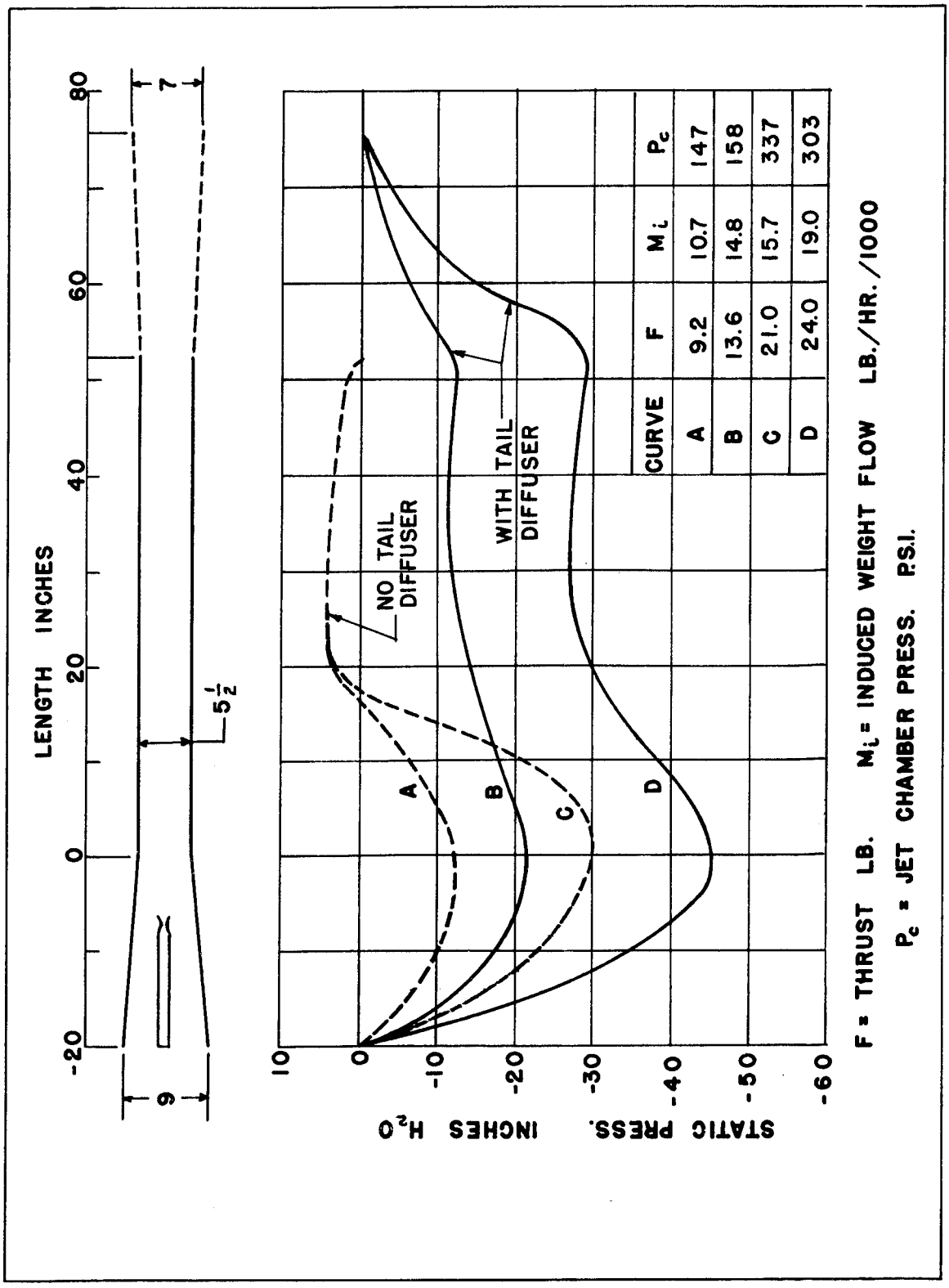


Fig. 10. Influence of exit diffuser on static pressure distribution.

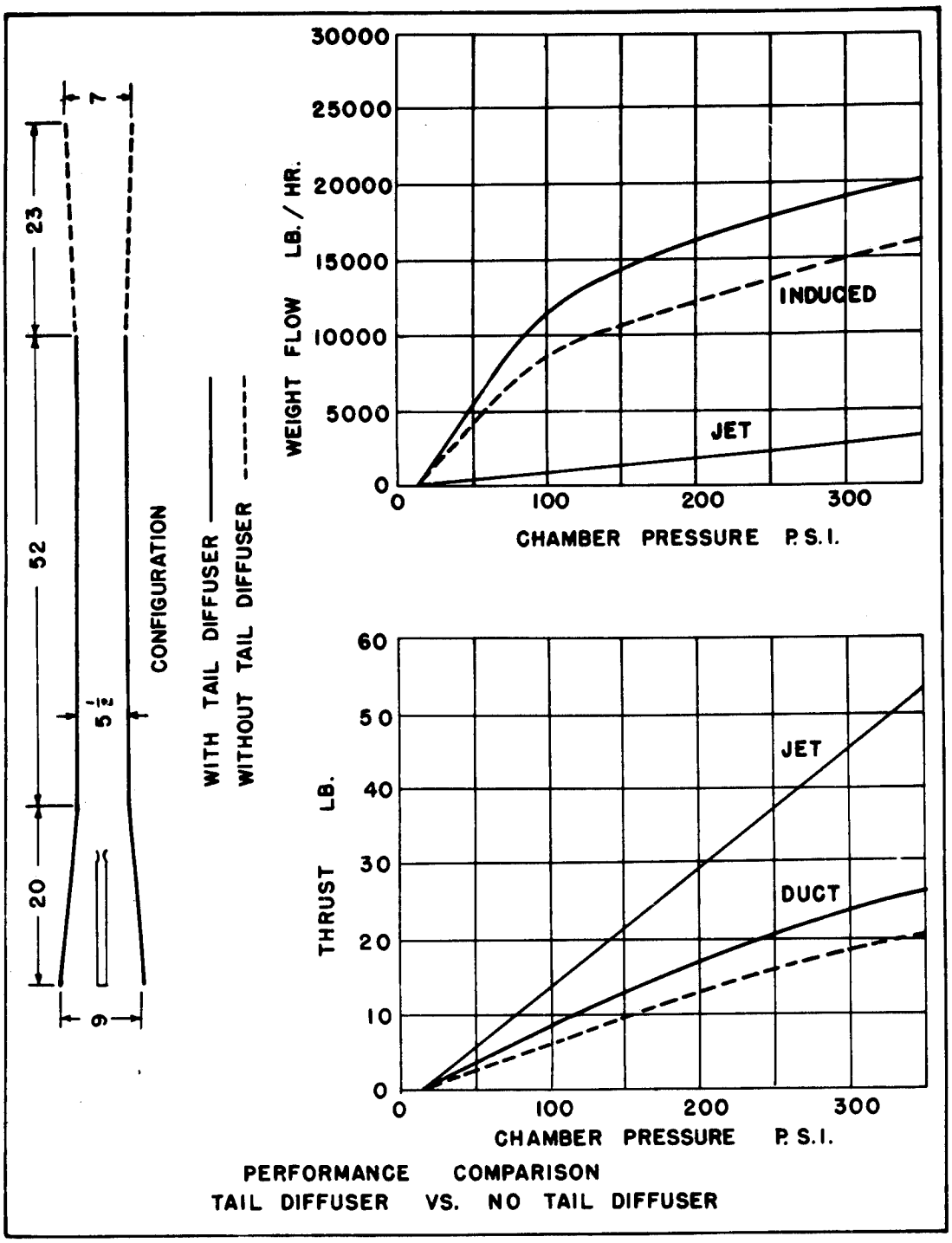


Fig. 11. Influence of exit diffuser on performance.

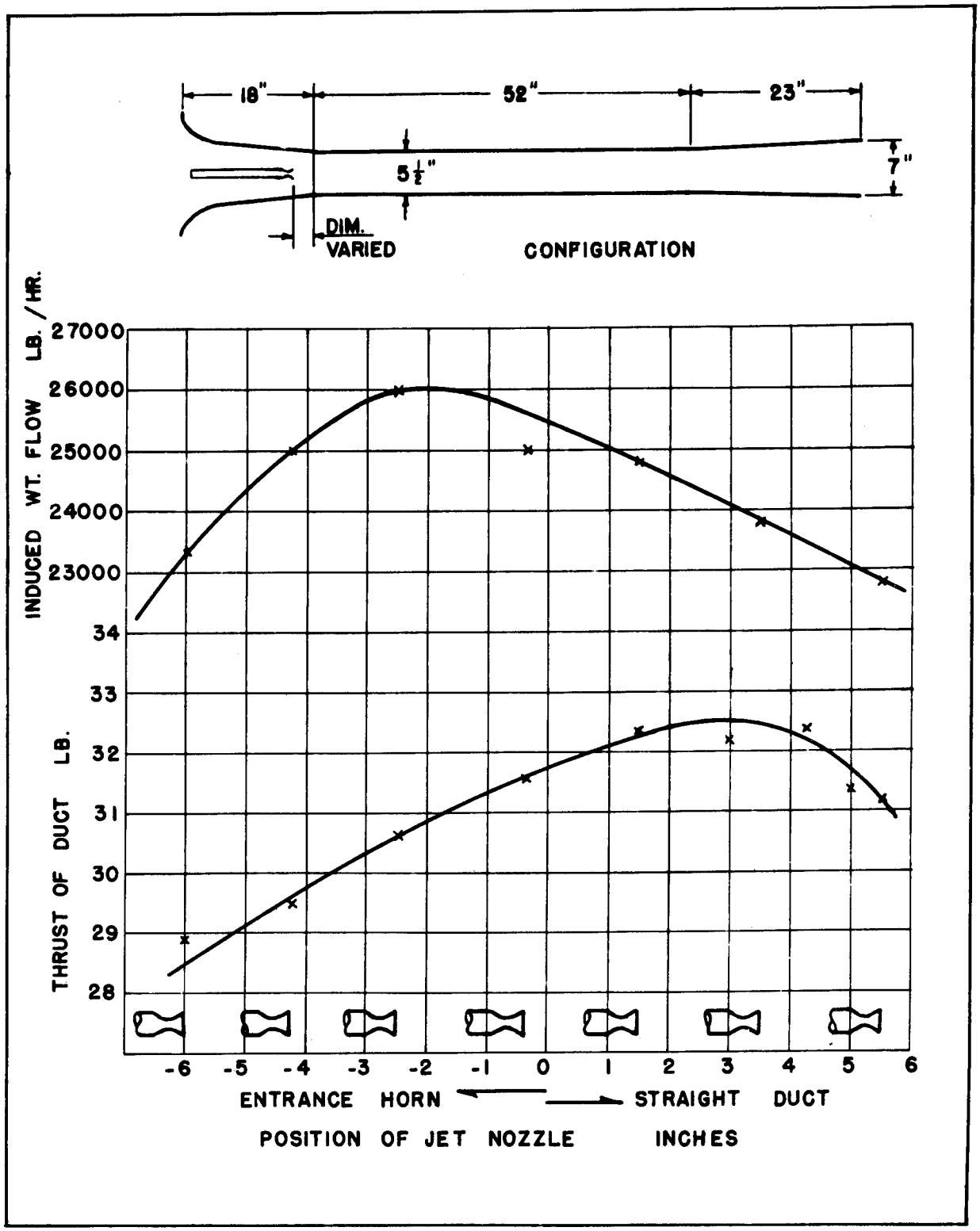


Fig. 12. Effect of primary jet location on performance.

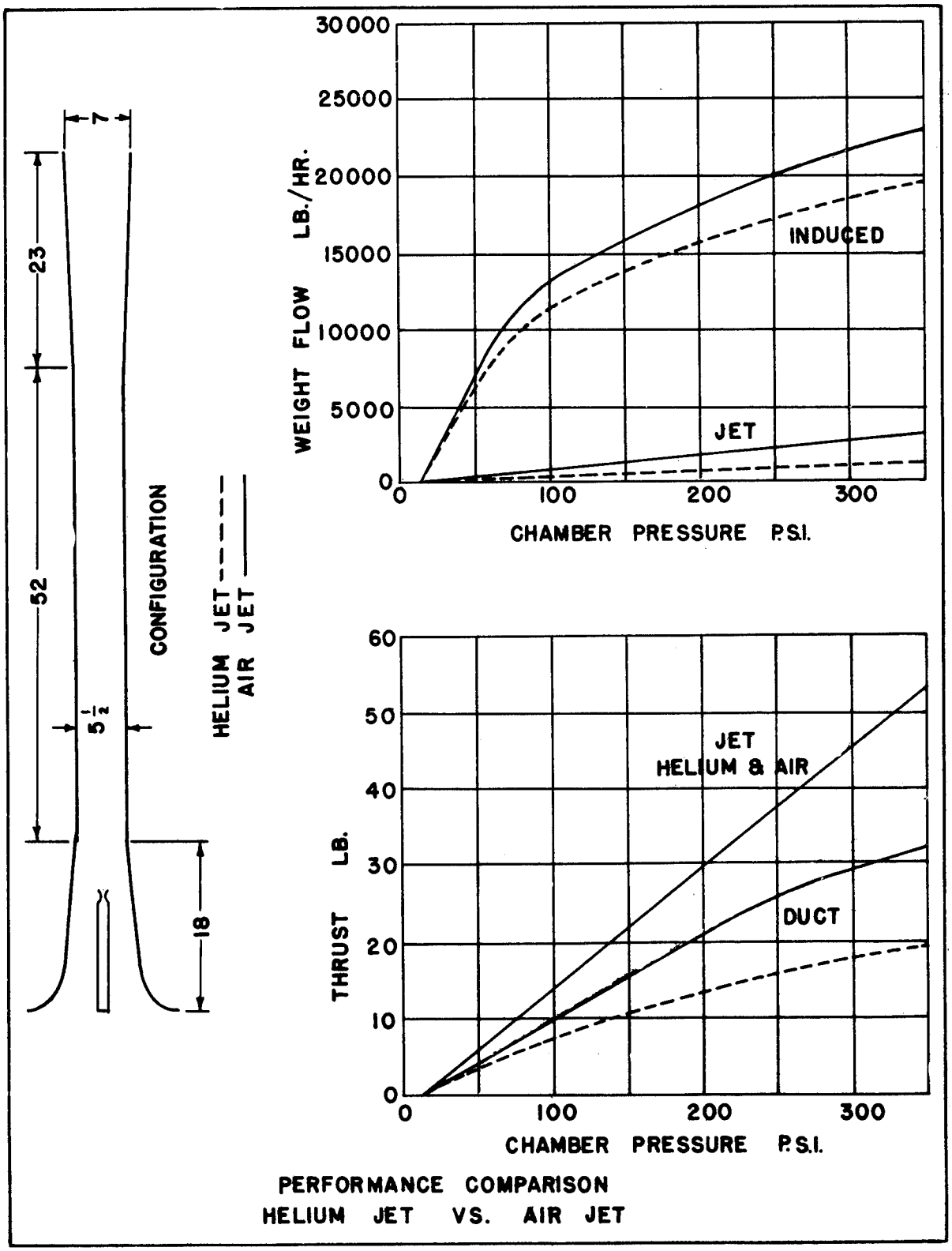


Fig. 13. Comparison of performance data, helium primary jet *vs.* air primary jet.

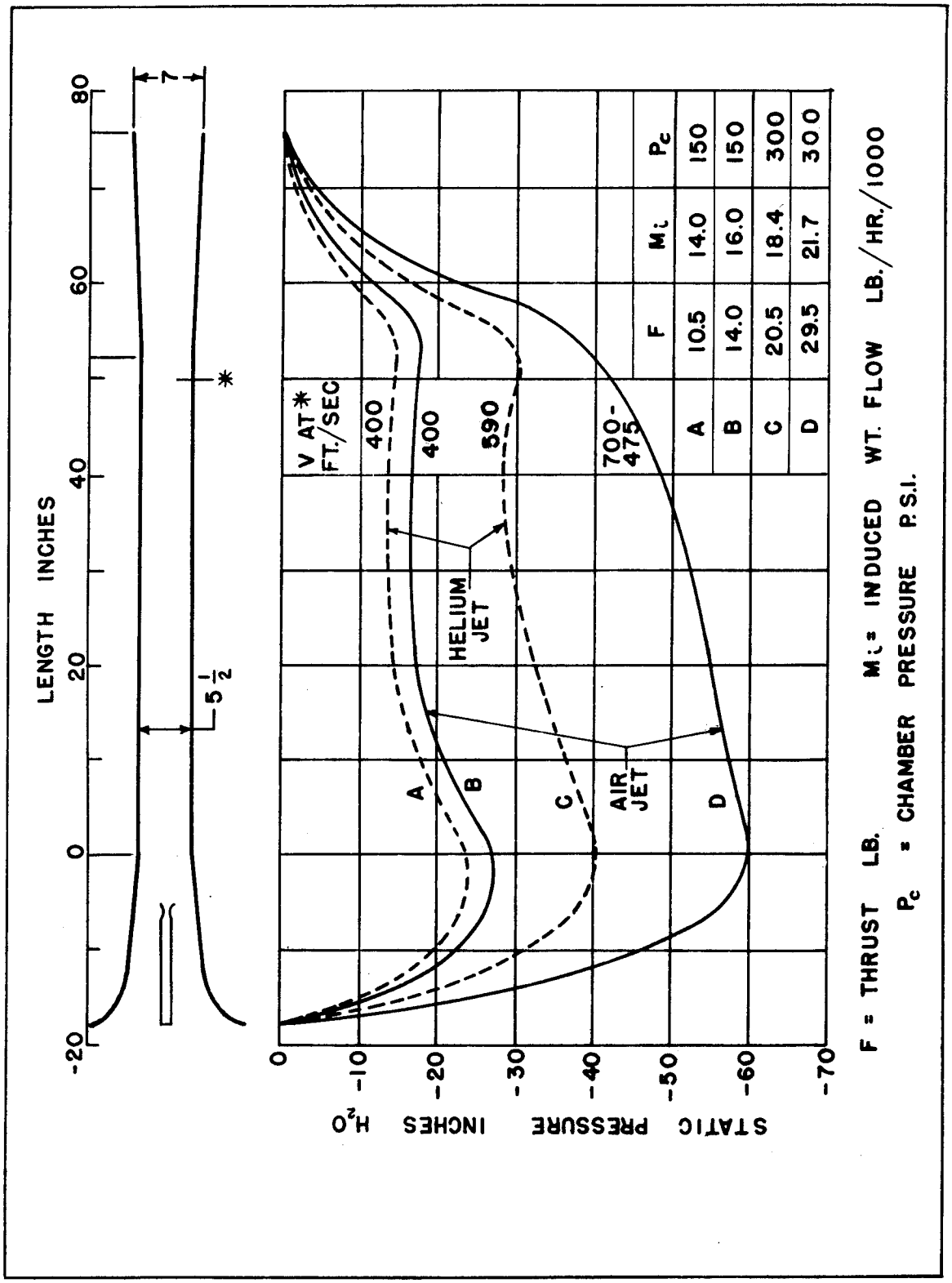


Fig. 14. Static pressure distribution comparisons, helium primary jet *vs.* air primary jet.

Some preliminary tests have been made to study ejector action in the case of primary and secondary fluids with dissimilar properties. One series of tests has been made using helium for the primary fluid. The results of the first tests are summarized in Figures 13 and 14.

The elementary one-dimensional ejector theory has been used to compare theoretical and experimental data with somewhat better agreement than was found in the case of the two-dimensional channel. Table I, for example, compares the calculated ratio of induced mass flow to primary flow with the experimental ratios for a particular test. The calculated values assume ideal diffuser efficiencies.

Future plans call for more detailed and refined investigations of the effects noted above. Specifically, it is intended, now that gross data are available, to study details of the mechanism of ejector action in more idealized configurations. The case of dissimilar primary and secondary fluid properties is particularly of interest and a continuation of these studies is proposed.

Table I.

| Primary Air Stagnation Pressure | Ideal $m_i/m_j$ | Experimental $m_i/m_j$ |
|---|---|---|
| 109 | 12.2 | 10.0 |
| 152 | 10.3 | 8.4 |
| 195 | 8.8 | 7.1 |
| 248 | 7.8 | 6.2 |
| 293 | 6.1 | 5.5 |

## *C. CONTRIBUTIONS TO THE FUNDAMENTAL THEORY OF TURBULENCE WITH PARTICULAR EMPHASIS ON THE CASE OF ISOTROPIC TURBULENCE. (JHU-Phase 2).*

*Submitted by: Ion Carstoiu, Johns Hopkins University.*

The theoretical work being done under this phase has been underway such a short time that no results of sufficient significance to report have been obtained as yet. However, it is felt that it may be of some interest to describe briefly the plan of attack that is being made on the problem. This attack is in two parts. The first consists of investigating the possible appearance of singularities or mathematical irregularities in the flow of a viscous fluid. The appearance of such irregularities would of course be of great conceptual importance in turbulence theory. The second approach is an exploration of the behavior of flow solutions as viewed in the Fourier transform space. An outline of these two investigations is given in the following paragraphs.

The Navier-Stokes equations, which describe the motions of a viscous fluid and which are generally accepted as forming a trustworthy foundation for turbulence theory, contain second

derivatives of the velocity with respect to the spatial coordinates. Past experience would tend to indicate that any initial lack of continuity in any of the derivatives would be ironed out by the action of viscosity. However, there is some evidence, both experimental and theoretical, that this may not be strictly true. Recent observations indicate that a turbulent wake preserves an unexpected sharpness of the boundaries between the turbulent and the non-turbulent regions. What degree of irregularity exists at such boundaries is not as yet known. Along quite different lines from the theoretical side, Jean Leray has investigated the flow of a viscous fluid using equations similar to the integro-differential equations of Oseen in which only the first derivatives of the velocity occur. Leray has shown that these equations have a solution which does not possess sufficient regularity for the second derivatives to be bounded at each instant of time. This solution is formed by a succession of regular solutions. It can be readily appreciated that such phenomena may prove of importance to the conceptual foundations of turbulence theory. The first part of our theoretical work on turbulence will be to explore some of the ideas described above.

Much of the serious work on turbulence that is being done throughout the world at the present time centers around the spectral distribution of energy in the turbulent field. Our second effort on the theoretical side will consist of formulating the Navier-Stokes equations in terms of variables in the Fourier transform space and then investigating the properties of the solutions of such equations. Particular effort will be made to see what statistical concepts in the transform space will lead to results that are compatible with experimental evidence.

### *D. STUDY OF PULSEJET OPERATION, WITH PARTICULAR REFERENCE TO THE EFFECT OF SHAPE. (CAL-1R1).*

*Submitted by: J.V. Foa and G. Rudinger, Cornell Aeronautical Laboratory*

It is well-known that the surface in a shallow water channel follows laws that are quite analogous to those applying to pressure waves in a duct. It has been planned to apply this method to study the influence of shape on the operation of pulsejet ducts. It appeared, however, from experiments with actual valveless pulsejet models, that the influence of shape on the combustion phenomena may be of considerable importance; unfortunately no way has yet been found to simulate combustion processes in the water analogy. It was felt, therefore, that this tool could be used with confidence only in the investigation of gas dynamic phenomena that are not obscured by concomitant combustion processes, such as, *e.g.*, flow oscillations in acoustic jets, in secondary streams of ducted pulsejets and in supersonic diffusers.

Because of the importance of qualitative observations of the entire flow in connection with the investigation of some of these problems,[4] a simple water table with transparent bottom was constructed so that illumination from below was possible. Coloring of the water facilitates detection of water waves and interfaces. It is planned to prepare a report on the techniques that have been used in connection with this work.

## *E. THEORY OF JET FORMATION. (NYU-7R2)*

*Submitted by: G.E. Hudson, New York University.*

To gain insight into the solution of problems of compressible viscous fluid flow over an edge, which is related to the operation of a jet propulsion device as described in Division II, Section F, five idealized fluid flow problems have been solved analytically.

The first problem considered the motion of two semi-infinite media both initially at the same pressure, density, and composition, and separated by a horizontal plane at $y=0$. The fluid was considered incompressible, initially irrotational and laminar, and the fluid above the plane was given an initial uniform velocity $u_0$ parallel to the plane, while that below the plane was initially at rest. Assuming viscous stresses in the fluid when the wall was suddenly removed, the subsequent velocity distribution was determined.

The second problem treated an incompressible homogeneous fluid flowing with an initial velocity $u_0$ in the x direction between two infinite smooth flat plates. The fluid not contained between the planes was originally at rest. The velocity distribution resulting when both plates were suddenly removed was calculated.

The third problem assumed that a parabolic rather than a uniform distribution of velocity existed between the two imaginary plates in the second problem and the velocity distribution was determined upon the removal of the plates.

The last two problems concerned flow initially contained in a tube of circular cross section immersed in a medium at rest. The fourth problem considered the flow in a smooth infinitely long tube of radius a. In this tube an incompressible homogeneous fluid was

---

[4]Project Squid, Annual Program Report, 1 January 1949, Cornell Aeronautical Laboratory, p. 108.

flowing axially, with initial velocity $W_0$, with respect to the fluid outside the tube. The resulting velocity distribution in space and time was found after the tube was suddenly removed. The fifth problem was similar to the fourth and was solved assuming an initial Poiseuille velocity distribution.

All these problems were soluble because the differential equations were reduceable to the linear heat conduction type of equation, and their solutions will be given in detail in a Technical Memorandum now in preparation. Further theoretical work will be done after more experimental data is obtained from the work discussed in the next section.

### *F. EXPERIMENTS ON GAS JET FORMATION. (NYU-7R1).*

*Submitted by: G.E. Hudson, New York University.*

The following experiment was performed to study in a very simplified form the initial stages of the formation of a jet of gas, one of the most important problems connected with flow at the exhaust port of a jet propulsion device. This experiment is the first step in an investigation to gather data on which a mathematical analysis of the problem can subsequently be based.

A body of slightly heated and relatively homogeneous gas is accelerated from rest out over the edge of a surface parallel to the direction of flow, into cooler stationary gas confined between parallel glass plates perpendicular to the optical axis of the Schlieren system. By earmarking small portions of the gas by creating local temperature gradients with small spark discharges or with heated wires, the motion of these portions of the gas can be followed. Examination of the preliminary runs has resulted in several minor improvements in the system, and analysis of the data will be started after a greater number of runs has been made.

### *G. LARGE AMPLITUDE GAS VIBRATION THEORY. (NYU-7R6).*

*Submitted by: G.E. Hudson and R. Shaw, New York University.*

The striking similarity in the behavior of the flow in and near many oscillating jet engines, and that of an open tube fitted with a piston which executes vibrations of large amplitude, indicates that an exhaustive mathematical analysis of the latter will throw considerable light on the gas motions inside the jet engines, in particular, pulse jets and Bodine type piston-driven engines.

The classical Riemann method of treating the non-linear equations which govern the large amplitude motions of the gas in the tube, has born little fruit in practical applications, where resort to cumbersome finite-difference schemes is usually made. As these give little information of a general character, and become unwieldy when applied to a problem of any complexity, an attempt is being made to exploit thoroughly the well-known fact that the equations

$$u_t + uu_x + \frac{2}{\gamma-1} cc_x = 0$$

$$c_t + uc_x + \frac{\gamma-1}{2} cu_x = 0$$

governing one-dimensional isentropic flow of a polytropic gas with adiabatic exponent $\gamma$, become linear upon interchanging the roles of the dependent variables, the flow velocity $u$ and the sound speed $c$, and the independent variables, $x$ and $t$. The resulting linear equations are tractable, however, only if this is done in the right way. If

$$\xi = \frac{c}{c_0}, \qquad \eta = \frac{\gamma-1}{2} \frac{u}{c_0},$$

with $c_0$ a constant reference sound speed, are taken as independent variables, the equations for

$$\tau = c_0 t$$

and, not $x$, but the quantity

$$\varphi = \frac{2}{\gamma-1} \eta t - x = ut - x$$

become simply the two ordinary linear wave equations

$$\tau_{\xi\xi} + \frac{2\lambda}{\xi} \tau_\xi - \tau_{\eta\eta} = 0$$

$$\varphi_{\xi\xi} + \frac{2(\lambda-1)}{\xi} \varphi_\xi - \varphi_{\eta\eta} = 0,$$

with

$$\lambda = \frac{1}{2} \frac{\gamma+1}{\gamma-1}$$

which are fully equivalent to the previous equations in any region where the mapping of $(x,t)$ on $(\xi,\eta)$ is one-to-one, that is, where the flow is not a simple wave or a constant state.

It is still necessary, however, to devise new methods for the solution of the rather peculiar initial value problems that arise when non-linear problems are reformulated in this

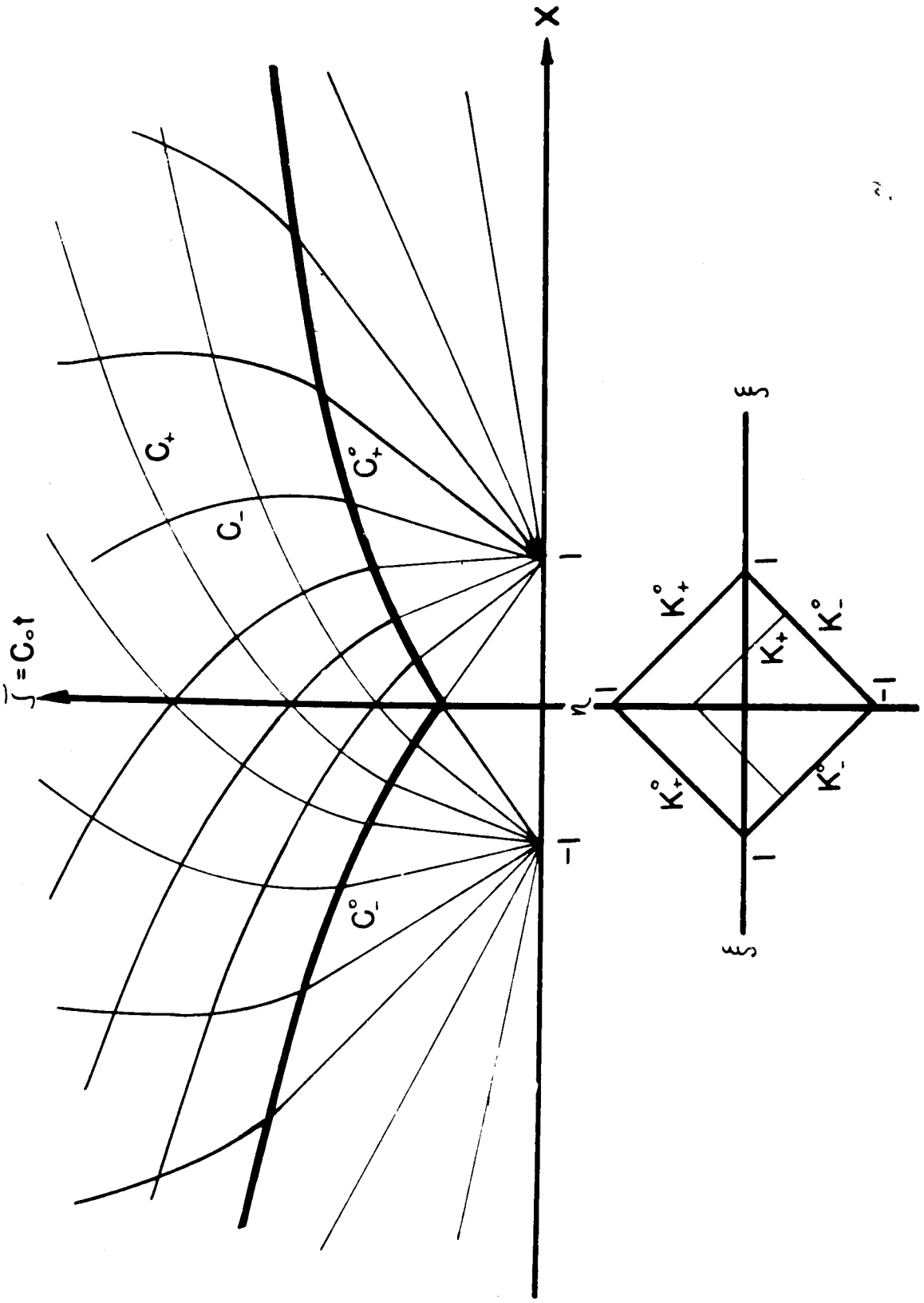


Fig. 15. Sketch of the interaction of two centered rarefaction waves showing the characteristics in the x,t plane and their images in the $(\xi,\eta)$ hodograph plane.

manner. To this end, and to get an insight into the structure of the kind of solutions required, first the simplest problems, then systematically more complex problems were considered.

The simplest problem is, of course, the interaction of two centered simple waves, as would occur in the expansion into a vacuum on either side of a slug of gas initially at rest ($u = 0$, $c = c_0$) in a region $-1 < x < 1$, of an infinite tube. The two initial characteristics (See Figure 15) $C_+^0$ and $C_-^0$, which form the boundaries between the two simple (rarefaction) waves and the region of interaction then map onto the initial cones

$$K_+^0: \quad \eta = +(1-\xi),$$

$$K_-^0: \quad \eta = -1(1-\xi).$$

On these cones the initial values of $\tau$ and $g$ turn out to be

$$\tau = \frac{1}{\xi^\lambda}, \qquad g = -\eta \, \frac{1-\xi^{-(\lambda-1)}}{1-\xi} \quad \text{on} \quad K_\pm^0$$

Solutions satisfying these conditions on both cones can be obtained only by placing appropriate singularities along the $\eta$ - axis, which corresponds to conditions of complete rarefaction ($c = c_0$ $\xi = 0$) at infinity in physical x, t = space.

The solution for $\tau$ is*

$$\tau = \frac{1}{\xi^\lambda} P_{\lambda-1}(z)$$

where $P_{\lambda-1}$ is a Legendre function of the first kind and

$$z = \frac{\xi^2 + 1 - \eta^2}{2\xi}$$

For integral values of $\lambda$ ($\gamma = 3/1,\ 5/3;\ 7/5, \ldots$),

$$g = \eta \sum_{m=1}^{\lambda-1} \frac{1}{\xi^m} P_{m-1}(z)$$

is the solution. For general values of $\lambda$ (or $\gamma$) numerous additional difficulties present themselves. A series representation

*This was also deduced from Riemann's results by C. DePrima, almost a century after publication.

$$g = \eta \sum_{m=0}^{\infty} \left[ \xi^{m+1-\lambda} P_{m+1-\lambda}(z) - \xi^{m} P_{m}(z) \right]$$

satisfies the initial conditions and formally satisfies the wave equation. However, some questions of convergence, existence of second derivatives, etc., have not as yet been completely discussed. More interesting from the point of view of general methods is the contour integral representation

$$g = \frac{\eta}{2\pi i} \int \frac{1 - \left( \frac{h^2+2zh+z^2-1}{2\xi h} \right)^{\lambda-1}}{1 - \left( \frac{h^2+2zh+z^2-1}{2\xi h} \right)} \frac{dh}{\xi h}$$

which also satisfies the initial conditions. It is not yet conclusively proved that this satisfies the wave equation for all $\lambda$. For integral $\lambda$ it reduces to the solution already obtained, however, and for the case of water waves ($\lambda = \frac{3}{2}$, $\gamma = 2$) the integral can be evaluated in terms of elliptic integrals, the functions which would be expected to appear in the solution for a number of other reasons.

The interaction of two symmetrical general simple waves, which would result if, instead of expanding freely, the gas were confined between two pistons moving symmetrically (i.e., along curves $x = +X(t)$, $x = -X(t)$, respectively), gives rise to an initial value problem of the type

$$\tau = \frac{a}{\xi^{\lambda}} + a_0 + a_1\xi + a_2\xi^2 + \cdots$$

on the same two cones $K_{\pm}^{o}$. Thus the solution can be obtained by a superposition of the above solution and solutions satisfying

$$\tau = \xi\eta \quad \text{on } K_{\pm}^{o}$$

For integral values of $\lambda$ a method has been devised whereby appropriate polynomial solutions can be obtained in all cases:

$$\tau = \xi^{\eta} - \frac{1}{2^{n-1}} f^{(n)}(\xi,\eta) \cdot (z-1);$$

for instance, when $\lambda = 1$, $\tau = \xi^5$ on $K_{\pm}^{o}$, we have

$$f^{(5)} = 31 + 56\xi + 66\xi^2 + 56\xi^3 + 31\xi^4 + (16 + 28\xi + 16\xi^2)\,\eta^2 + \eta^4.$$

The simple structure underlying all these polynomials, which is undoubtedly something like the structure of $g$ in the previous problem has not yet been recognized. Although the factor

$(z-1)$ vanishes on $K^o$, it is interesting to observe what happens to the $f^{(n)}$s. In the case of $\lambda = 1$, $f_1^{(n)}$ becomes, apart from a numerical factor,

$$\frac{1-\xi^n}{1-\xi} \quad \text{on } K_+^o$$

(compare the initial value for g above!), and similar things occur for other integral values of $\lambda$.

Finally, special solutions have been obtained which do one thing on $K_+^o$ and another on $K_-^o$. From such solutions one could construct representations of the interaction of dissimilar simple waves, occurring when the two pistons do not move symmetrically or when a simple wave is neglected on a moving wall. This, however, has not yet developed into anything like a general method for the treatment of such problems.

## *H. LARGE AMPLITUDE GAS VIBRATION SOURCE. (NYU-7R5).*

*Submitted by: G.E. Hudson, New York University.*

The theoretical work being done on all types of jet propulsion devices shows that when oscillations of finite amplitude occur in a gas-filled tube, the differential equations involved are no longer linear and are not readily solved. For this reason, experiments which are proving valuable in the development of a theoretical description of these motions have been devised to indicate, and to permit qualitative study of, the important phenomena. To produce gas oscillations, a piston 1½ in. x 1½ in. in cross section and having a total amplitude of motion of ¼ inch was installed at one end of a square brass tube that was open at the other end. The sidewalls of the tube are cut away for about six inches at the open end, and this cutaway section and the region outside the open end of the tube are sandwiched between vertical glass plates so that the flow is visible in the Schlieren field and is essentially two-dimensional. Schlieren photographs of the gas motion, which of course reaches its maximum amplitude when the piston is oscillated at the resonant frequency of the tube, show a pattern of flow that is very similar to that occurring at the end of the tailpipe of a pulsejet engine.

It was found that the flow pattern at the end of the tube was such that two very strong vortices were set up just inside the tube lips These vortices whirl in opposite senses in such fashion that the flow into the tube is along the axis. As outflow begins, these vortices are expelled from the tube and, still whirling, push the outside air away from the tube

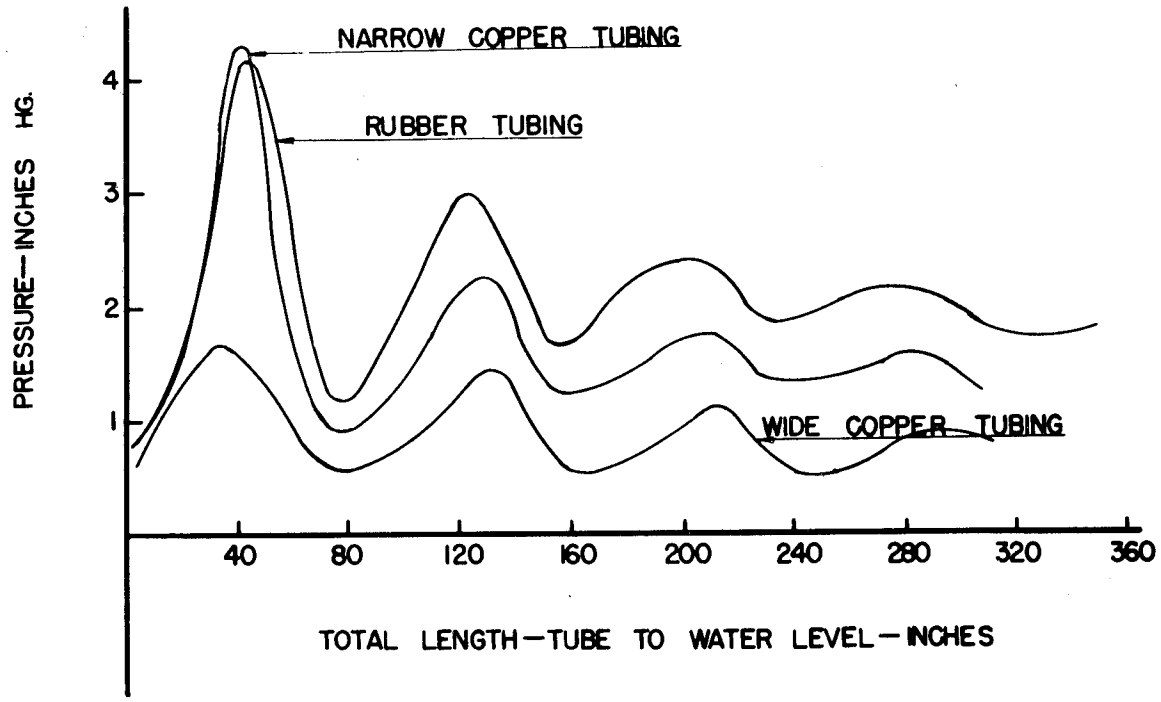


Fig. 16. Manometer figure for 3 tubes.

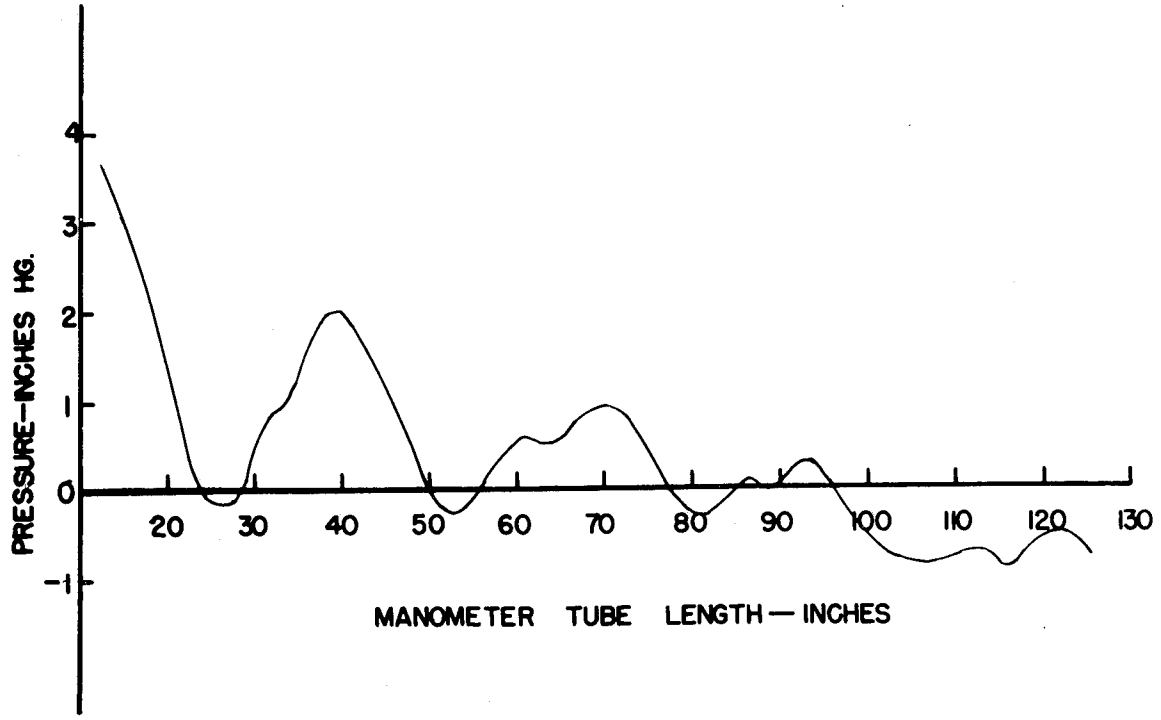


Fig. 17. Manometer figure for Dynajet.

mouth. As this occurs two more eddys are formed behind the first pair. These new eddys rotate in the opposite direction to the first two, and are apparently formed by the viscous drag between the surrounding air and the air coming out of the tube. As both pairs of eddys move away from the open end of the tube, the column of air in the tube becomes rarefied and finally comes to rest. Soon outside air starts to flow back into the tube, from above and below, necking off the outward flowing jet. Two small vortices are immediately generated just inside the lips of the tube, gradually growing in size and angular velocity until they are identical to the original pair. The flow into the tube then slows down and the cycle is repeated.

If the two lips of the tube are flared outward, however, the vortex and jet formation are almost totally absent even with the large amplitude of oscillation occurring near resonance, and the inflow and outflow both appear to be practically potential type flows. This difference in flow patterns is probably the basic reason that a flare at the end of the tailpipe of a small pulsejet produces an increase in thrust. A detailed study of the effect of flared tube lips can, however, only be made if the amplitude of gas oscillation is sufficient to cause detachment of a portion of the jet of gas expelled during each cycle.

To obtain these larger amplitudes of gas motion, a one-cylinder motorcycle engine is being modified to act as the oscillating piston assembly for a similar tube. The stroke of the piston will be 3 inches instead of ¼ in., and it is expected that a cyclic rate greater than 120 cps will be obtainable. This unit will be driven by a 3-horsepower electric motor and the resulting flow patterns will be observed by taking high speed Schlieren motion pictures.

During the course of the above experiments several other matters have been investigated, namely, test of an assumption concerning the dependability of manometer readings, and improvement and simplification of the Schlieren system now in use.

It has usually been assumed that while a manometer might be undependable for following the variation of a pressure changing fairly rapidly with time, it was dependable for measuring average pressure in cases where the pressure fluctuated very rapidly. A series of tests made during the past year has demonstrated, however, that when a water manometer was connected to a pressure pickup point near the closed end of the resonant tube described above, the average pressure readings obtained varied greatly as the length of the connecting tube was changed. Figure 16 shows the average pressure values obtained when the length of tubing connecting the manometer and the pick-off point was varied. These measurements were made for ⅛ in. I.D. Tygon tubing, and were repeated for both ⅛ in. and ⅜ in. I.D. rigid-walled tubing. The effect of greatly increasing the length of the tubing was also measured, and it was found that though

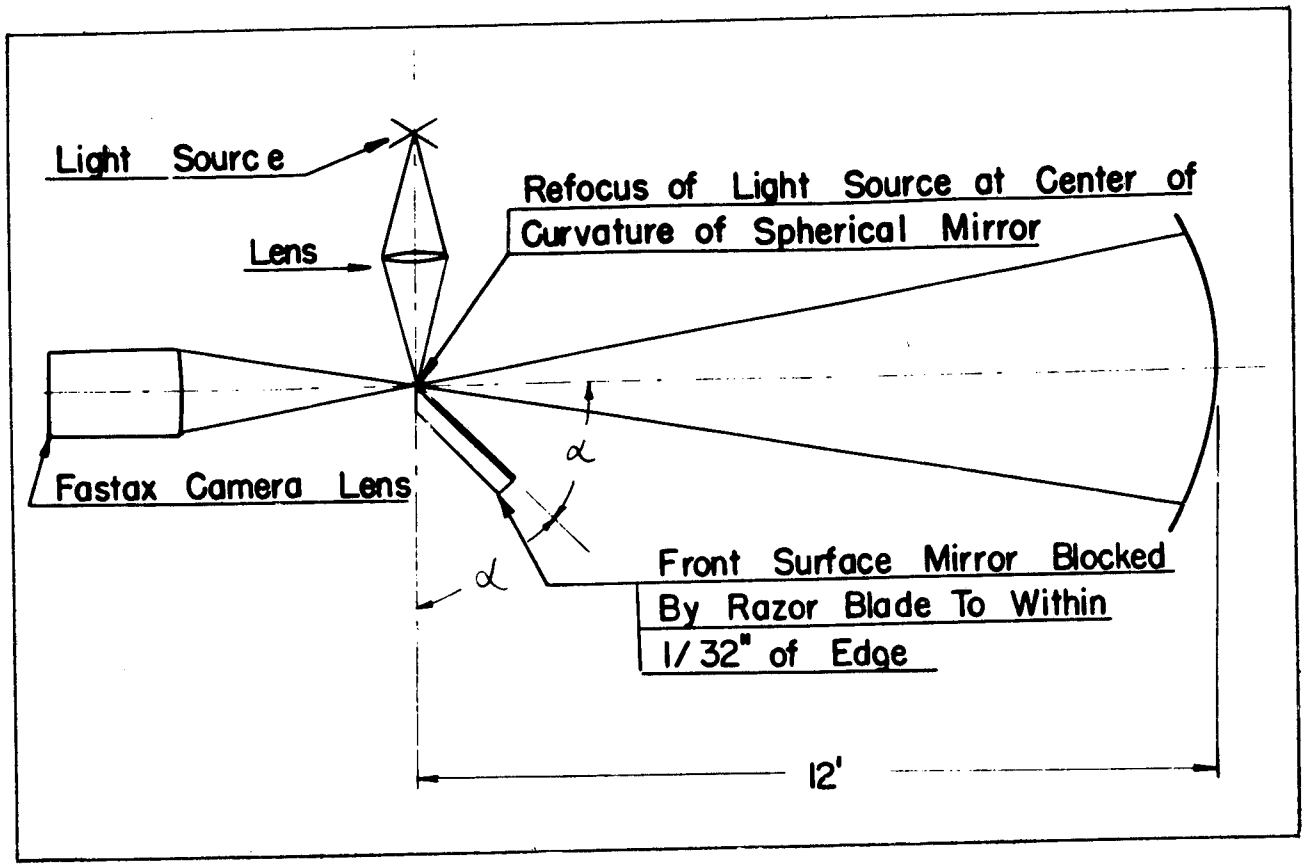


**Fig. 18.** Sketch (not to scale) of layout of parts for single mirror Schlieren setup with reflecting knife edge.

the average pressure readings seemed to be settling down to a fairly low average value near 25 feet, they gradually rose as the tube length was increased to 200 feet (not shown in Figure 16).

A series of tests was immediately made on a small pulsejet engine to determine whether a similar effect was present when a manometer was used to measure the average pressure in such an engine. The effect of variations between runs was compensated for by correcting the readings of the manometer whose tube length was changed, by the amount that the average of the readings of reference manometers of two differing but constant tube lengths, varied from the average obtained on a particular run chosen as standard. Though the fluctuation in the average of the readings for the reference manometers from one run to the next was severe, the plot of corrected readings for the manometer of varying tube length was remarkably smooth (See Figure 17.) and indicated that the corrections obtained by the use of the reference manometers satisfactorily

compensated for any variations between runs. The average pressure reading observed for any given engine will therefore be markedly affected by the length of manometer tube used. A Technical Memorandum on this subject is in preparation, and the actual average pressure present in the resonant tube and in the small pulsejet will be determined by calculation from instantaneous pressure records taken with the New York University pressure gauge system.

To obtain a Schlieren system of increased sensitivity, yet satisfactory definition, an improved single mirror Schlieren system using a 16-inch spherical mirror of 12 feet focal length has been been set up. In this system the knife edge is mounted at the focus of the mirror and is so inclined that it can at the same time be used as the effective source of the light (See Figure 18). With this arrangement the light incident on the mirror returns almost along the same path even when diffracted on its first passage through the occurrence, giving the desired increase in sensitivity with satisfactory definition.

## *I. STUDY OF THE MECHANISM OF THE ACOUSTIC JET. (CAL-1R2)*

*Submitted by: J.V. Foa and G. Rudinger, Cornell Aeronautical Laboratory.*

The term *acoustic jet* has been applied to devices in which thrust is produced by a piston oscillating in a tube. The specific impulse and thrust of an acoustic jet of infinite length have been analyzed previously for the case of sinusoidal piston oscillations.[5]

It was found, in agreement with experiments, that acoustic jets have extremely high values of specific impulse but that their thrust per unit area is very low at feasible operating frequencies and piston strokes.

The analysis has been extended to unsymmetrical piston motions. The case investigated was that of constant but unequal forward and backward velocities of the piston. The ratio of these velocities provided a new parameter in addition to piston stroke and frequency of the oscillations of the previous case. The result of the analysis was that, contrary to the case of sinusoidal motions, very large values of thrust could be obtained at any operating frequency by making the forward velocity of the piston sufficiently high. However, considering the difficulty of producing extremely high piston velocities, a fairer comparison between the two modes of operation considered would be based on equal maximum velocities in the two cases.

[5] Project Squid, Annual Program Report, January 1949, Cornell Aeronautical Laboratory, p. 112.

When that was done, it was found that the thrust produced by either type of piston motion was about the same.

On the basis of this theory, an acoustic jet of finite length operating at resonance frequency would produce several times as much thrust as an infinitely long unit due to wave reinforcement but not enough thrust per unit area to make the acoustic jet a practical unit for propulsion purposes. A more rigorous analysis would, of course, have to account for the three-dimensional phenomena that have been observed in the vicinity of the exit but it is doubtful that it would result in a radically different evaluation of this powerplant.

The acoustic jet appears to be a suitable model for theoretical and experimental investigations of certain non-steady flow phenomena. An example of this kind is the problem of periodic gas oscillations of large amplitude. With few exceptions, all non-steady flows of practical importance are periodic and no satisfactory method is available to analyze such flows. The method of characteristics can only be applied to problems where the initial conditions are given. In a periodic process, however, these are not known and one would have to start constructing a characteristics diagram from the known initial steady state. The difference between the first cycle and the final periodic state may be considerable, but it is quite impracticable to carry on the construction of a diagram for a number of cycles until at least an approximately periodic state is reached, because of the gradual accumulation of errors and because, in general, the time required for such an effort would be prohibitive.

Attempts were made to obtain periodic solutions by other means. Following a paper by Schultz-Grunow,[6] a modification of the method of characteristics was tried. A periodic state is characterized by the exact reoccurence of all conditions at regular time intervals. In particular, if a wave travel is plotted in a *state plane* (flow velocity u and speed of sound a as coordinates), the resulting path will be a closed curve or polygon.. Schultz-Grunow neglects the interaction of waves and assumes a *mean wave velocity* for which a reasonable constant value is taken. Since the time of wave travel follows from this assumption, the polygon may be drawn from an arbitrary starting point. The corner points are determined by the boundary conditions which either give one parameter as a periodic function of time or relate the state parameters in a manner that can be plotted as a fixed curve in the state plane.

[6] F. Schultz-Grunow, *Zeitschrift fur augewandte Math. and Mech.*, 25/27,155 (1948).

This method was somewhat extended and applied to the acoustic jet using mean wave velocities instead of selected fixed values. Mean values of thrust and specific impulse could thus be determined and were of the correct order of magnitude. It was also found that the frequency of resonance would decrease with increasing maximum piston velocity. A final evaluation will require further theoretical and perhaps experimental work.

In view of the importance of finding approximate periodic solutions other approaches were also explored. With the mean wave velocity assumed to be constant and neglecting interaction of waves and pressure drop during inflow, it is possible to solve the problem of the acoustic jet by setting up an infinite series of terms each of which represents the contribution from one wave reflection. The sum of the series could be obtained in a general form from which the pressure at the piston could be determined. This method may be of practical value, however, only if a satisfactory way can be found for taking into account the losses due to pressure drop at the exit during inflow and the like.

Another approach to the problem of periodic flows was based on a perturbation method for the solution of the Riemann functions. By substituting a series expansion for the Riemann functions, a linear system of differential equations for the terms of various order was derived. A general solution for the first order terms was obtained but it is doubtful whether the differential equations for the second order can be solved even for simple forcing functions. A report on this method is in preparation.

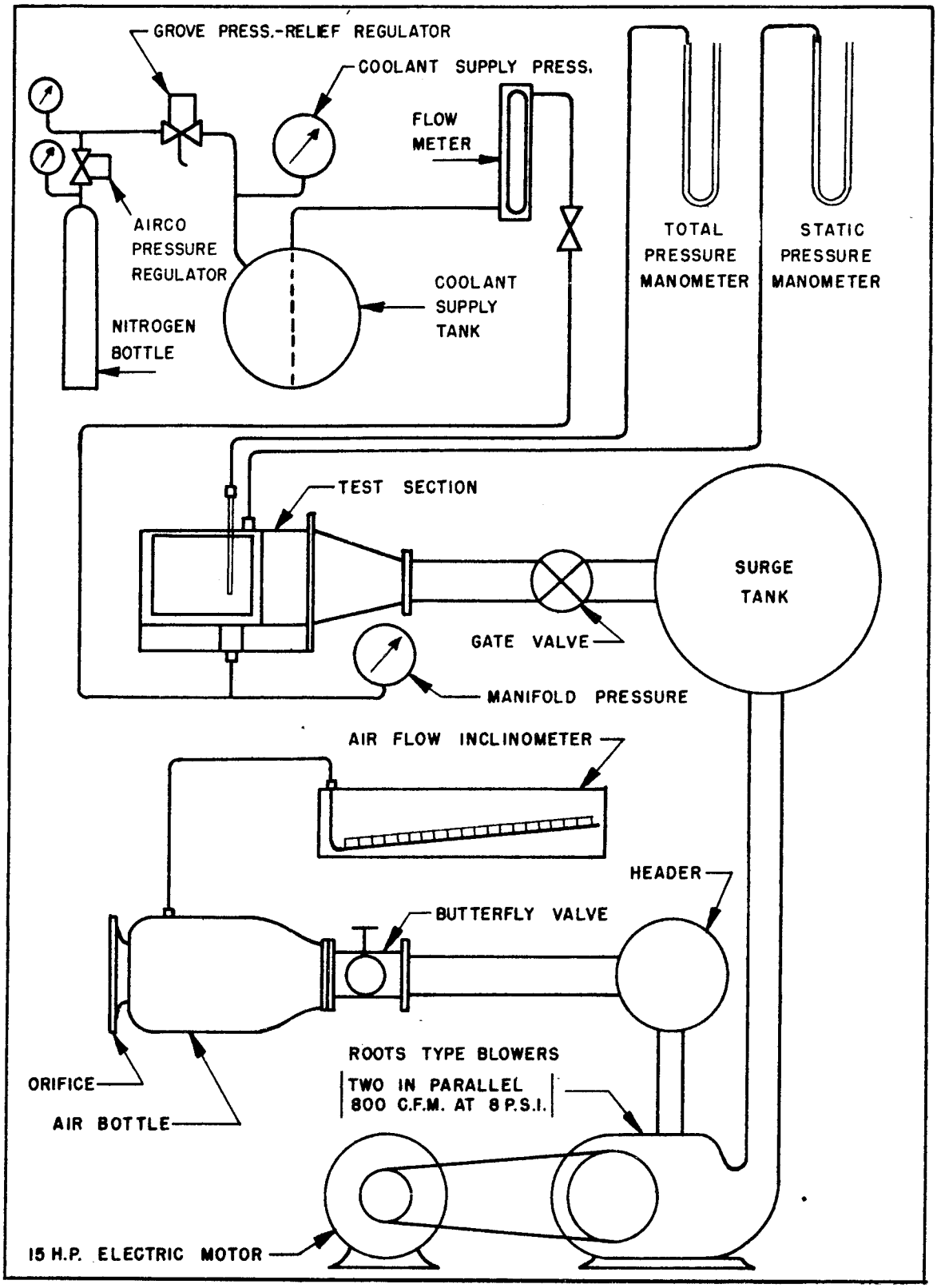


Fig. 1. Diagram of test apparatus.

# III. HEAT TRANSFER

## A. *TRANSPIRATION COOLING BY FLOW OF FLUID THROUGH PARALLEL DISKS. (PRF-7R10)*

*Submitted by: E.L. Knuth, Purdue University.*

The aims of this investigation are: to obtain fundamental data from which can be determined, for transpiration cooling of rocket motors through parallel disks, the critical coolant velocity when the coolant properties, propellant gas properties, propellant gas Reynolds number, and the configuration used for injecting the coolant are known; and the investigation of the effect of transpiration cooling through parallel disks on the heat transfer in a rocket motor.

A test section was designed and built for determining the relationship between the critical coolant velocity and the independent variables. Figure 1 indicates schematically the test apparatus while Figure 2 presents details of the test section. Note the shims in Figure 2, the thickness of which can be varied to give different slot thicknesses.

Critical velocity of injection was defined as *the average velocity of the coolant at the injection location at the time that the maximum rate of coolant is obtained without encountering separation of the coolant flow from the test section wall.*

Tests were conducted at the critical velocity of injection with various coolant densities, coolant viscosities, surface tensions, main stream Reynolds numbers, and coolant injector widths. Figure 3 is a plot of

$$\rho V\sqrt{\frac{W}{t}}\,\mu^{0.75} \quad vs. \quad Re,$$

where

Re = main stream Reynolds number

T = surface tension of injected liquid, lb./ft.

V = critical velocity of injection ft./sec.

W = width of slot, ft

$\rho$ = density of injected liquid, lb./ft.$^3$

$\mu$ = viscosity of injected liquid, lb./ft.-sec.

From this plot, the following empirical equation was obtained:

$$\rho\, V\sqrt{\frac{W}{T}}\,\mu^{0.75} = (8.25 \times 10^{-7})\, Re + 0.22$$

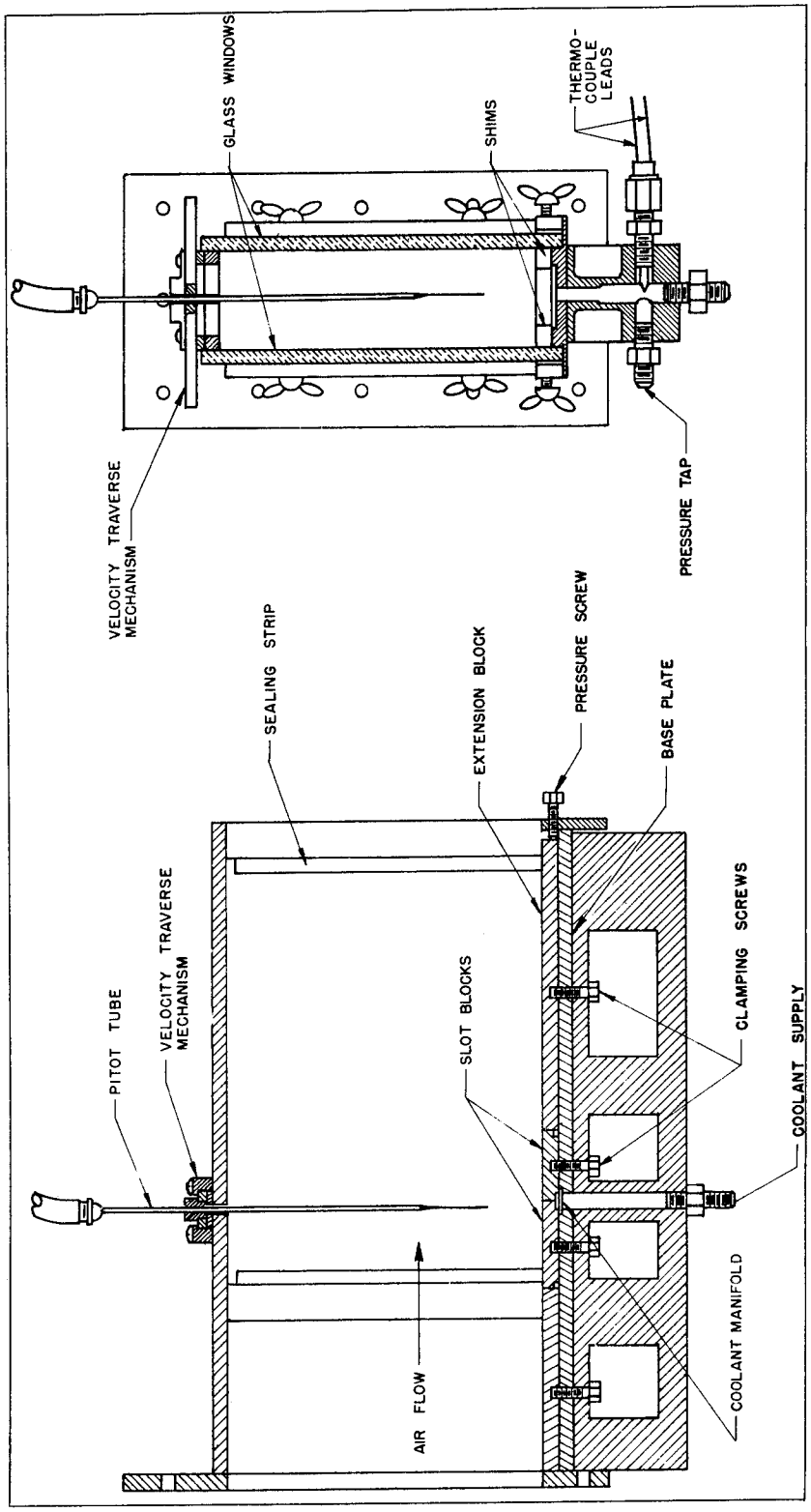


Fig. 2. Test Section

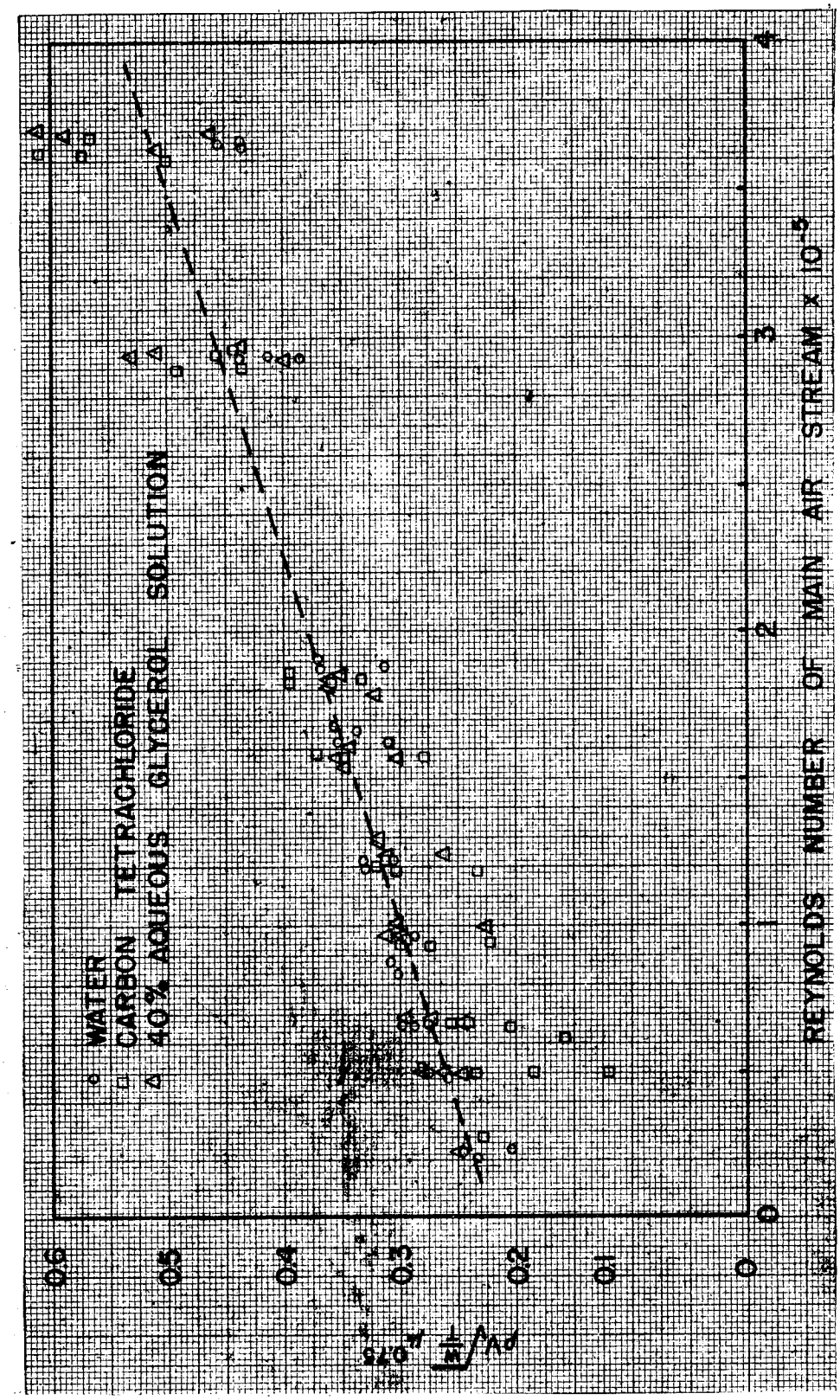


Fig. 3. Main stream Reynolds number *vs.* $\rho V \sqrt{\frac{M}{T}} \mu^{0.75}$

To check the validity of the foregoing equation over wider ranges of the variables than were originally investigated, more tests have been conducted. Wider fluid viscosity ranges were obtained by employing glycerol solutions, wider fluid density ranges by using zinc chloride solutions, and wider surface tension ranges by means of soap solutions. The slot width was varied by means of shims having different thicknesses. Data secured from the later tests are now being analyzed.

An apparatus has been designed for heat transfer studies using transpiration cooling. The apparatus is designed to investigate: correlation of cooling effect with critical velocity of injection; downstream cooling effect for one slot for various coolant and hot gas flows; and validity of the available theoretical equations for flow through laminations.

The research on the injection of fluids into an unheated gas stream is to be continued. The immediate plans are to study the following factors: the effect of gravity by inverting the test section; the effect of the size of the main stream duct by decreasing the size of the duct; the effect of varying the angle of injection of the coolant by changing the slot configurations; the effects when the liquid is injected at the junction of a flat and inclined surface; the effects when the liquid is injected at different distances upstream to an inclined surface; and the effects when the liquid is injected directly on an inclined surface.

Work with the injection of fluids into a heated gas stream will be initiated after the information discussed in the preceding paragraph becomes available. Apparatus for studying the injection of liquids in a heated gas stream is in the planning stage.

When the injection of fluids into both heated and unheated gas streams has been investigated sufficiently, the information obtained from these studies will be used in the design of a disk-type transpiration-cooled rocket motor. It is anticipated that a motor of the above type will be required in the investigation of motors operating at high combustion chamber pressures.

## *B. THEORY OF NON-LINEAR HEAT CONDUCTION IN SIMPLE METALS. (NYU-7R9).*

*Submitted by: G.E. Hudson and M.J. Storm, New York University.*

Investigations of heat transfer processes occurring in the metallic components of intermittent jet engines have indicated that, because of the dependence of specific heat, thermal

conductivity, and density upon the temperature, the temperature distributions calculated on the basis of the linear heat conduction equation may be significantly in error. The following theoretical study represents an attempt to improve the analysis.

Consider an isotropic solid through which heat is flowing but in which no heat is being generated. If T is the temperature of the solid at time t at the point (x,y,z), K is the thermal conductivity, and S the product of density multiplied by the specific heat at constant pressure, then the differential equation which governs the temperature of the solid is

$$\text{div } [K \text{ grad } T] = S \frac{\delta T}{\delta t} \tag{1}$$

Solutions of equation (1) can be obtained for the case of steady heat flow when the thermal conductivity is assumed to be a known function of temperature; and approximate solutions of the non-steady one-dimensional equation can be made under the assumption that the thermal parameters vary parabolically with temperature. Numerical calculations of specific cases can be made, but they possess the essential difficulty that statements of a general nature as to the effect of variations in the boundary conditions and geometry are very difficult to make.

Since the thermal parameters (K,S) are functions of temperature, equation (1) is non-linear. In the usual mathematical formulation it is assumed that the thermal parameters are constant, an approximation which holds for limited ranges of temperature, and the equation dealt with is then

$$\nabla^2 T = \frac{S}{K} \frac{\delta T}{\delta t} \tag{2}$$

Solutions of this linear equation when subject to various boundary conditions have been thoroughly investigated. In the case of metals, such theoretical treatments as (2) which assume that the thermal parameters are constant may be seriously in error, as the variation of these quantities can be quite large over wide temperature ranges.

In this study, an attempt is being made to take into account the physical theory underlying the variation with temperature of the thermal parameters, or of some appropriate combination of them, and then to use these facts to transform the non-linear equation into some form more amenable to mathematical analysis. To date, only the one-dimensional equation

$$\frac{\delta}{\delta x}\left(K \frac{\delta T}{\delta X}\right) = S \frac{\delta T}{\delta t} \tag{3}$$

has been treated.

It has been found possible to transform equation (3) into one where the thermal parameters appear only in the combination

$$\frac{d}{dQ} \ln\sqrt{\frac{S}{K}} \quad \text{where } Q = \int_{T_o}^{T} \sqrt{KS}\, dT,$$

$T_o$ being some arbitrary temperature. The transformed equation can then be linearized by the mathematical assumption that $\frac{d}{dQ} \ln\sqrt{\frac{S}{K}} = A$, a constant.

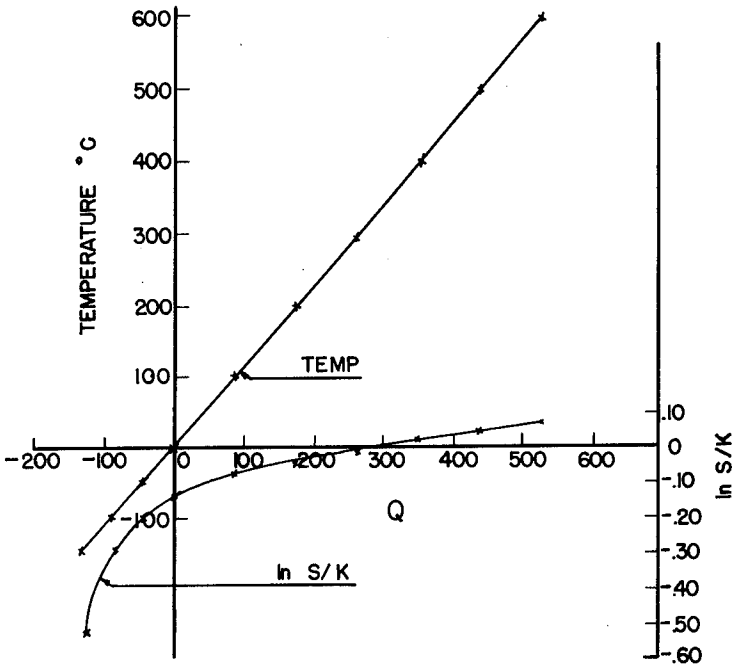


Fig. 4. Plot of $\ln \frac{S}{K}$ *vs.* Q.

Preliminary theoretical investigations indicate that the relation $\frac{d}{dQ} \ln\sqrt{\frac{S}{K}} = A$ holds for temperatures greater than the Debye temperature, which offers no serious obstacle to practical application of the heat conduction equation. This work also shows that in this temperature range, A is not an absolute constant but a slight function of temperature.

An analysis of available empirical data indicates that for simple metals like copper, A is essentially constant for temperatures greater than the Debye temperature; and that for a transition metal like iron, A is constant between the Debye temperature and the temperature at which the first phase change occurs. Over these temperature ranges $\frac{d}{dQ} \ln\sqrt{\frac{S}{K}}$ is more constant than either of the quantities S or K which are assumed to be constant in the usual linearized form of the heat equation

$$\frac{\delta^2 T}{\delta X^2} = \frac{S}{K} \frac{\delta T}{\delta t} \qquad (4)$$

The following curves (See Figure 4.) are plots of $\ln \frac{S}{K}$ versus Q, and T versus Q for copper. The Debye temperature for copper is 315°K which corresponds to Q = 36. It is seen that for Q > 36 curve (1) is essentially a straight line. Further investigation of the theoretical basis for the proposed relation between the thermal parameters is planned.

The linearized equation has already been solved for the case of a semi-infinite metal rod, and the solution for the finite case is now being worked on. Both solutions will be compared with those obtained from the usual linearized theory in order to estimate the errors involved in neglecting the variation with temperature of the thermal coefficients. The possibility of applying the method to different forms of the heat equation subject to appropriate boundary conditions will also be investigated.

## C. *FREE CONVECTION HEAT TRANSFER WITH COUNTERFLOW. (Del-1R1).*

*Submitted by: S.A. Guerrieri, University of Delaware.*

Heat transfer by free convection between a surface and a fluid in contact with it was first treated mathematically by Lorenz[1] in 1881. For the particular case of a vertical plane surface in air he postulated that upward flow of air along the plane took place because of density differences resulting from temperature differences. Further, he assumed that the air flow adjacent to the plane was laminar and that viscosity was independent of temperature.

Applying Newton's equation of motion to the air, he derived the following equation for steady state conditions:

$$h_{mean} = 0.548 \left( \frac{g \rho^2 C_p k^3 \Delta t}{\mu L T_o} \right)^{1/4} \qquad (1)$$

$h$ = mean coeff. of heat transfer by convection
$L$ = height of the surface
$\Delta_t$ = temperature difference between bulk of air and plane
$T_o$ = temperature of bulk of air
$\mu$ = viscosity of air
$g$ = local acceleration of gravity
$\rho$ = density of air at $T$
$C_p$ = specific heat of air
$k$ = thermal conductivity of air

Nusselt and Jurges[2] in 1928, derived an equation similar to the above on the basis of a somewhat different theoretical approach. Pohlhausen[3] integrated numerically the differential equations of Schmidt and Beckmann to derive an equation similar to the one given above but with a slightly different coefficient.

---

[1] L. Lorenz, *Wied. Ann.*, 13, 582 (1881).

[2] W. Nusselt, W. Jurges, *Z. Ver. aeut. Ing.*, 72, 597 (1928).

[3] E. Schmidt, W. Beckman, *Tech. Mech. Thermodynamics*, 341, 391 (1930).

Colburn and Hougen[4] derived an equation for heat transfer by free convection between a vertical plane surface and a fluid on the theory that the character of the flow changed from laminar to turbulent as the distance out from the surface is increased, (due to differences in buoyancy caused by differences in temperature) and that this change occurs at a critical value of the Reynolds number, $\theta u_\theta \rho/\mu$, where $\theta$ is the thickness of the laminar sublayer, $u_\theta$ is the velocity of the outer boundary of the laminar sublayer, $\rho$ and $\mu$ are the density and viscosity, respectively, of the fluid. Furthermore, assuming that the critical value of the Reynolds number is the same for this case as for fluid flowing through pipes, they were able to derive an expression for the thickness of the laminar sublayer and consequently an equation for the heat transfer coefficient by introducing the relation $h = k/\theta$ where h is the heat transfer coefficient and k is the thermal conductivity of the fluid. The theoretical equation so derived is:

$$h = 0.108\ k\ (\rho^2\ g\ \beta\ \Delta t/\mu^2)^{1/3} \qquad (2)$$

Both of these equations can be converted into the more generally preferred dimensionless forms whereby (1) becomes

$$hL/k = 0.548\ (L^3\rho^2\ g\ \beta\ \Delta t/\mu^2 \cdot C_p\mu/k)^{1/4} \qquad (3)$$

and equation (2) becomes:

$$hL/k \doteq 0.108\ (L^3\ \rho^2\ g\ \beta\ \Delta t/\mu^2)^{1/3} \qquad (4)$$

$hL/k = N_{Nu}$ = Nusselt number

$L^3\rho^2 g\beta\Delta t/\mu^2 = N_{Gr}$ = Grashof number

$c\mu/k = N_{Pr}$ = Prandtl number

One significant feature of these theoretical equations, which have been derived on the basis of simplified heat transfer mechanisms, is the remarkable agreement with the data over certain relatively wide ranges. Thus, when the flow is entirely laminar a slightly modified form of equation (3) employing the term $(N_{Gr}\ N_{Pr})^{1/4}$ fits the data for values of $(N_{Gr}\ N_{Pr})$ ranging from approximately $10^4$ to $10^9$. When the flow is such that turbulent sublayer is present beyond the laminar sublayer, that is for values of $(N_{Gr}\ N_{Pr})$ ranging from approximately $10^9$ to $10^{12}$ which is as far as present data extend, a modified form of equation (4) employing the term $(N_{Gr}\ N_{Pr}{}^a)^{1/3}$ appears to fit the data better. The derivation of equation (2) clearly brings out the relation between the thickness of the laminar sublayer and the Grashof number. In general, the thickness of the laminar sublayer appears to be inversely proportional to the

[4] A.P. Colburn, O.A. Hougen, *Univ. Wis. Eng. Expt. Sta. Bull*, 70, (1930).

Grashof number raised to a fractional power, the ¼ power when the flow is completely laminar, the ⅓ power when a turbulent sublayer is present beyond the laminar sublayer.

Similar correlations have been developed for horizontal cylinders, but little or no work has been done on free convection inside vertical tubes. However, it should be possible to evaluate heat transfer between tube wall and fluid for this case on the basis of existing correlations if care is taken to satisfy energy balances. For the case of free convection with counterflow, which is the one of interest in connection with the cooling of gas turbines, there are at present no means available to predict what the heat flow will be under a given set of conditions.

In the case of heat transfer in the cooling passages of turbine blades, the only condition which is different from ordinary problems of heat transfer is the change in the gravitational forces due to rotational effects. Because centripetal forces of rotation behave in the same way as gravitational forces, the effect of rotation of the turbine wheel may be considered simply as a multiplier of normal gravitational force (approximately 25,000 - 30,000 times at typical turbine blade speeds). Reference to equations (3) and (4) shows that the Grashof group increases by a like amount, assuming all other factors are kept constant. If the film thickness is in fact inversely proportional to the Grashof number raised to a power, the large reduction in laminar sublayer thickness and the corresponding increase in free convection heat transfer coefficient due to rotation is obvious. For example, if it is assumed that the conditions are such that a turbulent sublayer exists outside of the laminar sublayer, than, according to equation (4) the thickness of the laminar sublayer is inversely proportional to $(N_{Gr})^{1/3}$. If a turbine wheel speed is assumed, which increases gravitational force by 27,000 times, all other factors remaining the same, the laminar sublayer thickness is reduced to $^1/_{30}$ of that which would be obtained under natural gravity while the heat transfer coefficient would be increased to 30 times the value it would have had in a stationary passage. It is evident, therefore, that free convection can be an important factor, if not a controlling one, in heat transfer between wall and fluid inside the cooling passages of turbine blades. These considerations have not taken into account the effects of counterflow.

There are a number of methods by which turbine blades can be cooled. These methods will not be discussed but include various combinations of fluids flowing in passages open at the tips, or closed at the tips. In substantially all of these methods the heat transfer problem in the passages is one of natural convection with counterflow. However, the effect of counterflow. However, the effect of counterflow on the overall results cannot be predicted on the basis of present knowledge of heat transfer. Therefore, one of the principal objects of the

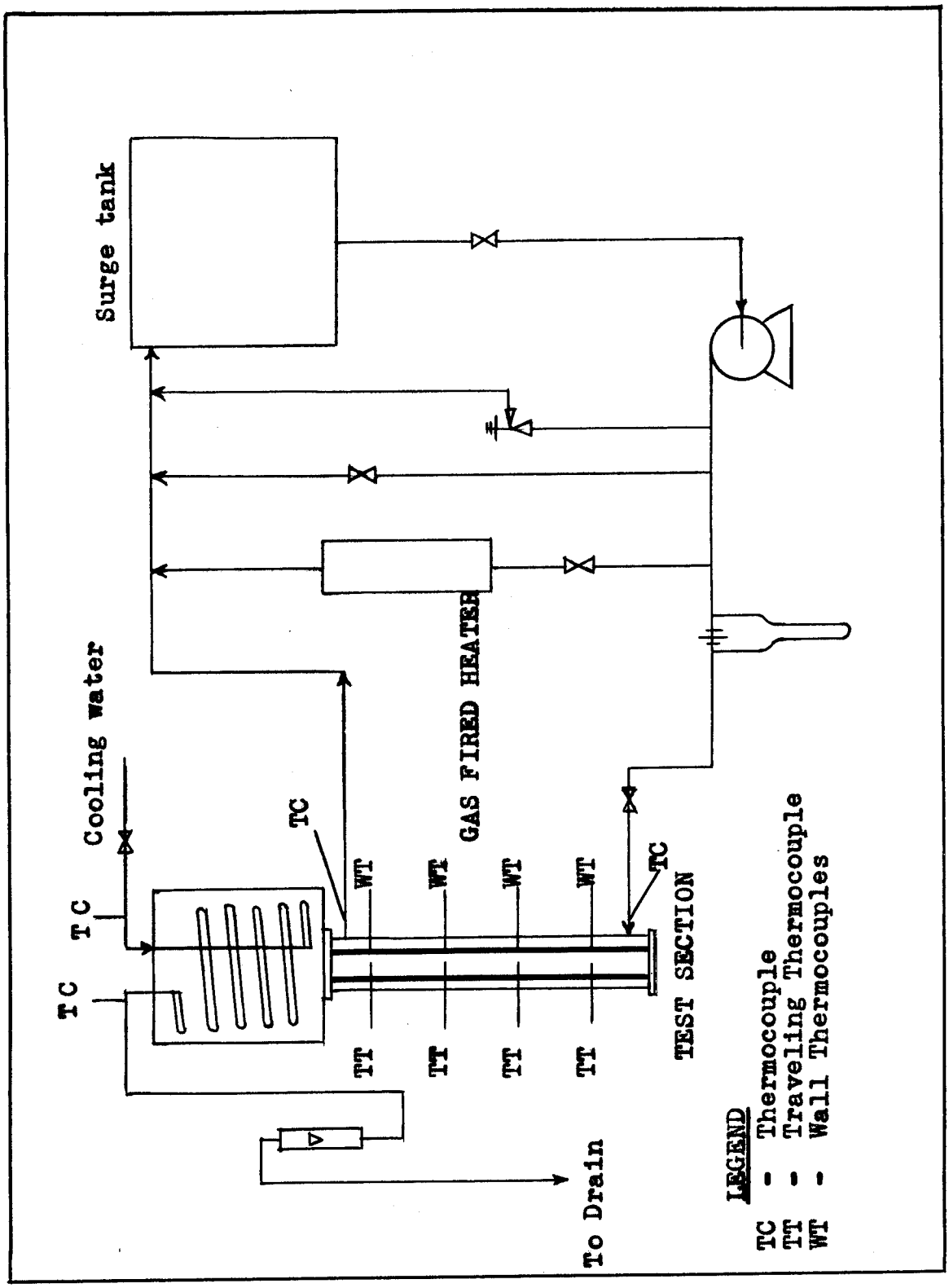


Fig. 5. Experimental apparatus for quantitative study.

present investigation is to study the effects of counterflow. Whether the net results of the counterflow is to increase or to decrease the thickness of the laminar sublayer can only be determined by tests. However, it is expected that the counterflowing fluid will have a profound influence on the heat transfer since it is ultimately the vehicle which carries away the heat which has been transferred.

To study the factors occurring in the Grashof, Prandtl and Nusselt groups above, under the flow condition existing in the passages of a blade, two general methods are possible. One method would be the use of a test turbine to study blade cooling under actual operating conditions. This method would be costly, difficult, and would not give fundamental knowledge of the actual heat transfer mechanism occurring with counter flow. The other method would be the use of a static model in which it would be possible to study the effects of the various controlling factors in turn over as wide a range as possible and determine suitable generalized relationships among the variables. The variables would be those changing the Grashof, Nusselt and Prandtl moduli, and also Reynolds modulus for the counterflowing fluid. This can be done by changing test conditions and test fluids.

The laws which hold for the heat transfer from the inside walls of a heated vertical cylinder to a fluid contained in the cylinder are being investigated with the following apparatus (Figure 5). A copper tube, 1.125 in. I.D. and 1.9 in. O.D., twenty-four inches long, is connected to the bottom of a chamber made from a section of 8-in. steel pipe in a vertical position. The copper tube is heated uniformly with hot oil which circulates in an annulus formed by the copper tube and a close fitting jacket. Thermocouples are provided to measure the tube wall temperature at four points approximately six inches apart. The traveling thermocouples which are used to obtain temperature profiles across the tube are located on the same plane as the tube wall thermocouples, thus making it possible to obtain temperature differences between the wall and the fluid at these locations. Thermocouples are used to determine the temperature change of the hot oil. The chamber above the tube contains a cooling coil to remove from the test fluid the heat which it has absorbed in the tube. Thermocouples are provided to determine the change in temperature of the cooling water passing through the coil; a rotameter is used to determine the flow rate.

The heating oil in the surge tank is maintained at the desired test temperature by recirculating it through a gas-fired heater by means of a turbine type pump. A high rate of flow is maintained through the heater and heat input to the system is controlled by varying the supply of gas to the burner. Hot oil from the pump is circulated through the annulus of the test apparatus at a controlled rate which is measured by a calibrated flow meter.

In order to coordinate the work at this university with certain parallel investigations at the Lewis Flight Propulsion Laboratory of the National Advisory Committee for Aeronautics, emphasis will initially be placed on experiments employing a closed system such as is shown in Figure 5. All runs which have been made to the present time have been with the closed system. In operation, the tube and the chamber is filled with the test liquid. Heating oil is circulated through the jacket at a predetermined rate and temperature, thereby heating the liquid in the tube. The addition of heat increases the temperature and decreases the density of the boundary layer; this layer rises along the inside wall of the tube to the large chamber above. The liquid so displaced is replaced by cooler liquid from the large chamber flowing down the center of the tube. In this manner, free convection of the test fluid is started which carries heat from the copper tube wall to the cooling coil in the large chamber.

During the past year, the apparatus for this work has been completed. All measuring devices have been calibrated; performance tests on the heating oil circuit have shown it to be possible to hold the temperature of the heating oil going into the jacket constant within $\pm 0.1^{\circ}F$. A tentative calibration of the thermocouples has been completed and several runs have been made with this unit using water as the test fluid. The temperature profiles made with the traveling thermocouple across the diameter of the tube were not symmetric about the center line of the tube. This discrepancy was believed to be caused by heat conduction along the thermocouple material since it extends through alternate hot and cold layers of fluid. A new method of fabricating the thermocouple junction has been proposed and is being tried out. During the runs thermal stresses set up between the jacket and the copper tube caused the failure of several of the connecting tubes for the traveling thermocouples. These have been redesigned and fabricated and several other minor changes have been made to reduce errors.

Present work with water will be continued to determine the influence of temperature difference, temperature level, physical properties of the fluid, and tube height on heat flux and temperature profiles. After these variables have been studied for water, a series of runs will be made with other fluids to give as wide a range as possible in the Grashof number.

When this work has been completed, another similar series of runs will be made with the tube open at the top and bottom and counterflow will be forced convection instead of natural convection. This will allow the rate of flow to be an independent variable.

A visual study of the flow patterns created by the transfer of heat by natural convection to gases with and without counterflow is to be made with the following apparatus (Figure 6).

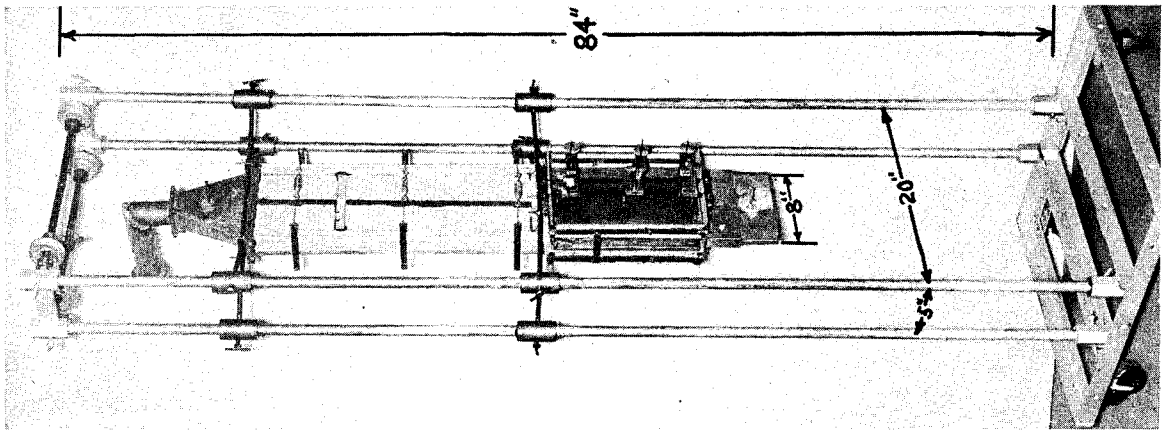


Fig. 6. Experimental apparatus for visual study.

The principal part of the equipment is the heating section which consists of two vertical parallel brass plates, eight inches wide, twelve inches high, three-eighths of an inch thick, and placed one inch apart; the thick plates are used in obtaining uniform wall temperatures. The other two sides are formed of glass to permit visual and photographic studies of the flow pattern. Mounted in back of each brass plate are transite boards to which are fastened the strip heaters that will heat the brass plates primarily by radiation. The strip heaters are arranged in banks of three heaters, with two banks behind each brass plate. Thus, there is a total of four banks, a total of twelve strip heaters. Each bank of heaters is connected through suitably wired magnetic double pole-double throw switches, wattmeter, and variable voltage transformers, to the 110 volt power lines (Figure 7). With the panel board constructed with four separate power inlets, it will be possible to control power input to any bank of strip heaters. Above the heating section there is a calming section approximately two feet long, which is constructed of transite boards and glass panels. The calming section of the apparatus is connected by flexible hose to the cooling air system which includes an orifice meter, a heater section that maintains the air supply at constant temperature, and a blower that forces the cooling air countercurrently through the apparatus.

In order to measure temperatures, three copper-constantan thermocouples are placed in each brass plate, at the top, middle, and bottom. Thermocouples are also placed to obtain the inlet and outlet gas temperatures.

In addition, three traveling thermocouples are placed at the top, middle, and bottom of one of the brass plates in order to take temperature profiles across the space between the two brass plates. These traveling thermocouples will be silver plated or gold plated and

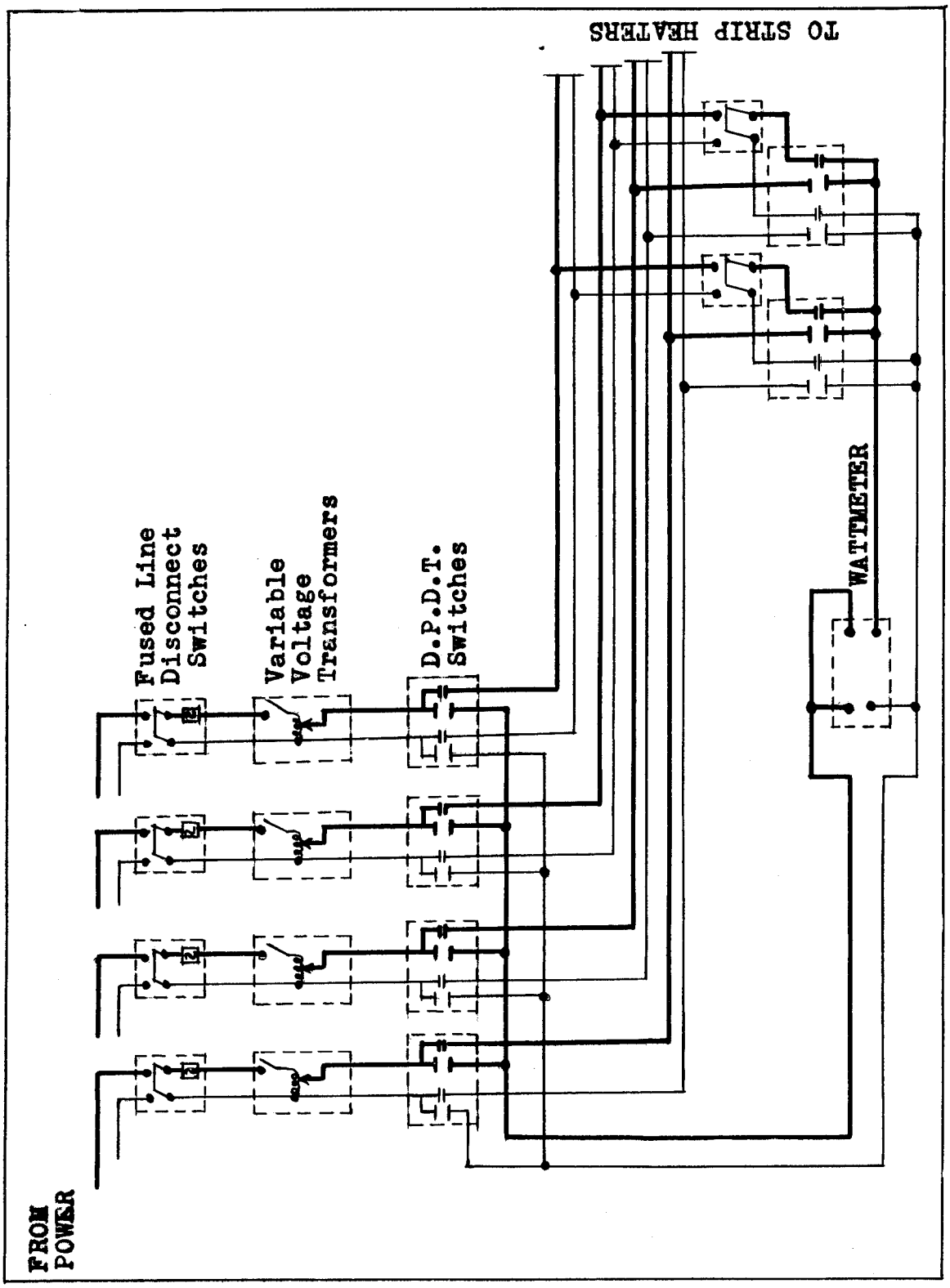


Fig. 7. Control panel wiring diagram for visual unit.

polished in order to minimize the errors created by radiation from the plates to the thermocouples.

The heating unit, calming section, and inlet and outlet parts are mounted together on four steel pipes in such a manner that the apparatus can be raised or lowered as needed (Figure 6).

In operation, the power input to the strip heaters is to be controlled so as to give the desired constant wall temperature at the face of the plate that is in contact with the gas layer. With the walls heated to the correct temperature, and heat transferring to the gaseous layer, the density of the layer will decrease. The layer then rises along the face of the vertical planes producing a flow pattern than can be visually studied by means of Schlieren or interference photography.

If counterflow patterns are desired, power is supplied to the heaters on the inlet gas duct, the blower is started and gas at a constant temperature slightly above room temperature is forced countercurrent to the upward flow of gas created in the heating section by means of natural convection. Thus flow patterns created by counterflow conditions can be readily studied.

During the last year, this apparatus was designed and completed. A tentative calibration was made on the thermocouples.

Experimental work with air will be started soon. A series of runs over a range of heat fluxes, temperature levels, and temperature gradients will be made. This will be followed by runs with other gases, lighter and heavier than air.

## *D. A THEORETICAL INVESTIGATION OF THE TEMPERATURE FIELD IN THE LAMINAR BOUNDARY LAYER (COMPRESSIBLE FLUID) ON A POROUS FLAT PLATE WITH FLUID INJECTION. (PIB-3R2).*

*Submitted by: S.W. Yuan, Polytechnic Institute of Brooklyn.*

The objective of the research under this problem assignment is to investigate analytically the velocity and temperature profiles in boundary layers on porous walls which are being cooled by fluid injection. After a review of the work completed during 1948, the analyses carried out this year and plans for next year are discussed.

In the early work,[5] a theoretical investigation of the flow of hot fluid over a complete porous flat plate under the condition of uniform fluid injection from the bottom of the plate was made. In the solutions of the laminar boundary layer equations, the momentum and energy equations were reduced to integral relation forms similar to the VonKarman integral relation of the Prandtl equation. The velocity and temperature profiles were assumed as polynomials of the fourth degree and also as exponential functions. The fluid mass density and viscosity were assumed to be constants which represent average values of their variation inside the boundary layer.

The velocity and the temperature profiles for different Prandtl numbers were calculated. The solution was also extended to the case where the coolant injection begins at any distance from the leading edge of the plate. The relations between the wall temperature and the rate of coolant injection were calculated for different Reynolds numbers, Prandtl numbers, and for a partially extended porous plate.

The investigation was extended to a laminar compressible boundary layer on a porous plate with fluid injection.[6] The assumptions made in this investigation were: (1) the inverse proportion between mass density and temperature inside the boundary layer was used, and the viscosity was assumed to be proportional to the square root and three-fourth power of the temperature; (2) the Prandtl number was assumed to be equal to unity, and the temperature inside the boundary layer was expressed by a certain parabolic function of the velocity inside the boundary layer; (3) the velocity profile mentioned in (2) was expressed as a linear function of the distance $y$, inside the boundary layer; and (4) the fluid flowing along the wall and the coolant flowing through the pores were assumed to be homogeneous. The relations between the wall temperature and the rate of coolant injection were calculated for different Mach numbers, Reynolds numbers, and viscosity variation with temperature.

A further investigation of the flow of a hot fluid over a porous flat plate under the condition of uniform injection from the bottom of the plate was made. In reference (6) the assumption was made, for Mach number equal to zero, that the fluid density varies inversely as a linear function of the distance $y$ inside the boundary layer; however, in this investigation, it was assumed that it varies inversely as a certain quartic function of the same

[5] S.W. Yuan, *A Theoretical Investigation of the Temperature Field in the Laminar Boundary Layer on a Porous Flat Plate with Fluid Injection,* Project Squid, Tech. Report No. 4, September, 1947.

[6] S.W. Yuan, "Heat Transfer in Laminar Compressible Boundary Layer on a Porous Flat Plate with Fluid Injection," *Jour. of the Aero. Sci.,* December, 1949.

distance y. The second degree term in the quartic function was now omitted in order to obtain an explicit solution.

In like manner the viscosity of the fluid was assumed to vary directly as the one-half power of the above-mentioned quartic function. Since the above-mentioned assumption would give a closer approximation to the actual phenomena due to the variation of fluid density and viscosity inside the boundary layer, it was the purpose of the investigation to determine the discrepancy between the results in reference (6) and those in the present case.

In the solution of the integral relation of the momentum equation, a process similar to that employed in reference (6) was carried out. The result was expressed by the relationship of length in the direction of flow to boundary layer thickness. The velocity and temperature profiles are then calculated for a Prandtl number equal to unity. From the temperature profiles the heat transfer characteristics of the flow can be established.

Since the quantity of heat per unit area removed from the plate is equal to the quantity of heat absorbed by the coolant at the surface of the plate per unit area, a relation between the wall temperature and the amount of coolant needed to cool the wall is established. The results of the above investigation can be summarized as follows:

(1) The boundary layer thickness along the direction of the flow in the present case (A) is larger than in case (B) given in reference (6). Furthermore, the difference of boundary layer thickness between cases (A) and (B) increases as the ratio of the free stream temperature $T_1$ to the wall temperature $T_W$, $(T_1/T_W)$, increases; the difference is about 15 per cent for $T_1/T_W = 2$, and about 30 per cent for $T_1/T_W = 4$.

(2) The temperature gradient at the wall for case (A) is less than that for case (B). This indicates that the heat transfer at the wall is greater in case (B) than in case (A).

(3) Thus for a predesignated wall temperature it is indicated that the rate of coolant injection is greater in case (B) than in case (A). More specifically, it appears that the mass coolant injection needed in case (A) is less than 10 per cent of that which is indicated in case (B).

The above investigation was submitted as a Technical Report entitled, *Further Investigation of Heat Transfer in a Laminar, Compressible Boundary Layer on a Porous Flat Plate with Fluid Injection - I.*

A further extension of the investigation of heat transfer in the laminar compressible boundary layer on a porous flat plate with constant fluid injection has been carried out. In this analysis, the mass density was assumed to vary inversely with a complete eighth-degree algebraic function of $y$, inside the boundary layer, and the viscosity directly with one-half power of the same eighth-degree algebraic function of $y$. The solution of the integral relation of the momentum equation was made possible by the transformation of the independent variable in the equation, as was done by Dorodnitzyn.[7] The result of this investigation should give more accurate information as to the relation between wall temperature and the rate of coolant injection. Furthermore, the relation between wall temperature and the rate of coolant injection can be calculated for a higher Mach number ($M>3$) than was possible with the method of the previous investigation.

A theoretical study of the heat transfer characteristics in a laminar compressible boundary layer on a partially porous flat plate with uniform fluid injection was completed. The plate is composed of an impermeable section followed by a porous (sweat-cooled) section. A previous investigation described in reference (6) was based on a fully porous flat plate with zero boundary layer thickness at the leading edge of the plate. The present investigation was carried out in order to provide better correlation with the experimental work in which only partially porous walls are usually studied.

Further assumptions made in this investigation were: the boundary layer thickness at the beginning of the porous section was taken to be that at the end of the impermeable section; the impermeable section of the plate was assumed to be thermally insulated; and the Mach number was assumed to be zero.

With the above assumptions, the velocity and temperature profiles along the plate were determined by means of the solution of the integral relation of the momentum and energy equations. A relation between wall temperature and the amount of coolant needed was established.

The results of this analysis show that the mean boundary layer thickness, i.e., area under the boundary layer thickness curve divided by the corresponding length of the porous plate, on a partially porous plate is considerably greater than the one on a corresponding fully porous plate. However, this difference of mean boundary layer thickness between two partially porous plates with, say $x_i = L/4$ and $x_i = L/2$ is slight, where $x_i$ is the distance

[7]Dorodnitzyn, *Laminar Boundary Layer in Compressible Fluids,* Central Institude of Aerodynamics, Moscow, 1942.

measured from the leading edge of the plate of total length L to the point where fluid injection begins. This phenomenon can be explained by the sharp increase of boundary layer thickness occuring near the leading edge of a plate. (A zero thickness of the boundary layer is taken at the leading edge). On the other hand, when the injection fluid begins at a certain distance from the leading edge of a plate, the boundary layer thickness at the beginning of the porous section is taken to be the same as that at the end of the impermeable section. This explains the phenomenon of the latter case.

It is interesting to note that when $x_i > L/2$ the difference of the mean boundary layer thickness for various partially porous plates is insignificant. However, a distinct difference in mean boundary layer thickness exists even between a fully porous plate and a partially porous plate with $x_i = L/20$.

For a predesignated wall temperature it is shown that the rate of coolant injection varies sharply between a fully porous plate and a partially porous plate. The difference of coolant injection becomes less as $x_i$ increases and approaches almost a definite value when $x_i > L/2$. The reason given in the previous paragraph also explains this phenomenon as the thicker the boundary layer, the less heat transfer at the wall.

The above investigation was published as Technical Report No. 13 entitled, *Heat Transfer in a Laminar Boundary Layer on a Partially Sweat-Cooled Plate.*

An investigation of heat transfer in the laminar compressible boundary layer on a porous flat plate with variable fluid injection is about completed. In this investigation two types of injection fluid variation with flow direction were considered: the case (1) where the injection fluid is assumed to decrease linearly with the distance from the leading edge, and (2) where the injected fluid is assumed to decrease bi-linearly with the distance.

A comparison was made between the results of this analysis and the one with uniformly distributed fluid injection on the basis of equal total amount of fluid being injected per unit time. For a predesignated wall temperature it shows that the injected fluid needed to maintain this wall temperature in case (1) is somewhat greater than in case (2). In both cases (1) and (2) the injected fluid required to maintain the same average wall temperature is less than in the case with uniform fluid injection. However, the differences in these required fluid injection rates for the above three cases are slight under the presently prescribed variable fluid injection profiles.

In order to investigate compressible laminar boundary layers with axial pressure gradients, heat transfer and fluid injection at the wall, the basic momentum and energy differential equations have been mathematically transformed into integral differential equations. The integration in these equations has been simplified by the use of Dorodnitzyn's type of change of variables (Ref. 3). Profiles in the form of fourth-degree polynomials satisfying appropriate boundary conditions have been assumed for both the velocity and temperature distribution through the boundary layer. In this manner two ordinary differential equations of the first order have been obtained. The dependent variables are the velocity boundary layer thickness and the temperature boundary layer thickness, while the independent variable is distance in the direction of flow; the equations thus derived are valid for any given distribution of normal fluid injection and temperature along the wall, as well as for any constant value of the Prandtl number. For the purpose of simplifying these equations, it has been assumed that the coefficient of viscosity varies in direct proportion to the absolute temperature. This may be considered as an approximation to the actual variation of viscosity coefficient with temperature.

As a preliminary investigation, the two ordinary differential equations have been solved for the case of a flat plate parallel to the stream with fluid injection. Among other results, the ratio of velocity thickness to temperature thickness has been determined as a function of Mach number for a given temperature at the wall. The solutions thus obtained have been compared with a solution already derived by the use of a known exact integral of the energy equation in this case. The close agreement between the two solutions showed that the use of an integral relation in place of the actual energy differential equation leads to satisfactory results. These results will also be useful in starting numerical solutions for flows with certain types of axial pressure gradients.

For the more general cases of flows with axial pressure gradients and fluid injection, the two basic ordinary differential equations have been made non-dimensional and have been converted into forms convenient for a numerical solution by means, for example, of the Kutta-Runge method.

The equations derived here imply singular points where either the boundary layer thicknesses are zero or where stagnation conditions occur, such as at the leading edge of an object. Consequently, such points must be given special investigation. Initial conditions at such points, which must be known in order to start numerical solutions, have been derived in detail for each of three different types of prescribed potential velocity distributions.

Certain general conclusions of a qualitative nature have been drawn from the initial conditions thus derived, as well as from the basic ordinary differential equations. After complete checking of the mathematical results obtained thus far, it is intended to begin a numerical solution for the case of a linearly varying potential flow velocity. Solutions thus obtained can then be compared with known solutions for incompressible flows. In this manner, the effects of parameters such as Mach number, fluid injection velocity, and wall temperature in the presence of an axial pressure gradient, favorable or adverse, can be determined.

A theoretical investigation of the heat transfer in the turbulent boundary layer on a sweat-cooled plate has been made. In this investigation the laminar sublayer was assumed to exist between the turbulent cone and the porous wall. In order to determine the thickness of the laminar sublayer as a function of the length in the direction of flow, the variation of the outer boundary velocity, $u_\delta$ of the laminar sublayer in the flow direction must be known. This velocity, $u_\delta$ is a constant in the laminar flow over a flat plate. Since the laminar sublayer is extremely thin, it was assumed that the turbulent stress near the wall was equal to the viscous stress of the laminar layer. With this assumption it was found that the velocity $u_\delta$ is a function of the thickness of the laminar sublayer as well as Reynolds number.

The velocity profile inside the laminar sublayer was assumed to be a certain exponential function in $y$, the distance inside the laminar sublayer, satisfying the required boundary conditions. Furthermore, the velocity profile varied linearly with $y$ when the velocity of injected fluid became zero. As the velocity of injected fluid increases, the slope of the velocity profiles at the wall decreases. This phenomenon indicates that the shearing stress at the wall decreases as the velocity of injected fluid increases. The solution of the integral relation of the momentum equation gives the thickness of the laminar sublayer as a function of length in the direction of flow.

Outside the laminar sublayer (i.e., $y>\delta$), the turbulent fluctuations in the stream cause diffusion of mass, heat, and momentum in a manner somewhat similar to molecular diffusion, but with very much higher rates. In regions where the velocity gradient of the mean speed is high, the rate of transport of any property across the stream can be taken as roughly proportional to the velocity gradient. Based on this approach, Reynolds analogy between heat transfer and momentum transfer across a turbulent stream was attained. Since there is no sudden change from laminar to turbulent flow at the outer boundary of the laminar sublayer, i.e. $y = \delta$, this point will be identified as the point where the turbulent diffusion rate becomes appreciable and the Reynolds analogy will be applied to the entire region $y \geq \delta$. The expression for the temperature ratio $(T_1 - T_W)/(T_W - T_O)$, where $T_1$ is the free stream

temperature, $T_w$ is the temperature on the hot side of the wall, and $T_o$ is the coolant temperature on the cold side of the wall, as a function of mass fluid injection was then obtained.

At the present time there is no available information on the turbulent wall shearing stress for a porous plate with fluid injection; however, the data obtained for an impermeable wall was used in the above analysis. It has been learned from the investigation described above that the viscous stress in the laminar sublayer decreases as the velocity of injected fluid increases, and the same reasoning would apply to the turbulent stress near the wall. The results obtained in the present investigation are valid only for very small mass fluid injection.

The future plans for this theoretical investigation of porous wall cooling can be divided into the following three categories.

(1) Investigation of heat transfer in the laminar compressible boundary layer on a flat plate with fluid injection will be extended as follows: temperature gradient along the wall will be taken into consideration; horizontal fluid injection along the wall will be analyzed-this will give some information on film cooling; consideration will be given to the most efficient method of porous wall cooling as indicated by the above investigations.

(2) It is intended that some information on porous wall cooling of turbine blades can be worked out from the investigation on porous wall cooling with axial pressure gradient.

(3) Further investigation of heat transfer in the turbulent boundary layer on a sweat-cooled wall will be carried out. The variation of physical properties (density, viscosity, conductivity) across the boundary layer will be taken into consideration. It is intended to extend the analysis by introduction of coolant in jets from a finite number of pores rather than as uniform flow from the wall.

## *E. AN EXPERIMENTAL INVESTIGATION OF THE LAMINAR BOUNDARY LAYER ABOVE THE SURFACE OF A POROUS FLAT PLATE WITH FLUID INJECTION. (PIB-3R1).*

*Submitted by: S.W. Yuan, Polytechnic Institute of Brooklyn.*

It is the object of this problem assignment to investigate experimentally the characteristics of boundary layers on porous walls with fluid injection. To date most of the effort has been confined to an investigation of the boundary layer characteristics without heat

transfer, that is with a *cold* flow. The equipment, tests and test results from this study will be discussed. Finally the design considerations for the contemplated high temperature tests will be discussed.

**Equipment.** A porous plate 26 inches by 4 5/16 inches has been mounted in the wall of a two-dimensional turbulence channel. At the leading edge of the porous section the boundary layer formed upstream of this point is withdrawn by a suction slot. Fluid is injected through the porous wall by means of a pressure chamber bell attached to the wall of the channel over the porous portion. Velocity surveys in the channel at various stations along the porous plate are made with a single wire, hot-wire anemometer.

Early in the year, an air compressor replaced the bottled nitrogen as the source of injected fluid. The large temperature drop obtained when the bottled nitrogen, under 2000 psi pressure, was expanded to pressures only slightly higher than atmospheric behind the porous plate was thereby eliminated. A large capacity commercial gas meter was secured and incorporated in the line between the compressor and the pressure bell behind the porous plate. This gas meter, in addition to providing a convenient instrument for the measurement of air flow, acts as a settling chamber to damp out pulsating delivery from the compressor.

Platinum wire rather than tungsten has been used in the construction of hot-wire anemometers. A single strand of .001-inch diameter platinum wire about one-half inch long, mounted normal to the direction of the air stream and parallel to the wall has been satisfactory.

Platinum has been found to possess several advantages. Velocity calibrations of tungsten wires were difficult to duplicate because of an oxide coating which formed after repeated use. The coating acts as an insulating layer and changes the heating characteristics of the wire. With platinum wire there is no difficulty in duplicating velocity calibrations from day to day. In addition, the platinum wires have been found to have four to five times the service life of the earlier tungsten wires. Moreover, platinum wire may be soldered to the mounting prongs with ease. Tungsten wire on the other hand must be copper plated before soldering and bared with nitric acid after soldering.

**Tests.** To determine the change in radiation effect of the wall on the hot wire due to the flow of injected fluid, the temperature of the porous plate during injection was measured with an iron-constantan thermocouple in conjunction with a precision potentiometer. Temperature measurements were made over a range of injection pressures, from 0 to 20 psi at

six stations along the porous plate, with zero free stream velocity. The results indicated only a small change in wall temperature and therefore in radiation correction due to fluid injection.

Chordwise velocity surveys of the porous plate with zero free stream velocity and a steady injection pressure of 5 psi were carried out to determine the distribution of injection velocity along the plate. Measurements of the rate of flow of injected fluid were made simultaneously, with a flow meter. Knowledge of the average injection velocity and quantity flow made it possible to compute an effective area of the plate.

In addition to these preliminary investigations, boundary layer velocity surveys were carried out at three chordwise stations along the plate. These surveys were made at various combinations of free stream velocity, suction at the leading edge slot, and injection velocity. In these tests the following procedure was used: After what appeared to be a laminar profile had been obtained with no injection and a given combination of leading edge suction and free stream velocity, injection was begun and the velocity profiles, with and without injection, and the corresponding boundary layer thicknesses compared.

**Experimental Results.** Temperature measurements with the iron-constantan thermocouple on the porous plate surface with a range of injection pressures from 0 to 20 psi indicate variations of no more than $1^{o}$-$2^{o}$ Fahrenheit from the existing atmospheric temperature. Thus the radiation corrections determined experimentally for a room temperature wall could be used for the porous wall with injection.

Chordwise surveys of the porous plate with zero free stream velocity and a steady injection pressure of 5 psi consistently yielded flow measurements of 17 cubic feet per minute. This indicated an effective area of 75 per cent of the actual area, based upon a measured mean injection velocity of 0.35 feet per second.

Comparison of boundary layer velocity profiles with and without injection indicate generally that under conditions which produce a laminar profile without injection, the addition of injected fluid at a velocity equal to 2.5 per cent of the free stream velocity produces a typically turbulent profile.

In addition to producing a turbulent boundary layer profile, the injection of fluid through the wall appears to thicken the boundary layer by as much as 25 per cent.

**Plans for Cold Tests.** To reach more definitive conclusions on the effect of injection upon boundary layer characteristics, more data should be collected to form a basis for judgment. Present plans contemplate continuation of present tests to collect this data.

**Design of High Temperature Channel.** During the second six months of this year design studies of a setup to investigate experimentally the velocity and temperature profiles in laminar and turbulent boundary layers in high temperature flows over porous walls, which are cooled by injection, have been made. To date all experimental work on the characteristics of heat insulating boundary layers on porous walls has been limited to small cylindrical porous tubes, through which hot gases have been induced, or to porous plugs in uncooled walls. In order to study the heat transfer properties of extended porous walls and to study the more fundamental characteristics of boundary layers on porous flat plates, a two-dimensional channel, one wall of which will be porous and cooled by injection is contemplated.

The following design conditions for this channel have been selected: maximum free stream velocity, 200 fps; maximum injection velocity, 1 fps; and maximum free stream temperature, 1500$^{0}$F. With an eight-foot channel maximum Reynolds numbers based on plate length of from approximately one to ten million, depending on the free stream temperature, will be obtained.

After considering several systems for achieving these design conditions, it was decided that, because of the high heat input required and the large mass of cooling fluid injected through the porous wall, to choose an open system with a direct-fired heater and with a blower on the cold side of the heater. Thus air at room temperature will be passed through the blower into the furnace, where it will be thoroughly mixed with the products of combustion and high temperature air from a gas burner of 1.6 million B.T.U./hour capacity. From the furnace the heated mixture will pass through a contraction cone into the test channel. Before being exhausted to the atmosphere, the working fluid will be quenched by water sprayed into the flow.

At the present time, considerable attention is being devoted to the selection of the channel cross-section height to width ratio. Because the porous sheets are not available in widths greater than fourteen inches it was considered desirable to make the duct cross section 2.5 by 12 inches. However, since one of the purposes of the experimental research is to investigate transition points, consideration is being given to the possibility of transition by transverse contamination from the corners of the duct. It may be found necessary to piece two porous sheets together in order that transition occur in the normal fashion at the duct centerline.

Bids for the blowers and furnace have been received. The design of the contraction cone and test channel awaits final decision on the duct cross section. The instrumentation required for the velocity and temperature profile surveys is being assembled.

## *F. CONVECTIVE HEAT TRANSFER IN HIGH TEMPERATURE GASES. (PRF-Ph. 5).*

*Submitted by: J.M. Smith, Purdue University.*

During the first nine months of 1949 convection heat transfer coefficients were measured experimentally for air flowing in a 2.0-inch I.D. nichrome pipe at bulk temperatures from 500°F to 1550°F and Reynolds numbers from 1600 to 14,000. The data were obtained under conditions of small temperature differences between the gas and pipe wall, with the gas being hotter than the wall in all cases.

The experimental data were found to fit the following equation, over the entire temperature range within the precision of the data:

$$\frac{h}{cG}\left(\frac{c\mu}{k}\right)^{2/3} = 0.023\left(\frac{DG}{\mu}\right)^{-0.22}$$

The experimental results were subject to significant random error, which may have masked an effect of temperature on the heat transfer coefficient.

Tests made with and without a disk and doughnut mixing device placed at the inlet to the test section of 2-inch pipe indicated that effects of turbulence caused by mixing could be significant. At the same Reynolds number, the Stanton number increased from two to four fold when the mixing device was present. The length to diameter ratio of straight pipe preceding the entrance to the test section was 25. This effect of mixing increased as the Reynolds number decreased.

In order to increase the accuracy of the measurements, the insulation on the test section has been removed and a water jacket will be installed. This will permit a heat balance to be obtained for each run. This will also greatly increase the temperature gradient near the tube wall. This work is now in progress.

It is planned to measure convection heat transfer coefficients with the revised equipment over the range of temperatures from 500 to 2000°F and Reynolds numbers from 2000 to 14,000. It is proposed to inaugurate during the next few months an investigation of heat transfer coefficients

at temperatures up to 3500°F and Reynolds numbers up to 200,000 from a different experimental approach using the facilities of the rocket laboratory now being constructed at Purdue University. It is proposed to obtain high temperature gases by the decomposition of hydrogen peroxide within the gases themselves.

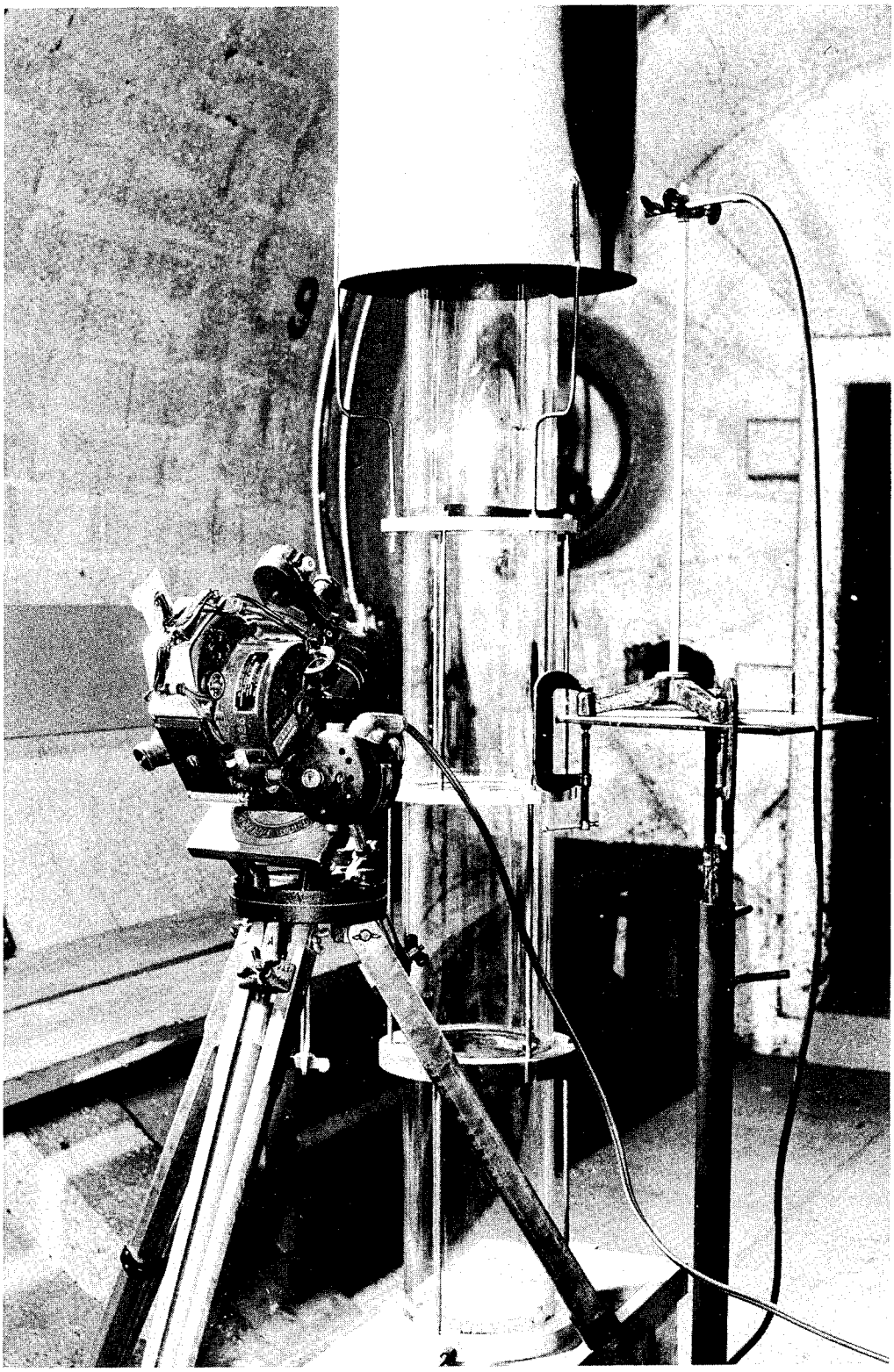

Fig. 1. Setup for the study of cellular flames at reduced pressure.

# IV. FLAME PROPAGATION

## A. *COMBUSTION TUBE EXPERIMENTS: STUDY OF FLAME STRUCTURE, EFFECTS OF DISUTRBANCES ON FLAME TRAVEL IN TUBES; AND STABILITY OF FLAME FRONTS. (CAL-2a).*

*Submitted by: J.V. Foa and G.H. Markstein, Cornell Aeronautical Laboratory.*

During preliminary experiments on flame propagation in tubes,[1] it had been found that within a certain range of mixture compositions hydrocarbon flames assumed a structure composed of many approximately hemispherical cusps, burning side by side in a horizontal layer in the vertical tube, with their convex side toward the unburned gas. This phenomenon occurred under flow conditions where stream turbulence was definitely absent, and had, therefore, to be ascribed to flow disturbances generated by the flame itself. It appeared to be of sufficient fundamental significance to justify a thorough investigation of the conditions for its occurrence and of the influence of various parameters on average cell size. The experiments were performed in vertical glass tubes, open at the top and closed at the bottom except for the inlet for the gas mixture. The flow velocity of the premixed gases was chosen low enough to insure laminar flow in the tube (the Reynolds number was about 500). The mixture compositions were selected so that the flames remained almost stationary a short distance below the top of the tube. In order to accomplish this over the whole range of air-fuel ratios within the limits of inflammability, the burning velocity was reduced by adding appropriate amounts of nitrogen. It was realized, of course, that this procedure introduced a certain ambiguity since it was generally not possible to vary one parameter such as type of fuel, air-fuel ratio or pressure, without having to readjust the amount of added nitrogen. However, preliminary work showed that as the air-fuel ratio approached the stoichiometric value from the rich side, the average cell size, after a small decrease for very rich mixtures, remained almost constant over a fairly wide range of compositions. Therefore, subsequent cell size determinations were carried out with mixtures on the rich side, but rather close to stoichiometric composition.

Average cell sizes were determined by counting the number of cells over the whole tube cross section. For this purpose photographs of the flames were taken under an oblique angle

[1]Project Squid, Annual Program Report, 1 January 1949, p 128.
G. H. Markstein, *Jour. Chem. Phys.*, 17, 428 (1949).

from below. In general, the mean value of at least five cell counts was taken. Since the flames were often subject to sudden disturbances by downdrafts, a large number of exposures had to be taken in order to obtain enough good pictures. This was accomplished by using a 35 mm movie camera, operated at 8 frames per second. Work at reduced pressures in the Cornell Aeronautical Laboratory Altitude Chamber was greatly facilitated by this procedure, using a camera with electric remote control. Figure 1 shows the setup in the Altitude Chamber, using a flame tube of 15.3 cm inside diameter. The shield on top of the tube served to protect the flame from drafts. The flames were ignited by means of a pilot flame burning on the nozzle visible on the right of Figure 1.

Table I.

| Fuel | Average cell size d (cm) |
|---|---|
| n-butane | 1.06 |
| iso-butane | 1.06 |
| butane-2 | 1.07 |
| iso-butylene | 1.07 |
| butadiene-1, 3 | 1.16 |
| propane | 1.16 |
| propylene | 1.18 |
| ethane | 1.60 |
| ethylene | 1.68 |

A comparison of a number of gaseous paraffinic and olefinic hydrocarbon fuels showed that cell structure occurred in rich mixtures in all cases with the exception of methane, which did not form cellular flames for any mixture composition. In all cases the cell structure disappeared almost abruptly giving way to a smooth flat flame when the air-fuel ratio was increased beyond a value close to stoichiometric.[2]

Average cell size at atmospheric pressure depended considerably on the type of fuel. Table I gives cell sizes in centimeters (cm), computed by the expression $d = D/\sqrt{n}$, where D is the tube inner diameter and n the average number of cells. The tube inside diameter was 10 cm; the compositions, as stated above, were chosen close to stoichiometric, with sufficient nitrogen added to keep the flame almost stationary.

Cell size is seen to depend primarily on the number of carbon atoms and, to a lesser degree, on the number of hydrogen atoms in the fuel molecule. No difference between normal and iso-structure was found.

The cellular flames of various fuels, and also of each fuel for various compositions, differed not only in cell size but also in what may be called *strength* of the structure. At present, this property can be described only in qualitative terms. A *strong* cell structure

[2]Project Squid, Quarterly Progress Report, 1 July 1949, pp. 43, 44.

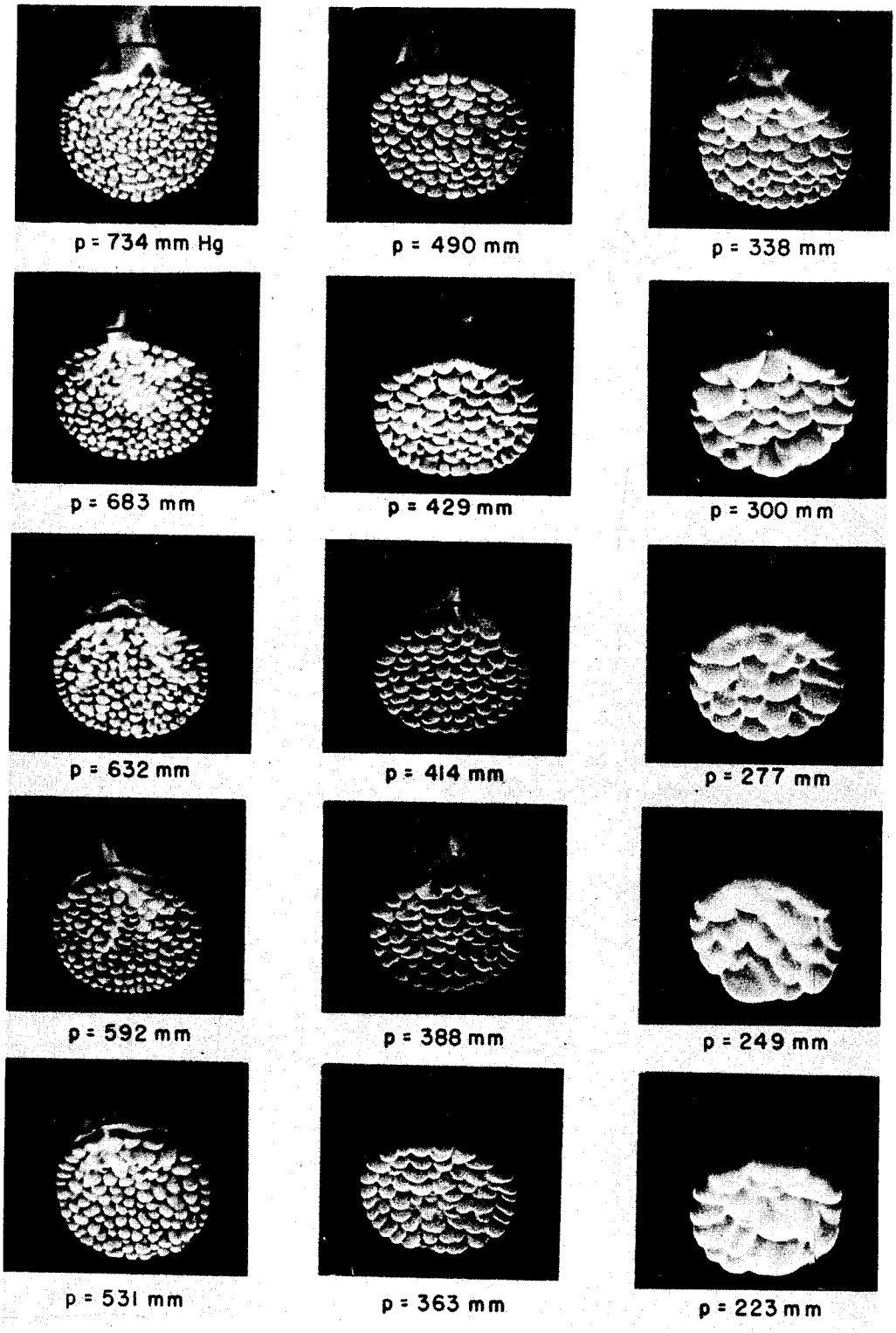


Fig. 2. Cellular butane-air-nitrogen flames at various pressures.

was characterized by sharply outlined, almost hemispherical cells, separated completely by dark ridges; the cells were in lively, irregular motion. Weak structures had shallow cells, the ridges often were almost as luminous as the rest of the flame, and the motion was more sluggish. For each fuel the strength appeared to increase somewhat when the air-fuel ratio was gradually changed from very rich toward stoichiometric, and dropped within a very short range of compositions before the structure disappeared completely at the limit. Ethane and ethylene had very weak structures; the other fuels did not seem to differ appreciably in this respect. There can be little doubt that the strength of the cell structure is related to the intensity of the flow disturbances set up by the flame and therefore to the amount of instability of the flame front. Attempts will be made to find a quantitative measure of the strength of flame structure.

For the determination of the pressure dependence of average cell size n-butane was chosen as fuel because it formed small cells and because its properties are closest to those of higher hydrocarbons which are important as practical fuels. Figure 2 shows a series of flame pictures, taken at atmospheric and various reduced pressures with the setup shown in Figure 1. A plot of average cell size and pressure is shown in Figure 3. Over most of the pressure range, the values determined in the 10 cm inside diameter tube and in the 15.3 cm inside diameter tube are seen to agree well. Except for the lowest pressures, the product pd decreased slightly as the pressure was reduced, as can be seen from the discrepancy between the experimental values and the curve pd = Const. drawn in. At the lowest pressures pd increased; however, this occurred at higher pressures in the 10 cm tube than in the 15.3 cm tube, and may have been caused by the fact that the number of cells became so small that the results were affected by the wall of the vessels.

A number of exploratory experiments were performed with gas mixtures containing a fourth component besides hydrocarbon fuel, air and nitrogen. It was found that hydrogen, added in small amounts, caused strong cell formation in *lean* mixtures of all hydrocarbons, including methane. Ammonia caused weak large cells to be formed in lean methane mixtures, but caused an increase of cell size and decrease of strength in rich mixtures of the higher hydrocarbons. Carbon monoxide had a similar effect on the cell structure of rich hydrocarbon flames. Replacement of the nitrogen by carbon dioxide gave slightly smaller cells in butane-air mixtures. Helium as diluent gas gave larger cells and suppressed the cell formation completely if added in larger amounts.

The investigation of the structure of almost stationary flames undoubtedly provides the best means of studying flame front stability under conditions where flow disturbances generated

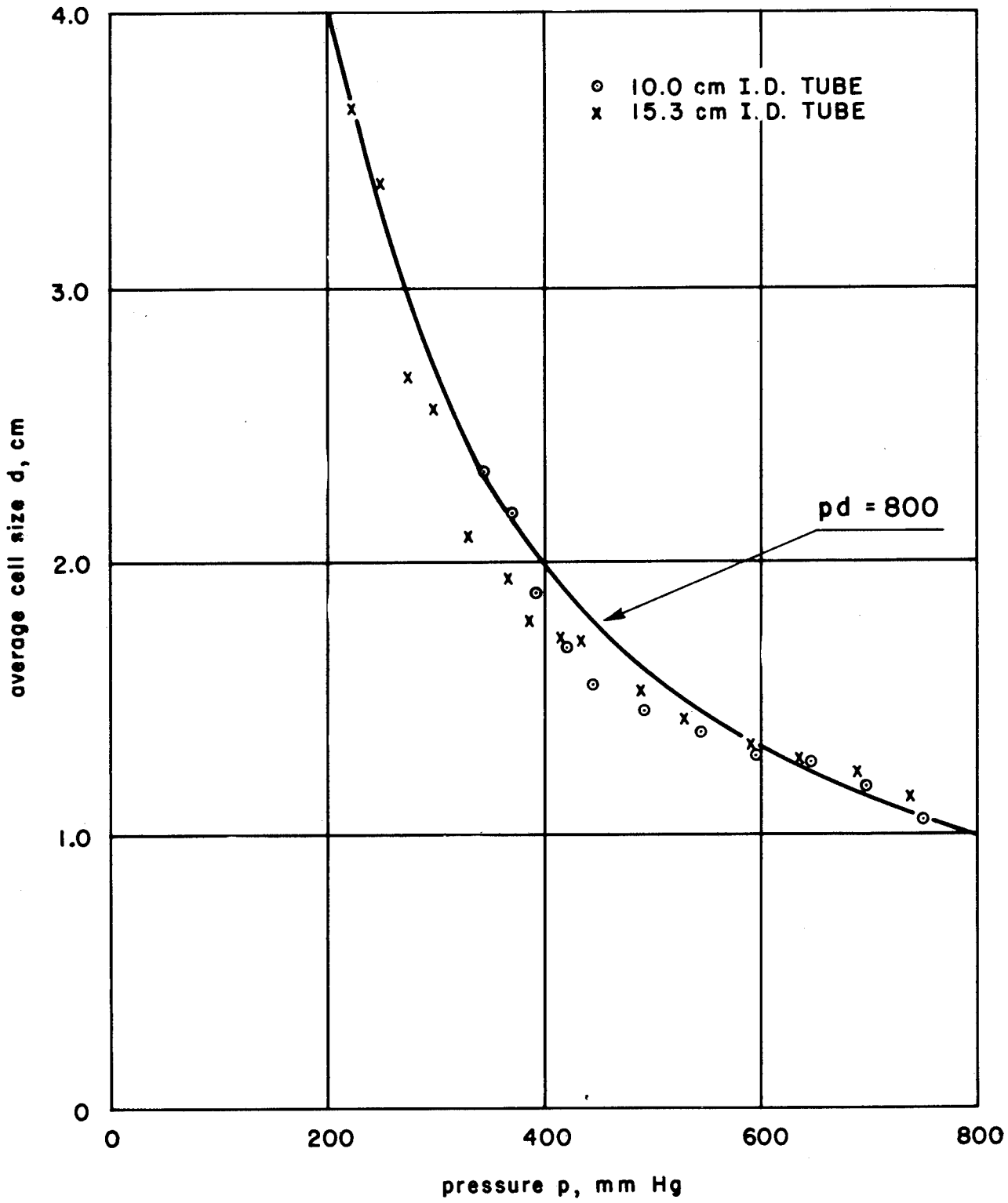


Fig. 3. Average cell size of butane-air-nitrogen flames *vs.* pressure.

outside the burning zone are suppressed as much as possible. However, it appears equally important to study the structure of flames propagating more rapidly through tubes. It has been known for a long time that unless extreme precautions are taken to damp the reflection of pressure waves at the ends of the tube, flame propagation in tubes is invariably accompanied by organ-pipe oscillations which often may reach violent intensities. During this *vibratory flame motion* the apparent flame speed increases considerably, and the flame thus acquires the characteristics of a *high speed turbulent flame*. Furthermore, the excitation of oscillations by the flame is important because of the obvious connection with practical problems, such as rough burning, valveless pulsejets, etc.

While this phenomenon has been studied extensively in the past, the aspect of flame structure has been almost entirely neglected in spite of its fundamental importance, because of the proportionality between flame speed and flame surface area.

Because of the extremely rapid changes of flame structure during the vibratory phase of propagation, high speed motion picture techniques must be employed. The low luminosity of the flames precludes, however, direct photography; shadowgraph and Schlieren methods have to be used instead. In tubes of circular cross section, this is possible only by means of a parallel beam of light passing axially through the tube and through a plane glass window at the closed end.

Exploratory work was done with the same glass tubes which were used in the study of stationary cellular flames. Later, a metal tube was employed which, by means of the ionization flame timer,[3] allowed the registration of flame position along the tube on an oscillographic record. A pressure pickup of the condenser type developed by New York University[4] was connected near the closed end of the tube; pressure was registered both on the oscillographic record and simultaneously on the high speed movie by means of a second oscilloscope. Recently a tube of rectangular cross section with glass windows at the sides and at the closed end has been built, which will allow transversal as well as axial shadowgraph or Schlieren movies to be taken. The experimental conditions were similar to those in the study of almost stationary flames, but fast-burning mixtures without nitrogen addition were used so that the flames propagated rapidly from the open top to the closed bottom of the tube.

---

[3] Project Squid, Annual Program Report, 1 January 1948, p. 106.

[4] Project Squid, Annual Program Report, 1 January 1949, pp. 14-16.

The work performed until now has indicated clearly that during the phase of vibratory flame motion cells appear and disappear periodically in the rhythm of the oscillation.[5] During the period of *uniform flame motion* preceding the vibratory phase, markedly different structures were observed according to whether the air-fuel mixture used gave rise to cellular or non-cellular stationary flames upon the addition of nitrogen. In no case was the flame completely devoid of structure, but the *non-cellular* mixtures showed only few separating ridges, often tapering out and disappearing somewhere in the middle of the tube cross section, while the *cellular* mixtures showed a large number of cells similar to the stationary flames. This difference of structure disappeared during the vibratory phase; however, vibrations started earlier during flame travel and with the first harmonic of the tube in the *cellular* mixtures, while the period of uniform motion was longer, giving way to vibrations of the fundamental frequency for the *non-cellular* mixtures.

This result was first obtained with butane-air and methane-air mixtures[6] and later confirmed when it was found that addition of hydrogen to lean mixtures, which caused cell formation, also gave rise to first-harmonic oscillations.

Theoretical work on the problem of flame front stability and on the excitation of vibrations by flames has been continued. The purely hydrodynamical treatment of flame front stability by Landau,[7] which regarded the flame front as a surface of discontinuity between two regions of constant density, temperature and initial velocity, did not seem to be adequate for explaining the experimentally-found dependence on mixture composition. Furthermore, it predicted a linear increase of instability with the wave number (i.e., the reciprocal of the wave length) of the disturbance, while the observed uniformity of cell size suggested a maximum of instability for a certain wave length. An attempt was therefore made to treat the problem more rigorously by taking the finite thickness of the combustion zone into account and by including the equation of heat balance, and possibly one or more diffusion equations. This attempt was unsuccessful, not only because of the formidable mathematical difficulties, but because one can hardly hope to solve the stability problem, i.e., the first order perturbation problem, since the zero order problem, namely, the calculation of the burning velocity, is still far from a satisfactory solution.

---

[5] Project Squid, Quarterly Progress Report, 1 July 1949, pp. 44-47.
[6] Project Squid, Quarterly Progress Report, 1 October, 1949, pp. 33-34,
[7] L. Landau, *Acta Physicochimica, URSS,* 19, 77 (1944).

However, as long as the wave length of the flow disturbance is large compared to the thickness of the combustion zone, the effect of the disturbance will consist essentially of a deformation of the combustion zone as a whole without causing changes in its internal structure. Thus it may be assumed that chemical kinetics, heat conduction, and diffusion can enter the problem only by the dependence of the local burning velocity on the curvature of the flame front. Under these assumptions it is possible to split the problem into two separate ones: a purely hydrodynamic treatment of the Landau type, into which the chemical kinetics, etc., are introduced merely by a single parameter which characterizes the dependence of burning velocity on curvature; and the calculation of this parameter, which involves only the heat conduction and diffusion equations. The hydrodynamic problem has been solved. The solution indicates that if the curvature dependence is such that a portion of the flame front convex toward the unburned gas propagates slower and a portion concave toward the unburned gas propagates faster than the plane flame front (a dependence which one would normally expect), then the instability of the flame front goes through a maximum with respect to the wave length of the disturbance. The calculation of the curvature parameter remains a difficult problem which is related to the unsolved problem of burning velocity. For the special cases, however, where all the diffusion coefficients are equal among themselves and to $\lambda/c_p\rho$, where $\lambda$ is the heat conductivity, $c_p$ the specific heat at constant pressure and $\rho$ the density, the problem has been solved. (These cases include, of course, those where flame propagation is governed exclusively by heat conduction or by diffusion of one single chemical species.) The result for this case was introduced into the solution of the hydrodynamic problem; with reasonable assumptions for the value of the density ratio between unburned and burned gas and for the thickness of the combustion zone, a maximum instability was obtained for a wave length of the order of one centimeter. In view of the approximations involved in a first order perturbation treatment of this kind, this value agrees very well with the order of magnitude of the experimentally determined cell sizes. Furthermore, the result showed that as long as the curvature parameter remains constant the wave length for maximum instability should be proportional to the thickness of the combustion zone; since the latter is roughly inversely proportional to pressure, the result is in qualitative agreement with the experimentally-found pressure dependence of average cell size.

Since the curvature dependence of burning velocity should determine the conditions at the tip of a Bunsen flame, exploratory experiments were performed in order to find possible correlations between the appearance of the tip and the composition of the combustible mixture. It was found that in all cases so far investigated those mixtures which were capable of forming cellular flames in tubes formed open-tip flames, while the others formed closed-tip flames. Further work will have to be done before this statement could be considered correct under all possible conditions of flow velocity and composition.

Since the experiments on cellular flames were performed in vertical tubes, the effect of gravity on flame stability should be taken into account. It is not difficult to include an acceleration term in the hydrodynamical treatment. The result showed that gravity, under the conditions under which the experiments were performed, has a stabilizing effect which increases with the wave length of the disturbance. Thus, if both the curvature dependence of burning velocity and gravity are taken into account, instability occurs only over a finite range of wave lengths.

The importance of the effect of acceleration on flame front stability goes beyond the influence of gravity. During the vibratory phase of flame motion the flame front is subject to alternating accelerations, which should alternately increase and decrease the stability. This conclusion is in agreement with the experimental result that vibratory flame motion is accompanied by periodic appearance and disappearance of cellular structure. The periodic change of structure will in turn cause periodic variations of flame surface area and thus the the rate of burning and heat release. As was shown by Rayleigh,[8] a periodic heat addition in proper phase with the density variation leads to spontaneous excitation of organ-pipe oscillations in tubes. The importance of phase relations in the case of vibratory flame motion is apparent from the experimental finding that various harmonics and the fundamental frequency of the tube are excited in sequence as the flame moves along. A theoretical study of vibratory flame motion on the basis of this hypothetical mechanism has been started.

The planning of future experimental work, both on stationary cellular flames and on vibratory flame motion, will be guided to a considerable extent by these theoretical developments.

## *B. BURNER EXPERIMENTS. (CAL-2R6).*

*Submitted by: G.H. Markstein, Cornell Aeronautical Laboratory.*

Attempts to adapt the technique of intermittently illuminated particles for flow visualization in Bunsen flames subjected to periodical disturbances were not successful although the same technique is satisfactory for steady flames. Promising results were obtained, however, by injecting titanium tetrachloride vapor in several thin jets into the unburned gas,[9] and photographing the resulting smoke traces.

---

[8]Lord Rayleigh, *Theory of Sound,* Vol. II, Dover, New York, 1945, p. 226.

[9]Project Squid, Quarterly Progress Report, 1 October,1949, pp. 34-36.

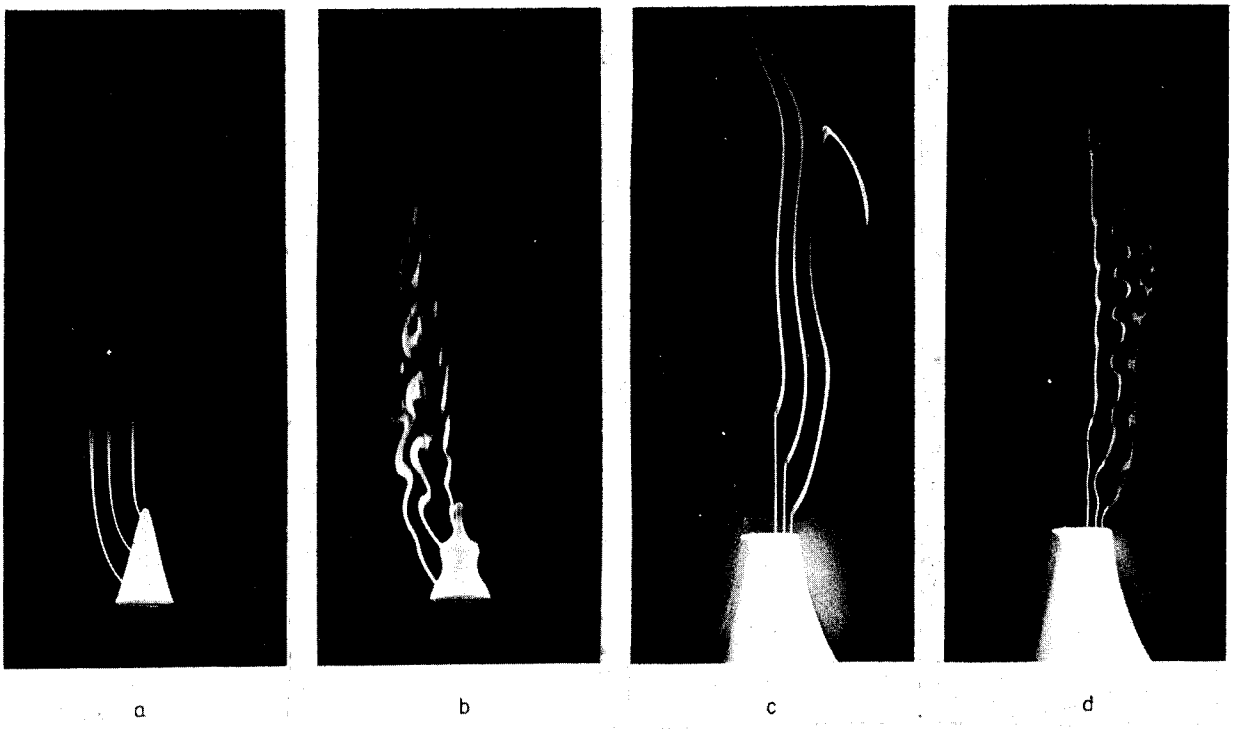


**Fig. 4.** Flow patterns in burner flames visualized by smoke traces.

a. Undisturbed flame; direct photograph.
b. Flame disturbed by sound of of 250 c.p.s. stroboscopic direct photograph.
c. Undisturbed flame; flash photograph.
d. Flame disturbed by sound of 250 c.p.s. flash photograph.

Since the smoke became brightly luminous in the burned gas, direct photographs were first taken for cases of undisturbed and acoustically disturbed flames, the latter through a synchronized stroboscopic disk. Examples are shown in Figures 4a and 4b. These were not entirely satisfactory, however, as the traces were invisible in the unburned gas, and low frequency disturbances always present in the burned gas caused considerable blurring of their upper regions. These defects were eliminated by electronic flash illumination of the smoke; results are shown in Figures 4c and 4d. Figure 4d shows clearly the presence of flow disturbances in the unburned gas. A corresponding photograph taken with the unlit gas jet subjected to the same acoustical disturbance showed that in the same region the flow remained undisturbed with exception of the jet boundary; this demonstrated strikingly the modification of the flow disturbance by the flame.

Work is continuing on further modifications of this technique in order to enable a quantitative evaluation of the flow patterns.

## *C. A STUDY OF FLAME CHARACTERISTICS, MAINLY OF FLAME TYPES INTERMEDIATE BETWEEN SELF-PROPAGATING AND DIFFUSION FLAMES. (DEL-2R1).*

*Submitted by: Kurt Wohl, University of Delaware.*

This problem is concerned with the structure and stability of flames burning above tubes in air and in an inert gas atmosphere at normal and elevated pressure. The investigation includes laminar and turbulent flames, flames which burn in homogeneous inflammable gas mixtures (self-propagating flames), and flames which depend on the supply of external oxygen (diffusion flames). The combustible gas mixtures to be studied are butane-air and methane-air mixtures. Other combustible mixtures may follow. The work is a continuation of previous studies.[10] [11] [12]

With laminar flames, special attention is being given to flames burning in air at fuel-air ratios around the upper limit of inflammability where the transition occurs between self-propagating and diffusion flames. It has been observed that the separation of a Bunsen flame into an inner cone, which is thought to be characteristic of self-propagating burning zones, and an outer diffusion zone still exists beyond the upper limit of inflammability, and that these two zones melt together into one diffusion zone at a fuel concentration which is considerably above that of the limit mentioned. The explanation of this observation is not obvious so that a further study of the transition range between self-propagating and diffusion flames is indicated. Such a study seems especially desirable since combustion in jet propulsion engines occurs in an inhomogeneous gas stream which is partially over-rich so that the flames produced are of this transitional type.

The transition between laminar self-propagating and diffusion flames can be followed with the help of the true or apparent burning velocity which can be calculated from the area of the inner cone by the method of Gouy, and also with the help of the blowoff velocity, and the dead space between flame and burner rim.[12] In order to separate the effect of external oxygen on combustion from that of the oxygen of the original gas mixture, the same experiments will be carried out with an atmosphere of nitrogen surrounding the flame. These experiments, as far as they are carried out at atmospheric pressure, require only long tubes

[10] K. Wohl, N.M. Kapp, C. Gazley, The Stability of Open Flames, *Third Symposium on Combustion, Flame and Explosion Phenomena*, Williams and Wilkins Co., Baltimore, Md., 1949, pp. 3-21.
[11] Ibid., pp. 288-300.
[12] K. Wohl and N.M. Kapp, *Flame Stability at Various Pressures*, Meteor Report UAC-42, October 1949.

of various diameters which may be surrounded by a rectangular box with two opposite plane glass walls. Blowoff is observed directly, burning velocity and dead space will be determined by direct photography and also by Schlieren photography. At elevated pressure the burner tube is surrounded by a pipe of 8 inches diameter through which a slow stream of air or nitrogen is flowing. Two opposite windows of 2 inches width and 8 inches height are inserted for observation and for taking of direct and Schlieren pictures. The pressure combustion chamber has been described in reference 12. It can at present be operated up to a pressure of 7 atmospheres. In the transition region between self-propagating and diffusion flames, the local chemical composition of the flame gases between the visible primary and secondary burning zones and in the cold stream near the burner port will be ascertained with the help of a watercooled probe which has passed preliminary trials successfully.

With turbulent flames the interest will be concentrated on the size, shape and instantaneous structure of flames, as revealed by direct, shadow, Schlieren, and stereoscopic shadow photography, and by high speed shadow and Schlieren motion pictures. The average local chemical composition of flame gases also will be determined with the probe mentioned. First, turbulent flames will be investigated which burn in free air or in nitrogen at ordinary pressure. In order to be able to study flames above tubes at high velocity, blowoff has to be prevented. This is conveniently done by arranging at the burner rim a wreath of small pilot flames. This makes it necessary to cool the burner wall. The pilot gas will consist of a stoichiometric mixture of butane and oxygen. The holes in the burner rim for the pilot gas have a diameter of 0.1 mm; the accuracy is sufficient to give a uniform height of pilot flames. The distance between the holes is 2 mm. Two tubes with such ports have been constructed, one of 0.3-inch and one of 1-inch diameter. The tubes provide for insertion of several screens. The uppermost screen is placed one tube diameter below the rim of the tube. The other screens can be placed under the first with ½ inch distance between them. In this way a flat velocity profile is produced. The degree of turbulence will be varied by using screens of different mesh, one of 100 mesh to make the flow streamlined, the other of about 6 mesh to create turbulence artificially.

## *D. A STUDY OF THE STABILITY CONDITIONS, THE FLUCTUATIONS, AND OTHER PROPERTIES OF TURBULENT FLAMES WITH THE HELP OF THE HOT-WIRE ANEMOMETER. (DEL-2R2).*

*Submitted by: Kurt Wohl, University of Delaware.*

This problem is concerned with the question of how the properties of high velocity flames, such as ignitability, stability and *burning velocity*, depend on turbulence and other types of

fluctuations in the unignited gas stream and in the ignited gas stream upstream of, and inside, the flame. Attention will be given to the fluctuations which occur in the close vicinity and in the wake of the flame holder in either case, when the gas stream does not burn, and when a flame is attached to the flame holder.

The flames studied are stabilized by a flame holder in a high velocity stream of a homogeneous propane-air mixture. The combustion section is a rectangular duct with a cross section of 1.5 inches $x$ 2 inches, the two opposite 2-inch walls consisting of plane glass plates. The maximum cold gas velocity obtainable is 500 ft./sec. The gas mixture passes through a wide calming section and a set of screens before entering the chamber so that the velocity profile is flat. The state of turbulence of the cold gas can be varied by insertion of various screens immediately upstream of the flame holder. The apparatus is shown in the status report of June 6, 1949, of the Office of Naval Research Project NR-061-055. The emphasis is placed on the measurement of fluctuations with the help of the hot-wire anemometer. However, measurements are also made of the static pressure and head pressure, and of the local composition of the gas upstream of, and inside, the flame. Water-cooled instruments for measuring these quantities have been constructed which can be operated within the flame. Flame shape and a structure will be ascertained with the help of instantaneous Schlieren photography. For this purpose two parabolic mirrors of 8 inches diameter are available.

It is intended to use the hot-wire anemometer in the cold gas stream and in the flame. The functions which it has to fulfill in these two cases are quite different. In the cold stream the hot-wire anemometer will be used in the conventional manner for determining the local average velocity and the intensity and scale of velocity fluctuations. The effect of the state of turbulence in the cold gas and of the flow pattern and the fluctuations in the cold gas near the flame holder on different flame properties is different according to the property considered. It appears that the *burning velocity* of turbulent flames is hardly affected by moderate degrees of turbulence in the cold stream. On the other hand, the question whether a combustible mixture will *ignite* at a certain place, will greatly depend on the state of the cold gas at this place. Flame *stability* is determined mainly by the conditions in the protected region behind the flame holder. It is known that the structure of this region is quite different according to whether a flame is attached to the flame holder or not. Still, there is a relation between the flow pattern behind a flame holder in case of burning and the flow pattern of the cold gas at the downstream end of the flame holder. It is therefore important to determine the latter. It has been shown[13] that the blowoff velocity from

[13] B.Lewis and G.vonElbe, *Jour. Chem. Phys.*, 11, (1943), p. 75-97.

wires of different diameters which were placed in the axis of the duct could be well correlated with the help of the velocity gradient of the gas stream at the wall of the wire within a range of diameters from 0.107 cm to 0.211 cm. (This is the same type of correlation which applies to the blowoff velocity of a Bunsen flame from tubes of different diameters.) The correlation fails for smaller and larger diameters. On the other hand, Scurlock finds in the case of cylindrical flame holders placed with their axis perpendicularly to the direction of flow that 'increasing turbulence intensity decreases the stability limits. The effect of turbulence of the same intensity and scale becomes less as the ratio of stabilizer to scale increases.'[14]

These investigations seem to need extension in many directions. More attention should be given to the effect of high intensity fluctuations of various scales in the cold gas stream on the properties of a flame. Two-dimensional and three-dimensional flames attached to cooled cylinders (with their axis parallel to the direction of flow) and to cooled thin plates (with their side walls parallel to the direction of flow), respectively, should be investigated more systematically. The spreading of a flame from the wake of a flame holder into the bulk of the gas stream should be studied more closely, especially with respect to the composition limits for spreading. One might also use a thin-walled tube in the axis of the duct as a flame holder. When no gas flows through this tube, it is about equivalent to a full cylinder. When a stream of nitrogen, air, or another gas is passed through the tube with increasing velocity, the specific flow pattern behind the tube will gradually disappear and conditions will approach that of a Bunsen flame burning above a tube in a gas stream. (The only difference would be the opposite curvature of the wall which separates the stream of the combustible mixture and of the *foreign* gas.)

The research plan as outlined includes a study of velocity fluctuations of high amplitude and frequency. For this reason the constant temperature (constant resistance) type of hot-wire anemometer has been chosen, rather than the constant current or constant voltage type; for the constant temperature method is essentially a zero method. Correspondingly, the time lag of the hot-wire response is minimized, and the response can be made linear up to nigh amplitudes.

After considerable experimentation with various circuit designs, stable operation was achieved with the direct-coupled push-pull amplifier described by E. Ossofsky.[15] The

[14] A. Scurlock, Meteor Report No. 19, Massachusetts Institute of Technology, May 1949.
[15] E. Ossofsky, *Rev. Scient. Instr.* 19, (1948), pp. 881-889.

construction of this unit has been completed. The necessary power supplies are all regulated such that an input variation of 80 to 130 volts gives output variations of less than 0.01 per cent. Preliminary tests have shown that the amplifier has satisfactory drift and noise characteristics, and that it records fluctuations in an air stream of an average velocity of 500 ft./sec. Preparations are under way to calibrate the instrument with respect to average velocity and fluctuations. The latter calibration will be performed with the help of an electrical signal, consisting of a square wave of known frequency and amplitude.

The hot-wire probes consist of tungsten wires with a diameter of 0.0002 inch to 0.0004 inch and $^1/_{16}$-inch length welded to chromel supports. This welding is accomplished by means of a tweezer-welding device. Two of these units are in operation, one using a condenser discharge through a thyraton tube, the other using a high current, low voltage transformer. They have both given satisfactory results with the transformer device having the advantage of simplicity.

As was mentioned, at attempt will also be made to measure the fluctuations in the immediate vicinity of the flame and in the flame itself with a hot-wire anemometer. The function of the instrument in this case is not merely to measure velocity changes. In the flame, fluctuations in temperature, composition and velocity occur, and the hot-wire anemometer responds to all of them. These three kinds of variations, however, are strongly (though not entirely) coupled. Moreover, the hot-wire anemometer primarily registers wire temperatures. Thus strong temperature changes of the environment have by far a larger effect on the wire than all other changes. It is therefore expected that semi-quantitative information will be obtained on the local temperature fluctuations in a flame. The information is called semi-quantitative because it will hardly be possible to measure true temperature changes. However, it should be possible to ascertain quantitatively the frequency distribution and scale of these fluctuations, their relative amplitude, and whether the fluctuations are to some degree periodic phenomena or whether they are true random or turbulence phenomena. Such information is considered essential for understanding the stability, the average and true burning velocity, and the size of turbulent flames. What correlation between these fluctuations and the state of turbulence of the approaching stream can be observed, remains to be seen.

It is intended for this purpose to use a hot-wire anemometer with a relatively thick platinum wire. Even with this instrument it is, of course, not possible to measure temperatures which approach the maximum adiabatic flame temperatures. Preliminary experiments with thermocouples have shown, however, that the temperature in the protected region behind a cooled flame holder (extending downstream about twice the characteristic thickness of the flame

holder) is very far below such temperatures. It follows moreover from the width of the average burning zone of a turbulent flame that the average temperature increases only gradually to its maximum value. The average temperature at the upstream boarder of the apparent burning zone must therefore be relatively low so that it should be possible to operate in this region with a platinum wire, provided the wire is so thick that it does not respond *in full* to the instantaneous temperature pulses. For the purpose of recording temperature fluctuations the circuit will be modified to keep the *voltage* across the hot wire constant. It is then possible to pass only a small current through the wire so that the temperature of the wire will be only slightly above the average temperature of the environment. Moreover, with this arrangement the current has to be reduced when the temperature (i.e. the resistance) increases. As a consequence, the rate of heat production in the wire will decrease with increasing temperature. Therefore the excess temperature of the wire above the temperature of the environment will decrease with increasing temperature of the environment. This is obviously favorable for an extension of the upper temperature limit to which the hot-wire anemometer can be used.

Table II.

Lean propane-air mixture, average velocity 100 ft./sec. Duct 1.5 in. $x$ 2 in., flame holder a rod of ½-in. diameter and 3-in. length mounted axially. Distances in inches, pressures in inches $H_2O$.

| Distance behind flame holder | | 1 | 3 | 4 | 8.5 |
|---|---|---|---|---|---|
| Static Pressure | Value at axis. | 7.8 | 7.5 | 5.3 | 0.8 |
| | Average value at four edges | 7.8 | 7.6 | 5.3 | 0.8 |
| Head Pressure | Value at axis. | 8.3 | 7.7 | 7.4 | 6.6 |
| | Average value at four edges | 10.2 | 10.1 | 10.3 | 8.0 |
| Pitot Pressure | Value at axis. | 0.5 | 0.2 | 2.1 | 5.8 |
| | Average value at four edges | 2.4 | 2.5 | 5.0 | 6.5 |

A few preliminary measurements of pressure and composition in flames are presented which were obtained with the help of the cooled probes described above. Table II contains data on the static pressure and head pressure in flames. It is seen that the static pressure is uniform across any cross section. The change of the three pressures with increasing distances from the flame holder reflects the increase of gas velocity through combustion. The Pitot pressure shows a minimum at the axis throughout. Close to the flame holder this is probably due to low velocity along the axis of the duct, far away from the flame holder it may be due to low density (high temperature) along the axis of the duct. Preliminary measurements have also been made of the oxygen content in a rich propane-air flame in the axis of the duct

| Table III. | | | |
|---|---|---|---|
| Average gas velocity (ft./sec.) | 40 | 100 | 140 |
| Oxygen content (%) | 0.5 | 4.4 | 9.5 |
| (The theoretical oxygen content is zero.) | | | |

one inch behind the flame holder. Table III shows that combustion at this point becomes less and less complete as the gas velocity is increased.

## *E. LOCAL VELOCITY IN FLAMES USING STROBOSCOPICALLY ILLUMINATED POWDER PARTICLES. (DEL-2R4).*

*Submitted by: Kurt Wohl, University of Delaware.*

It is planned to measure the local gas velocities in laminar and turbulent Bunsen flames of the self-propagating and the diffusion type. This work is to supplement the investigation of the structure, local temperature and composition of such flames. Several questions appear to be of interest; e.g,, how does secondary burning influence the velocity pattern in the upper region of self-propagating laminar flames; how does the velocity field around the base of a laminar flame above the burner port change when the flame passes over from the self-propagating type to the diffusion type; how is the gradual disappearcnce of primary burning with increasing fuel content of the combustible mixture reflected in the general velocity pattern of a laminar flame; what is the average velocity distribution in turbulent flames, including the affected environment.

The method which recommends itself for these studies is that of stroboscopic illunination of powder particles which are admixed to the gas stream in the burner tube or to the surrounding gas atmosphere. The method has been used in this department previously under the sponsorship of Pratt and Whitney Aircraft.[16] At that time the velocity distribution in the column of buoyant gases above the primary Bunsen cone had been studied at medium average gas velocities with the help of flash bulbs as a light source. The limited brightness of this light source made it necessary to use powder of as large a diameter as 40 microns for gas velocities of about 50 ft./sec. It was, however, found that the discrepancy between particle velocity and gas velocity which was caused by the inertia of these particles is suprisingly small. This is probably due to the non-spherical shape and the rotational motion of the particles used. (The inertia effect at flame temperatures is, of course, in any case smaller than that at room temperature due to the increase of viscosity).

[16]Pratt and Whitney Aircraft Co., Summarizing Report of September 1948.

The development of the high intensity flash tubes of the General Electric Company now permits the use of powder particles of much smaller size at much higher velocities. This will make it possible to determine the velocity pattern even in regions of strong acceleration without serious distortion, and to study whirl formation and low frequency fluctuations.

In the present setup a General Electric flash tube FT-429 (2000 Volts, 480 wattsec.) is used in conjunction with a circuit which gives a duration of illumination of 0.002 sec. The lamp is placed closely behind a rotating slotted disk which intersects the light beam several times during this period. The burner tube is placed closely in front of the disk; with the help of two slits a thin sheet of light of 4 inches height is produced which passes through the axis of the burner. A mirror behind the burner intensifies the illumination. It is hoped to obtain a flash tube of the type described which is straight, 4 inches long, and silvered on the back.

The powder is introduced into the stream by letting part of the air enter the powder container near the bottom tangentially at high velocity and by letting the air leave the container tangentially at low velocity. Powder particles of various description (magnesium oxide, titanium oxide, ground mullite, silica flour or other white sand) and of an average diameter between 5 and 25 microns have been used. It seems that a diameter of 5 microns does not constitute the lower limit. In all these cases it is essential to free the powder from fine dust by elutriation. The best results so far have been obtained with Scotch Beads (Minnesota Mining and Manufacturing Company) with diameters between 5 microns and 50 microns. This material is free from fine dust. It colors the flame yellow so that a didymium filter has to be used for photographing the particles in flames.

## *F. THEORY OF FLAME SPEEDS. (Pr-2R3).*

*Submitted by: R.N. Pease, Princeton University.*

There has been no very active work on the theory of flame speeds in the past year, though some calculations on the $H_2$-$O_2$-$N_2$ system have been made. One serious uncertainty in all such work is the actual composition of burned gas. Apart from some earlier studies of the water-gas equilibrium in hydrocarbon flame gases, there is relatively little known. A project for sampling just ahead of, and also behind, the flame is under consideration.

In this general field may be mentioned preliminary experiments on the photochemical explosibility of hydrogen-chlorine mixtures. An attempt is being made to evaluate the lower-

limit intensity of radiation which will just generate an explosion. It has been possible to obtain some semi-quantitative comparisons, but difficulties remain in the reproducibility of data.

## G. *SMALL FLAME TUBE OBSERVATIONS AND THEORY. (NYU-7R3).*

*Submitted by: G.E. Hudson and I. Amron, New York University.*

Previous to 30 September 1949, this problem was NYU-1R1 entitled, Study of Effective Flame Speeds, Pressures, Temperatures, and Effective Gas Flow Speeds in Flame Tubes with Turbulence.

The experiments with the large flame tube were completed during the early part of the past year, and a report on part of this work was published.[17] A more complete report on the large flame tube studies has been submitted to and accepted by the *Journal of Applied Physics* for publication in the January or February 1950 issue of that journal. In addition, Project Squid Technical Report No. 17 entitled, *A Study of High Velocity Flames Developed by Grids in Tubes: The Role of Turbulence in Combustion Processes,* was prepared.

Experiments are to continue along the same lines using a ¼-scale model of the large flame tube to determine the effect of change in scale on the phenomena previously observed, and to examine in greater detail the relation between ionization, pressure, and flame fronts; primarily during the initial expansion of the gas through the grid. Attempts will also be made to determine the effects of all the controlled variables, one at a time, upon the flame velocity; to follow the accompanying pressure fluctuations with several pressure measuring stations; and to study the lateral variation in flow velocity with the three-dimensional Schlieren system (Div. 8, Sec. B). Further theoretical work will be done as data from these experiments become available.

In order to improve the reproducibility of both the high velocity and slow flames, an auxiliary apparatus has been designed and is under construction which will permit accurate and simple control of such factors as gas composition, humidity of the gas, initial temperature of gas mixture, spark energy, tube length, and distance from the grid to closed end of

[17] *Third Symposium on Combustion and Flame and Explosion Phenomena,* Williams and Wilkins Co., Baltimore, Md., 1949, pp. 168-176.

tube. It is felt that control of these factors will considerably simplify the detection of small differences in flame velocity due to varying grid geometry, relative grid position, and percentage of open grid area.

Preliminary qualitative observations have indicated that there is no appreciable scale effect but detailed investigation of these problems awaits completion of the considerable amount of construction work required, much of which must be done to closer tolerances than the larger tube if the measurements are to be dependable.

# V. CHEMICAL REACTION KINETICS

## A. *KINETICS OF COMBUSTION OF GASEOUS BORON COMPOUNDS. (Pr-2R2).*

*Submitted by: R.N. Pease, Princeton University.*

Substances like diborane ($B_2H_6$) and aluminum borohydride ($Al(BH_4)_3$) are potential fuels of high heat release and easy ignitibility. They have been investigated with respect to stability (ease of decomposition) and explosibility with oxygen.

**Diborane.** ($B_2H_6$; b.p. - 92.5°C) is unusual in structure in that two of the six hydrogens appear to act as bonding agents between the two boron atoms. This gives it an ethylene-like structure, and in formal analogy to the well-known polymerising tendency of ethylenic linkages (as in synthetic rubber or polythene itself), the first steps in the pyrolysis of diborane produce higher boranes with loss of hydrogen. Since this reaction occurs at fairly low temperatures (~100°C), it has an important bearing on the question of the stability of diborane, and quantitative investigation is justified on this account alone.

Measurements of the rate of pyrolysis of gaseous diborane have been undertaken in the range, 80° to 160°C, and pressures of 20 to 200 mms. Hg. It is found that at 100°C and 100 mms initial pressure, the half-life is about 10 hours, and roughly doubles for every 10° decrease in temperature. Diborane is thus considerably less stable than a hydrocarbon of corresponding molecular weight - for ethylene the temperature range would have been perhaps 300°-400° higher.

Diborane is not sensitive to glass surface or to solid decomposition products. Added hydrogen (a pyrolysis product) has a pronounced stabilizing effect; an equal pressure of hydrogen decreases the net rate of pyrolysis by a factor of 3 to 4. An inert gas such as nitrogen has no effect on the rate.

Only preliminary results are available on the oxidation rate. The indications are that at low pressures (~ 10mm) there is no explosion with oxygen even up to 100°C. Further work is in progress in this connection.

**Aluminum Borohydride.** ($Al(BH_4)_3$; b.p. - +44.5°C) is also a novel compound in many respects, containing as it does the negative ion $(BH_4)^-$, the structural analog of methane ($CH_4$)

and the positive ammonium ion $(NH_4)^+$. It is subject to complete hydrolysis yielding aluminum hydroxide, boric acid, and hydrogen, and consequently must be carefully shielded from water or water vapor.

The stability of the vapor is not very different from that of diborane. Thus at 160°C and 100 mm the half-life may be estimated at about 100 minutes, compared to an extrapolated value of about 10 minutes for diborane. The rate of decomposition at 160°C is unaffected by glass surface, or by solid products, or by addition of hydrogen (in distinction to diborane). Details of the decomposition reaction are not clear. There is some evidence that the six potential molecules of hydrogen per molecule of borohydride are given off in two sets of three, the first at temperatures of 100°-200°C, and the last three on heating to 500°-600°C. A solid product is deposited.

The oxidation of aluminum borohydride possesses interesting features. At low pressures ($\sim$ 10 mm) spontaneous explosion occurs with oxygen at room temperature provided there is a small amount of water vapor present. In bone-dry gases there is no explosion until the temperature reaches 100°-110°C, where decomposition is becoming appreciable.

Aluminum borohydride acts as an igniter of paraffin hydrocarbon-oxygen mixtures, provided the mixture carries a small amount of moisture. With mono-olefin hydrocarbons (ethylene or butylene) ignition occurs even with dry mixtures after a short induction period. In this case evidence has been obtained of a preliminary interaction between the borohydride and the olefine. This reaction is slow but detectable at room temperature, accounting for the induction period. At higher temperatures ($\sim$ 85°) it appears that a boron trialkyl is formed. This is believed to be the source of the spontaneous ignition, since earlier tests of boron triethyl $(B(C_2H_5)_3)$ had shown that this compound ignites spontaneously in oxygen even in absence of moisture.

Future work on this problem will involve the interaction of diborane and oxygen; and the aluminum borohydride-olefine-oxygen system.

## *B. INTERACTION OF HYDROGEN ATOMS WITH OXYGEN AND HYDROCARBONS. (Pr-2R4).*

*Submitted by: R.N. Pease, Princeton University.*

The initial step in most chain-reaction processes is the primary formation of an active particle (a free atom or unsaturated radical). Since this ordinarily requires a relatively

high temperature or actinic radiation for its production, it is usually rate-limiting. However, by producing such particles in an electric discharge at low pressure and subsequently mixing with normal reactants, the corresponding reaction may be studied at room temperature.

Experiments of this sort have been carried out employing atomic hydrogen from a Wood's discharge tube, in which wall re-combination is reduced by coating with phosphoric acid, and by adding a small amount of water vapor. When such atomic hydrogen is led into a mixture of hydrocarbon and oxygen all at room temperature and a few tenths millimeter pressure, the hydrocarbon is oxidized as shown by the production of aldehydes and ketones. Such an attack on the hydrocarbon molecule would normally occur only at 300°-500°C. if there were no active particles initially present.

Although quantitative analysis for all the products of reaction is incomplete, it was possible to demonstrate some outstanding trends. Thus it was surprising to find that only traces of organic peroxides were formed since it had been expected that reactions such as

$$R^* + O_2 \rightarrow ROO^* \rightarrow + RH \rightarrow ROOH + R^*$$

would occur. Actually, with isobutane ($(CH_3)_3CH$) as the hydrocarbon the principal products (10%-25% of isobutane introduced) were roughly equi-molecular amounts of acetone ($(CH_3)_2CO$) and formaldehyde ($H_2CO$) with a rather larger amount of water. This points to an overall reaction

$$(CH_3)_3CH + 1.5\ O_2 \rightarrow (CH_3)_2CO + H_2CO + H_2O$$

The initial attack on the isobutane might be

$$(CH_3)_3CH + HO_2 \rightarrow (CH_3)_3C^* + H_2O_2 \searrow H_2O$$

$$(CH_3)_3C^* + O_2 \rightarrow (CH_3)_3COO^*$$

$$(CH_3)_3COO^* \rightarrow (CH_3)_2CO + CH_3O^*$$

$$CH_3O^* + HO_2 \rightarrow H_2CO + H_2O_2 \searrow H_2O$$

The last reaction is preferred to

$$CH_3O^* + H\ (\text{or } RH) \rightarrow CH_3OH$$

since alcohols, though present, did not seem to be a major product. All this has to remain tentative in view of the incomplete analytical data, but the relatively low yields of peroxide and alcohol require some modification of current views.

A rough comparison of relative reactivities of a number of hydrocarbons was obtained by estimating total aldehydes and ketones. On this basis the ratios found (for like conditions of reaction) were 100 isobutane : 60 n-butane : 33 propane : 5 methane. Likewise among the mono-olefines the ratios were (taking isobutane as 100)- 230 butene-2 : 170 butene-1 : 190-propene.

It is believed that this still remains a promising method of attack, providing suitable analytical methods can be made available. For this purpose studies are planned involving complete analysis of such products.

## C. *KINETICS OF NON-CATALYTIC COMBUSTION OF AMMONIA.* (Pr-2R5).

*Submitted by: R.N. Pease, Princeton University.*

Ammonia ($NH_3$) stands in sharp contrast to the gaseous boron compounds just discussed. Although the heat of combustion is considerable (86.7 Cal. per mole $NH_3$), it is almost impossible to sustain a flame of ammonia in air. Even the catalytic oxidation over platinum gauze, the basis of nitric acid manufacture, is commonly operated with the gauze at a temperature in the neighborhood of 1000°C. This inertness is the more surprising in that ammonia as an electron-donor molecule might be expected to interact with oxygen, which is electron-defficient.

A study of the ammonia-oxygen system in quartz vessels has assisted in clarifying this question. It has been found that appreciable reaction rates for a 50 per cent mixture are only attained at 600°-700°C, which makes ammonia rather more inert than the saturated hydrocarbon, methane ($CH_4$). However, as the percentage of ammonia is *decreased,* the rate of oxidation *rises* rapidly. This effect is so marked that at 600°C for equal total flow rates more than twice as many moles (or grams) of ammonia oxidize in a 15 per cent mixture as in a 50 per cent mixture (fractional conversions were 75 per cent and 9 per cent, respectively). It may be said therefore that ammonia is an inhibitor for its own oxidation. Fundamentally its apparent inertness must be ascribed to this characteristic. This is unusual since for most common fuels the reaction rate increases rapidly with increasing concentration.

The reason for this effect is not completely clear. It is believed to be traceable to some step in the chain-reaction mechanism. Nevertheless, there are surface effects as well, in which ammonia might act as a catalyst poison.

The results summarized above are based on a flow system at one atmosphere. These data are now being amplified by experimental work in a static constant-volume system, with variable pressure and composition.

## *D. PHOTO IGNITION. (NYU-7R7).*

*Submitted by: H.A. Taylor and M.D. Scheer.*

The mechanism of ignition of fuel oxidant mixtures is not well understood, and it is the purpose of this study to make some contribution to the eventual solution of this problem by studying the chemical kinetics of the oxidation of hydrocarbon-oxygen mixtures in the presence of free methyl radicals produced by the photolysis of azomethane.

Gaseous azomethane liberated by heating from the cuprous chloride salt is added to a propane-oxygen mixture in a glass reaction vessel mounted within a temperature controlled oven. The reaction vessel is irradiated by an ultra-violet arc light; and the resulting reaction followed manometrically and by analyzing its products.

Preliminary tests of the photolysis of azomethane alone were made at 35°C to determine whether the mercury arc had sufficient intensity to penetrate the walls of the reaction vessel. The results were satisfactory in that approximately 20 per cent decomposition was observed after 5 hours of irradiation. A gas analysis of the resulting products checked with that obtained by previous investigators.

The stability in darkness of various azomethane-oxygen mixtures has also been studied. A 50 per cent oxygen-azomethane mixture was introduced into the reaction vessel at a temperature of 35°C and at a total pressure of 20 mm of Hg. No pressure change was observed after 24 hours, so it was concluded that there was no appreciable thermal reaction between the azomethane and the oxygen at or near room temperature. A cursory study of the photolysis of azomethane-oxygen and azomethane-propane mixtures will next be made. When this has been completed, the reaction produced by irradiation of azomethane-propane-oxygen mixtures will be thoroughly studied over the 25°-200°C temperature interval at pressures from 200-400 mm of mercury. This pressure temperature range was chosen so as to fall below the *slow reaction region* of propane oxidation, yet in the region in which one molecule of azomethane decomposes for each quantum of light absorbed.

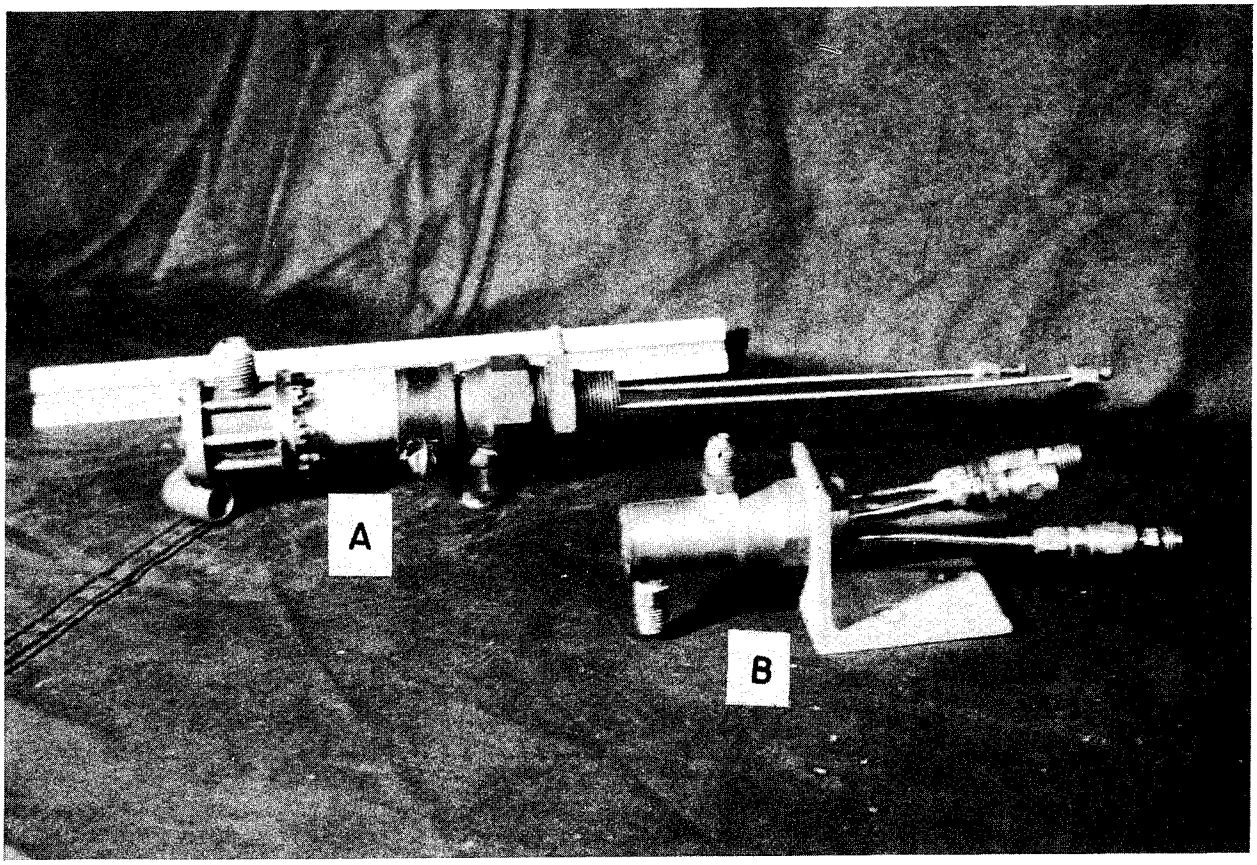


Fig. 1. Gaseous propellant rocket motors.

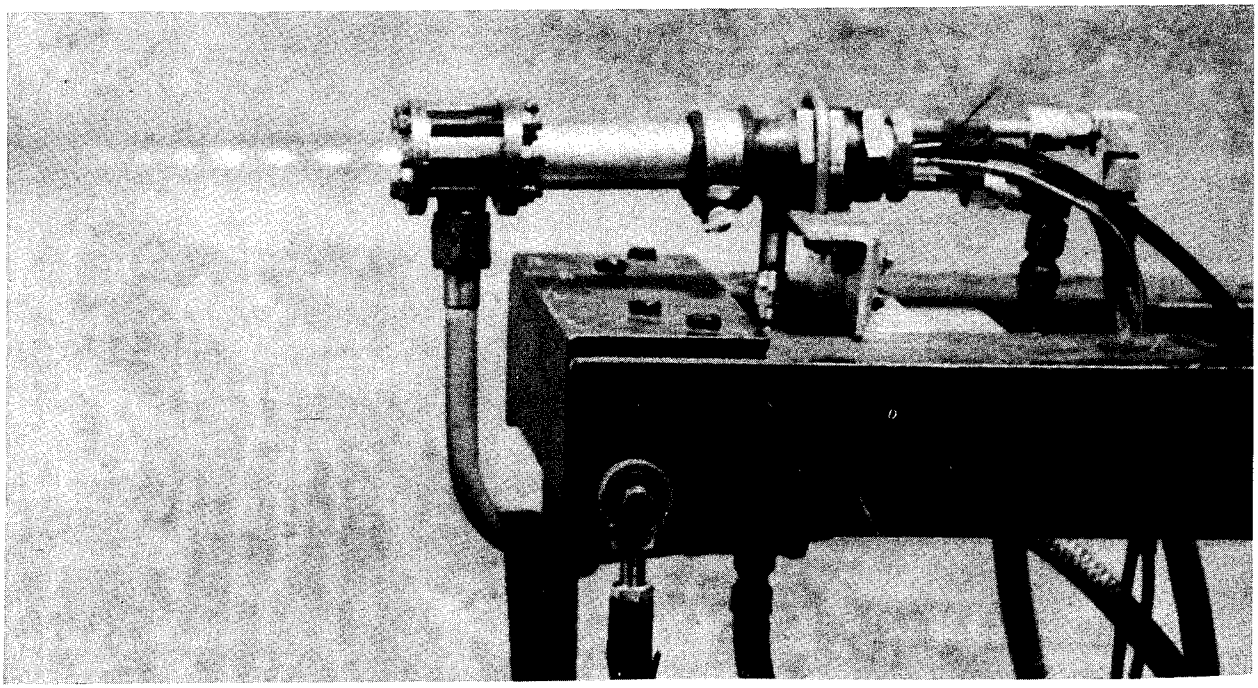

Fig. 2. Firing test: gaseous propellant rocket motor.

## *E. FUNDAMENTAL STUDIES OF L* REQUIREMENTS IN ROCKETS. (Pr-Ph. 5).*

*Submitted by J.V. Charyk, Princeton University.*

Work under this phase assignment was initiated in October 1949. The purpose of this study is to attempt a more complete understanding of the combustion processes which occur in rocket motors, and to translate this knowledge into basic parameters for design purposes. In this connection, special rocket motors of simplified design are being constructed and testing equipment is being installed. The experimental study is designed to reduce the number of variable factors to a minimum and to investigate separately these factors over a wide range of operation.

In liquid propellant rocket motors, the characteristic velocity, $c^*$, is found, for a constant mixture ratio and chamber pressure, to be a function of a parameter, $L^*$, which is defined as the ratio of the combustion chamber volume to the throat area. The value of $L^*$ for which an optimum value for $c^*$ is obtained, can as a rule only be found experimentally since the complex phenomena occurring in liquid propellant rocket motor combustion chambers have, to date, seriously limited any theoretical approach to the problem.

Involved in the establishment of a value for $L^*$ are such physical and chemical factors as mixing, atomization, evaporation, the kinetics of liquid phase and gaseous phase reactions, etc. These individual processes themselves are not well understood and their complicated interplay in rocket motor combustion chambers has precluded any general theoretical approach to the $L^*$ problem.

The present investigation is directed towards an evaluation of the effect of the following factors on $L^*$: time required for reaction in the gaseous phase; gaseous mixing; and turbulence introduced by particular injector configuration.

It is hoped that it will be possible to eliminate the effect of mixing by the use of a premixing chamber in which the fuel and oxidizer are mixed prior to injection into the motor. If successful, the remaining influencing factor will be the residence time required for complete chemical reaction. Whether or not turbulence caused by the injector design influences this time factor will be investigated by using multi-holed injectors ranging from a single hole to a porous plug. In this preliminary work, the characteristic parameter of rocket combustion, namely $c^*$, will be measured and, for a particular configuration, the value of $L^*$ which gives optimum $c^*$ will be sought experimentally.

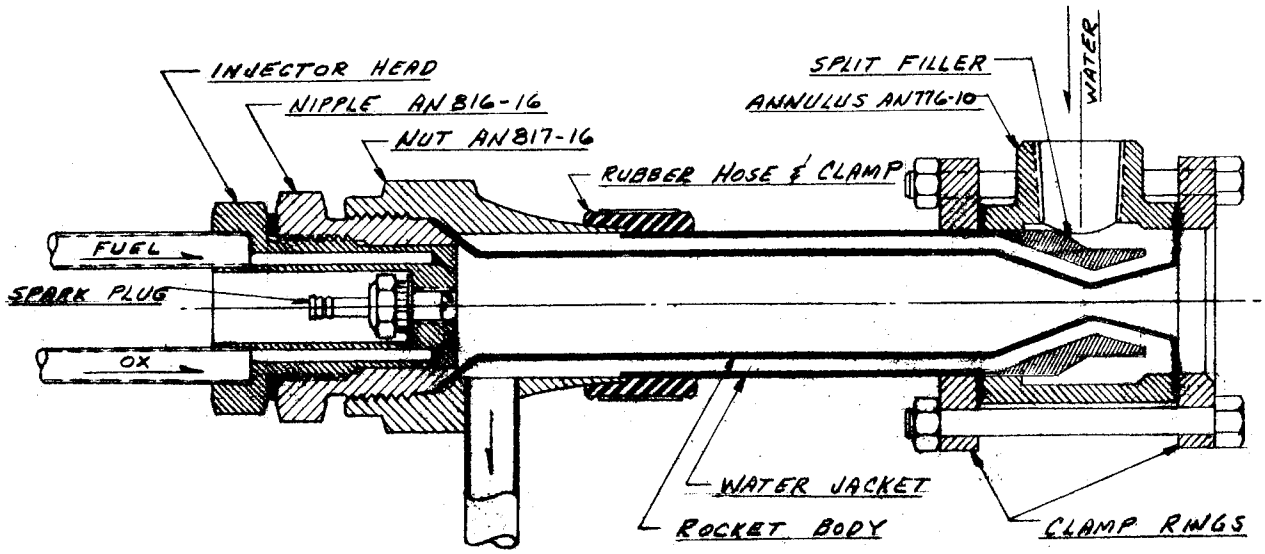


**Fig. 3.** Assembly, 10 pound thrust gaseous rocket motor.

The size of the test rocket also enters the problem in that the $L^*$ for optimum performance, at least as far as liquid propellant rockets are concerned, is known to be a function of scale. This effect can be investigated in the present experimental setup only up to motors of about 50 pound thrust. Whether this limitation will be serious remains to be seen.

The rocket motors to be used in these studies are based on a design, developed at Princeton University for laboratory work, which permits great flexibility at small cost.

Figures 1 and 2 show two small rocket motors that have been built and tested. Rocket motor A is designed for 10 pound thrust and motor B for 3 pound thrust at a chamber pressure of 300 psia. The larger motor is constructed as shown in Figure 3, with a stainless steel body and standard Army-Navy steel fittings. The fuel and oxygen enter the combustion chamber through the two lines as indicated. Only 2-hole injectors have been employed, although it is planned to use 4, 8, 16, or more holes, and, if possible, a porous plug injector. A spark plug ignites the mixture. Cooling water enters near the exhaust nozzle and is circulated through a water jacket in the annular space outside the rocket body.

With the exception of the injector head and the split ring filler around the nozzle, all parts of the rocket motor assembly are easily obtainable. Many parts are standard Army-Navy fittings, as indicated, while the rocket body, fuel lines, and water jacket are standard size stainless steel, copper, and brass tubing. The throat is formed by an inexpensive spinning process and the spark plug is of standard manufacture. Since only the internal conditions in

the rocket are of importance, no streamlining of the exterior is required. Thus rocket assemblies may be made simply and economically for a range of thrusts from 5 pounds to 50 pounds with various lengths, nozzle throat areas, and rocket body diameters. The component parts for such a series of rocket motors have been obtained and are presently being assembled.

The instrumentation and layout of the testing laboratory are designed for a high degree of accuracy in all important measurements. In order to accomplish this, provisions have been made to install two separate measuring systems at each point where such accurate observations must be made.

A special test stand has been built for the measurement of thrust. Four ball-bearing end rods are used to support an aluminum cradle and form a parallelogram-type stand that is free to move in the longitudinal direction. A straight, horizontal steel tube transmits the thrust force axially to a single linkage which converts this thrust to a vertical force acting directly onto the platform of a bench-type Toledo scale, the dial of which may be read accurately to $\frac{1}{20}$ pound. For additional accuracy, a diaphragm acting on a water column is placed in series with this scale.

The pressure in the combustion chamber is taken from two separate taps drilled in the injection head with lines leading to two independent indicating and recording pressure gauges.

Controlling and metering the flow of gases into the rocket motor is of considerable importance. The high pressure of the gases in the bottles is reduced to any desired value through adjustable pneumatic regulators which are remotely operated and activated by helium or nitrogen. Another set of remotely-operated, electric valves are placed in the test cell to control the flow of the gases into the combustion chamber. As a means of accurately determining the mass flow of gas, two sets of flowmeters are employed in series. One set is a visual flowmeter with attached recorders. The other set is a standard orifice-type meter with accompanying mercury manometers.

A visual flowmeter is inserted in the coolant flow lines, and two independent sets of readings of the coolant temperatures at entrance and exit are observed by the use of liquid-filled, bulb-type thermometers and recording thermocouples for heat transfer measurements.

It is expected that the instrumentation will be completed and that test work will be initiated by the latter part of January.

## *F. INVESTIGATION OF IGNITION LAG OF SELF-IGNITING (HYPERGOLIC) PROPELLANTS. (PRF-7R3)*

*Submitted by: S.V. Gunn, Purdue University*

The object of this problem is to obtain data regarding the effects of temperature, mixture ratio, manner of mixing, and various additives upon the ignition lag of spontaneously inflammable (hypergolic) liquid propellants. In that connection it has been necessary to develop an accurate *timing device* which measures the ignition lag accurately and from which the information can be obtained conveniently and expeditiously.

Most of the work done has been in connection with the development of the ignition lag timer. The main specifications for the timing device were that: (a) it should instantly record when the fuel and oxidizer make contact with each other when one is poured into the other in an open cup test;[1] (b) it should instantly record when visible light is emitted from the reaction; and (c) it should provide a photographic record of the elapsed time between items (a) and (b). An electronic timing device has been developed that satisfies the above requirements and in addition, by a suitable modification, it can be made sensitive to physical phenomena other than emitted light. A detailed description of the electronic timer and its design has been prepared.[2]

Electronic Timing Device. The electronic timing device is comprised of the following components: triggering pulse generator, single sweep voltage generator, cathode-ray oscillograph, phototube and phototube amplifier, signal generator, and oscillograph-record camera. Figure 4 illustrates diagrammatically the arrangement of the components. The operating principle is described briefly below.

Before an ignition lag determination is made, the single sweep voltage generator is adjusted so that the impact spot of the electron beam is located at the extreme right of the screen of the oscilloscope. At the instant the propellants come into contact with each other, a triggering voltage pulse is communicated to the single sweep voltage generator; the method employed for bringing the propellants together is discussed later. The single sweep voltage generator, upon receipt of the triggering pulse, causes the beam to deflect to the left at a uniform rate. Simultaneously, the signal generator, by intensity modulation of the beam at

---

[1]Project Squid, Annual Program Report, January 1949, p. 92-95,

[2]S.V. Gunn, *The Effect of Temperature Upon the Ignition Lag of the Rocket Bipropellant System, Red Fuming Nitric Acid and Aniline,* M.S. Thesis, Purdue University, August 1949.

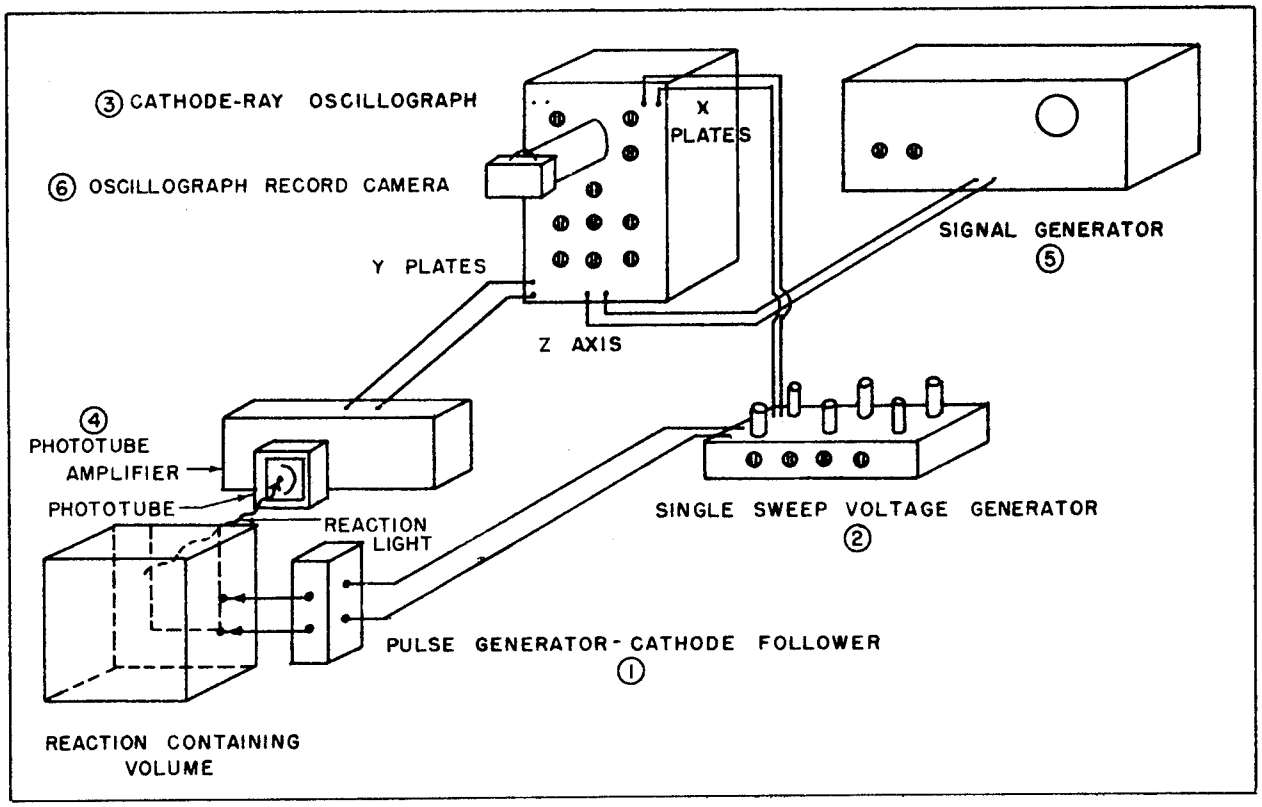


Fig. 4. Schematic diagram of components of electronic ignition lag timer.

a pre-set frequency, causes the trace to appear as a series of uniformly spaced dots; the distance between dots is a time unit equal to the period of the modulation frequency. At the instant visible light is emitted by the reaction of the propellants, the phototube and phototube amplifier cause a voltage pulse to be applied to the vertical deflection plates of the cathode ray oscillograph, and a rapid vertical deflection of the dotted line is produced. The ignition lag is determined from the photographic record of the behavior of the dotted trace, by counting the number of spaces between the horizontal dots and multiplying that number by the pre-set period of the signal generator. A typical ignition lag record is illustrated in Figure 5; a photograph of the complete timer is presented in Figure 6.

To check the accuracy of the electronic timer, a calibration device was constructed. Calibration tests were unable to detect any inaccuracies in the time interval measurements obtained with the electronic timer. A brief description of the calibration device appeared in a previous quarterly report.[3]

[3]Project Squid, Quarterly Progress Report, April 1949, p. 34.

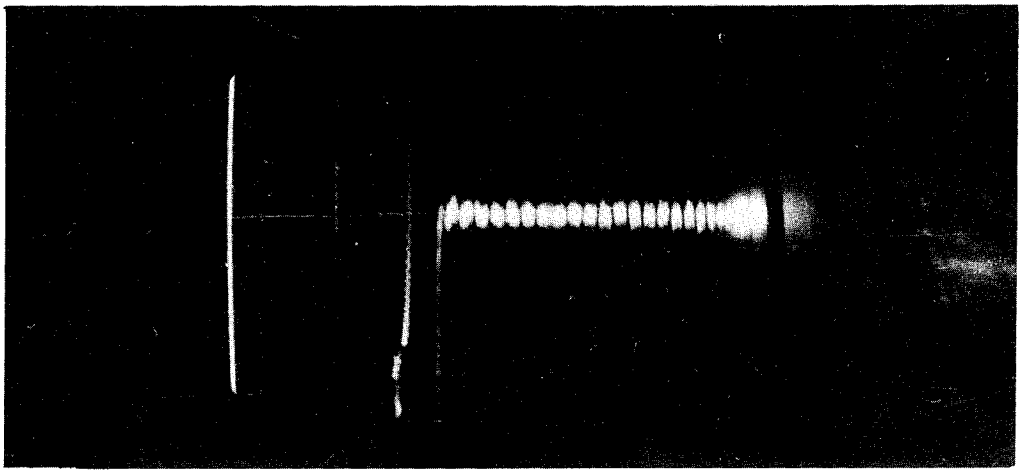

Fig. 5. Representative photographic record of normal ignition lag determination.

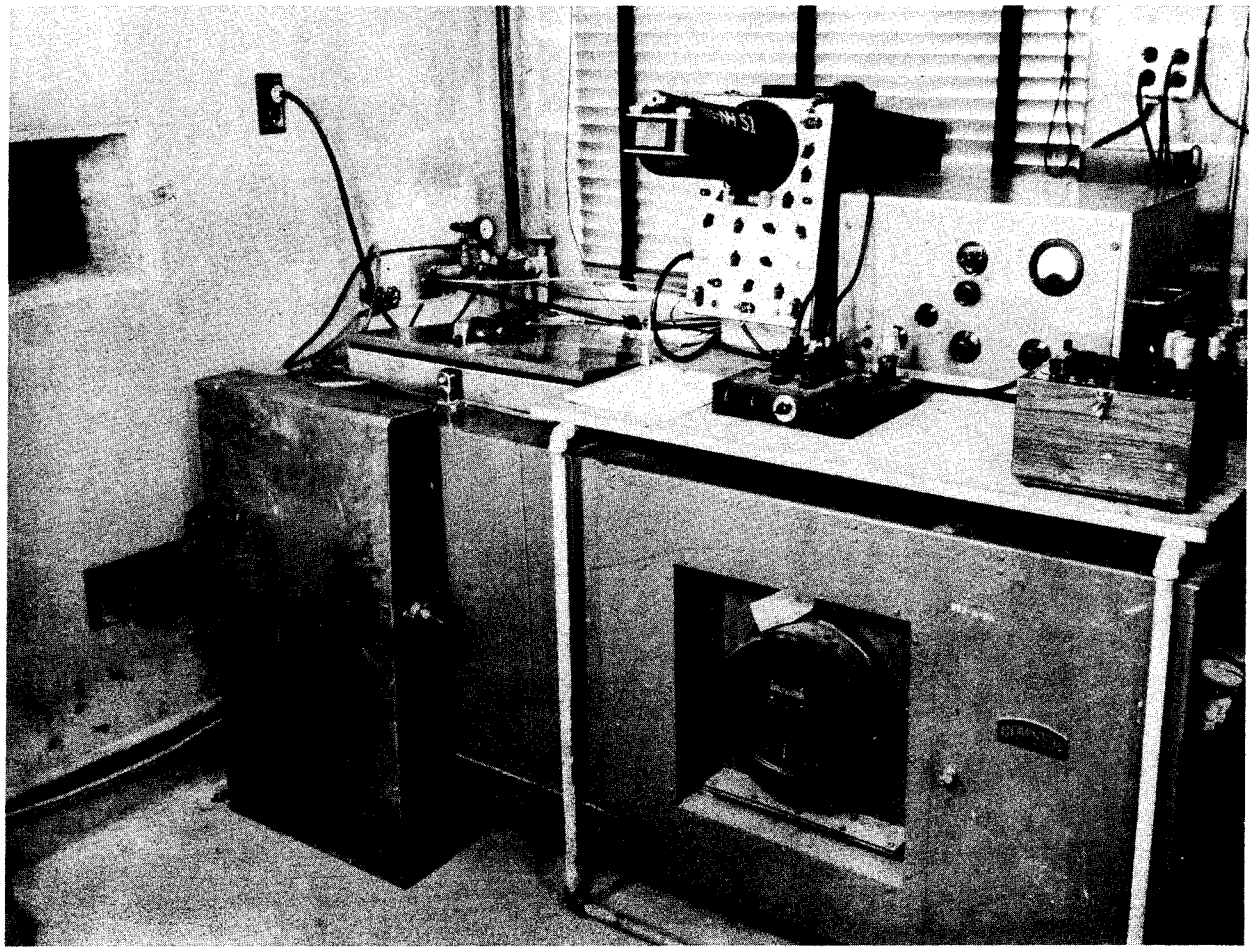

Fig. 6. Electronic ignition lag timer assembled in control room.

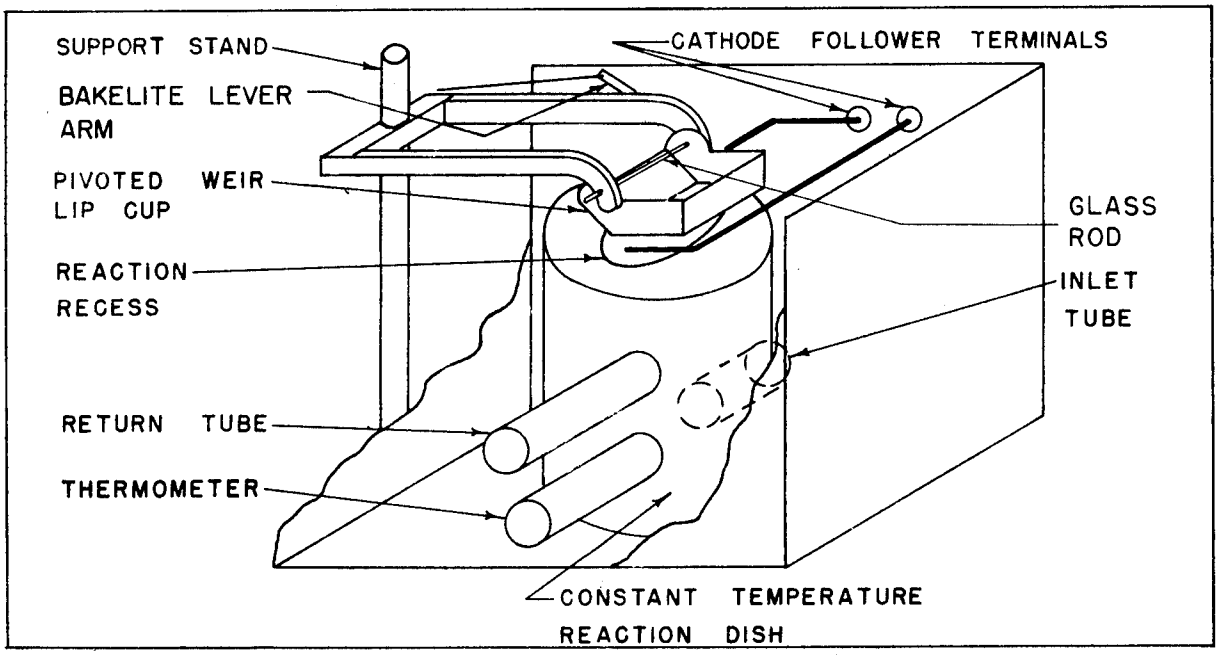


**Fig. 7.** Section schematic view of reaction box.

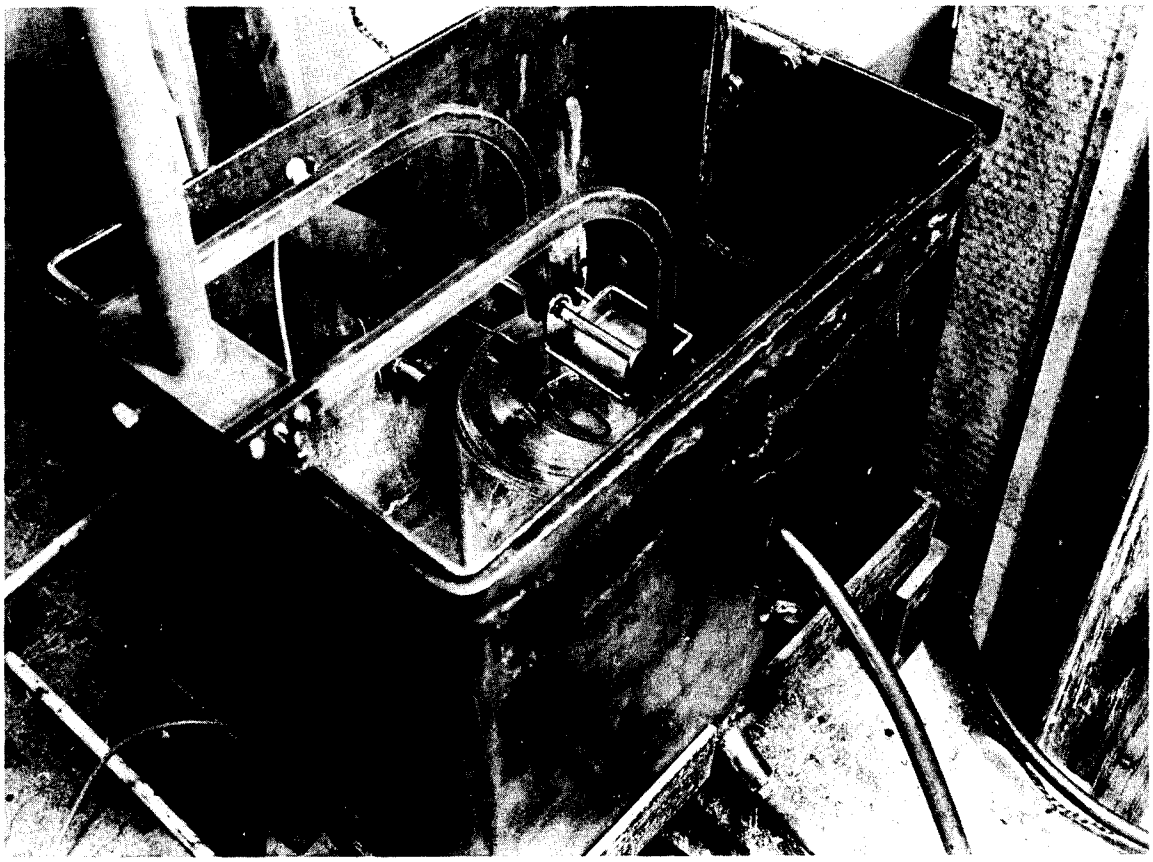

**Fig. 8.** Reaction apparatus assembled in reaction chamber.

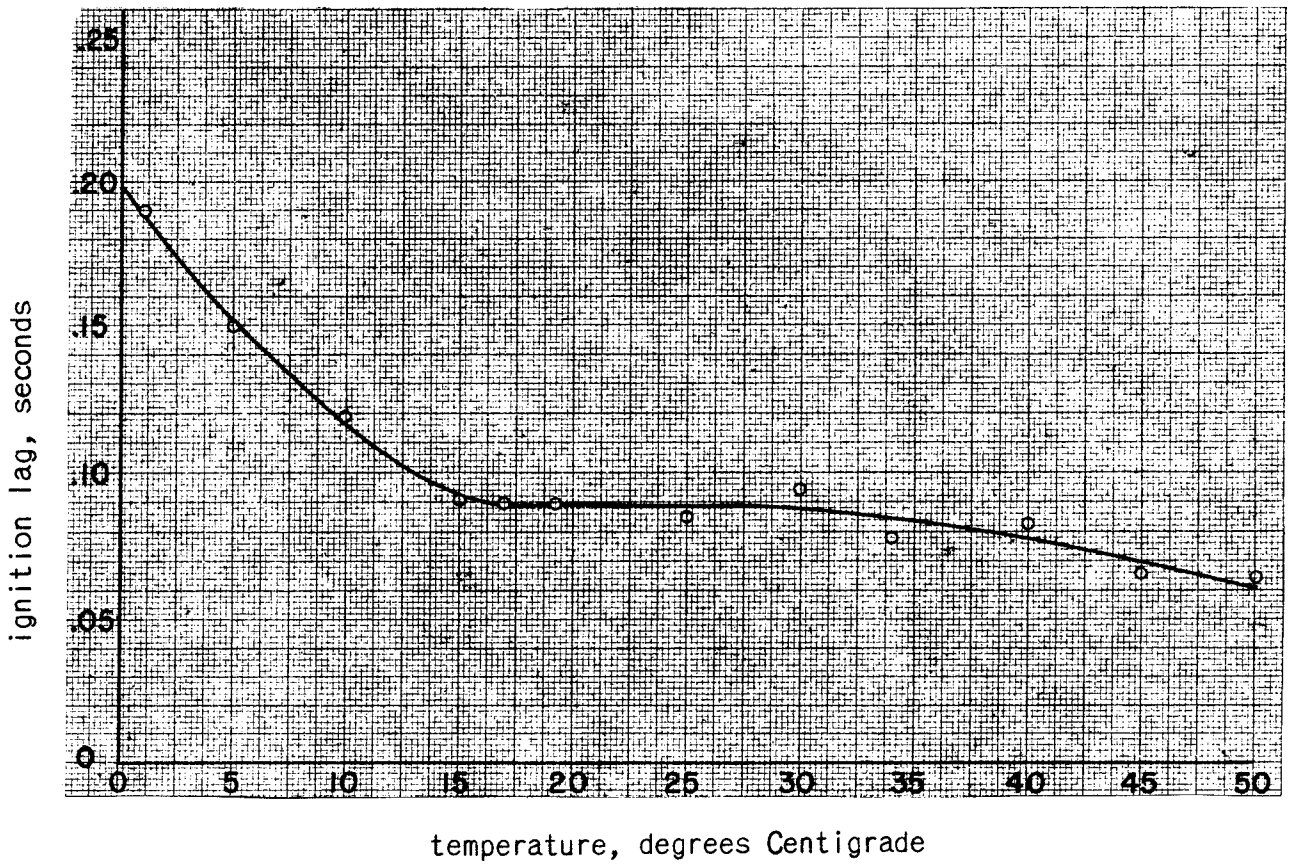


Fig. 9. The effect of temperature upon the ignition lag of the rocket bipropellant system, red-fuming nitric acid and aniline.

Open-Cup Ignition Lag Experiments. The reaction apparatus for the open-cut tests was designed so that the temperature of the liquid propellants and the mixture ratio can be controlled. For a given set of determinations the type of mixing is substantially a constant condition. The reaction apparatus has been described in detail (See footnote 2.) but a brief description of its principal features and method of operation is presented below. (See Figure 7.)

The primary elements of the reaction apparatus are: a constant temperature reaction dish, and a weir-lip cup. Figure 7 and Figure 8 are a schematic drawing and a photograph of the reaction apparatus. The rectangular weir-lip cut, made of stainless steel, is rotatably mounted upon a stationary glass rod. The weir-lip cup is arranged so that it can pour its contents, a known weight of fuel, into the recessed reaction dish located below it and containing a known weight of oxidizer. Two lead-wires, one from the weir-lip cup and the other from the reaction dish recess, are connected to the input terminals of the pulse generator. When the liquid poured from the weir-lip cup makes contact with the liquid in the reaction dish, the triggering pulse voltage, discussed earlier, is produced.

Fig. 10. Representative photographic record of ignition lag determination with pre-ignition glow.

Ignition lag determinations have been made for the red fuming nitric acid (RFNA)-aniline propellants, over the temperature range 0° to 50°C. Figure 9 presents the data obtained.

More recent ignition lag measurements conducted with RFNA and aniline in a darkened room produced a record indicating a *pre-ignition* glow prior to full ignition; a phenomena not recorded in any of the earlier experiments conducted under the same conditions, but in a lighted room. Several check experiments were conducted in the darkened room and in every case the photographic records showed a pre-ignition glow at the same time interval after the propellants came into contact with each other. The ignition lag values in all cases were identical with those obtained in earlier experiments. Figure 10 is a photograph of a record with pre-ignition glow.

A series of experiments were conducted to determine the effect of aging (darkening due to preoxidation in storage) of the aniline upon the ignition lag and the pre-ignition glow. The experiments were conducted with RFNA and: the clear liquid produced by condensation of the vapors from the distillation of aniline which had darkened during storage; aniline which had darkened during storage; and the residue remaining after the distillation of darkened aniline.

All of the experiments were conducted at room temperature (65°F to 70°F). The results obtained may be summarized as follows: the clear distillate produced an ignition lag of 0.09 seconds and a pre-ignition glow at about 0.04 seconds; the moderately darkened aniline produced an ignition lag of 0.11 seconds and a pre-ignition glow at about 0.05 seconds; and the residue produced an ignition lag of 0.12 seconds, with no discernable ignition glow.

The investigations planned for the next few months are concerned with the following: the ignition characteristics of RFNA and furfuryl alcohol, and also mixtures of furfuryl alcohol in aniline to determine whether or not the pre-ignition glow discussed above is characteristic of all hypergolic reactions with RFNA; the ignition characteristics of aniline, furfuryl alcohol-aniline mixtures, and butyl mercaptans with white fuming nitric acid; the ignition characteristics of AN-F-58 jet engine fuel, with butyl mercaptans as additives, and white fuming nitric acid (WFNA); the effect of temperature, particularly low temperatures, upon the ignition lag of fuels hypergolic with WFNA; the effect of metallic salt additives, to the fuel or WFNA, on the ignition characteristics of fuels hypergolic with WFNA; and the effects of mixing by variation of the configuration of the fuel streams discharged by the weir-lip cut, upon ignition lag.

The long range objective is to study the correlation of the type of mixing currently being employed, with ignition lag obtained when the fuels are brought together in the form of well-defined jets in the actual rocket motor.

## *G. CATALYSIS OF THE REACTIONS OF NON-SELF-IGNITING PROPELLANTS. (PRF-7R5).*

*Submitted by: C.H. Trent and C.M. Ehresman, Purdue University*

This problem is concerned with the study of the reactions of hydrocarbon fuels, such as AN-F-58 jet engine fuel, with white fuming nitric acid, the ultimate objective being to make the reactions self-igniting (hypergolic), if possible, by the addition of substances broadly classified as catalysts. In the past year the main problem has been attacked on three fronts: research on the behavior of liquid hydrocarbons with the gases produced by boiling WFNA; the determination of the chemical species formed as the result of the reaction between AN-F-58 jet engine fuel and WFNA; and measurement of the temperature history for the reactions between liquid hydrocarbons and liquid WFNA.

Vapor Phase Studies and Construction of Ignitor. A survey of the literature revealed that no investigations have been reported regarding the reactions between hydrocarbons and vaporized WFNA as processes leading to the combustion of the hydrocarbons. Recently Lloyd has outlined the effect of carbon/hydrogen ratio, density, vapor pressure, viscosity, and inflammability limits of hydrocarbon fuels on their combustion with air in gas turbine power plants.[4]

[4]P. Lloyd, " The Fuel Problem in Gas Turbines," *Internal Combustion Turbines,* American Society of Mechanical Engineers, April 1949, p. 220.

From exploratory experimentation it was found that hydrocarbon mixtures such as gasoline and kerosene will ignite spontaneously in an atmosphere composed of the gases produced by boiling WFNA if the gases are at a sufficiently high temperature. The preliminary experiments with gasoline[5] indicated that to secure its spontaneous combustion the WFNA vapors must be at a temperature exceeding approximately 350°C. Experiments of the aforementioned character are to be continued with improved apparatus for obtaining quantitative data on the factors influencing the combustion of hydrocarbons in WFNA vapor. It is also planned to determine if there is any correlation between the combustion of liquid hydrocarbons in WFNA vapor and their combustion in air.

The information obtained from the preceding preliminary experiments was employed in constructing an experimental ignitor for the propellants WFNA and AN-F-58 jet engine fuel.[6] The ignitor consisted essentially of an electrical resistance heater over which a stream of liquid WFNA was passed; the heater rapidly vaporized a portion of the WFNA. Downstream from the end of the heating section, a fine stream of liquid hydrocarbon fuel was injected into the hot vapor and immediate ignition occurred. The combustion was observed to continue even after the heating element was disconnected from the electrical energy supply. Two small experimental ignitors of the type described above were built; one using glass parts and the other stainless steel. The object was not to develop a practical ignitor but to demonstrate the principles involved. Nevertheless, it is of interest to describe the experiences with these experimental ignitors.

The major difficulty encountered was with the heated wire employed for vaporizing the WFNA. Coils made from chromel wire proved satisfactory for several experiments but finally broke. Tungsten wire was immediately oxidized by the hot WFNA vapor. Tests with the experimental ignitors demonstrated that in the design of a practical ignitor, attention must be given to the corrosion resistance, at high temperatures, of the metal utilized for the heating coil, and provision must be made to prevent the wire from sagging and short-circuiting. Platinum wire properly suspended should be satisfactory. Undoubtedly, heating the liquid fuel prior to injecting it into the WFNA vapor will aid the ignition problem. The essential components of the experimental ignitor are illustrated in Figure 11.

The Reaction Between WFNA and AN-F-58 Jet Engine Fuel. Several attempts have been made to determine the course of the reaction between WFNA and AN-F-58 jet engine fuel by allowing

[5]Project Squid, Annual Program Report, January 1949, p. 95.
[6]Project Squid, Monthly Progress Memorandum, February 1949, pp. 5-6.

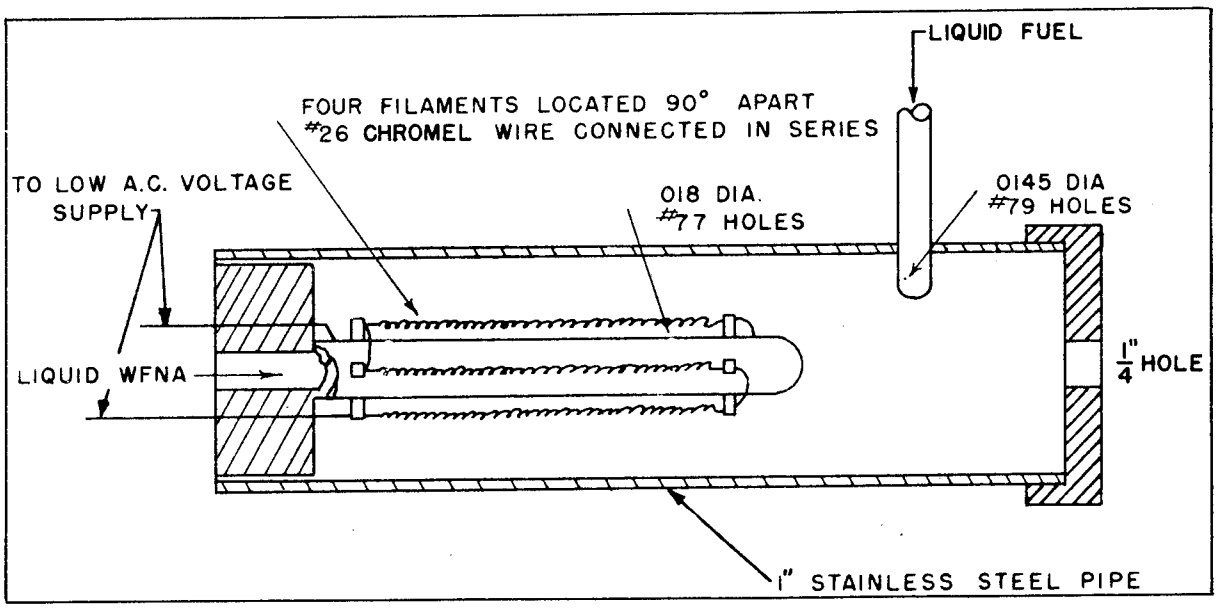


Fig. 11. Schematic drawing of ignitor for WFNA-hydrocarbon rocket propellants.

the two liquids to remain in contact with each other for known periods of time, quenching the reaction by dilution with water, and then analyzing the reaction mixture for the compounds formed.[7] These experiments were planned with the object of segregating the compounds produced in greatest yield at different reaction times, and in that manner to obtain information regarding the course of the reaction. It was postulated that this information might serve as a guide in selecting catalytic agents for accelerating the reaction. AN-F-58 jet engine fuel contains a large number of isomeric hydrocarbons. Furthermore, since only small quantities of fuel could be used with safety (5 g of jet fuel were employed in all experiments), it was impossible to isolate sufficient quantities of the reaction products for purification and subsequent characterization by macrochemical methods.

To simplify the problem, a series of isomeric hydrocarbons containing the 10-carbon-atom skeleton were selected to replace the original jet fuel. The following hydrocarbons were chosen for further experimentation: n-Decane; 2-, 3-, 4-, and 5-Methylnonane; 1-Decene; 1,9-, 1,3-, 4,6-, and 1,2-Decadiene; 1,9-, and 4.6-Decadiine; 1-, and 5-Decine; and saturated cyclic hydrocarbons and some benzene homologs. The above hydrocarbons with the exception of the acetylene derivatives are assumed to be typical of the major constituents in AN-F-58 jet engine fuel.

[7]Project Squid, Monthly Progress Memorandum, June 1949, p. 45.

Currently the synthesis of 1.9-decadiene is in progress; the other compounds are yet to be synthesized. Subsequently all of the aforementioned hydrocarbons will be reacted with liquid WFNA and the identification of the reaction products will be attempted.

**Temperature Measurements on the WFNA-Hydrocarbon System.** It has been observed that when WFNA is added to various types of hydrocarbon compounds there is an increase in the temperature of the system.[8] The temperature increases to a maximum at a rate which depends upon the nature of the hydrocarbon and the apparatus; the effect on the rate of temperature rise of the quantity of reactants has not yet been determined. The initial exploratory experiments indicated that not only the maximum temperature reached, but also the rate at which the temperature increases is related to the structure of the hydrocarbon molecule. A survey of the literature failed to produce any published data on the rate of temperature rise of the maximum temperature reached when a liquid hydrocarbon fuel is reacted with liquid WFNA, or for fuels hypergolic with WFNA.

It appears logical to hypothecate that one of the differences in the reaction of fuels which are either non-hypergolic or hypergolic with WFNA should be the initial rates of the temperature rise when reacted. To establish this point, experiments were conducted to obtain data on the initial rates of temperature rise of several hydrocarbons having different molecular structures when reacted with liquid WFNA at ambient temperature. Experiments were also conducted with fuels which are hypergolic with WFNA. It was believed that from such data judgments would be possible regarding the type of hydrocarbon structure which reacts most rapidly with WFNA.

The first set of experiments was conducted with the low boiling fractions, each having a boiling range of 10° C, obtained from the rectification of AN-F-58 jet engine fuel. These fractions were reacted with WFNA as a 2-phase system, and the maximum temperature reached was measured by means of a glass-sheathed iron-constantan thermocouple placed as close as possible

Table I. Reaction of pure olefins with white fuming nitric acid.

| Hydrocarbon | WFNA g | Fuel g | Initial Temp. | Max. Temp. | T | Calculated T/t |
|---|---|---|---|---|---|---|
| 1-Dodecene | 24 | 5 | 86 F | 241 F | 155 F | ----- |
| 1-Octene | 24 | 5 | 86 F | 241 F | 155 F | 135.5 F / sec |
| 1-5-Hexadiene | 24 | 5 | 86 F | 243 F | 157 F | 550 F / sec |

[8] Project Squid, Monthly Progress Memorandum, April 1949, p. 4-5.

to the interface between two liquids. The comparison of the bromine number of each fraction with the maximum temperature reached indicated that fractions having a higher bromine number and, therefore, a higher degree of unsaturation gave the largest values of maximum temperature. The mono-olefins 1-dodecene and 1-octene, and also the diolefin 1,5-hexadiene gave a much higher maximum temperature than did the AN-F-58 fraction.[9] With 1,5-hexadiene (Table I) the reaction proceeded rapidly with an average initial rate of temperature rise of roughly 550°F/sec; these data do not take into account any lags in thermocouple response and should, therefore, be regarded as orders of magnitude only. The above results indicate in a general way that the presence of olefinic hydrocarbons in petroleum fuels is favorable to initial reaction with liquid WFNA. To what extent unsaturation affects the reactions will be determined by obtaining the time-temperature curves for the hydrocarbons listed on page 134.

**Table II.** Reaction of hypergolic fuels with WFNA and RFNA.

| Propellant Combination | Flame | Initial Temp. | Temp. of 1st break | Time to 1st break | Temp. of 2nd break | Time to 2nd break | Calculated T t (1) | Calculated T/t (2) |
|---|---|---|---|---|---|---|---|---|
| 1. Aniline & WFNA | delay | 77 F | 212 F | 0.18 sec | 289.4 F | 0.13 sec | 750F sec | 595F sec |
| 2. Aniline & WFNA | none | 77 F | 221 F | 0.15 sec | 293 F | 0.20 sec | 720F sec | 360F sec |
| 3. Aniline & WFNA | long delay | 86 F | 129 F | 0.07 sec | 271 F | 0.11 sec | 614F sec | 1273F sec |
| 4. Aniline | Immediately | 86 F | 212 F | 0.01 sec | 302 F | 0.14 sec | 1400F sec | 643F sec |
| 5. Furfuryl Alcohol & WFNA | Immediately | 86 F | 230 F | 0.11 sec | 352 F | 0.03 sec | 1309F sec | 4067F sec |

The rates of temperature rise were also measured for the aniline-WFNA and furfuryl alcohol-WFNA propellants which are hypergolic.[10] The WFNA was added to the fuel contained in a glass reaction vessel enclosed in a stainless steel case sufficiently ventilated to allow the reaction to proceed against the constant pressure of the atmosphere. The temperature changes were measured by a platinum-platinum-10% rhodium thermocouple immersed in the fuel and calibrated for use in conjunction with a Consolidated recording oscillograph. A record was thereby

[9]Project Squid, Monthly Progress Memorandum, October 1949, p. 3.
[10]Project Squid, Monthly Progress Memorandum, November 1949, p. 2.

obtained of time versus temperature for the reaction. Unfortunately, because of the apparatus employed, the time-temperature curves obtained for the hypergolic fuels, and also for the non-hypergolic hydrocarbon fuels, were not reproducible to the desired degree of precision. The results should, therefore, be regarded as only a qualitative measure of the temperature changes. Those experiments which are in fair agreement with each other are presented in Tables I and II. The O/F mixture ratio for the hypergolic fuels was 3/1 employing 4g of fuel and 12g of oxidizing agent.

The geometry of the reaction vessel, the position and response rate of the thermocouple, and the method of introducing the oxidant affect the shape of the time temperature curve. A slight modification of any one of the above factors produces a different curve the same ame acid-fuel combination. For example, when aniline and WFNA are reacted in an elliptically shaped recess 2 in. long, 1 in. wide, and 1 in. deep (reactions 1 and 2, Table II) the values obtained for the slopes of the time-temperature curve are quite different than when this system is reacted in a cylindrical beaker 1.5 in. in diameter (reaction 3). Furthermore, experiments carried out in a vessel 1.5 in. in diameter and having the thermocouple sealed into the hemispherical bottom gave curves which were neither consistent with themselves nor with the previous experiments.

Currently these experiments are being continued employing different types of reaction apparatus with the objective being to develop an apparatus that gives reproducible results. After the latter problem is solved, time-temperature data for the reaction behavior of liquid WFNA and the hydrocarbons listed on page 134 will be determined.

## *H. OXIDATION OF CHROMIUM ALLOYS. (PRF-Ph-3).*

*Submitted by: H.J. Yearian, Purdue University*

This problem is a study of corrosion in connection with jet propulsion devices; the purpose of the research is to identify the corrosion as affected by the chemical and physical properties of the materials and the conditions of exposure.

X-ray diffraction measurements of the scale (corrosion products) formed on 5 per cent to 26 per cent chromium steels when oxidized in oxygen at temperatures of 700°C to 1160°C for periods ranging from ¼ hour to 100 hours confirm the correlations previously established[11]

[11]Project Squid, Annual Program Report, January 1949.

between oxidation resistance and the presence of $Cr_2O_3$ together with the absence of $Fe_3O_4$. Comparable results are obtained for air oxidations. An additional spinel structure of larger parameter is also found. The possible interpretations of this structure are discussed.

The temper-color films formed beneath the scale in oxygen and air, and the scale-free films produced in shorter times and at lower temperatures have been stripped and examined by transmission electron diffraction and electron micrography. The diffraction shows that essentially all films have similar crystal structure; the chief component is a chrome-rich $\alpha Fe_2O_3$-$Cr_2O_3$ phase together with a small amount of $Fe_3O_4$-$FeCr_2O_4$. This result applies only to the thin films, which micrographs show have a texture of coarseness increasing with rate of attack, and on which the incipient scale grows from localized centers.

X-ray diffraction determinations have been made of the scale formed on chromium steels when oxidized in one atmosphere of pure oxygen for 20 hours at 700°C to 950°C, for ten hours at 1000°C and 1100°C, and for seven hours at 1160°C. The results at intermediate temperatures, reported previously,[12] is reproduced with the added results discussed above as Table III. The oxides formed in 20 hours at 600°C were too thin for X-ray examination but were electrolytically stripped and examined by transmission electron diffraction (Table VI).

In Table III the letters S, M, W, indicating strong, medium, and weak intensity diffraction patterns, are entered in columns referring to the three principal phases observed, namely: O, the $Fe_3O_4$ magnetite type spinel with a lattice parameter a = 8.385±0.01 KX where 1 KX unit = 1.00202 Angstrom units (an entry with * indicates a similar spinel structure with a = 8.430± 0.01 KX); X, the $\alpha Fe_2O_3$ hematite type phase with not more than 10 per cent $Cr_2O_3$ in solid solution; and $X_c$, the $Cr_2O_3$ type phase with not more than 10 per cent $\alpha Fe_2O_3$ in solid solution, a number in this column refers to a phase with this percentage of $Cr_2O_3$ in solid solution with $\alpha Fe_2O_3$. Where it has been possible to separate the scale into layers, the distribution of the phases through the scale is shown by a bar placed over the symbol if the phase increases toward the inside of the scale; where complete segregation has been found, the whole symbol is displaced upward or downward corresponding to outside or inside respectively.

The extension of the measurements to higher or lower temperatures confirms the correlation of oxide type and oxidation resistance discussed previously.[13] An X phase occurs under

[12] Project Squid, Annual Program Report, January 1949.
[13] *Ibid.*

**Table III.** Scale on Chromium Steels Oxidized in One Atmosphere Dry Oxygen

S,M,W = strong, medium, weak diffraction patterns.

O = $Fe_3O_4$ (magnetite) type spinel with with phase lattice parameter a = 8.385 ± 0.01 KX

O* = $Fe_3O_4$ (magnetite) type spinel phase lattice parameter a = 28.430 ± 0.01 KX

X = $\alpha Fe_2O_3$ (hematite) phase, not more than 10% $Cr_2O_3$ in solid solution

$X_c$ = $Cr_2O_3$ phase, not more than 10% $\alpha Fe_2O_3$ in solid solution; Note: A number in the third column indicates an $\alpha Fe_2O_3$ phase with this percentage of $Cr_2O_3$ in solid solution.

( ) = Sometimes found

" = $\alpha Fe_2O_3$ on surface oriented with (111) phase parallel to surface.

Bar above or below intensity symbol = Phase increases toward outside or inside of scale respectively.

Intensity symbol displaced upward or downward = Complete segregation of phase on outside or inside of scale respectively.

| Temp. deg.C | Hrs. | Per Cent Cr Alloy | | | | | | | | | | | | | | |
|---|---|---|---|---|---|---|---|---|---|---|---|---|---|---|---|---|
| | | 5% | | | 11% | | | 13% | | | 17% | | | 26% | | |
| | | O | X | $X_c$ | O | X | $X_c$ | O | X | $X_c$ | O | X | $X_c$ | O | X | $X_c$ |
| 700 | 20 | W | S | - | | | | - | S | S | - | S | M | - | M | S |
| 775 | 20 | W | S | - | - | S | W | - | S | M | - | M | S | *W | W | S |
| 825 | 20 | S | S | - | - | S | W | M | (W) | S | - | S | M | *W | W | S |
| 900 | 20 | M | S | - | - | M | (?) | M | S | (S) | (W) | S | W | *W | S | W |
| 950 | 20 | S | S | - | S | M | - | M | S | - | M | S | - | *S | - | S |
| 1000 | 10 | S | M | - | S | M | - | S | W | - | S | S | - | *S | - | S |
| 1100 | 10 | S | S | - | | | | S | S | 25M | | S | 15S | *S | - | S |
| 1160 | 7 | | | | | | | | | | | S | 15W | *M | S | - |

nearly all conditions. On any given alloy $X_c$ is present at low temperatures but as the temperature increases the amount of the phase decreases and is eventually replaced by an increasing amount of the O phase. An exception to the latter trend is shown by the 26 per cent alloy for which the O* spinel of large parameter occurs at all temperatures above 700°C, even at 1160°C where the $X_c$ phase has disappeared, and no O structure is found. The transition temperature, above which $X_c$ is absent and O present, increases with increasing chromium content of the alloy and corresponds to the temperature at which the rate of metal loss attains a value of approximately 100 mg/cm$^2$/day.[14]

It has not been possible to find the distribution of $Cr_2O_3$ through the scale since it is observed only when the scale is too thin to be separated into layers. Under conditions of rapid attack, where both O and X structures occur, the trend is for X to become more prevalent toward the surface and O toward the inside of the scale; for the highest rates, this segregation becomes complete.

Coincident with rapid attack a strongly oriented material is formed on the scale surface (symbol "). This structure was tentatively assigned to $Cr_2O_3$ on the basis of the single strong reflection of interplanar spacing d=2.28 - 2.30 KX observed with the Phillips spectrometer.[15] This seems improbable since the pattern is observed most readily on the lowest chrome alloys. More complete investigation by grazing incidence photographs, for which reflections from many planes can be observed, has now established that the whole pattern can be accounted for by $\alpha Fe_2O_3$ oriented with its (111) plane parallel to the specimen surface. The geometry of the Phillips spectrometer is such that the second order diffraction from the plane (d= 2.288 KX), which does not appear in randomly arranged powder samples, is strong because of this particular orientation. With this crystal orientation, the direction of growth perpendicular to the specimen surface is in a crystallographic direction for which layers of oxygen and iron ions alternate and the preferential growth is presumably influenced by this arrangement. That the presence of chromium is not essential to the formation of this oriented structure is evidenced by the recent observation that it may be formed on a chromium-free cast iron.

Wherever this oriented structure is indicated in the table, it is probable that no other phase is present on at least the extreme surface, even in those cases for which observations on mechanically separated layers could not be effected.

---

[14] *Corrosion Handbook*, John Wiley and Sons, p. 644 ff.
[15] Project Squid, Annual Program Report, January 1949.

Table IV. Scale on Chromium Steels Oxidized in One Atmosphere Dry Oxygen.

S,M,W = strong, medium, weak diffraction patterns.

O = $Fe_3O_4$ (magnetite) type spinel with phase lattice parameter a = 8.385 ± 0.01 KX.

O* = $Fe_3O_4$ (magnetite) type spinel phase lattice parameter a = 28.430 ± 0.01 KX

X = $\alpha Fe_2O_3$ (hematite) phase, not more than 10% $Cr_2O_3$ in solid solution.

$X_c$ = $Cr_2O_3$ phase, not more than 10% $\alpha Fe_2O_3$ in solid solution; Note: A number in the third column indicates an $\alpha Fe_2O_3$ phase with this percentage of $Cr_2O_3$ in solid solution.

( ) = Sometimes found

" = $\alpha Fe_2O_3$ on surface oriented with (111) phase parallel to surface.

Bar above or below intensity symbol = Phase increases toward outside or inside of scale respectively.

Intensity symbol displaced upward or downward = Complete segregation of phase on outside or inside of scale respectively.

| Temp. deg.C | Hrs. | Per Cent Cr Alloy | | | | | | | | | | | | | | |
|---|---|---|---|---|---|---|---|---|---|---|---|---|---|---|---|---|
| | | 5% | | | 11% | | | 13% | | | 17% | | | 26% | | |
| | | O | X | $X_c$ | O | X | $X_c$ | O | X | $X_c$ | O | X | $X_c$ | O | X | $X_c$ |
| 825 | 2 | (?) | S | (?) | - | S | (?) | - | S | W | - | S | M | - | M | S |
| | 20 | S | S | - | - | S | W | M | (W) | S | - | S | M | *W | W | S |
| 900 | ½ | S | S | - | M | S | VW | S | S | W | M | S | W | - | M | S |
| | 5 | S | S | - | | | | (M) | S | M | - | S | W | - | M | S |
| | 20 | W | S | - | - | M | (?) | M | (S) | (S) | (W) | S | W | *W | S | W |
| | 100 | W | S | - | | | | - | M | W | - | S | - | (*W) | S | 75W (W) |
| 1000 | ½ | S | S | - | S | S | W | M | S | W | M | S | W | - | - | S |
| | 20 | S | M | - | S | M | - | S | W | - | S | S | - | *S | - | S |

The results of structure determinations as a function of time of oxidation are shown in Table IV, using the same notation as above. It is evident that the O* structure increases in time more rapidly than either X or $X_c$. Under conditions of rapid attack on a small amount of $X_c$ may be found in short but not in long oxidations. This need only require that the material grow less rapidly than other phases present, not that it disappear; it may still be present in small amounts. The O phase, on the other hand, increases more rapidly than the X phase under these conditions.

Results of oxidations in dry air over a limited range of temperatures, are shown in Table V. The general trends are the same as those established for oxidation in a pure oxygen atmosphere. There is some indication of a slightly larger portion of the O spinel, and it is noted

Table V. Scale on Chromium Steel - Dry Air.

S,M.W, = strong, medium, weak diffraction patterns.

O = $Fe_3O_4$ (magnetite) type spinel with phase lattice parameter a = a = 8.385 ± 0.01 KX.

O* = $Fe_3O_4$ (magnetite) type spinel phase lattice parameter a = 28.430 ± 0.01 KX.

X = $\alpha Fe_2O_3$ (hematite) phase, not more than 10% $Cr_2O_3$ in solid solution.

$X_c$ = $Cr_2O_3$ phase, not more than 10% $\alpha Fe_2O_3$ in solid solution; Note: A number in the third column indicates an $\alpha Fe_2O_3$ phase with this percentage of $Cr_2O_3$ in solid solution.

( ) = Sometimes found.

" = $\alpha Fe_2O_3$ on surface oriented with (111) phase parallel to surface.

Bar above or below intensity symbol = Phase increases toward outside or inside of scale respectively.

Intensity symbol displaced upward or downward = Complete segregation of phase on outside or inside of scale respectively

| Temp. deg.C | Hrs. | Per Cent Cr Alloy 5% | | | 11% | | | 13% | | | 17% | | | 26% | | |
|---|---|---|---|---|---|---|---|---|---|---|---|---|---|---|---|---|
| | | O | X | $X_c$ | O | X | $X_c$ | O | X | $X_c$ | O | X | $X_c$ | O | X | $X_c$ |
| 775 | 20 | S | S | - | - | S | - | *VW | S | S | *W | S | S | *M | - | S |
| 825 | 20 | M | S | - | - | S | M | *W | M | M | *M | - | S | *M | VW | S |
| 900 | 5 | M | M | - | | | | - | S | S | W | M | S | *M | - | S |
| | 20 | S | M | - | | | | M | S | - | W | - | S | *S | - | S |
| | 100 | S | W | - | | | | W | S | - | - | S | - | *M | - | S |

that the X phase disappears at 900°C on the 26 per cent alloy instead of at 1000°C, but the only striking difference is the occurrence, at the lower temperatures, of the O* spinel on 13 and 17 per cent alloys as well as on the 26 per cent alloy. The relative amount of this material increases, at a given temperature, with chromium content of the alloy. These results, therefore, give evidence that a decrease in the severity of oxidation conditions and a high chromium content of the alloy favor the formation of the large parameter spinel. It is to be noted that in all cases so far observed this structure is found only in the presence of $Cr_2O_3$ ($X_c$), and there are indications that it is accompanied by a reduction in the amount of $\alpha Fe_2O_3$(X).

Interpretation of the two spinel patterns found is an open question. One would expect to find spinels with a lattice parameter approaching a=8.34 KX if the percentage of chromium increased toward the composition $FeCr_2O_4$ (chromite) as has been suggested by chemical analysis.[1]

[16]H.H. McCullogh, *Ohio State Engineering Experiment Station News*, December 1947, p. 38.

No such value is found. It is thought the expected variation may be masked by a compensating variation of the structure.[17] This could be due either to deviations from stoichiometric proportions (an excess of oxygen in the structure lowers the parameter) or to a partial or complete change from the *inverted* to the *normal* metallic ion arrangement, which should increase the parameter. The O* structure might also be accounted for on this basis, having perhaps a deficiency of oxygen (formed in the presence of chromium) or having reverted to the normal arrangement.

Since no systematic investigation of tnese points has been found in the literature, attempts have been made to synthesize iron and iron-chromium spinels having different lattice parameters, with the idea that if this is possible, chemical analysis can be used to correlate lattice parameter measurements with composition. Several variations of two basic methods of precipitation of the hydroxide and heating to obtain the oxide have been used. In most cases the material is too finely divided to give good diffraction patterns and in any case control of the degree of oxidation is not good. When the preparation of magnetite is done in air, a slightly low value of parameter, a=8.37±.005 KX is found. On heating in air at 250°C, this material converts to the magnetic ferric oxide form $\alpha Fe_2O_3$, which has the same structure as magnetite, but a low parameter, 8.33 KX, associated with the deficiency of metal ions in the lattice. When the preparation is carried out under nitrogen, a parameter of 8.38 to 8.39 KX is found. Whether the parameter can be raised as high as the value 8.43 found for O*, or whether this is only possible in the presence of chromium or by solution of chromium, is yet to be determined. Some high temperature reductions of $\alpha Fe_2O_3$ and mixtures of this with $Cr_2O_3$ are now being tried. Preliminary reduction experiments with carbon and with chromium metal, as well as by heating the oxalate, give spinels with a=8.38 ±.005 KX.

The thin oxide films formed on 5 to 26 per cent chromium steels under a variety of conditions have been stripped and examined by transmission electron diffraction and electron micrography. Three methods of stripping are being used. These are an electrolytic method using KCl saturated with hydrogen as electrolyte, dissolution of the metal by bromine in methanol, and a second electrolytic method using perchloric acid and acetic anhydride. The ease of stripping increases in this order. Since no significant difference has yet been observed in the structure of films removed in the various ways, we assume, tentatively, that no changes are produced during stripping.

The structures found by electron diffraction of the films produced by heating in one atmosphere of oxygen at temperatures of 600°C to 1000°C for times of ¼ to 20 hours are summarized

[17]Project Squid, Annual Program Report, January 1949.

**Table VI.** Structure of Oxide Films - One Atmosphere Oxygen.

O = $Fe_3O_4$ - $FeCr_2O_4$ type spinel

X = $\alpha Fe_2O_3$ - $Cr_2O_3$ type; position left to right indicates increasing amounts of $Cr_2O_3$ in solution or as a mixture

Symbol in upper line = thin film

Symbol in lower line = thicker film

——— = grey film too thick for diffraction

| Temp. deg.C | Hrs. | Per Cent Cr Alloy 5% | 11% | 13% | 17% | 26% |
|---|---|---|---|---|---|---|
| 600 | 20 | $X_4$ / $X_3$ | $X_4$ / ? | $X_4$ / $X_4$ | $X_4$ / $X_4$ | 0 $X_4$ / 0 $X_4$ |
| 700 | ½ | $X_4$ / $X_4$ | $X_4$ | $X_4$ / 0 $X_3$ | 0 $X_4$ / $X_4$ | 0 $X_4$ / $X_4$ |
| | 1 | 0 $X_4$ / 0 $X_4$ | | 0 $X_2$ | $X_4$ / $X_4$ | $X_4$ / $X_4$ |
| | 20 | 0 | | 0 $X_3$ | 0 | 0 $X_4$ |
| 800 (Scale Removed) | ½ | 0 | 0 $X_2$ | 0 $X_1$ | 0 $X_2$ | 0 $X_1$ |
| | 1 | 0 $X_3$ / $X_3$ | | 0 $X_3$ / 0 $X_2$ | 0 $X_4$ | 0 $X_4$ |
| | 2 | 0 $X_3$ | | 0 $X_4$ | 0 $X_4$ | 0 $X_4$ |
| | 20 | 0 | | 0 $X_3$ | 0 $X_3$ | 0 $X_3$ |
| 900 | ¼ | 0 $X_3$ / $X_3$ | | 0 $X_4$ | $X_4$ | 0 $X_4$ |
| | ½ | $X_2$ / 0 $X_2$ | 0 - $X_3$ | 0 $X_3$ | 0 $X_3$ | 0 $X_4$ |
| 1000 | ¼ | 0 $X_1$ / 0 $X_2$ | | 0 $X_1$ | 0 $X_3$ | 0 $X_4$ |
| | ½ | 0 $X_2$ / 0 $X_1$ | $X_3$ | $X_3$ | 0 $X_3$ | 0 $X_3$ |

in Table VI. For the times and temperatures below the line shown, a more or less heavy scale was formed which could be removed mechanically before stripping the film. These data, therefore, represent a thin temper-color oxide film as formed on the metal under a heavy scale. (The scale structure is included in Tables III and IV.) For times and temperatures above the

line indicated, no removable scale was formed. In stripping these latter films, a grey film too thick for electron penetration sometimes separates from the remainder of the film. This is shown by a horizontal line at the bottom of the rectangle. Independent of the presence or absence of the grey film, there frequently is a separation into a thin and a thick transparent component. The diffraction results for the former are shown in the top line, and for the latter in the bottom line of symbols. Which of these components lies next to the metal has not yet been determined, but there is some evidence that it is the thinner one.

The symbol O at the left indicates the presence of an $Fe_3O_4$-$FeCr_2O_4$ phase. This material is usually present only in small amounts, with the consequence that the lattice parameter can not be determined with accuracy, but it seems to be definitely smaller than that for $Fe_3O_4$ and possibly as low as that for $FeCr_2O_4$. The symbol X designates an $\alpha Fe_2O_3$-$Cr_2O_3$ type structure. It is entered at a position from left to right, corresponding to increasing amounts of $Cr_2O_3$, which represents the best fit of the pattern. This position may correspond to a solid solution or to a mechanical mixture of the two phases, since it is questionable whether the two patterns could be distinguished if both were present.

Inspection of the table shows that the films consist chiefly of a $Cr_2O_3$-rich oxide and a small amount of spinel. There may be a significant trend toward less $Cr_2O_3$ as the temperature is increased, but, broadly speaking, no systematic variation of oxide type with alloy composition, time or temperature of exposure, is evident. Essentially the same inconclusive results are obtained for similar oxidations in air, for long oxidations at lower temperatures and for cyclic heating in air to 650°C. Yet there must be some differences in properties of the films formed under these widely different conditions since the degree of protectiveness they afford the metal is known to vary greatly. One must exercise caution, however, in interpreting these electron diffraction patterns. Since the electron beam can effectively penetrate a film thickness of not more than $10^{-5}$ cm, portions of the film thicker than this contribute little or nothing to the diffraction pattern observed.

In order to assist in the diffraction interpretations and to seek variations in the film properties, electron micrographs have been taken of the stripped films. These observations may be summarized as follows.

The films from which a heavy scale has been removed are continuous and have a generally uniform thickness except at grain boundaries, over carbide inclusions of the metal, etc. This thickness varies only two or threefold for different metal grains and for the range of alloys and exposures covered in table VI. Although over regions measured in microns the films are

uniform, there are local variations, or a texture, on a tenths of a micron scale. When examined from a statistical point of view, this local roughness seems to vary in a systematic way, in that the texture becomes coarser as the temperature of oxidation is raised or the percentage of chromium in the alloy is decreased. It may also be more pronounced for short than for long times of oxidation. Thus there would seem to be a correlation between coarseness of texture and oxidation rate. Similar considerations apply to those films from which a superficial grey film was removed during stripping.

The situation is quite different when no material is removed from the film before examination. Whether the film is grown under the conditions of Table VI, in oxygen or air, by continuous heating at lower temperatures, or by cyclical heating in air to 650°C, the result is always a thin film of the same general nature as described above, on which grow nodules or excresences of irregular shape. These crystalline masses increase in size and frequency with increasing time and temperature of oxidation and with decreasing chromium content of the alloy, i.e., with decreasing oxidation resistance. Thus it is suggested that after the thin film is formed the principal metal loss is in the growth of the large particles. These eventually coalesce to form the continuous grey film removed in stripping and ultimately form the bulk scale. These particles are too large to be penetrated by the electron beam and so contribute nothing to the electron diffraction pattern except possibly at their edges; thus the electron diffraction results apply only to the thin, more or less uniform, film.

If it be true that the film next to the metal is not appreciably different on the different alloys, then a logical hypothesis to explain the known differing degree of protectiveness which it provides would be to assume that the variation in rate of attack is associated with variations of the type and number of local imperfections in the film, as indicated by the localized growth of protuberances on it. This hypothesis is consistent with all the previous data on the 5 to 26 per cent chromium steels. It has also been tested on a total of ten steels by oxidation at 310°C in air. In all cases increased rate of attack is correlated with an increased roughness of oxide texture as shown by electron micrographs. If this correlation continues at higher temperatures, the next step will be to find the nature and cause of these imperfections.

Measurements of the electrical properties of the oxide scale and film have been started, since these properties may be of importance in determining the rate of oxidation. The electrical resistance of the oxide, for example, may be the limiting factor, as has been shown by Wagner and Mott. Since the metal diffuses to the oxide surface in the form of positive ions, a positive space charge will be built up and stop the process if negative charge cannot be conducted through the layer to neutralize this space charge.

Preliminary resistance measurements of a stripped oxide film have been made. The resistance of an approximately 1 x 2 mm film is extremely high at room temperature ($3 \times 10^{11}$ ohms) and falls very rapidly with increase in temperature ($4 \times 10^{8}$ ohms at 100°C) corresponding to an effective activation energy for conduction of approximately 0.7 electron volts. Other films are observed to have a much lower resistance or to permanently fall to the lower value on heating. For these, the activation energy is approximately 0.3 electron volts. The cause and interpretation of these changes is being investigated. To improve the measurements, the whole furnace tube and leads will have to be electrostatically shielded. Calculation of resistivity of the oxide is dependent upon mounting the film on optically flat quartz so that its thickness can be measured by the shift of interference fringes.

Even if the resistance of the film is low, there is another possible electrical mechanism which might limit the outward flow of negative charge (either electrons outward or positive *holes* inward). When contact is made between a metal and a *semi-conductor,* such as an oxide, a potential hill is formed which may act as a barrier to the flow of charge. Since the height and nature of this barrier is determined essentially by the difference in work functions (the energy to remove an electron) of the two materials, experiments by which this difference may be estimated have been started.

The method in use is to measure the contact potential between the specimen and a standard surface. This gives the difference in work function of the two surfaces. Comparison of such measurements before and after oxidation of the metal surface will determine the difference in work function of the metal and oxide. (There are several complicating factors in the interpretation of these data which will have to be considered in some detail.)

The measurements to date have been made at room temperature only, and indicate that well-aged as-machined surfaces of 446, 430, and 410 commercial chromium alloys (nominal chromium content, 23 to 30, 14 to 18, 10 to 13 per cent respectively) have nearly the same work function. On polishing with 3/0 paper their work functions fall by 0.20 to 0.25 volts, the decrease being progressively greater in the sequence 446-430-410. On standing in air at room temperature, the values rise by approximately 0.1 volt over a period of hours; this may be due to a slow approach to an equilibrium following the abrasion or to the formation of an oxide film. Electrolytic polishing lowers the work function of the 430 and 410 alloys by an additional 0.2 volts, and this is followed by a rapid rise, presumably due to oxidation.

When these surfaces are oxidized for 5 minutes in one atmosphere of oxygen, at 670°C, the work functions of the three surfaces increase 0.7 to 1.2 volts in the sequence 410-430-446.

This is followed on standing in air by a rather rapid decrease to values of 0.2 to 0.4 volts.

Interpretation of these data, as applying in detail to the actual oxidized metal surface and the oxide in contact with it, is perhaps questionable, but the change produced on oxidation is large enough that one is probably correct in concluding that the oxide has a higher work function than the metal. This, if true, has the consequence that the potential hill between oxide and metal would not form a barrier to the passage of electrons, but would be a barrier to the flow of positive *holes*. Which type of semi-conductor the actual oxides are, electron conductor or hole conductor, is not known. This is one of their properties which should be investigated.

The X-ray diffraction studies will be extended to higher temperature oxidations in air and in oxygen at reduced pressures. Attempts to synthesize and analyze spinels of variable parameter will be continued.

The problem of the thin film, including its growth; the structure of the crystalline nodules formed on it; the nature and cause of film imperfections and their correlation with oxidation resistance will be extensively investigated by electron diffraction in reflection and transmission, by electron micrographs, and by microchemical analysis.

Measurement of electrical properties, particularly the resistance, will be continued, with the intent of finding correlations with oxidation resistance. It is hoped that these measurements may be extended to include Hall effect of determinations of the sign of electrical carrier. It may also be possible to devise equipment suitable for measuring the contact potential between metal and oxide at the temperature of oxidation.

# VI. SPECTROSCOPY OF COMBUSTION

## A. *IDENTIFICATION OF EMITTERS OF VAIDYA HYDROCARBON FLAME BANDS. (NYU-7R8).*

*Submitted by: G.M. Murphy and L. Schoen.*

The identity of the emitter or emitters of the so-called Vaidya hydrocarbon flame bands, found in the ultraviolet region of most hydrocarbon flame spectra, has never been established conclusively.

It is felt that observation of the spectrum emitted by the flame produced by the reaction of a deuterated hydrocarbon with atomic oxygen should provide evidence for the identity of the emitter, since an isotopic shift of the lines emitted by radicals containing deuterium atoms would be observed. For example, if the emitters include the diatomic radicals $O_2$, $C_2$, CH, OH, etc., shifts of the CH and OH lines will be observed.

Deutero-acetylene will be prepared by means of the reaction between calcium carbide and deuterium oxide. A sample of calcium carbide of high purity has been donated for this purpose by the National Carbide Corporation.

The apparatus consists of a discharge tube approximately 2 meters long and 20 mm in diameter from which a stream of oxygen atoms is drawn into a pyrex glass reaction vessel to encounter a stream of acetylene molecules. The emitted radiation is focused through a quartz window onto the slit of a spectrograph. The dissociation potential used to produce the oxygen atoms is supplied by a 3 K.V.A. high voltage transformer, and a high-speed 3-stage mercury diffusion pump provides the source of vacuum.

The flame itself is spherically shaped, structureless, and pale blue in color. By suitable regulation of the flow velocities, it may be held on the nozzles for as long a time as desired, and satisfactory spectra have thus been obtained with a medium quartz spectrograph at exposure times of approximately 30 minutes. The spectra are similar to those of a normal hydrocarbon flame at atmospheric pressure, exhibiting OH, CH, and CC bands as well as the hydrocarbon flame bands. The flame bands show up particularly well in the region 3000-4000 Å where there is no overlapping.

At present a new discharge tube, water cooled and of greater current carrying capacity has just been completed for use with a new reaction vessel of improved design. It is expected that the intensity of the flame will be increased to the point where it will become convenient to use a 3 meter grating spectrograph, which has recently been made available by the Chemistry Department.

## *B. INVESTIGATION OF THE EFFECT OF COMBUSTION CONDITIONS ON THE SPECTRA OF HYDROCARBON FLAMES AT LOW PRESSURES. (CAL-2R9).*

*Submitted by: J.T. Grey, Cornell Aeronautical Laboratory.*

Knowledge of the chemical processes by which any propulsive combustion proceeds can lead to improved performance. Such knowledge is obtained in part by applying the techniques of spectroscopy to flames. In this project contributions to a better understanding of the mechanisms of hydrocarbon combustion are being sought through a study of the influence of the experimental parameters on the spectra of hydrocarbon flames burning at low pressure. Emphasis has been placed upon the variation of intensity of the $C_2$, CH, and OH bands with the experimental parameters, total burner pressure, oxygen-fuel ratio, partial pressure of fuel, and the total mass flow. In these studies, the oxygen-fuel ratio has been varied quite widely and the total burner pressure has been varied from 20-40 mm. Results of the study are discussed in Technical Memorandum, CAL-24.

Within the limits of the variables examined, the intensity of the OH bands was found to be independent of the mass flow and the partial pressure of methane, and to increase linearly with burner pressure up to about 25 mm., in which region the slope of the curve began a gradual progressive increase.

The CH bands were also found to be independent of the mass flow, to increase linearly with increasing partial pressure of methane and also with decreasing oxygen-fuel ratio, and to increase with burner pressure up to about 25 mm., in which region a decrease in the slope occurred.

The intensity of the $C_2$ bands was found to increase linearly with increasing partial pressure of methane and to increase with burner pressure up to about 25 mm., in which region a gradual progressive decrease in the slope of the curve was observed.

The fact that in the case of the CH bands linear increases were observed for not only the partial pressure of methane but also the oxygen-fuel ratio, which represents the recipro-

cal of the methane partial pressure, indicates that the spread of experimental parameters was insufficient to establish the dependence uniquely. An elaboration of this point figures in the current work.

It may be significant that the changes in intensity with change in pressure for the $C_2$, CH, and OH bands were observed in the same burner pressure region. The formation of these radicals,[1] moreover, may be inter-related, according to the reaction $C_2 + OH = CO + CH$. Hence, with increasing CH intensity, a decrease in $C_2$aand OH intensity would be expected, and although the equilibrium above should not be affected by pressure changes, it must be remembered that the further polymerization of carbon to and beyond $C_2$ would be increased by increasing pressure. This, in turn, would lead to a decrease in CH intensity. The experimental findings seem to follow this pattern, for above about 25 mm. pressure, the CH and $C_2$ bands decrease in intensity and the OH bands increase in intensity. This is as expected from the assumption of further polymerization of $C_2$ with increasing pressure. Below this region, the CH band and $C_2$ band intensity decreases markedly and the OH band intensity decreases at a much slower rate. The decrease in the $C_2$ band intensity here is possibly due to a decrease in the rate of polymerization of methane residues. In applied combustion, these relationships are important, since $C_2$ represents the initial step in soot formation.

During the third quarter of the year, no experiments were conducted, although a limited amount of planning and reassessment was accomplished. Further calibration of all the spectrographic equipment involved and the determination of the limit of resolution of the spectrograph are now being pressed to a conclusion. In evaluating the limit of resolution of determining the rotational temperature from the individual lines in the band spectra and comparing the results with those reported by other investigators, it will be necessary to analyze the bands of interest and calculate the rotational temperatures therefrom. Further, certain physical changes have been accomplished in the apparatus to facilitate the determination of the change in relative number of emitters in the different parts of the flame and the estimation of the absolute number of emitters per unit volume in the different zones of the flame.

In planning the work program for the current year, it was decided to concentrate on emission work in the ultraviolet region, because of the time and financial limitations of the project, and to forego work in the infrared region, because of the uncertainties and delays which would occur in implementing such a study. However, it was decided to do a limited amount of absorption work in the ultraviolet region, since the necessary instrumentation could be obtained at the Laboratory and because this field of study has been relatively unexplored.

---

[1]A.G. Gaydon, *Spectroscopy and Combustion Theory*, Chapman & Hall, London (1947), p. 46.

Specifically, the redefinition of the objectives of this study has led to the following plans: to determine the effective temperature of some emitters in the methane and oxygen flame at low pressures by determining the rotational temperatures of the OH and CH bands at 3064Å and 3900Å, respectively, as a function of (a) the partial pressure of methane at the burner exit, (b) the partial pressure of oxygen at the burner exit, (c) the total pressure in the burner, and (d) the flow rate at the burner exit; to determine the change in the relative number of emitters (CH, OH, $C_2$) in the different zones of the flame as a function of the above parameters; to estimate the absolute number of these emitters per unit volume in the different zones of the flame, by estimating the absolute intensities of the above bands, as functions of the parameters; and to detect the presence of various fragments (CH, OH, $H_2CO$, etc.) in the different zones by observing the ultraviolet absorption spectrum of the flame, and, possibly, to estimate the relative changes in the concentration of these fragments by following the intensity of absorption as a function of the parameters.

# VII. INSTRUMENTATION AND TESTING EQUIPMENT

## *A. DEVELOPMENT OF OPTICAL TECHNIQUES FOR MEASURING THE STATISTICAL PROPERTIES OF TURBULENCE (INTENSITY, SCALE, CORRELATION, SPECTRUM, ETC.) IN HIGH VELOCITY FLOWS FOR WHICH MEASURABLE DENSITY FLUCTUATIONS OCCUR. (JHU-Ph.1)*

*Submitted by: L.S.G. Kovasznay, Johns Hopkins University.*

This phase has as its broad purpose the measurement of the statistical properties of turbulence in compressible flows by optical techniques. The use of optical methods appears expecially promising for flows with velocities sufficiently high that the frequency response of conventional techniques, i.e., hot wires, is exceeded or where the temperatures are sufficiently high that it is difficult to introduce instruments in the stream.

The development of optical techniques for turbulence measurements is one portion of a larger research effort to devise general methods for investigating turbulence at high speed so that these techniques can be used as standard laboratory tools. This work has been underway for about 2½ years with the initial emphasis on hot-wire anemometry at supersonic flow. The work on hot-wire techniques is continuing under its original sponsorship outside of Squid.

This phase on optical techniques under Squid sponsorship has been underway only a short time and the present report gives an outline of the preliminary work that has been done and indicates the present direction of the effort.

Possible optical techniques for measuring turbulence can be based on one of the three well-established techniques; shadow, Schlieren, interferometer, or some new one. Our past work has been based on the shadow method and we expect to explore the possibilities of the interferometer.

The shadowgraph method is suited to obtain quantitative information on turbulent density fluctuations as has been reported in detail.[1] The method is briefly as follows: A shadow

[1] Leslie S.G. Kovasznay, *Technique for the Optical Measurement of Turbulence in High Speed Flow, Heat Transfer and Fluid Mechanics Institute,* Berkeley, California, June 1949. Published by the American Society of Mechanical Engineers in a volume.

picture of the turbulence pattern is taken by a short duration spark. The pictures exhibit a random character. Two identical slides are made of the pattern and superimposed face to face. The average transparency of a set of two slides depends on their relative position. If they are in register, the average transparency is maximum and, if they are shifted far from matched positions, their average transparency is minimum since it varies depending on the probability of dark and light areas being matched. The variation of transparency with relative displacement gives the correlation coefficient (autocorrelation coefficient) of the two-dimensional pattern. With certain mathematical operations (Fourier transforms) the statistical properties of the three-dimensional density fluctuations can be determined.

Since the shadowgraph method principally responds to second spatial derivatives of the air density, it overemphasizes the high frequency contribution to the spectrum by the fourth power of the frequency.

The interferometer technique has not been tried out as yet for measuring turbulence although some time records were taken from the relative motion of the fringes as described by Ladenburg, Winckler and Van Voorhis.[2]

The fringe shift in the interferometer is proportional to the average density along the beam of light and therefore responds principally to the low frequency part of the spectrum of density fluctuations. Since the interferometer's resolution in space is somewhat inferior, we plan to take fast time records of the fringe shifts instead of short duration flashes. The time-correlation (auto-correlation) of the fringe shift fluctuation can be measured either by tracing the fringe shifts or by using the technique already developed for the evaluation of shadow pictures. The interferometer technique is in a preliminary trial stage. We are using a borrowed interferometer and if the preliminary results seem promising we plan to set up our own interferometer. Fortunately, the quality of interferometer in this case is not very critical since only the relative motion of the fringes with respect to time has any importance.

The Schlieren technique was disregarded since the normal knife-edge type arrangement gives a preferred direction and the circular type Schlieren does not have the necessary definition or isotropy of response to trust it for quantitative measurements.

Since all the optical techniques are sensitive to the density of the medium, the validity and accuracy of the optical evaluation of turbulence shadow-pictures must be checked in tur-

[2]R. Ladenburg, J. Winckler and C.C. vanVoorhis, " Interferometer Studies Faster than Sound," *Phys. Rev.*, Vol. 73, No. 11, (1948), pp. 1359-1377.

bulent flows where the density fluctuations are not due to compressibility but to heat added. In view of this fact a steady turbulent flow has been set up with the possibility of heat addition and preliminary experiments with both techniques are currently being made by varying the parameters that seem to be significant. The optical measurements will be checked against standard hot-wire measurements so the reliability of the optical measurements can be established.

The whole phase fits into the research on pulse jets by offering techniques for defining and measuring quantitative statistical properties of turbulence under flow conditions where optical methods are still feasible but hot-wire probes cannot be seriously considered.

This appears to be useful because the turbulence properties seem to influence combustion so fundamentally that some understanding of turbulent phenomena is imperative to be able to handle combustion problems successfully.

## *B. 3-DIMENSIONAL SCHLIEREN APPARATUS. (NYU-8R4).*

*Submitted by: J.H. Hett, New York University.*

In high speed photography of jets of burning gas, it is not possible to discern the third dimension along the line of sight so necessary in analysis of the formation and decay of a jet of gas and swirling combustion. For this reason a preliminary study of the possibility of making two pictures of the flow at each instant from two different angles, as is done in making stereoscopic or 3-dimensional photographs, was undertaken. An angle of stereopsis of $15^{\circ}$ was chosen and gave satisfactory results when the slow moving gas flow around a Bunsen burner was observed in a Schlieren system.

With this data a system was designed for insertion into a standard 2-mirror Schlieren system as follows. The parallel beam of light from the first Schlieren mirror is split by plane mirrors into an upper and lower half which intersect in the field of interest at an angle of $15^{\circ}$. After the beams pass through this field, they are reflected from another set of plane mirrors so placed to reform two adjacent parallel beams which are reflected from and brought to a focus by the second parabolic mirror. At this focus, as usual, there is a knife edge. The light passing the knife edge enters the high speed movie camera, forming two adjacent images of the occurrence as seen from two different angles of view on each frame of the film.

These two images may be recombined on a projection screen using deviating prisms and crossed polaroids; the screen is viewed through crossed polaroids. The two images, of course, may be measured directly with a comparator.

## C- *A DUAL PATH PYROMETER FOR FLAME TEMPERATURE MEASUREMENT. (NYU-8R1).*

*Submitted by: J.H. Hett and J.B. Gilstein, New York University.*

The method of measuring instantaneous temperatures, developed during the past year, involves observation of an isolated region of the continuous background of the spectrum of a flame with a dual path pyrometer. Description of the system has been given by Hett and Gilstein.[3]

In brief, light emitted by a fluctuating flame is focused by a lens through a filter on a photomultiplier tube, forming light path No. 1; and at the same time light is reflected from a mirror on the far side of the flame through the same lens and filter onto a second photomultiplier tube forming path No. 2, twice as long as path 1. The outputs of both photomultiplier tubes are fed to DC amplifiers, and thence to cathode ray tubes, where the traces are recorded with a 35 mm. drum camera. The system is calibrated by using a standardized strip lamp, and the intensities measured over the two paths through the flame are used to calculate the temperature. During the year, three temperature measurement stations were mounted on the PJ-31 pulse jet, one at the combustion chamber near the spark plug; a second, 2 inches from the end of the tailpipe; and a third, halfway between the first two. The data were recorded with the sixteen channel instrument trailer constructed last year, and are now being reduced.

The chief difficulties encountered in the field were: noise in the photomultipliers, which has been much reduced by limiting the band width of the output signal and also experimentally, by cooling the photomultiplier tubes; and instability of the DC amplifiers, which has been traced to rapid aging of the tubes and resistors and to differential heating of the circuit components. The amplifiers have, therefore, been rebuilt using precision wire-wound resistors wherever necessary.

The maximum temperature reached during each cycle in the PJ-31 is 2450°C at low fuel rates, but the minimum temperature is more difficult to determine due to the large errors associated with the use of the strip lamp for calibration of temperatures below 1450°K. An

[3] J.H. Hett and J.B. Gilstein, *Journal of the Optical Society of America,* Vol. 39, No. 11, November 1949, p. 909.

approximate check on these minimum temperatures was obtained by the following experiment. A General Radio strip camera was sighted through a quartz window into the combustion chamber of a PJ-31 engine while it was run at a specific fuel pressure, so that the peak temperature would be known from former temperature runs. The film record thus made of instantaneous flame radiation showed that the luminosity was never zero at any point during the cycle. By knowing the exposure curve of the film, and by measuring the maximum and minimum film densities, the minimum temperature was determined as $1406^{\circ}K \pm 30^{\circ}$. This essentially confirms the low point temperatures as determined with the dual path pyrometer. The possibility that this minimum radiation was from the wall of the engine is excluded by the fact that just after the engine stopped, no radiation was observed on the film. It would also seem to explain the re-ignition of the fuel in the jet, at least for the operating conditions used.

Work on the large jet ceased at the end of September, and preparations are now being made to use the equipment on laboratory jets in order to check temperatures of hydrocarbon flames. These measurements will be checked against those obtained by the two-color method of measuring temperature, using the ratio of emissivity obtained from the present dual path method.

In January, attempts will be made to measure rocket exhaust temperatures at the Malta Test Station of the General Electric Company, Malta, New York.

## *D. EFFECT OF TEMPERATURE ON PRESSURE GAUGES. (NYU-8R2).*

*Submitted by: J.H. Hett and R.W. King, Jr., New York University.*

Experiments have been made involving the cooling of a large part of the pressure gauge body, including the edge of the diaphragm. This has substantially improved the cooling rate so that shorter fire tubes may be used in the chamber ahead of the gauge, and the overall frequency response in the system is now 5500 cycles per second, as against 3000 cps. for the older cooling chamber.

Work is also proceeding on plastic-bonded multiple layer diaphragms in the hope of reducing still further the temperature dependence of the gauge; the electronic circuits in the pressure gauge have been improved by eliminating the small AC output signal which formerly limited the low frequency response.

A description of the pressure gauge system, without the latter developments, is scheduled to appear in the February 1950 issue of the *Review of Scientific Instruments.*

## *E. FREQUENCY RESPONSE AND DYNAMIC CALIBRATION OF PRESSURE GAUGES WITH COOLING CHAMBERS. (NYU-8R3).*

*Submitted by: J.H. Hett, New York University*

In calibrating pressure gauges it would be highly desirable to be able to apply pressure waves of known shape and amplitude at frequencies up to 5000 cycles per second. So far it has not been possible to do this and at present the method of calibration used is the bursting diaphragm method. Some time ago an attempt was made to use a Dilks speaker for this purpose, but the maximum pressure available at 2000 cps was found to be only ¼ psi. Such an amplitude is scarcely above the noise level of a gauge designed for maximum pressures of 60 psi.

A preliminary model of a high speed rotary valve, similar to a siren has been constructed but has been found to need redesign before further progress can be made. It is expected that these tests will be supplemented by shock tube calibrations.

## *F. A RESISTANCE-TYPE ELEMENT FOR THE MEASUREMENT OF OSCILLATING FLUID VELOCITY IN LIQUID FLOW. (NYU-4R3).*

*Submitted by: J.H. Hett, New York University.*

A thermistor, which is a thermally sensitive resistor made of solid semi-conductive material, is in general far more rugged than a comparable hot-wire system. Experiments were made in the laboratory to determine the suitability of a thermistor for the measurement of the instantaneous rate of fluid flow. These showed that a thermistor with an associated compensating circuit could be used successfully at frequencies up to 1000 cycles per second. A bead type thermistor was therefore mounted in the PJ-31 gasoline feed line and the output was recorded photographically after passing through the compensating circuit. The system was found to be unsatisfactory due to the variable temperature of the gasoline, which caused errors comparable to the flow signal. Further work on this installation stopped when the field station closed on October 1st.

It is planned to add a circuit to compensate for variations in fluid temperature and to use the apparatus as an operating instrument on a laboratory jet.

## *G. X-RAY STUDIES OF HOT WALL TEMPERATURES. (PIB-3R3).*

*Submitted by: A. Bender, Polytechnic Institute of Brooklyn*

The object of this research is to develop a workable X-ray diffraction thermometer capable of measuring the surface wall temperatures of a combustion chamber. A complete description of the work on this problem undertaken during 1949 was contained in the July Quarterly Progress Report[4] and in a Technical Memorandum.[5]

It had been found during the preliminary studies on the development of an X-ray thermometer that the position of the diffraction lines of the X-rays could be recorded photographically and calibrated to indicate surface temperatures to within ± 15°F up to 1200°F, the highest temperature obtainable with the heating equipment used at that time. The objection to this photographic technique was that long exposures, on the order of one hour, were required for a single temperature determination. To increase the time sensitivity, it was decided to use a Geiger-Muller tube and counter system to locate the diffraction lines. With a G-M tube, a North American Philips counting unit, and a Brown recorder it has been found possible to locate diffraction lines within a time interval of the order of a second,

It is planned to continue this research by determining the simultaneous effects of mechanical strain and temperature on the diffraction lines and by developing a servo-circuit for making the G-M tube self-seeking. Research is also being conducted on the use of X-ray absorption techniques for the determination of the density distribution in supersonic flows.

## *H. DEVELOPMENT OF A HIGH TEMPERATURE METALLOSCOPE. (CAL-3R1).*

*Submitted by: L.K. Porter and L.W. Smith*

In order to obtain photomicrographs of metal structures at high temperatures and thereby to assist in the study of such metallurgical factors as recrystallization, phase changes, phase melting, strain under high temperature loading, and high temperature phase identification, a high temperature metalloscope has been under development.

A vacuum-tight furnace had been designed and built with a platinum-wound heating element, chromel-alumel thermocouple, and a quartz viewing window. The vacuum system consisted of a two-stage oil diffusion pump and a Megavac forepump with Pirani and ionization gauges for the measurement of vacuum as high as $10^{-5}$ mm. of mercury. The optical system consisted of a microscope, light source, and cameras for photo and cine-micrography.

---

[4]Project Squid, Quarterly Progress Report, July 1949.

[5]A. Bender and I. Fankuchen, *Surface Temperature Determination by X-ray Diffraction Technique,* Project Technical Memorandum PIB-5, June 1948.

It had been found that steel specimens would severely oxidize under the operating conditions of the vacuum system; therefore, aluminum specimens were selected and used in the development of the metalloscope. No changes in micro-structure had been noted in heating 24 ST aluminum until a temperature of 935°F has been reached. The change was attributed to a melting of a ternary eutectic.

Severe outgassing of the refractory and parts of the vacuum furnace was encountered when the furnace was heated to high temperatures. A test was conducted with no specimen to determine whether the specimen contributed to the outgassing. No difference was detected in the amount of outgassing with or without a specimen. Therefore, the furnace was rebuilt to eliminate all refractory material except that required to support the platinum wire heating element. Also, in order to increase the pumping speed, the inlet to the furnace was increased to one-inch diameter. The outgassing was reduced considerably by the redesigned furnace, and further reduction was accomplished by raising the temperature in small increments and allowing the vacuum pumping system sufficient time to remove the outgassing occurring for each increase in temperature.

In an attempt to obtain satisfactory photomicrographs, it was found that the light source necessitated an excessively long exposure time. Vibration of the forepump caused a blurring of the images when long exposures were used. Flash lighting techniques were tried. However, the quality of the flash photomicrographs was unsatisfactory, and continued efforts to improve the definition and focus were hindered by an optical system which could not be improved without major changes. Experimentation was continued with the 16 mm. movie camera, and attempts, to obtain still photomicrographs were discontinued. The movie camera gave satisfactory results since the field of the 16 mm. camera was extremely small by comparison with the field obtained with an 8 inch by 10 inch view camera.

Although aluminum was useful as a specimen in the development of the high temperature metalloscope, the requirements for the study of other metals would necessitate a change in the operating conditions of the metalloscope. In the case of steel, the vacuum would have to be higher than $10^{-5}$ mm. of mercury or a very pure inert gas or a hydrogen atmosphere would have to be used. Furthermore, the change in microstructure would have to be visible under the etched or oxide-coated surface of the specimens; if not, then suitable pretreatments, coatings, or the introduction of an etchant at high temperatures would have to be used. It appears that the development of a universal high temperature metalloscope is practically impossible. Each metal used and each change in microstructure would require special equipment and procedures.

A summarizing report, Technical Memorandum CAL-31, was written to complete this phase of the project. This problem was terminated on 1 October 1949.

## *I. DESIGN, CONSTRUCTION, AND INSTRUMENTATION OF A ROCKET TEST FACILITY. (PRF-7R1).*

*Submitted by: C.M. Beighley, D.L. Dynes, R.L. Schock,*
*Purdue University*

The Purdue Rocket Laboratory is a research facility in which rocket motors can be tested with combustion pressures up to 2000 psi. The design basis and detailed description of the laboratory have been presented in an earlier report,[6] so that only a brief description of its general features is presented here.

There are two test cells and a common control room between them. The test cells, fuel and oxidizer weighing tanks, the instruments, the propellant feed system to the rocket motors, and the control apparatus were designed and constructed so that rocket motors operating at pressures up to 2000 psi can be tested with safety. The capacities of the propellant weighing tanks are such that a 1000-pound thrust rocket motor can be operated for approximately 60 seconds, and stored nitrogen is used for pressurizing the propellants. By pumping directly to the rocket motor from the propellant storage tanks located outside the laboratory, it will be possible to operate for longer durations and test larger thrust cylinders. Although the structure is adequate for testing rocket motors up to 10,000-pound thrust, the maximum thrust to be tested in the laboratory is limited to 3000 pounds.

The present investigations employ white fuming nitric acid (WFNA) and AN-F-58 jet engine fuel as the propellants. With minor modifications, however, other propellant systems can be employed.

Currently only one test cell, designated as test cell No. 1, is fully instrumented and in operation. The apparatus for test cell No. 2 is being installed, and the experience derived from the operation of test cell No. 1 is being applied to test cell No. 2 to secure more convenient operation and improved measurement accuracy.

The research projects either planned for or being conducted in the Purdue Rocket Laboratory are as follows: the effect of temperature, mixing, and additives on the ignition.

---

[6]W.J. Hesse, *The Design and Instrumentation of a Rocket Test Pit,* M.S. Thesis, Purdue University, January 1948.

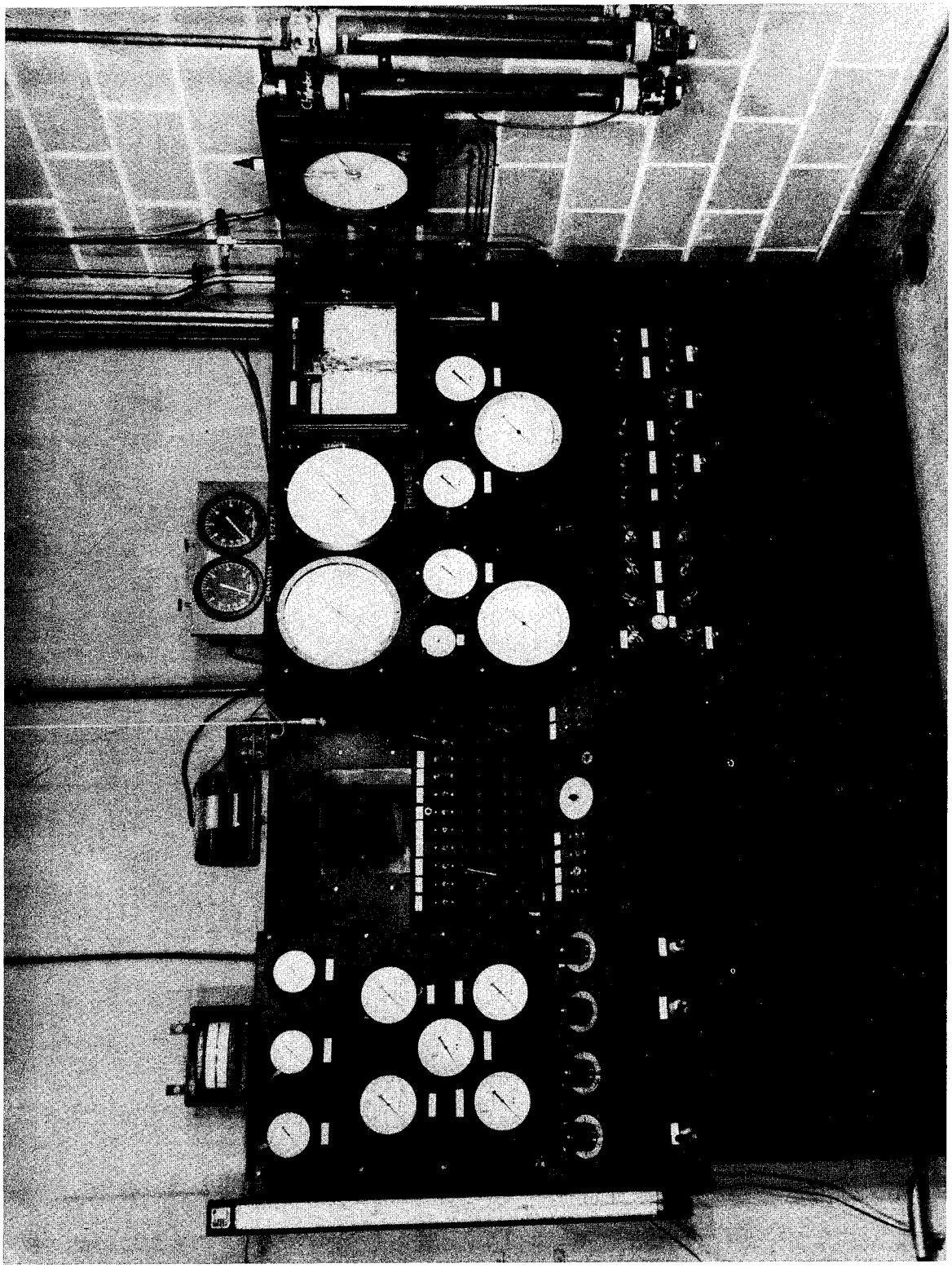

Fig. 1. Control panel for test cell No. 1.

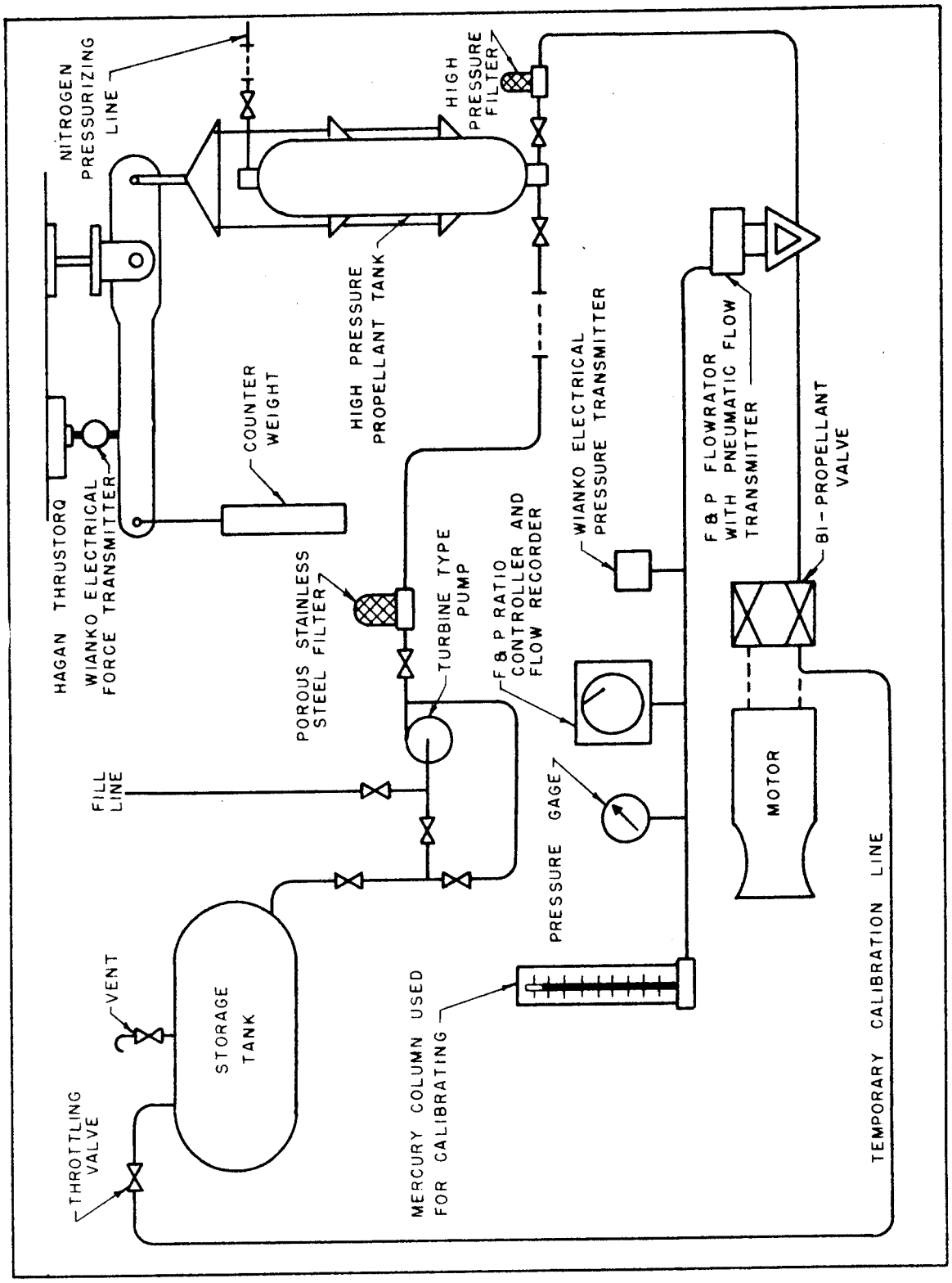


**Fig. 2.** Schematic diagram of propellant flow rate calibration system.

characteristics of self-igniting (*hypergolic*) propellants (See Div. V, Sec. F.); catalysis of the reaction between WFNA and AN-F-58 jet engine fuel (See Div. V, Sec. G.); the performance characteristics of rocket motors operating at combustion chamber pressures ranging from 300 to 1500 psia (See Div. I, Sec. A.); the effect of combustion chamber pressure on the heat transin rocket motors (See Div. I, Sec. B and Div. I, Sec. C.); and such broad problems as the development of more reliable and accurate methods for measuring the physical quantities determining rocket motor performance.

Table I. Summary of Instrumentation Methods.

| Quantity | Measuring Instrument | Method for Recording and/or Indicating. |
|---|---|---|
| Thrust | Hagan Thrus-Torq | 1. Heise pressure gauge<br>2. Esterline-Angus strip chart recorder |
| | Wiancko force transmitter | 1. Oscillograph |
| Chamber Pressure | Bourdon tube | 1. Heise pressure gauge<br>2. Esterline-Angus strip chart recorder |
| | Wiancko pressure transmitter | 1. Oscillograph |
| Injector Pressures | Bourdon tubes | 1. Heise pressure gauges |
| Propellant Flow Rates | Wiancko force transmitter on tank weighing system | 1. Brown automatic potentiometer |
| | Fischer and Porter flowrators with pneumatic transmission. | 1. Pressure Gauge<br>2. Fischer and Porter Chart recorder |
| | Wiancko pressure transmitter | 1. Wiancko pressure transmitter recording on oscillograph |
| Water Flow Rates | Sharp edge orifice | 1. Barton differential pressure gauges. |
| Temperatures | Thermocouples | 1. Brown automatic potentiometers |

As far as it is feasible it has been endeavored for obvious reasons to duplicate each variable to be measured . Table I summarizes the instrumentation methods being used.

Figure 1 is a photograph of the instrument panel for test cell No. 1. Figure 2 is a schematic diagram illustrating the method used for calibrating the devices employed for measuring the flow rates of the propellants.

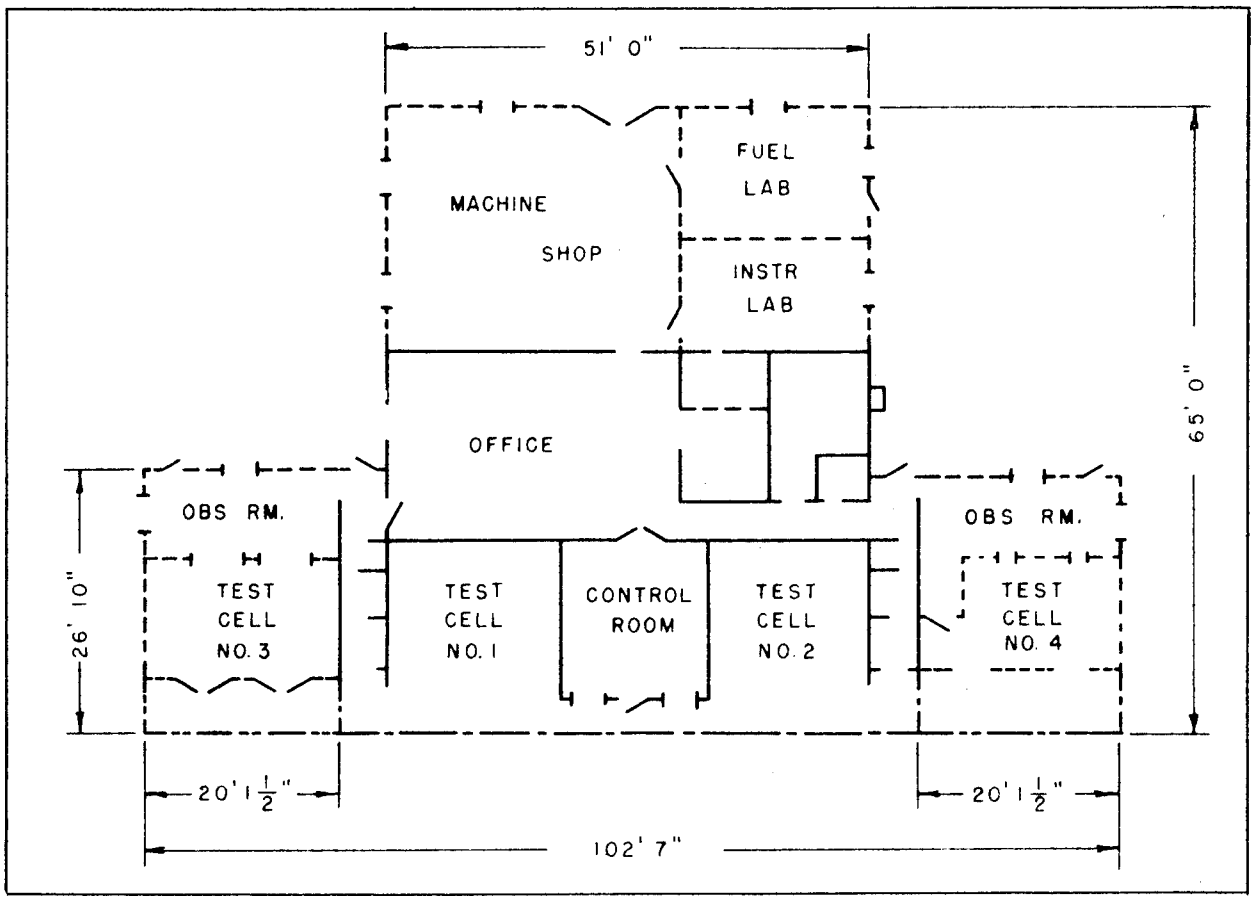


Fig. 3. Purdue Rocket Motor Laboratory

The work in progress and future plans for this problem are divided for convenience into three categories: the completion of the installation of equipment in test cell No. 2; the expansion of the laboratory; and improvement in instrumentation.

As pointed out above, effort is being expended to place test cell No. 2 into operation; it is planned to utilize test cell No. 2 for problem PRF-7R9 (Div. I, Sec. C.). The equipment for test cell No. 2 has been designed, constructed and is being installed. Because of the experience with the operation of test cell No. 1, a number of changes have been made in test cell No. 2. To illustrate, stainless steel tubing and tube fittings with Teflon seats are being substituted for stainless steel pipe and pipe fittings; the latter gall during installation and leak unless *back-welded.* The braided flexible stainless steel tubes connecting a weighing tank to supply and discharge lines are being replaced with U-shaped tube-turns. •All of the instruments will be equipped with electrical transmission to the recording and indicating instruments, for safety and improved accuracy.

The present laboratory is too crowded for safety and is being expanded. Furthermore, the current source of electricity, a 30-KW Buda-Lanova Diesel generator, is unsatisfactory. The Purdue Research Foundation has appropriated $30,000 for enlarging the Rocket Laboratory and for a 150-KW electric power line connecting the laboratory to the Purdue University power line approximately one mile away. Figure 3 illustrates the plan of the Rocket Laboratory with the new additions. The space assignments are indicated in the sketch. It is expected that the installation of the power line will be completed by 1 March 1950 and the extension to the building by 1 October 1950.

The methods being employed for measuring propellant flow rates - tank weighing with electrical transmission (Wiancko force transmitter) and rotometers - work satisfactorily but can be improved. A method for differentiating the output of the Wiancko thrust ring to give the flow rate directly has been investigated;[7] the method seems to be satisfactory. More testing is required to establish its sensitivity and accuracy. Preliminary investigations have been made, as a thesis project, of an electromagnet flow meter.[8] It appears that a flow meter of that type should be particularly suited to measuring the flow rate of corrosive liquids, but further study is required to establish the factors governing its operation. Another advantage of this flow meter is its rapid response rate.

Another instrumentation problem being studied is the possibility of transmitting the output of a single Wiancko pickup to three different instruments; a Brown automatic electronic balancing recording potentiometer, a Consolidated oscillograph, and an indicating milliammeter. The objective is to arrange the instrumentation so that a central recording system with one set of recording instruments can be employed for recording the test data from all test cells; a switch is used to connect the instruments to the desired test cell. The Brown potentiometers will record the rocket motor performance parameters; the indicating milliammeters will be located in the central room to guide the operator conducting the test; and the oscillograph will record the transient data.

---

[7]Franklin Micheals, *Measurement of Liquid Rocket Propellant Flow Rate,* M.S. Thesis, Purdue University, August 1949.

[8]Edward Bennet, *A New Electronic Flow Meter,* M.S. Thesis, Purdue University, June 1949.

# VIII. HEAT RESISTANT MATERIALS

## *A. THE EFFECT OF HIGH RATES OF HEATING ON HEAT CAPACITY AND CONDUCTIVITY OF STEEL SPECIMENS. (NYU-2R1).*

*Submitted by: J.H. Hett, New York University.*

Study of the effect of rapid heating on the specific heats of low carbon steel was terminated at the end of September. This problem was undertaken because no information was available concerning the thermal conductivities and heat capacities of steels at high rates of heating. This information is needed to understand the temperature and stress distributions in rocket walls, important factors in the design of rocket engines.

Attempts to compute the complete specific heat versus temperature curve during extremely rapid heating were unsuccessful because the results obtained by differentiating graphically the curve of temperature versus time as recorded on film proved to be insufficiently accurate. Accordingly, only the temperature of the specimen (0.4 per cent carbon steel) was recorded during the rapid heating runs. By examining this trace for slight dips or discontinuities, the location of the peaks in the specific heat curve can be found since $C_p \sim \frac{1}{\frac{dT}{dt}}$. Comparisons were made between these peaks and those on the static curves of specific heat for similar steel specimens published by the Iron and Steel Institute.

Although the equilibrium phase diagram of the iron-carbon system correctly accounts for these static curves, it was found that during rapid heating, when the rate of rise of temperature became comparable to or greater than the transformation process rate, the peaks were greatly affected.

On consideration of the effect of heating at rates comparable to the transformation process rate, it was felt that the phase transformations would be spread over large temperature intervals, because the temperature of the specimen would continue to rise while they were still proceeding.

In addition, during the very slow heating of 0.4 per cent carbon steel, the $A_3$ transformation ($\alpha$ iron to $\gamma$ iron) goes to completion at about 770°C and the Curie point at 769°C

(the temperature at which ferromagnetism disappears) does not show up on the specific heat curve, because $\gamma$ iron is non-magnetic. If, however, the effect of rapid heating is to spread these transformations over a wide temperature range, it would be expected that the Curie point would show up as a small dip on the temperature record, since $\alpha$ iron, which is magnetic, would still be present because the $\alpha$ to $\gamma$ iron transition would not have gone to completion by the time 769°C was reached.

Rapid heating runs made during this study showed only one sharp dip in the temperature trace at 769.4°C ± 3.4°C on all four experimental runs. Since only one dip was observed and this at the Curie point temperature, it was concluded that the $A_1$ (during which cementite disappears) and the $A_3$ transformations were spread over an appreciable temperature interval during rapid heating. A report on this work will soon be submitted to the *Journal of Applied Physics.*

## *B. HIGH TEMPERATURE TENSILE TESTING OF SHEET MATERIALS. (CAL-3R2).*

*Submitted by: L.W. Smith, Cornell Aeronautical Laboratory.*

As part of a program of study of sheet materials for jet engine service, some attention has been given to basic mechanisms of high temperature deformation. Through consideration of the variables of stress, strain, strain rate, and temperature it was possible to establish a testing technique and method of data analysis for evaluating the activation energies associated with high temperature deformation.[1] Results obtained from this earlier testing, using a number of commercially available sheet alloys, suggested a high temperature deformation mechanism which, on an atomic scale, closely resembled that of metallic self-diffusion.

For purposes of clarifying such a concept, additional high temperature deformation tests were conducted on several relatively pure metals for which the activation energies of self-diffusion were known from radioactive tracer diffusion experiments. True stress-true strain tensile tests at various strain rates were conducted on electrolytic copper in the temperature range of 800°F to 1400°F and on Armco iron in the 800°F to 1200°F temperature range.

As was the case for the commercial alloys previously reported, the activation energies for deformation of the relatively pure copper and iron materials were found to decrease with applied stress. This is consistent with the picture of easier diffusion or relative movement of the atoms during the course of plastic flow at higher stress levels due to the greater

[1] James Miller and Glen Guarnieri, *High Temperature Deformation Characteristics of Several Sheet Alloys,* Project Squid, Technical Memorandum CAL-17, 20 April 1948.

elastic dilation or opening of the atomic lattice. Extrapolation of the stress versus activation energy curve to the zero stress ordinate yielded activation energy values for both metals of the same order of magnitude as their self-diffusion energies.

| Metal | Extrapolated Zero Stress Activation Energy from Deformation Tests. cal/mol | Activation Energies of Self-Diffusion from Diffusion Tests cal/mol |
|---|---|---|
| Copper | 61,000 ± 3,000 | 57,200[2] |
| Iron | 80,000 ± 5,000 | 77,000[3] |

Since the stress tests and the diffusion experiments were made with different lots of material of different purities, more exact agreement between the two methods for determining the activation energy values could not be expected. Impurities or alloy additions definitely raise the magnitude of the energy values obtained. This should be particularly true where the foreign atom is dissolved interstitially in the lattice and thereby interferes with the shearing action taking place between matrix atoms during their rearrangement.

According to a dislocation or diffusion type deformation mechanism, the role of interstitial solute elements should be of importance. Creep test specimens of Armco sheet iron are being prepared in which the carbon content will be varied from approximately 0.1 to 0.001 per cent by wet hydrogen and carburizing treatments. Such a series of tests conducted in the temperature range where carbon is interstitially dissolved should help in clarifying the effect of interstitial elements on creep strength. Similar testing could be extended eventually to more highly carburized specimens of the same iron to provide a systemitized evaluation of the effect of carbon on creep strength in iron and particularly in steel.

## *C. CYCLIC LOADING EFFECTS ON CREEP PROPERTIES OF SHEET MATERIALS. (CAL-3R3).*

*Submitted by: L.W. Smith, Cornell Aeronautical Laboratory.*

The creep of metals at high temperatures under fluctuating load conditions is being studied to evaluate the effect of the following variables: frequency of sine wave stress variation; amplitude of fluctuating load; magnitude of static load; and temperature (cold working and annealing range).

---

[2] F. Seitz, *Physics of Metals*, McGraw-Hill Book Co., Inc. New York, 1943, p. 180.

[3] E. Birchenall, R.F. Mehl, "Self Diffusion in Iron," *Mining and Metallurgy*, Vol. 28, November 1947, p. 555.

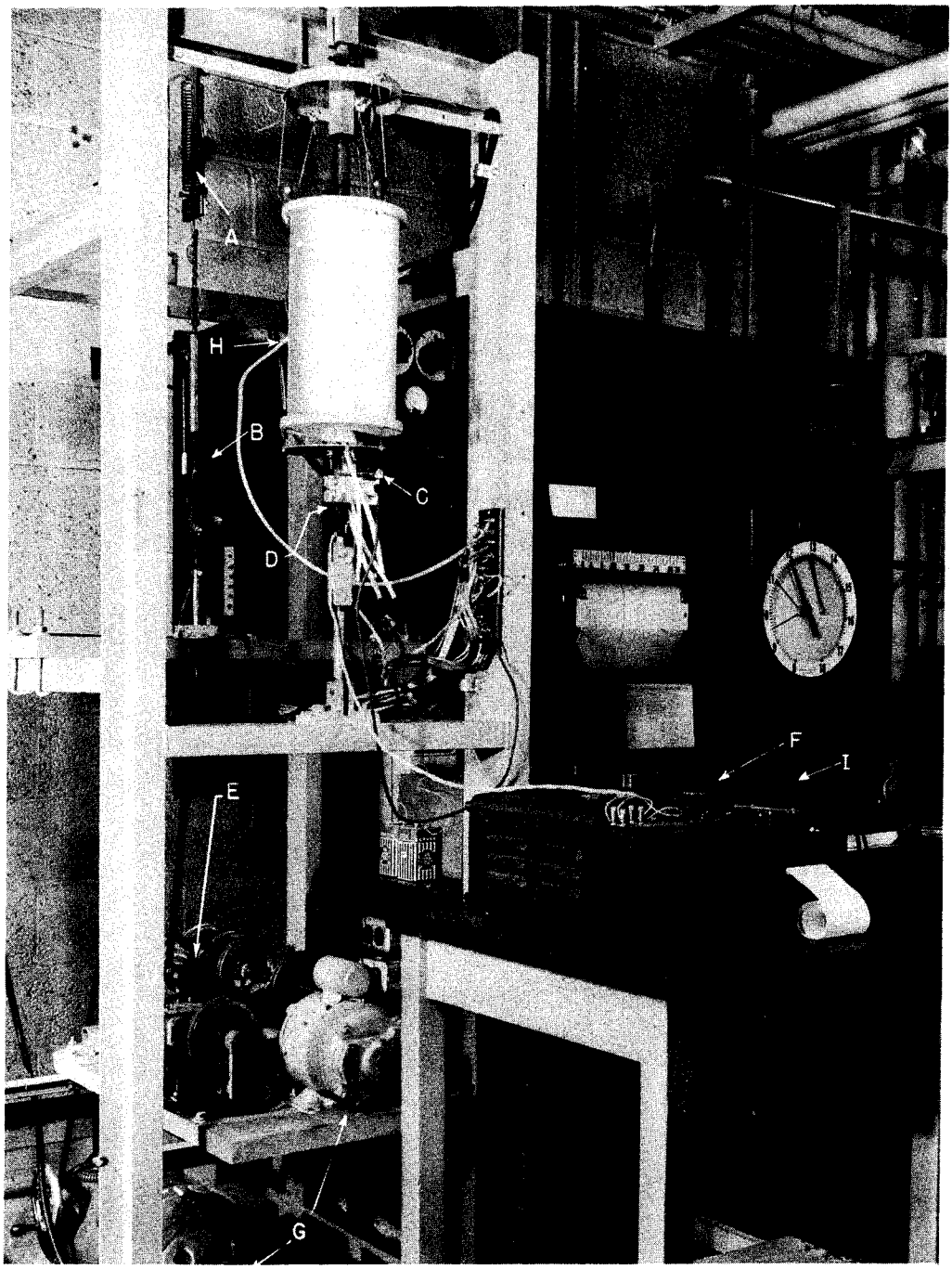


Fig. 1. Dynamic creep test unit.

A. Spring
B. Stress take-up motor
C. Strain gauge
D. Strain gauges for stress calibration
E. Adjustable crank
F. Strain analyzer and recorder
G. Drive motors
H. Furnace
I. Strain indication

Fluctuating-load high temperature creep experiments have been in progress on Armco iron. This material was chosen to eliminate the effect of precipitation hardening microstructure of phase changes as additional variables. Tests have been run at a mean stress level of 6000 psi and 1000°F. Amplitudes of fluctuating stress are varied between 0 and 50 per cent of the mean static stress. Mean stress and temperature are maintained constant while amplitude and frequency of the fluctuating stress is varied for each test. Equipment has been constructed to produce a fluctuating load on the specimen corresponding to a sine wave variation.

Equipment consists of a standard beam-loaded creep test unit as shown in Figure 1. Fluctuating loads are applied by a crank mechanism through a spring attached to the beam. This equipment is capable of frequencies up to 100 cycles and with slight modifications to 2000 cycles of stress per minute. The amplitude of the fluctuating stress can be varied by springs of various stiffness factors and can be determined very accurately by means of an SR-4 strain gauge.

Data to date are not conclusive. However, tests at temperature and stress mentioned above indicate that the effect of low frequencies on strain rate is negligible. Strain rate is accelerated with fluctuating loads when these are above 25 per cent of the mean stress.

The purpose of the present investigation is to determine the effect of temperature, stress, amplitude and frequency of fluctuating stresses on metals. Future tests will be run to study the effects of these variables on alloy metals for higher temperature applications.

## *D. FATIGUE FAILURE CHARACTERISTICS OF SHEET MATERIALS FOR HIGH TEMPERATURE APPLICATIONS. (CAL-3R4).*

*Submitted by: L.W. Smith, Cornell Aeronautical Laboratory.*

One of the original material problems under the Squid Project was an evaluation of materials that could be used for intake valves in pulsejet engines. This evaluation naturally led to high temperature fatigue studies. Specimens were loaded in bending and vibrated with frequencies of the same order of magnitude as those occurring in pulse jet engines.

A testing machine, previously reported,[4] was developed for use with sheet stock speci-

[4] F.J. Gillig and L.W. Smith, *Pneumatic Vibrator for Determination of High Temperature Fatigue Properties of Sheet Materials,* Project Squid Technical Memorandum CAL-10, December, 1947.

mens at temperatures up to 1800°F. The specimen is loaded and controlled pneumatically, making use of resonance frequencies. The specimen is made to vibrate at its natural frequency by air streams from two nozzles on either side of the flat specimen. Its tendency to vibrate at the natural frequency is reinforced by a compression wave which travels back and forth through a U-tube connecting the two nozzles. As the specimen approaches one nozzle, the opening of that nozzle is restricted. This generates a compression wave which travels through the U-tube, with the speed of sound, to the other nozzle. When the distance of travel is correctly adjusted, the compression wave arrives at the second nozzle at the proper time to reinforce the natural vibration of the specimen. The amplitude of vibration can be controlled by the quantity of air which is fed to the nozzles under pressure. The natural frequency of vibration for a given material depends on the physical dimensions of the specimen. The short-time high-temperature fatigure properties of three heat-resistant alloys and cold-rolled plain carbon steel have been evaluated on this pneumatic fatigue tester. The results are comparable on a qualitative basis. The evaluation of the short-time high-temperature fatigue properties of S-816, 25-20-2 Si, regular Inconel, and AISI-1010 was made at temperatures of 1200°F, 1400°F, 1600°F, and 1800°F. Alloy S-816 was tested only at 1600°F and 1800°F because the deflections required to cause short-time failures of the .040-inch sheet material were beyond the capacity of the testing machine. The plain carbon steel, AISI-1010, was evaluated only at 1400°F for comparison. The resistance to high-temperature fatigue failure is in the following decending order: S-816, 25-20-2 Si, Inconel, AISI-1010.

It has been postulated that high-temperature deformation processes are dependent upon the interrelation between stress, time, temperature, and strain rate. This can be summarized into two opposing mechanisms: strain-hardening and recovery. In order to investigate the existence of a balance between strain-hardening and recovery as a basic fatigue mechanism, some tests were interrupted at intervals and the specimen held at temperature for a short time before restarting. This should have the effect of allowing recovery from prior strain hardening and of decreasing fatigue life. Preliminary tests indicate that this is true. Increasing the frequency of vibration (strain rate) should increase fatigue life as should also small amounts of cold work and understressing. It is planned to investigate these effects further.

Photomicrographs of the failed specimens show the existence of a temperature at which failure changes from the normal transgranular type that occurs at room temperature to an intergranular type which seems to be subject to the corrosion effects of the atmosphere in the furnace used to heat the specimen. Similar effects are encountered in creep testing where it is also known that strain rate affects the temperature at which the change occurs.

In order to produce quantitative data on alloys rather than the qualitative comparisons made to date, it will be necessary to conduct the tests on constant-load type fatigue machines. This will also allow greater flexibility in testing and enable other tests to be made to further establish the strain hardening-recovery mechanism.

A technical memorandum report, CAL-30, has been written summarizing the fatigue studies conducted to date.

## *E. SIGMA PHASE STRENGTHENING OF HIGH TEMPERATURE SHEET ALLOYS. (CAL-3R5).*

*Submitted by: L.W. Smith, Cornell Aeronautical Laboratory.*

In an effort to enhance the many desirable features of the chromium-nickel stainless steels for high temperature service, the role of the sigma phase constituent in such alloys has been under study. Emphasis has been placed upon short-time high-temperature creep properties as correlated with various sigma phase microstructures and patterns of distribution.

The initial phase of this investigation has been concerned with the testing of a 25Cr-20Ni-2Si (type 314) stainless steel. Aging tests in the 1200°F to 1800°F temperature range on both annealed and cold-worked stock, established the characteristics of sigma formation in this alloy. On the basis of the results obtained, it was possible to prepare creep and tensile specimens with six different initial microstructures for testing in the 1200°F to 1600°F temperature range. These tests have been such as to provide stress values necessary to give 0.2 per cent, 1.0 per cent and 5 per cent deformation in time periods ranging from 2 minutes to 100 hours. The relationship of room temperature ductility with respect to sigma phase pattern was established by bend testing of specimens aged in the 1200°F to 1800°F temperature range.

The details of this study have been reported as CAL Technical Memorandum No. 26, 1 May 1949. The following conclusions were established.

The sigma phase, in general, increases appreciably the tensile and yield strengths of the 25Cr-20Ni type of alloy at temperatures up to 1400°F.

The creep strength may be increased for relatively short life applications involving deformation of the order of one per cent per hour for temperatures up to approximately 1400°F.

Where slow strain rate conditions are involved, as in long-time service applications, the sigma phase lowers creep resistance.

The pattern of distribution of the sigma constituent in the austenite matrix is quite significant in controlling the magnitude of the above mentioned effects. The finer the sigma particle size, the greater is the decrease in long-time creep strength relative to the fully austenitic-structure. This is quite likely due to the large number of grain boundary discontinuities introduced into the microstructure which provide additional dislocations leading to plastic flow under slow strain rate and high temperature conditions.

Sigma phase materially decreases the room temperature ductility of the parent alloy although increasing ductility is restored at temperatures above 1000°F to 1200°F. This property depends upon the sigma distribution, the better ductility characteristics being obtained with the finer and more random occurrence of the sigma.

Room temperature bend properties of the sheet alloy are decreased as the result of sigma formation with time at temperatures in the range of 1200°F to 1800°F. This condition may be improved, where practical, be controlling the pattern of sigma formation.

Cold working in conjunction with the selection of exposure temperature provides a convenient and flexible means for controlling the mode of distribution of the resultant sigma constituent.

While the sigma phase can be readily formed and manipulated in the two per cent silicon analysis (type 314), greater difficulty is encountered in promoting this constituent in the low silicon grade (type 310). Smaller quantities of this phase and more sluggish reactions are the case for the 310 analysis.

The possibility of deliberately utilizing the sigma phase in the 25Cr-20Ni-2Si stainless steel for improvement of the high temperature strength properties of this alloy would seem to have some merit for the shorter time service applications. It is unlikely that similar long-time high-temperature gains can be made in this manner.

Investigation of the sigma phase in the chromium-nickel steels is continuing with current studies being made on 25Cr-12Ni (type 309) and the 18Cr-14Ni-2Mo (type 316) sheet stock. After establishing the sigma forming characteristics of these alloys, creep and tensile tests will be conducted on sigmatized specimens similar to those made with the 314 grade. An attempt

will be made not only to obtain specific data but to determine under what temperature, time, and stress conditions sigma phase might be utilized to advantage in the various chrome-nickel steels studied.

# APPENDIX A. REPORTS PUBLISHED DURING THE YEAR 1949

## *TECHNICAL MEMORANDA*

### Polytechnic Institute of Brooklyn

| *Title and Author* | *Memorandum No.* | *Distribution* |
|---|---|---|
| Heat Transfer in Laminar Boundary Layer (Compressible Fluids) on a Porous Flat Plate with Fluid Injection,- S.W. Yuan. | PIB No. 19 | Internal |

### Cornell Aeronautical Laboratory

| | | |
|---|---|---|
| Spectroscopic Study of Combustion,-G.H. Rothgery, J.T. Grey | CAL No. 24 | Internal |
| Confidential Memo | CAL No. 25 | General |
| The Effect of Sigma Phase on the Short Time High Temperature Properties of 25 Chromium-20 Nickel Stainless Steel,- G.J. Guarnieri, J. Miller, F.V. Vawter. | CAL No. 26 | Internal |
| Valveless Pulse Jet Investigation, Part I,- J.G. Logan,Jr. | CAL No. 27 | General |
| An Experimental Investigation of the Effect of Inlet Ducts on the Performance Characteristics of a Pulse Jet,- J.G. Wilder, Jr. | CAL No. 29 | Internal |

### New York University

| | | |
|---|---|---|
| A Mobile High Capacity Blower Unit,- D. Kasner, M.W. Woody. | NYU No. 5 | General |

### Princeton University

| | | |
|---|---|---|
| The Kinetics of the Reaction of Aluminum Borohydride Vapor with Olefins,- R.S. Brokaw. | Pr. No. 9 | Internal |
| The Thermal Oxidation of Ammonia with Oxygen,- E.R. Stephens Parts I and II. | Pr. No. 10 | Internal |
| Confidential Memo | Pr. No. 11 | Internal |

| *Title and Author* | *Memorandum No.* | *Distribution* |
|---|---|---|
| A Further Study of the Kinetics of Thermal Decomposition of Aluminum Borohydride,- R.S. Brokaw. | Pr. No. 12 | Internal |
| Hydrocarbon Oxidation Initiated by Atomic Hydrogen,- E.J. Badin. | Pr. No. 13 | Internal |
| Preliminary Report on the Kinetics of the Thermal Decomposition of Diborane,- R.P. Clarke | Pr. No. 14 | Internal |
| Purdue University | | |
| Some Thermodynamic Properties of the Nitroparaffins,- G.L. Dorsey, L.H. Going, D.E. Holcomb. | Pur No. 5 | Internal |
| The Calculated Performance of Hydrocarbon White Fuming Nitric Acid Propellants at High Chamber Pressures,- C.H. Trent, M.J. Zucrow. | Pur No. 6 | Internal |

## *TECHNICAL REPORTS*

| | | |
|---|---|---|
| Compressible Flow Through Reed Valves for Pulse Jet Engines, I. Hinged Reed Valves,- P. Torda, I.P. Villalba, J.H. Brinck. | T.R. No. 9 | General |
| Compressible Flow Through Reed Valves for Pulse Jet Engines, II. Clamped Reed Valves,- P. Torda. | T.R. No. 10 | General |
| Approximate Theory of Compressible Air Inflow Through Reed Valves for Pulse Jet Engines,- P. Torda. | T.R. No. 12 | General |
| A Water Analogue of the Isentropic Flow of Compressible Gases Which Have Arbitrary Ratios of Specific Heats,- R.F. Probstein, G.E. Hudson. | T.R. No. 15 | General |
| Flame and Particle Motions in a Small Pulse Jet Engine,- Paul Elias. | T.R. No. 16 | General |
| A Study of High Velocity Flames Developed by Grids in Tubes: The Role of Turbulence in Combustion Processes,- M.W. Evans, E.L. Miller, L.J. Schoen, M.D. Scheer. | T.R. No. 17 | General |

## *OTHER REPORTS*

| | | |
|---|---|---|
| Annual Report | 1 January 1949 | General |

| *Title and Author* | | *Distribution* |
|---|---|---|
| Quarterly Progress Report | 1 April 1949 | General |
| Quarterly Progress Report | 1 July 1949 | General |
| Quarterly Progress Report | 1 October 1949 | General |
| Our Present Knowledge of Certain Properties of Gases and on Future Research,- K. Herzfeld. | 11 November 1949 | Limited |

## *JOURNAL ARTICLES*

### Polytechnic Institute of Brooklyn

| *Title and Author* | *Magazine* |
|---|---|
| Heat Transfer in Laminar Compressible Boundary Layer on a Porous Flat Plate with Fluid Injection,-S.W. Yuan | Journal of Aeronautical Sciences, 16, Issue No. 12 (1949). |

### Cornell Aeronautical Laboratory

| | |
|---|---|
| Flame Propagation Studies,- G.H. Markstein. | Research Reviews. (In press) |
| Note on the Use of the Shock Tube as an Intermittent Supersonic Wind Tunnel,- G. Rudinger. | Physical Review, 75, Issue No. 12 (1949). |
| The Effect of Sigma Phase on the Short Time High Temperature Properties of 25 Chromium-20 Nickel Stainless Steel,- G.J. Guarnieri, J. Miller, F.J. Vawter. | ASM Trans. 1950. (In press) |
| Cell Structures of Propane Flames Burning in Tubes,- G.H. Markstein. | Journal of Chemical Physics, 17, 428-9. (1949). |
| Evaluation of Metals for High Temperature Service,- G. Guarnieri. | Research Reviews. (In press). |
| On the Hydrodynamic Stability of Flame Fronts,- H. Einbinder. | American Physical Society. (In press). |
| A High Temperature Metalloscope,- E.H. Kinelski. | Research Reviews. |
| On the Addition of Heat to a Gas Flowing in a Pipe at Subsonic Speed,- J.V. Foa, G. Rudinger. | Journal of Aeronautical Sciences, 16, Issue No. 2 (1949) |

## New York University

| | |
|---|---|
| Augmented Flames in Half Open Tubes,- M.W. Evans, M.D. Scheer, L.J. Schoen, E.L. Miller. | Journal of Applied Physics. (In press). |
| Pyrometer for Measurement of Instantaneous Temperatures of Flames,- J.H. Hett.. | Journal of Optical Society of America. (In press) |
| A Frequency Modulation Pressure Recording System,- J.H. Hett, R.W. King, Jr. | Review of Scientific Instruments. (In press) |

## Princeton University

| | |
|---|---|
| The Kinetics of the Reaction of Aluminum Borohydride Vapor with Olefins,- R.N. Pease, R.S. Brokaw. | Journal of Am. Chemical Society (In press). |
| Kinetics of the Non-Catalytic Oxidation of Ammonia. Flow Experiments,- R.N. Pease, E.R. Stephens. | Journal of Am. Chemical Society (In press). |
| The Oxidation of Butene-1 Induced by Aluminum Borohydride,- R.N. Pease, R.S. Brokaw, E.J. Badin. | Journal of Am. Chemical Society (In press). |
| The Spontaneous Ignition of Aluminum Borohydride Vapor in Oxygen,- R.N. Pease, P.C. Hunter, E.J. Badin. | Journal of Am. Chemical Society (In press). |
| Ionization Flame Detector | Review of Scientific Instruments, 20, 349-52 (1949). |

## Purdue University

| | |
|---|---|
| Stability Conditions and Propagation Velocities of Propane-Air Flames in an Independently Controlled Annular Flame Holder,- H.J. Buttner. | Journal of Physics and Colloid Chem. (In press). |
| The Flame Propagation of Air Propane Mixtures in a Controlled Turbulence,- H.J. Buttner, F.W. Bowditch, W.W. Floyd. | Journal of Physics and Colloid Chem. (In press). |
| Some Thermodynamic Properties of Nitro-Paraffins,- D.E. Holcomb. | (In press). |
| 1,3-Dinitropropane,- J.P. Kipersky, D.E. Holcomb, H.B. Hass. | Journal of Am. Chemical Society, 71, 516, (1949). |
| Heats of Combustion of Nitrogen Containing Compounds,- M.V. Sullivan. | Journal of Physical Chemistry, (In press). |

# APPENDIX B. OUTLINE OF STUDIES CONDUCTED BY AFFILIATED UNIVERSITIES

Studies sponsored by Project Squid and conducted at the affiliated universities are divided into various phases of work. Each phase is, in turn, divided into specific research problems. For the convenience of the reader the work of each university is outlined below.

## POLYTECHNIC INSTITUTE OF BROOKLYN

### *PHASE 3*

*Phase Leaders: R.P. Harrington and S.W. Yuan*

(a) To investigate the metallurgical, fabrication, and design problems involved in cooling rocket and intermittent jet motors by the diffusion of fluids through porous metal combustion chamber liners. (b) To study analytically and experimentally (1) the diffusion of fluids through porous media under high pressures and temperatures and (2) the effects (of this diffusion) on the internal aerodynamics. (c) To study problems in the field of physical-chemistry pertinent to (a) and (b) with consideration given to the clogging of pores, the use of catalysts embedded in the liner walls, and endothermic diffusion processes.

PIB-3R1. An experimental investigation of the stability of the laminar boundary layer above the surface of a porous flat plate with fluid injection.

PIB-3R2. A theoretical investigation of the temperature field in the laminar boundary layer (compressible fluid) on a porous flat plate with fluid injection.

PIB-3R3. Measurement of pulsejet wall temperatures by X-ray diffraction methods.

## CORNELL AERONAUTICAL LABORATORY

### *PHASE 1*

*Phase Leaders: J.V. Foa and G. Rudinger*

In connection with jet propulsion engines: (1) to study the mechanism of nonsteady flow in simple ducts with particular reference to acoustic jets, inflow and outflow phenomena in jet engines, and the stability of shock waves in diffusers, and (2) to study the operation of shrouded pulsejets.

CAL-1R1. Study of pulsejet operation with particular reference to the effect of shape, using the analogy between surface gravity waves in water and pressure waves in gases.

CAL-1R2. Study of the mechanism of the acoustic jet.

CAL-1R6. Propagation and stability of shock waves in supersonic diffusers.

CAL-1R7. Investigation of valveless pulsejet.

CAL-1R8. Study of the operation of shrouded pulsejets.

### *PHASE 2a*

*Phase Leaders: J.V. Foa and G. Markstein*

In connection with jet propulsion engines: to investigate ignition and flame propagation and stability as affected by physical parameters with particular reference to the interaction between flow disturbances and flame propagation.

CAL-2R3. Combustion chamber experiments.

CAL-2R5. Combustion tube experiments: study of flame structure, effects of disturbances on flame travel in tubes, and stability of flame fronts.

CAL-2R6. Burner experiments.

### *PHASE 2b*

*Phase Leaders: P.K. Porter and J.T. Grey*

In connection with jet propulsion engines: to study the mechanism of combustion and attendant reactions through the application of spectrographic and other techniques.

CAL-2R9. Investigation of the effect of combustion conditions on the spectra of hydrocarbon flames at low pressures.

*PHASE 3*

*Phase Leaders: P.K. Porter and L.W. Smith*

To study the physical properties and mechanism of failure of materials for high-temperature application in connection with jet engines.

CAL-3R1. Development of a high-temperature metalloscope.

CAL-3R2. High-temperature tensile testing of sheet materials.

CAL-3R3 High-temperature short-time creep testing of sheet materials.

CAL-3R4. High-temperature fatigue testing of sheet materials.

CAL-3R5. Sigma phase strengthening of high-temperature sheet materials.

## UNIVERSITY OF DELAWARE

*PHASE 1*

*Phase Leader: S.A. Guerrieri.*

Heat transfer in passages with free convection and counterflow: (a) the visual study is to be carried out using a vertical rectangular duct having two opposing glass walls with provision to heat the middle portion. Free convection will be upward but arrangement will be made to force air downward at a controllable velocity. By means of spark photography, the resulting gas can be studied. (b) the quantitative study is to be carried out with emphasis on the cooling effect of liquid under conditions of free convection with forced counterflow. Various liquids will be chosen so as to give a wide variation in the Grashof number.

Del-1R1. The quantitative study is to be carried out with emphasis on the cooling effect of liquid under conditions of free convection with forced couhterflow. Various liquids will be chosen so as to give a wide variation ih the Grashof number.

Del-1R2. The visual study is to be carried out using a vertical rectangular duct having two opposing glass walls with provision to heat the middle portion. Free convection will be upward but arrangement will be made to force air downward at a controllable velocity. By means of spark photography, the resulting flow can be studied.

### *PHASE 2*

*Phase Leader: Kurt Wohl*

To investigate experimentally several of the basic problems associated with gaseous combustion including: (a) flame type intermediate between self-propagating and diffusion flames, (b) the stability conditions, the fluctuations, and other properties of turbulent flames, (c) the temperature distribution in flames, (d) the local velocities in flames with the help of the method of stroboscopically illuminated powder particles, and (e) sampling in nonhomogeneous gas streams.

Del-2R1. A study of flame characteristics, mainly of flame types intermediate between self-propagating and diffusion flames.

Del-2R2. A study of the stability conditions, the fluctuations, and other properties of turbulent flames with the help of the hot-wire anemometer.

Del-2R3. A study of the temperature distribution in flames of various types.

Del-2R4. A study of the local velocity in flames using stroboscopically illuminated powder particles.

Del-2R5. A study of sampling in nonhomogeneous gas streams.

## JOHNS HOPKINS UNIVERSITY

### *PHASE 1*

*Phase Leader: Leslie S.G. Kovasznay*

To develop optical techniques for measuring the statistical properties of turbulence (intensity, scale, correlation, spectrum, etc.) in high-velocity flows for which measurable density fluctuations occur.

*PHASE 2*

*Phase Leader: Ion Carstoiu*

To make contributions to the fundamental theory of turbulence with particular emphasis on the case of isotropic turbulence.

## NEW YORK UNIVERSITY

*PHASE 2*

*Phase Leader: J.H. Hett. Associate: A.M. Nathan*

In connection with rockets and pulsejets: to develop theoretical methods for the calculation of transient temperature distributions and thermal stresses in solids in which heat capacities and conductivities are functions of the temperature; to measure these thermal parameters under conditions of high rates of heating which may involve absorption lag, and to study and test the theory of thermal radiation from solids and gases in relation to the measurement of temperature.

NYU-2R1. The effect of high rates of heating on heat capacity and conductivity in steel specimens.

*PHASE 3*

*Phase Leader: G.E. Hudson*

In connection with pulsejets: to observe valve, particle, and flame motions, and to record thrusts and instantaneous pressures, temperatures, and flow speeds in and near standard or idealized components of pulsejets and related devices, and to use these observations in theoretical and analogue treatments of pulsejets.

NYU-3R7. Theory of pulse jets.

*PHASE 4*

*Phase Leader: J.H. Hett*

In connection with rockets and pulsejets: to develop and use instruments for recording thrust and transient pressures, temperatures, densities, and radiations of hot oscillating gases, and gas and liquid velocities.

NYU-4R3. A resistance-type element for the measurement of oscillating fluid velocity in liquid flow.

*Phases 2, 3, and 4 have been revised and as of 1 October 1949 are combined in Phases 6, 7, and 8.*

## *PHASE 6*

*Phase Leader: G.E. Hudson*

*Associates: J. Jeffress and J. Lenelson*

In connection with pulsejets, ramjets, rockets: to investigate both by theory and experiment (a) combustion and fluid flow processes in pulsejets having simple or idealized configurations, and (b) high effective burning rates and large amplitude gas vibrations in jet propulsion devices.

NYU-6R1. Idealized pulsejets.

NYU-6R2. Oscillating piston engine.

NYU-6R3. Theory of the oscillating piston engine.

## *PHASE 7*

*Phase Leaders: G.E. Hudson and I. Amron*

*Associates: R.J. Kraushaar, J. Neuringer, M.D. Scheer, L. Schoen, R.P. Shaw, M.Storm*

In connection with jet propulsion devices: to make an experimental and theoretical study of the physical phenomena whose fundamental importance is indicated by the studies of Phase 4, including: fluid jet formation; the interaction of combustion and fluid flow; large amplitude gas vibrations in tubes; and ignition and combustion.

NYU-7R1. Experiments on gas jet formation.

NYU-7R2. Theory of jet formation.

NYU-7R3. Small flame tube observations and theory.

NYU-7R4. Theory of swirling combustion.

NYU-7R5. Large amplitude gas vibration source.

NYU-7R6. Large amplitude gas vibration theory.

NYU-7R7. Photo-ignition

NYU-7R8. Hydrocarbon flame bands.

NYU-7R9. Theory of non-linear heat conduction in simple metals.

*PHASE 8*

*Phase Leader: J.H. Hett*

*Associates: R.W. King, J.B. Gilstein*

In connection with jet propulsion devices: to develop further and use pressure, temperature, fluid velocity, and density instrumentation, and other pertinent observational techniques needed to collect the data for the studies and investigations of Phases 6 and 7.

NYU-8R1. Temperature measurement.

NYU-8R2. Effect of temperature on pressure gauges.

NYU-8R3. Frequency response and dynamic calibration of pressure gauges with cooling chambers.

NYU-8R4. Three-dimensional schlieren apparatus.

## PRINCETON UNIVERSITY

*PHASE 2*[1]

*Phase Leader: R.N. Pease*

To study (1) the characteristics of combustion in high-velocity fuel-oxidant streams, ignitibility, efficiency, after-burning, thrust, etc.; (2) effects of sub-atmospheric pressures;

[1]This phase is jointly sponsored with the Bureau of Ordnance, U.S. Navy, APL-JHU associated contract NOrd-7920 Task PN-3.

(3) interactions between ionization and flame, (4) observation of optical and mass spectra, and (5) theory of adiabatic exothermic reaction.

Pr-2R1. Development of a low-pressure burner.

Pr-2R2. Kinetics of combustion of gaseous boron compounds.

Pr-2R3. Theory of flame speeds.

Pr-2R4. Interaction of hydrogen atoms with oxygen and hydrocarbons.

Pr-2R5. Kinetics of noncatalytic combustion of ammonia.

Pr-2R6. Photochemical explosion of hydrogen-chlorine mixtures.

*PHASE 3*

*Phase Leader: J.V. Charyk*

To study theoretically and experimentally certain of the basic problems associated with steady-burning propulsive devices of the ducted type. These are: (1) investigation of the mixing of a supersonic (hot or cold) stream with a subsonic stream; (2) investigation of ejector performance; (3) investigation of the combustion chamber problems in steady-burning ducted propulsive devices.

Pr-3R1. Investigation of ejectors and mixing of subsonic and supersonic fluid streams.

Pr-3R2. Investigation of mixing of rocket exhaust jet with induced air stream; problems of fuel injection and subsequent burning in mixture.

*PHASE 4*

*Phase Leader: A. Kahane*

To investigate theoretically and experimentally the feasibility of a valveless intermittent-jet engine.

Pr-4R1. Investigation of a valveless intermittent-jet engine.

### *PHASE 5*

*Phase Leader: J.V. Charyk*

To make preliminary studies of rocket motor performance under certain particular conditions with a view to gaining some insight into the factors affecting combustion in a rocket and to endeavor to translate such information into the establishment of basic parameters governing rocket combustion chamber processes.

## PURDUE UNIVERSITY

### *PHASE 3*

*Phase Leader: H.J. Yearian*

To undertake the study of corrosion in connection with jet propulsion devices. The purpose of the research is to identify the corrosion products, and to investigate the process of corrosion as affected by the chemical and physical properties of the materials and the conditions of exposure.

PRF-3R1. Oxidation of heat-resistant alloys.

### *PHASE 5*

*Phase Leader: J.M. Smith*

To determine, for liquid-fuel rockets and jet engines, the radiation factor and its contribution to heat-transfer coefficients inside a pipe with gas flow at low and also at high temperatures.

PRF-5R1. Convection heat-transfer coefficients for gases at high temperatures.

PRF-5R2. Relative importance of convection and radiation heat transfer for gases at high temperatures up to 2000°F.

### *PHASE 7*

*Phase Leader: M.J. Zucrow*

To investigate rocket motor and liquid propellant parameters at high chamber pressures.

PRF-7R1. Design, construction and instrumentation of a rocket test facility.

PRF-7R2. Preliminary analysis of heat transfer in a high-pressure rocket motor.

PRF-7R3. Investigation of ignition lag of spontaneously ignitible propellants.

PRF-7R5. Catalysis of the reaction of nonhypergolic propellants.

PRF-7R7. Investigation of various methods for calculating propellant performance at high pressures.

PRF-7R8. Experimental investigation of effect of combustion chamber pressure upon rocket-motor performance.

PRF-7R9. Experimental investigation of effect of combustion chamber pressure upon heat transfer in rocket motors.

PRF-7R10. The cooling of rocket-motor nozzles by transpiration cooling through parallel discs.

# APPENDIX C. DISTRIBUTION LIST

1. Army-Navy-Air Force Guided Missiles Mailing List No. 10 dated 15 January 1950, as amended, Parts A, B, C, DP.
2. Dr. R. Courant, New York University.
3. Dr. E. R. Gilliland, Massachusetts Institute of Technology.
4. Dr. A.B. Kinzel, Union Carbide and Carbon Research Laboratory.
5. Mr. E.S. Roberts, Chemical Construction Co.
6. Dean H.S. Taylor, Princeton University.
7. Dr. Theodore von Karman, Scientific Advisory Board, United States Air Force.
8. Dr. J.V. Charyk, Princeton University.
9. Dr. F. Clauser, Johns Hopkins University.
10. Dr. J.V. Foa, Cornell Aeronautical Laboratory.
11. Dr. R.P. Harrington, Polytechnic Institute of Brooklyn.

12./32. Dr. G.E. Hudson, New York University (Attn: M. W. Woody).

33. Dr. M.J. Zucrow, Purdue University.
34. Dr. K. Wohl, University of Delaware.
35. Dr. G. Markstein, Cornell Aeronautical Laboratory.
36. Prof. R.N. Pease, Princeton University.
37. Dr. P. Libby, Polytechnic Institute of Brooklyn.
38. Dr. S.A. Guerrieri, University of Delaware.
39. Prof. L. Lees, Princeton University.
40. Dr. G. Rudinger, Cornell Aeronautical Laboratory.
41. Mr. J.M. Smith, Purdue University.
42. Dr. S.W. Yuan, Polytechnic Institute of Brooklyn.
43. Dr. M. Balicki, Polytechnic Institute of Brooklyn.
44. Dr. P.K. Porter, Cornell Aeronautical Laboratory.
45. Dr. H.J. Yearian, Purdue University.
46. Dr. I. Fankuchen, Polytechnic Institute of Brooklyn.
47. Dr. J.T. Grey, Cornell Aeronautical Laboratory.
48. Mr. H.J. Shafer, Princeton University.
49. Dr. A.P. Colburn, University of Delaware.
50. Dr. G.S. Meikle, Purdue University.
51. Mr. H.K. Moffitt, Cornell Aeronautical Laboratory.
52. Mr. E.E. Miller, Chief, Division of Research Information, N.A.C.A.,
53. Mr. R.J. Woodrow, Princeton University.
54. Dr. H.K. Work, New York University.

55. Mr. R. Spence, Johns Hopkins University.
56. Prof. A. Kahane, Princeton University.
57. Mr. H.L. Pool, Princeton University.
58. Mr. L.W. Smith, Cornell Aeronautical Laboratory.
59./70. Chief of Naval Research, Code 429, Washington, D.C.
71. Commanding Officer, Office of Naval Research, New York.
72. Commanding Officer, Office of Naval Research, Chicago, Illinois.
73. Commanding Officer, Office of Naval Research, Pasadena, Calif.
74./75. Chief of Bureau of Aeronautics, Experimental Engines Branch.
76. Chief of Bureau of Aeronautics, Fuels and Lubricants Branch.
77. Chief of Bureau of Aeronautics, Ships Installations Division.
78. Mr. P. Kratz, Office of Naval Research Representative, Philadelphia.
79. Mr. A.G. Leigh, Office of Naval Research Representative, Rochester.
80. Dr. A. Kuethe, Office of Air Research, Wright Field.
81. Dr. G. Samaras, Office of Air Research, Wright Field.
82./83. Guided Missiles Division, Bureau of Ordnance, (Mr. F. Tanczos).
84. Mr. W. Worth, Power Plants Laboratory, Wright Field.
85. Dr. C.F. Yost, Directorate of Research and Development, United States Air Force, Washington, D.C.
86. Aeromarine Co., Vandalia, Ohio (Mr. W. Tenney).
87. University of California, Berkeley, Calif. (Prof. R. Folsom).
88. Columbia University Library, New York.
89. Guggenheim Aeronautical Laboratory, Pasadena, Calif. (Prof. C. Millikan).
90. University of Minnesota, Minneapolis, (Dr. B. Crawford).
91. Officer in Charge, Naval Ordnance Test Station, Pasadena, Calif.
92. Commanding Officer, Office of Naval Research Branch Office, San Francisco, Calif.
93. Purdue University, Lafayette, Indiana. (Mr. J. Moriarty).
94. Commanding Officer, Office of Naval Research, Boston, Mass.
95. Office of Assistant Naval Attache for Research, Navy 100, FPO, N.Y.
96. Mr. H.S. Avery, American Brake Shoe Co., Mahwah, New Jersey.
97. Dr. J.B. Austin, U.S. Steel Laboratory, Kearney, New Jersey.
98. Committee on Undersea Warfare, National Research Council (Mr. J.S. Coleman).
99. The Director, U.S. Navy Electronics Laboratory , San Diego, Calif. (Ref 617-206).
100. Mr. G. Sands, Union Carbide and Carbon Research Laboratory.
101. Prof. L. Crocco, Aeronautical Engineering Department, Princeton, New Jersey.
102. Mr. F.A. Parker, Princeton University.
103. Dr. Martin Summerfield, Princeton University.

104. Dr. J.H. Wakelin, Princeton, New Jersey.
105. Mr. C. Denney, American Helicopter Co.
106. Dr. Bernard Lewis, Bureau of Mines,

TITLE: Annual Program Report - Project Squid - 1 January 1950 - and Appendixes A-C

ATI- 77 625

REVISION: (None)

ORIG. AGENCY NO.: (None)

PUBLISHING AGENCY NO.: (None)

AUTHOR(S) : Beighley, C. M.; Warner, C. F.; Zucrow, M. J.; and others
ORIG. AGENCY : Polytechnic Institute of Brooklyn, N. Y.; Cornell Aeronautical Lab.,*
PUBLISHED BY : (Same) for USN Project Squid

| DATE | U.S. CLASS. | COUNTRY | LANGUAGE | PAGES | ILLUSTRATIONS |
|---|---|---|---|---|---|
| Jan' 50 | Unclass. | U.S. | English | 193 | photos, tables, diagrs, graphs |

ABSTRACT:

Progress made in the development of project Squid, a cooperative program of fundamental research in jet propulsion, is presented. Experimental investigations were continued on jet propulsion engines, including rocket, rocket-ramjet, ramjet, valveless intermittent ramjet, valveless pulsejet, and shrouded pulsejet engines. Studies related to jet propulsion development are reviewed under the subject headings of fluid mechanics, heat transfer, flame propagation, chemical reaction kinetics, spectroscopy of combustion, instrumentation and testing equipment, and heat resistant materials. An outline is given which indicates the various phases of work being conducted by each affiliated university.

* Inc., Buffalo, N. Y.; University of Delaware, Newark; and others

DISTRIBUTION: Copies obtainable from CADO.

DIVISION: Power Plants, Rocket (4)
SECTION: General (0)

SUBJECT HEADINGS: Project Squid
Propulsion - Development

Central Air Documents Office
Wright-Patterson Air Force Base, Dayton, Ohio

CADO ['CAL INDEX

USN Contr. Nos. N6-ORI-11, 98, 104 and others